Characterization of *Populus* x *canescens* LysM-Receptor Like Kinases LYK4/LYK5 and LysM-Receptor Like Protein LYM2 and their Roles in Chitin Signaling

Dissertation

for the award of the degree

"Doctor rerum naturalium"

of the Georg-August-Universität Göttingen

within the doctoral program in Biology
of the Georg-August-University School of Science (GAUSS)

submitted by

Mo Awwanah

from Pamekasan, Indonesia

Göttingen, 2020

Thesis Committee

PD Dr. Thomas Teichmann
(Department of Plant Cell Biology, Georg-August-Universität Göttingen)

Prof. Dr. Volker Lipka
(Department of Plant Cell Biology, Georg-August-Universität Göttingen)

Members of the examination board

Referee : **Prof. Dr. Volker Lipka**
(Department of Plant Cell Biology, Georg-August-Universität Göttingen)

2nd Referee : **PD Dr. Thomas Teichmann**
(Department of Plant Cell Biology, Georg-August-Universität Göttingen)

Further members of the examination board

PD Dr. Marcel Wiermer
(Department of Plant Cell Biology, Georg-August-Universität Göttingen)

Prof. Dr. Andrea Polle
(Department of Forest Boatny and Tree Physiology, Georg-August-Universität Göttingen)

PD Dr. Till Ischebeck
(Department of Plant Biochemistry, Georg-August-Universität Göttingen)

Prof. Dr. Stefan Jakobs
(Department of Nanobiophotonics, Max Planck Institute for Biophysical Chemistry, Göttingen)

Date of oral examination: March 2nd, 2020.

Declaration

Promovierenden-Erklärung
der Georg-August-Universität Göttingen

Die Gelegenheit zum vorliegenden Promotionsvorhaben ist mir nicht kommerziell vermittelt worden. Insbesondere habe ich keine Organisation eingeschaltet, die gegen Entgelt Betreuerinnen und Betreuer für die Anfertigung von Dissertationen sucht oder die mir obliegenden Pflichten hinsichtlich der Prüfungsleistungen für mich ganz oder teilweise erledigt.

Hilfe Dritter wurde bis jetzt und wird auch künftig nur in wissenschaftlich vertretbarem und prüfungsrechtlich zulässigem Ausmaß in Anspruch genommen. Insbesondere werden alle Teile der Dissertation selbst angefertigt; unzulässige fremde Hilfe habe ich dazu weder unentgeltlich noch entgeltlich entgegengenommen und werde dies auch zukünftig so halten.

Die Ordnung zur Sicherung der guten wissenschaftlichen Praxis an der Universität Göttingen wurde von mir beachtet.

Eine entsprechende Promotion wurde an keiner anderen Hochschule im In- oder Ausland beantragt; die eingereichte Dissertation oder Teile von ihr wurden nicht für ein anderes Promotionsvorhaben verwendet.

Mir ist bekannt, dass unrichtige Angaben die Zulassung zur Promotion ausschließen bzw. später zum Verfahrensabbruch oder zur Rücknahme des erlangten Grades führen.

Göttingen, January 31st, 2020

Mo Awwanah

I. Table of Contents

II. List of Figures

III. List of Tables

IV. List of Supplemental Figures

V. List of Supplemental Tables

VI. List of Abbreviations

α	anti
°C	degree Celsius
µg	microgram
µl	microliter
µm	micrometer
ω	omega
aa	aminoacids
AM	Arbuscular mycorrhiza
Arg	Arginine
AS	Alternative splicing
Asn	Asparagine
Asp	Aspartic acid
APS	Ammoniumpersulfate
At	*Arabidopsis thaliana*
AT	Annealing temperature
ATP	Adenosintriphosphat
Avr	avirulence
BAK1	BRI1-ASSOCIATED KINASE 1
BLASTP	Basic Local Alignment Search Tool (for Protein)
bp	base pair
BG	β-1,3-glucanase(s)
BRI1	BRASSINOSTEROID INSENSITIVE 1
$CaCl_2$	Calcium chloride
CalS	Callose Synthase
CBB	Coomassie Brilliant Blue
CBM	Carbohydrate-binding module
CC	coiled-coil
CC-NBS-LRR	Coiled-coil nucleotide binding site leucine rich repeat
cDNA	complementary DNA
CDPK/CPK	CALCIUM DEPENDENT PROTEIN KINASE
CEBiP	CHITIN ELICITOR BINDING PROTEIN
CERK1	CHITIN ELICITOR RECEPTOR LIKE KINASE
CesA3	cellulose synthase subunit
CLSM	Confocal laser scanning microscopy
cm	centimeter
CML	CALMODULIN LIKE
CO	Chitoologisaccharide(s)
Col-0	Columbia-0
Co-IP	co-immunoprecipitation
Com.	Complementation
CTAB	Cetyl Trimethyl Ammonium Bromide
CTP	CHLOROPLAST-TARGETED PROTEIN
DEPC	Diethyl pyrocarbonate
DAMP	damage-associated molecular pattern
ddH2O	double-distilled water

DMSO	Dimethylsulfoxid
DNA	Deoxyribonucleic acid
DTT	Dithiothreitol
DUF	Domain of unknown function
E. coli	*Escherichia coli*
e.g.	exempli gratia
EDTA	Ethylenediaminetetraacetic acid
EFR	elongation factor thermo unstable receptor
EF-Tu	elongation factor thermo unstable
eGFP	enhanced-GFP
ER	endoplasmic reticulum
etc.	Et cetera
ETI	effector-triggered immunity
EtOH	Ethanol
flg22	flagellin22
FLS2	FLAGELLIN SENSING 2
FRET	Förster resonance energy transfer
FT	CONSTANS (CO)/FLOWERING LOCUS T
g	gram
GABI	Genomanalyse im biologischen System Pflanze
gDNA	genomic DNA
GFP	Green fluorescent protein
GlcNAc	N-acetyl-D-glucosamine
Glu	Glutamic acid
Gly	Glycine
GN8-Bio	biotinylated chitin oligosaccharide
GPI-anchor	glycosylphosphatidylinositol-anchor
GSL	GLUCAN SYNTHASE-LIKE/CALLOSE SYNTHASE
GTP	guaninetriphosphosphate
h	hour(s)
HCl	Hydrogen Chloride
HCL	HAIR CURLING
HEPES	4-(2-hydroxyethyl)-1-piperazineethanesulfonic acid
HMGB	High mobility group box
HR	hypersensitive response
ID	intracellular domain
Ile	Isoleucine
kDa	kilo Dalton
KOH	Potassium hydroxide
l	liter
LCO	Lipochitooligosaccharide(s)
Leu	Leucine
LiCl	Lithium Chloride
Lj	*Lotus japonicus*
LOF	loss of function
LRR-RLK	leucine-rich repeat receptor-like kinase

LRRs	leucine rich repeats
LYK	LysM receptor-like kinase
LYM	LysM-containing receptor-like proteins
LYP	LysM-containing protein in rice
Lys	Lysine
LYS	LysM receptor kinase gene in *Lotus japonicus*
LysM	lysin motif
MAMP	microbe associated molecular pattern
MAPK	mitogen-activated protein kinase
M	Molar
min	minute(s)
ml	milliliter
MltD	membrane-bound lytic murein transglycosylase D
mm	Millimeter
MP	Movement protein
MPK	MAPK
mRNA	Messenger RNA
MS	Murashige-Skoog
Mt	*Medicago truncatula*
MurNAc	*N*-acetylmuramic acid
MUSCLE	Multiple Sequence Comparison by Log- Expectation
Myc	myc- factors
n	Number of replicate
NaCl	Natrium Chloride
NBS	nucleotide binding site
NFP	NOD FACTOR PERCEPTION
NFR	NOD FACTOR RECEPTOR
Nfs	Nod-factors
nM	nanomolar
NPR	NONEXPRESSOR OF PATHOGENESIS-RELATED GENE
NTC	No template control
OD_{600}	optical density at a wavelenght of 600 nm
OG	Oligogalacturonide(s)
ORF	Open reading frame
Os	*Oryza sativa*
p	promoter
pa	*Parasponia andersoni*
PAMP	pathogen associated molecular pattern
Pc	*Populus* x *canescens*
PCR	Polymerase Chain Reaction
PD	plasmodesma(ta)
PD-PM	Plasmodesmal plasma membrane
PDCB	Plasmodesmata callose-binding protein
PDBG	Plasmodesmata β-1,3-glucanase
PDLP	PD-Located Protein
PGN	Peptidoglycan

PhyML	a phylogeny software based on the maximum-likelihood principle
PKA-Cα	Protein kinase A catalytic subunit
PLS	PD localization signal
PM	plasma membrane
PMA	proton pump ATPase
Pre-mRNA	Precursor mRNA
Pro	Proline
PRR	pattern recognition receptor
PRX	Peroxidase
psi	Pounds per Square Inch (a unit of pressure)
Pt	*Populus trichocarpa* Nisqually
PTI	PAMP-triggered immunity
pv	pathovar
PVP	Polyvinylpyrrolidone
R-	resistance
RBOHD	Respiratory burst oxidase homolog protein D
REV	REVOLUTA
RFP	Red fluorescent protein
RLK	receptor-like kinase
RLP	receptor-like protein
RNA	ribonucleic acid
ROS	reactive oxygen species
rpm	rounds per minute
RT	room temperature
(q)RT-PCR	(quantitative) reverse transcriptase PCR
s	second(s)
SA	Salicylic acid
SD	Standard Deviation
SDS	Sodium dodecyl sulfate
SDS-PAGE	Sodium dodecyl sulfate polyacrylamide gel electrophoresis
SEL	size exclusion limit
Ser	Serine
sgRNA	Single guide RNA
SND	*SECONDARY WALL-ASSOCIATED NAC DOMAIN*
SNP	Single nucleotide polymorphism(s)
SP	Signal peptide
SPFH	stomatin/prohibitin/flotillin/HflK/C
spp.	Several species
SRC	short-rotation coppice
SYMRK	SYMBIOSIS RECEPTOR KINASE
SYTA	synaptotagmin A
t	Terminator
TBS-T	Tris buffered saline - Tween-20
T-DNA	transfer-DNA
TEMED	Tetramethylethylenediamine
TF	Transcription factor(s)

TIR	Toll-Interleukin-1 receptor
TIR-NBS-LRR	Toll-Interleukin-1 receptor nucleotide binding site leucine rich repeat
Thr	Threonine
TM	transmembrane domain
TMV	tobacco mosaic virus
TTSS	type III secretion system
UBQ	Ubiquitine
v/v	volume per volume
vRNA	Viral RNA
w/v	Weight per volume
WGD	Whole genome duplication
WRKY	Transcription factor with WRKY amino acid sequence at the N-terminus
WT	wild type
ZAT	Zinc finger protein

1. Summary

Poplar is a model tree to study the molecular biology of woody plant species. It also has commercial benefits as it is used as a renewable energy resource. Poplar plantations suffer from poplar rusts caused by *Melampsora* fungi. Fungal pathogens are recognized by plants via LysM domain-containing receptors that perceive a major component of fungal cell walls, the β-1,4-linked N-acetylglucosamine polymer chitin, which functions as a pathogen associated molecular pattern (PAMP). Chitin perception triggers defense responses that contribute to plant immunity. The components of chitin receptors have been well characterized in some plant species such as the model plants *Arabidopsis thaliana* (*At*) and *Oryza sativa* (*Os*). In *A. thaliana*, the perception of chitin and initiation of chitin-induced immune responses require the LysM Receptor-like Kinase (LysM-RLK) CHITIN ELICITOR RECEPTOR KINASE 1 (AtCERK1). Two additional LysM-RLKs, AtLYK4 and AtLYK5 exhibit chitin-triggered AtCERK1-dependent phosphorylation and may function as co-receptors of AtCERK1. In rice, the LysM Receptor-like Protein (LysM-RLP) CHITIN ELICITOR BINDING PROTEIN (CEBiP), associates with OsCERK1 in order to trigger chitin-induced plant defense. *AtLYM2*, the homolog of *CEBiP* in *A. thaliana*, is not involved in AtCERK1-mediated chitin responses, but mediates chitin-induced suppression of plasmodesmal flux independent of AtCERK1. This study analyses chitin receptor components in the hybrid poplar *P. x canescens* (*Pc*) (*P. tremula* x *P. alba*).

In Chapter 1, identification and functional characterization of poplar lysin motif receptor-like kinases (LysM-RLKs) encoded by *AtLYK4*/*AtLYK5* homologs are described. *In silico* analysis revealed that four homologs of *AtLYK4* and two homologs of *AtLYK5* are present in the *Populus trichocarpa* (*Pt*) Nisqually genome. Of these, two *PcLYK4* and one *PcLYK5* homologs represent pseudogenes due to internal stop codons. The homologs *PcLYK4-1*, *PcLYK4-2* and *PcLYK5-2* have an open reading frame, which code for proteins with three extracellular LysM domains, a transmembrane domain and an intracellular, inactive kinase domain. All identified *PcLYK4*/*PcLYK5* genes are expressed in roots, wood, developing xylem, bark and leaves. Subcellular localization studies by transient expression of the poplar *PcLYK4/PcLYK5* genes in *Nicotiana benthamiana* as well as analyses of stably-transformed *Arabidopsis thaliana* showed that PcLYK4/PcLYK5 proteins localize at the cell periphery, indicating plasma membrane localization similar to their homologs in Arabidopsis. Functional characterization was carried out by testing the complementation of the Arabidopsis double knock-out mutant, *Atlyk4-1 Atlyk5-2*, which does not show chitin

triggered reactive oxygen species (ROS) production and mitogen-activated kinase (MAPK) phosphorylation. Transgenic expression of *PcLYK4-1*, *PcLYK4-2* and *PcLYK5-2* partially restored the chitin sensitivity of *Atlyk4-1 Atlyk5-2*. Upon chitin treatment, PcLYK4/PcLYK5 proteins are internalized into endosomes. The chitin-triggered endocytotic removal of PcLYK5-2 was shown to be AtCERK1-dependent.

In Chapter 2, the role of poplar LYM2 homologs in chitin-triggered responses was analysed. Two *AtLYM2* homologs, *PcLYM2-1* and *PcLYM2-2*, were identified in poplar. The second homolog, *PcLYM2-2*, is subject to mutually exclusive splicing of the first exon, which generates two protein variants with distinct N-teminal LysM domains, designated as PcLYM2-2.1 and PcLYM2-2.2. All identified PcLYM2 proteins are likely GPI-anchored proteins. Analysis of the transcript abundance showed that all *PcLYM2* genes are expressed in roots, wood, developing xylem, bark and leaves. *PcLYM2-1* exhibits higher mRNA levels in all analysed tissues compared to *PcLYM2-2*. The differential splicing of *PcLYM2-2* pre-mRNA is tissue-specific, resulting in high levels of *PcLYM2-2.1* in wood and developing xylem in contrast to the high levels of *PcLYM2-2.2* in bark and leaves. A chitin pull-down assay showed that all PcLYM2 homologs can bind the PAMP chitin, with PcLYM2-1 having the highest binding capacity compared to both PcLYM2-2 splicing variants. To analyze the role of PcLYM2 proteins in chitin signaling, poplar knock-out lines were generated through a CRISPR/Cas9 approach. Knocking out *PcLYM2* genes in poplar did not affect chitin-induced ROS production and MAPK activation, suggesting that PcLYM2 is not involved in these two chitin-induced responses. Subcellular localization studies revealed that all identified PcLYM2 proteins localize at the plasma membrane and plasmodesmal-PM, indicating a plasmodesmata-related function. Plasmodesmal flux analysis with the *Pclym2-1 Pclym2-2* double knock-out mutants suggests that PcLYM2 proteins mediate chitin-triggered plasmodesmal closure. Moreover, knocking out *PcLYM2-1* is sufficient to abolish this response, suggesting that PcLYM2-1 plays a major role in poplar in particular for mediating this response. Individual functions of the two splicing variants PcLYM2-2.1 and PcLYM2-2.2 in the regulation of plasmodesmal flux or other ligand-induced processes remain to be identified. Expression levels in different tissues suggest that PcLYM2 proteins may have a potential to form tissue-specific complexes through homo- or heterodimerization depending on their abundance in the corresponding tissues.

2. General Introduction

2.1 The Plant Immune System

The ability to perceive environmental signals is crucial for plants to survive since they are exposed to various kinds of environmental conditions during their life cycle, including abiotic and biotic stresses. In response to biotic factors, plants employ different molecular programs to discriminate between beneficial and pathogenic microorganisms. Both beneficial and pathogenic microbes produce signaling molecules that are known as microbe-associated molecular patterns (MAMPs), which have beneficial or pathogenic effect in plants, leading to the establishment of a symbiotic relationship or defense responses (Antolín-Llovera et al., 2014). Beneficial microorganisms such as symbiotic rhizobia and mycorrhizal fungi produce Nod Factors (NFs) and Myc factors (also known as Myc-LCOs), respectively as a signal for symbiosis, which are composed of four to five N-acetylglucosamine (GlcNAc) residues and the non reducing sugar (acyl chain) is de-N-acetylated or N-acetylated (Mulder et al., 2006; Radutoiu et al., 2007; Maillet et al., 2011; Miyata et al., 2014; Antolín-Llovera et al., 2014).

Pathogens are recognized by plants upon the perception of either pathogen-associated molecular patterns (PAMPs) or damage-associated molecular patterns (DAMPs) (Antolín-Llovera et al., 2014). PAMPs are 'non-self' molecules derived from foreign microorganisms that generally have conserved chemical structures within a group of microorganisms (Choi and Klessig, 2016), such as bacterial lipopolysaccharides, flagellin22 (flg22), elongation factor (EF-Tu), lipoproteins, peptidoglycans and fungal chitin. While attacking the plants, pathogens might also induce cell damage or wounding that causes the release of DAMPs, which are 'self' molecules originated from host plants (Boller and Felix, 2009). Several types of DAMP in plants have been reviewed by Choi and Klessig (2016) that include polypeptides/peptides, cell wall-derived substances, extracellular ATP (eATP) and high mobility group box (HMGB) proteins. Systemin, a peptide defense signal that contains 18 amino acid residues, was found in Solanaceous species and is able to trigger the synthesis of wound-inducible proteinase inhibitor proteins (Boller and Felix, 2009). Examples of cell wall-derived substances are the pectic polysaccharide homogalacturonan (a linear polymer of 1,4-linked α-D galacturonic acid) and the fragments of this polymer called oligogalacturonides (OGs) (Choi and Klessig, 2016). The perception of both, PAMPs or DAMPs leads to the activation of plant defense. Plant innate immunity that is initiated upon the perception of PAMPs is termed PAMP-triggered immunity (PTI). PTI is the first

layer of plant defense against initial attempts by pathogens to invade plants. However, well-adapted pathogens can suppress PTI by releasing virulence factors known as effectors. Some bacterial pathogens deliver effectors into the host cells through a needle-like structure, the type-III secretion system (TTSS). Effectors can be recognized by intracellular immune receptors of plants such as the Nucleotide-binding Leucine-rich Repeat (NB-LRR) proteins, leading to the activation of effector-triggered immunity (ETI) in plants (**Figure 2.1** from Dodds and Rathjen, 2010; Macho and Zipfel, 2014). ETI can lead to a hypersensitive response (HR) manifested as cell death, which is qualitatively stronger and faster than PTI (Dodds and Rathjen, 2010).

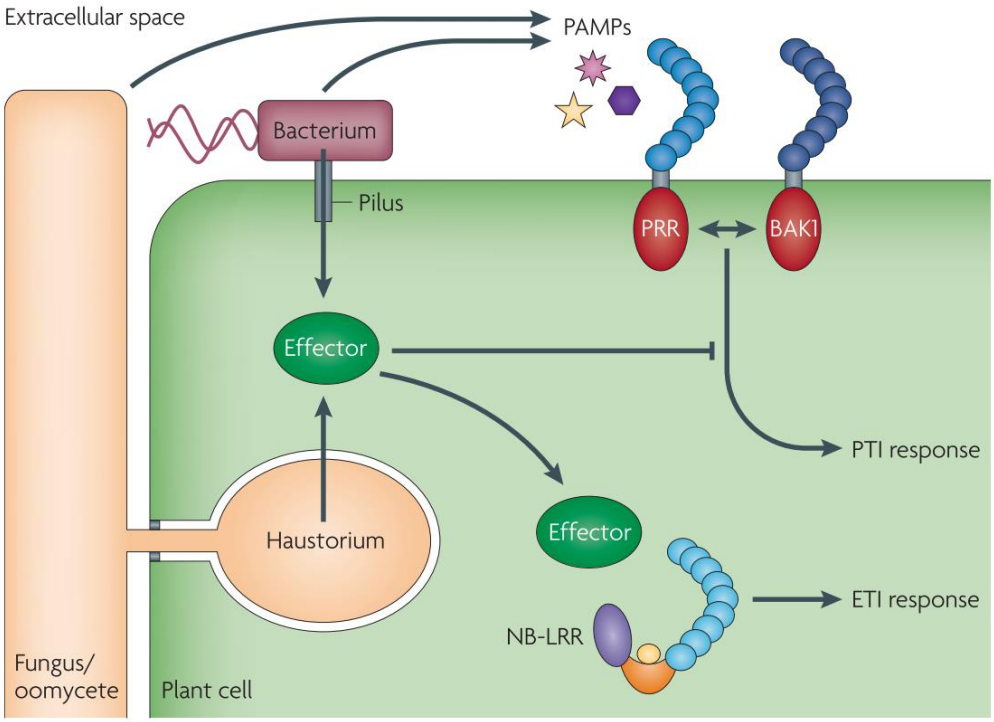

Figure 2.1. Non-self recognition in plants. Plants recognize potential attackers such as pathogenic bacteria and fungi that grow in the extracellular spaces through the perception of elicitors (PAMPs) from the corresponding pathogens by surface-localized receptors, which results in the establishment of PAMP-triggered Immunity (PTI) responses. However, some pathogens have special structures such as fungal haustoria or bacterial type-III secretion pilus to deliver effectors into the plant cells in order to breach the PTI. Plants recognize effectors through Nucleotide-binding Leucine-rich Repeat (NB-LRR) proteins, which leads to Effector-triggered Immunity (ETI). Schematic picture adopted from Dodds and Rathjen (2010).

The discrimination between beneficial and pathogenic microorganisms in plants is mediated by surface-localized pattern recognition receptors (PRRs) that perceive microbial signals (Antolín-Llovera et al., 2014; Macho and Zipfel, 2014). Plant PRRs are surface-localized proteins such as receptor-like kinases (RLKs) or receptor-like proteins (RLPs) (Macho and Zipfel, 2014). RLKs have an ectodomain responsible for ligand binding, a

transmembrane domain and an intracellular kinase domain for signal transduction. RLPs lack the intracellular kinase domain. Plant PRRs are able to activate one or more signaling pathways and often form a complex with other co-receptors to initiate plant immune signaling (Macho and Zipfel, 2014; Miyata et al., 2014). An example of dual function of a receptor in discriminating pathogenic and beneficial microbes is the bifunctionality of CHITIN ELICITOR RECEPTOR KINASE 1 (CERK1) in rice. OsCERK1 was reported to regulate both chitin-triggered immunity induced by fungal pathogens and the establishment of mycorrhization with Arbuscular Mycorrhizal (AM) fungi (**Figure 2.2**) (Miyata et al., 2014). The following sections describe in more detail the view on how surface-localized receptors mediate the recognition of beneficial and pathogenic microbes.

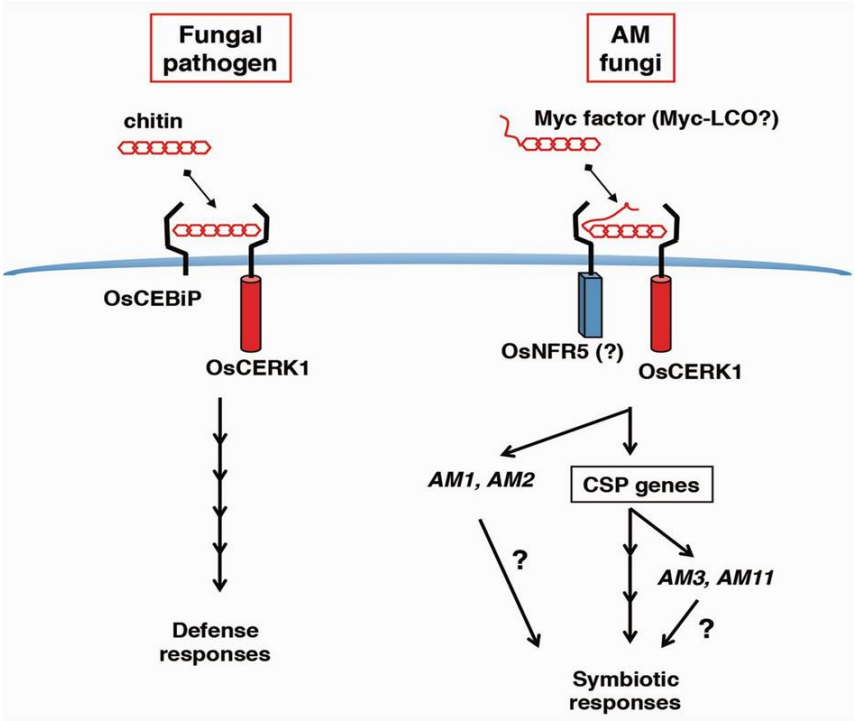

Figure 2.2. Discrimination between pathogenic and beneficial microbes by plants through the recognition of MAMPs by surface-localized PRRs. The schematic picture describes the dual function of a PRR, CHITIN ELICITOR RECEPTOR KINASE 1 (CERK1) in rice, which is able to perceive both fungal chitin to trigger defense responses, and mycorrhizal lipo-chitooligosaccharide (Myc-LCO) to establish symbiotic signaling. In order to exhibit different functions, CERK1 associates with another PRR such as CHITIN ELICITOR BINDING PROTEIN (CEBiP) for chitin perception or the Nod Factor Receptor 5 (NFR5) for Myc-LCO recognition. AM1, 2, 3, and 11 = Arbuscular mycorrhizal symbiotic marker genes. CSP = common symbiotic pathway. Modified from Miyata et al. (2014).

2.2 LysM-RLKs/RLPs and MAMP Perception

2.2.1 LysM-RLKs/RLPs

Lysin Motif (LysM) is a motif composed of 44-65 amino acids (aa) that was first found as a C-terminal direct repeat in the lysozyme of Bacillus phage ø29 (Garvey et al., 1986). The motif is termed as LysM domain since it is mostly found in bacterial autolysins and involved in bacterial cell wall degradation due to its capability to recognize peptidoglycan (PGN) (Bateman and Bycroft, 2000; Zhang et al., 2007). LysM-containing proteins are present in most living organisms ranging from bacteria, fungi, plants and animals, but not in archaea. However, the presence of this motif in eukaryotic proteins was suggested as the result of horizontal gene transfer from bacteria (Bateman and Bycroft, 2000). LysM motifs can be positioned at the N-terminal, central and C-terminal regions of a protein (Buist et al., 2008). The presence of multiple LysM motifs within one LysM domain is possible and usually they are separated by conserved residues of Thr, Ser, Asp and Pro. In plants, the amino acid linkers between LysM domains contain a conserved CxC motif that functions as disulfide bridge (Buist et al., 2008; Arrighi et al., 2006; Radutoiu et al., 2003; Mulder et al., 2006; Petutschnig et al., 2014; Liu et al., 2012).

Liu et al. (2012) characterized the three dimensional structure of a LysM-containing protein using the ectodomain of *Arabidopsis thaliana* CHITIN ELICITOR RECEPTOR KINASE 1 (CERK1), a plasma membrane-localized LysM-RLK that was characterized as the main chitin receptor in Arabidopsis (Miya et al., 2007; Petutschnig et al., 2010). The three LysM domains of AtCERK1 are tightly packed in a globular structure, and the secondary structure of each LysM domain shows a βααβ conformation with the two β strands forming an antiparallel β sheet. The same protein conformation was also observed in the crystal structure of the *Lotus japonicus* LjLYS6 ectodomain, a LysM-RLK that is closely related with NFR1 (Bozsoki et al., 2017). This secondary structure is similar to the three-dimensional structure of LysM from *Escherichia coli* membrane-bound lytic murein transglycosylase D (MltD), a protein that was suggested to be involved in the biosynthesis of the flagellum, reported by Bateman and Bycroft (2000). This structure also resembles the secondary structure of *Bacillus subtilis* ykuD described by Bielnicki et al. (2006), thus, indicating the conservation of the LysM domain in prokaryotes and eukaryotes.

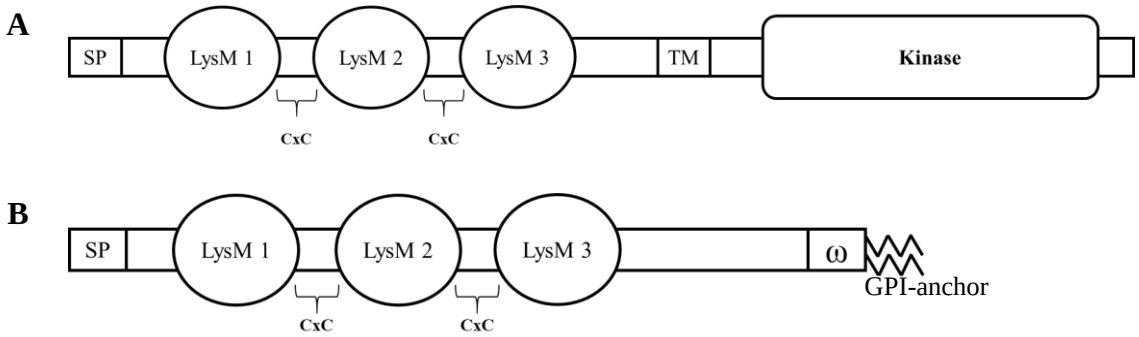

Figure 2.3. Multiple LysM domains separated by a CxC motif in plant LysM-RLKs (A) and LysM-RLPs (B). Schematic picture of the LysM-RLK is modified from the sheme of LysM-RLK CERK1 described in Petutschnig et al. (2014) and NFP in Arrighi et al. (2006), and the scheme of LysM-RLP is illustrated based on the described CEBiP in rice (Hayafune et al., 2014; Gong et al. (2017). SP = signal peptide, LysM = Lysin motif, TM = transmembrane domain, ω = omega site.

LysM-containing molecules that function as surface-localized receptors in plants are classified into LysM-receptor like kinases (LysM-RLKs) and LysM-receptor like proteins (LysM-RLPs). LysM-RLKs consist of extracellular LysM domains, a transmembrane domain and an intracellular kinase domain (**Figure 2.3A**). LysM-RLPs also have LysM motifs at the ectodomain but lack a transmembrane domain, exploiting a GPI-anchor instead at the C-terminal region in order to attach to the plasma membrane of plants (**Figure 2.3B**). Also, an intracellular kinase domain is missing in LysM-RLPs. LysM-containing proteins are involved in multiple functions including hydrolysis of bacterial peptidoglycan (PG), in the development of spores in sporulating bacteria and they are components of receptors to recognize pathogens or symbionts in plants (Buist et al., 2008; Antolín-Llovera et al., 2014). Functional characterization of a chitinase, a LysM-containing protein from the fern *Pteris ryukyuensis*, showed that a tyrosine of the chitinase LysM motif is a determinant in binding to five GlcNAc residues, leading to its antifungal activity (Onaga and Taira, 2008). Plant LysM-receptor like kinases (LysM-RLKs) and LysM-receptor like proteins (LysM-RLPs) play a major role in the discrimination between beneficial and pathogenic microorganisms, through their binding capacity to N-acetyglucosamine-containing ligands such as lipo-chitooligosaccharides (LCO), chitoologisaccharides (CO) and peptidoglycans (PGN) (Buist et al., 2008; Antolín-Llovera et al., 2014; Buendia et al., 2018).

2.2.2 LysM-RLKs/RLPs in Chitin Perception

Chitin is a major component of fungal cell walls that serves as a pathogen-associated molecular pattern (PAMP) composed of β-1,4-linked N-acetylglucosamine (GlcNAc) (Kaku et al., 2006). Chitin is considered as a general elicitor that triggers defense signaling in plants,

including monocots and dicots. N-acetylglucosamine-containing ligands like chitin can be recognized by LysM-containing receptors (Buist et al., 2008; Antolín-Llovera et al., 2014). The components of chitin receptors have been well characterized in some plant species such as the model plants *Arabidopsis thaliana* and *Oryza sativa*. The first component of a chitin receptor complex that was characterized is CHITIN ELICITOR BINDING PROTEIN (CEBiP), which was identified as a glycoprotein that plays a major role in chitin perception and signaling in rice (Kaku et al., 2006). OsCEBiP harbors three LysMs at the ectodomain, and the central LysM is vital for binding to chitin due to the presence of hydrophobic residues especially Ile122, acting as the binding site (Hayafune et al., 2014). Hydrophobic residues important for chitin-binding at the central LysM domain are conserved among CEBiP of different plant species (Liu et al., 2016). In contrast, the other two LysM domains are unable to recognize chitin on their own (Liu et al., 2016).

Hayafune et al. (2014) described the molecular binding mechanism of chitin to OsCEBiP as a sandwich-type dimerization, in which one chitin oligomer binds to the mirrored-sites of two OsCEBiP molecules simultaneously, leading to the homodimerization of this receptor. OsCEBiP preferably binds longer-chain (heptamer-octamer) of chitin oligosaccharides and requires N-acetyl groups for binding, e.g. OsCEBiP does not bind chitosan (de-acetylated chitin) (Hayafune et al., 2014). Binding of OsCEBiP to chitin occurs in a sliding mode along the chitin oligomer, hence, longer chains of chitin (hepta or octamer) offer more optimal interaction (Liu et al., 2016). Liu et al. (2016) examined the binding affinity of the OsCEBiP ectodomain to chitin, and found that the LysM domain of OsCEBiP is sufficient for binding chitin. Moreover, this binding does not introduce conformational change to the secondary structure of OsCEBiP.

Gong et al. (2017) reported that OsCEBiP is not a transmembrane protein and further described that it employs a GPI anchor for plasma membrane positioning. The fact that OsCEBiP has no intracellular kinase domain indicates that OsCEBiP has to interact with another receptor kinase for chitin signal transduction from the plasma membrane to the cytoplasm (Kaku et al., 2006). Shimizu et al. (2010) characterized ten genes encoding OsLysM-RLKs and reported that nine of them are expressed in rice cells. OsLysM-RLK9 which was then assigned as OsCERK1 showed high homology to AtCERK1, a plasma membrane-localized LysM-receptor like kinase that was characterized as the main chitin receptor in *Arabidopsis thaliana* (Miya et al., 2007; Petutschnig et al., 2010; Liu et al., 2012). Shimizu et al. (2010) described that OsCERK1 has a domain organization similar to AtCERK1, with an intracellular serine/threonine kinase domain, a transmembrane domain

and three extracellular domains (Miya et al., 2007; Wan et al., 2008). *OsCERK1* expression is up-regulated by elicitor treatment (Shimizu et al., 2010). The role of OsCERK1 in chitin perception and signaling is indispensable (Kouzai et al., 2014), since chitin-induced hydrogen peroxide production is abolished in OsCERK1-disrupted lines: The OsCERK1 loss-of-function lines also showalteration of chitin-induced gene expression, and these lines are more susceptible to the rice fungus *Magnaporthe oryzae*. Functional characterization by qPCR showed that the $GlcNAc_8$-induced gene expression was suppressed in *OsCERK1* knock-down lines, but the binding of biotinylated chitin oligosaccharide (GN8-Bio) to microsomal membranes was not affected by knocking down *OsCERK1* (Shimizu et al., 2010). This observation suggests that OsCERK1 is not responsible for binding chitin but important for chitin-mediated downstream signaling in rice, further indicating that OsCERK1 might be a potential interacting partner of OsCEBiP that was suggested to be the main chitin receptor in rice. Yeast two-hybrid assays using the extracellular domain of OsCEBiP and OsCERK1 show that these two proteins can interact and form a heterodimer. In addition, homodimerization of the molecules can also occur.

CHITIN ELICITOR BINDING PROTEINs similar to OsCEBiP have been identified in many other plant species, which indicates that chitin-triggered defense signaling is quite conserved in plants (Kaku et al., 2006). In *Arabidopsis thaliana*, chitin induced MAPK activation and ROS burst are mediated by CERK1 (Miya et al., 2007). Chitin-induced MAPK activation, ROS production and defense gene expression are abolished in this mutant. Complementation of *Atcerk1* with WT AtCERK1 restores the chitin response, indicating that AtCERK1 plays an essential role in chitin perception and signaling in *A. thaliana*. Petutschnig et al. (2010) reported that the three extracellular LysM domains of AtCERK1 are required for binding chitin without the necessity of any other co-receptors, leading to the auto-phosphorylation of AtCERK1 that is necessary to activate downstream signaling pathways. Thus, AtCERK1 has capability to perceive chitin by itself (Iizasa et al., 2010; Petutschnig et al., 2010; Liu et al., 2012) which was also confirmed through the evaluation of chitin-binding properties of the ectodomain and chimeric receptors consisting of combinations of ecto/cytosolic domains of AtCERK1 and OsCERK1 (Shinya et al., 2012). Similar to the molecular binding of chitin by OsCEBiP, AtCERK1 homodimerizes upon binding to a chitin oligomer consisting of eight GlcNAc residues, in which four GlcNAC moieties bind to each AtCERK1 at the LysM2 domain which harbors a binding site (Liu et al., 2012). The intracellular serine/threonine kinase domain of AtCERK1 has protein kinase activity, and functional characterization using the kinase dead variant proved that the kinase

activity is necessary for its chitin-dependent phosphorylation *in vivo* (Petutschnig et al., 2010).

In addition to AtCERK1, two LysM-RLKs, AtLYK4 and AtLYK5, are required for proper chitin-induced signaling in *A. thaliana*. Petutschnig et al. (2010) performed a proteomics approach and identified AtLYK4 and AtLYK5 as chitin binding proteins. AtLYK4 and AtLYK5 are also plasma membrane-localized proteins. However unlike AtCERK1, these two LysM-RLKs lack kinase subdomains necessary for enzymatic activity (Wan et al., 2012; Cao et al., 2014). The importance of AtLYK4 in chitin signaling was proven by generating *Atlyk4* mutants that showed reduction of both chitin-triggered gene expression (*WRKY53, MPK3, ZAT12*) and cytosolic calcium elevation as well as increased susceptibility to *Pseudomonas syringae* pv tomato DC3000 and *Alternaria brassicicola* (Wan et al., 2012). The role of AtLYK5 in chitin perception is still under debate. Analyses of a Ler *Atlyk5* mutant (*Atlyk5*-1 or CSHL_GT7089) showed that loss-of-function mutations of *AtLYK5* have no significant effect on the expression of chitin-induced genes (Wan et al., 2012). However, Cao et al. (2014) reported that AtLYK5 is the major chitin receptor and essential for the chitin-induced responses in *A. thaliana* based on the analyses of a Col-0 *Atlyk5* mutant (*Atlyk5*-2 or SALK_131911C). The *Atlyk5*-2 mutant has reduced chitin-triggered ROS production, MAPK activation, calcium influx, as well as expression of chitin responsive genes (*AtWRKY29*, *AtWRKY30*, *AtWRKY33*, and *AtWRKY53*). However, Gubaeva et al. (2018) claimed that the observed defects in chitin-induced responses of the *Atlyk5*-2 mutant could not be reproduced by their group and others. Therefore, Desaki et al. (2018) suggests the need of further investigations on the chitin receptor model with regard to the role of AtLYK5.

Atlyk4-1 *Atlyk5*-2 double knock-out mutants are insensitive to chitin, with respect to chitin induced MAPK activation and ROS burst. AtLYK5 was shown to associate with AtCERK1 after chitin treatment and this interaction is essential for chitin-induced AtCERK1 homodimerization and phosphorylation (Cao et al., 2014). Erwig et al. (2017) expressed the intracellular domains (IDs) of AtLYK4, AtLYK5 and AtCERK1 as well as the enzymatic loss-of-function version of AtCERK1 (AtCERK1-LOF) in *E. coli* and performed *in vitro* kinase assays, which revealed that only AtCERK1-ID showed autophosphorylation and that AtLYK4-ID and AtLYK5-ID are direct phosphorylation targets of AtCERK1-ID *in vitro*. They also examined the importance of AtCERK1 kinase activity for AtLYK5 phosphorylation *in planta* by expressing AtLYK5 together with AtCERK1 or with AtCERK1-LOF in the *Atcerk1*-2 background. Western blots of plants expressing both

AtLYK5 and AtCERK1 showed a protein mobility shift of AtLYK5 as well as AtCERK1 after chitin treatment, indicating phosphorylation. In contrast, no mobility shift was observed in the western blots of plant expressing AtLYK5 together with AtCERK1-LOF. Taken together, their data suggest that the interaction of AtCERK1 with AtLYK5 and AtLYK4 is required for effective chitin signaling. In addition, AtLYK5 showed AtCERK1-dependent endocytosis after chitin treatment while AtCERK1 stays in the plasma membrane, indicating that the interacting proteins might dissociate after chitin perception. The necessity of AtCERK1 kinase activity in AtLYK5 endocytosis was examined by expressing *AtLYK5_mCitrine* in the *AtCERK1*- and *AtCERK1-LOF*-expressing plants, showing that no endocytosis of AtLYK5_mCitrine in the AtCERK1-LOF background occured. AtLYK5-containing endosomes may not contain active chitin receptor complexes required for initiating signal transduction since AtLYK5 harbors an inactive kinase (Erwig et al., 2017).

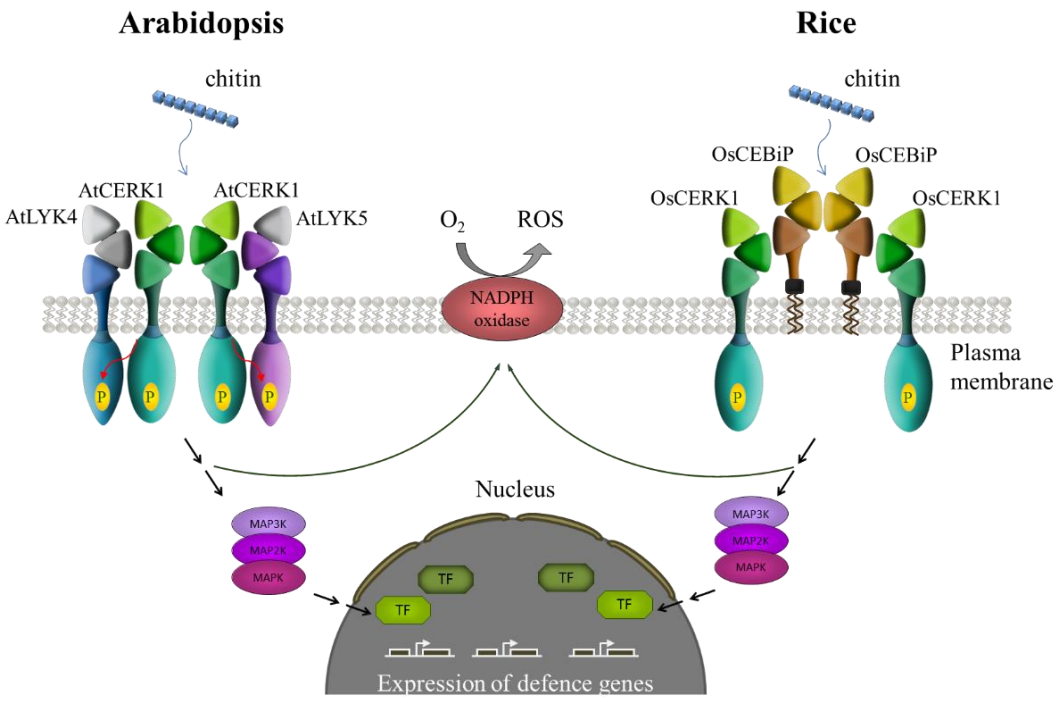

Figure 2.4. Current model of chitin perception in Arabidopsis (A) and rice (B). (A) Chitin perception and signaling in Arabidopsis are mediated by AtCERK1 and two additional LysM-RLKs, AtLYK4 and AtLYK5. The perception of chitin leads to AtCERK1 homodimerization and autophosphorylation, which recruits and phosphorylates AtLYK4 and AtLYK5, leading to chitin-induced defense responses such as ROS production, MAPK activation and expression of chitin-responsive genes. In rice, chitin recognition is mediated by CEBiP, which associates with CERK1 to initiate chitin-induced signaling. Image by Elena Petutschnig and Mascha Muhr based on updated information from current publications of Arabidopsis (Miya et al., 2007; Wan et al., 2008; Petutschnig et al., 2010; Liu et al., 2012; Wan et al., 2012; Cao et al., 2014; Erwig et al., 2017) and of rice (Shimizu et al., 2010; Hayafune et al., 2014; Liu et al., 2016).

The above descriptions indicate the presence of different chitin receptor systems in plants as it was emphasized by Shinya et al. (2012) and shown in **Figure 2.4**. In rice, the major component of the chitin receptor complex is LysM-RLP (OsCEBiP), which requires association with LysM-RLK (OsCERK1) for chitin perception and signal transduction (Kouzai et al., 2014). In Arabidopsis, the components of the chitin receptor complex are LysM-RLKs, with AtCERK1 as the main receptor that interacts with AtLYK4 and AtLYK5 for chitin recognition and a proper signal transduction (Cao et al., 2014; Erwig et al., 2017). Shinya et al. (2012) analysed a putative association of AtCERK1 with LysM-RLPs by characterizing the OsCEBiP homologs AtLYM1, AtLYM2 and AtLYM3 in Arabidopsis. Only AtLYM2 showed a high chitin-binding affinity similar to OsCEBiP. However, knocking-out or overexpressing LYM2 did not affect the primary chitin-induced defense response, e.g. chitin induced MAPK activation and ROS burst, indicating that AtLYM2 is functional in chitin-binding but does not contribute to the primary chitin signaling. Faulkner et al. (2013) reported that AtLYM2 plays a role in a chitin-responsive signaling pathway independent from that of AtCERK1. AtLYM2 is a plasma membrane-localized protein with plasmodesmata association that was shown to mediate reduction of chitin-triggered plasmodesmal flux in a CERK1-independent manner.

2.2.3 LysM-RLKs/RLPs in Nod Factor and Myc Factor Perception

Besides binding to long chitin oligomers (heptamer-octamer) to initiate plant defense signaling, some LysM-RLKs such as OsCERK1 binds shorter chitin oligomers that consists of only four to five GlcNAc residues, leading to the activation of symbiotic signaling (Zhang et al., 2015). The establishment of symbiosis signaling relies on the recognition of Nod-factors (Nfs) or Myc factors (Myc-LCOs) produced by rhizobial bacteria or mycorrhizal fungi, repectively. Nfs are linear β-1,4-linked N-acetylglucosamine (GlcNAc) oligosaccharides consising of usually four to five GlcNAc residues (Mulder et al., 2006), and function as signaling molecules for the establishment of *rhizobium-legume* symbiosis (Liang et al., 2013). Nfs are produced by rhizobia when they sense chemical signals, usually flavones, released by the roots of host plants (Madsen et al., 2003). The characteristics of Nfs are strain-specific comprising different numbers of sugar residues, and different chemical composition and structure of the acyl chain, which varies and determines their host specificity (Mulder et al., 2006; Geurts and Bisseling, 2002).

In *Lotus japonicus*, the perception of Nfs is mediated by the LysM-RLKs NOD FACTOR RECEPTOR 1 (NFR1) and NFR5 (Madsen et al., 2003; Radutoiu et al., 2003; Broghammer et al., 2012), which recognize Nfs through the LysM domains (Radutoiu et al., 2007) and act upstream of SYMBIOSIS RECEPTOR KINASE (SYMRK), a gene required for rhizobial and mycorrhizal invasion in legumes (Radutoiu et al., 2003). In *Medicago truncatula*, the establishment of symbiosis is mediated by the homolog of LjNFR1, LYK3 (Smit et al., 2007; Limpens et al., 2003), and the homolog of LjNFR5, NOD FACTOR PERCEPTION (NFP) (Arrighi et al., 2006). MtNFP likely mediates the early Nf perception and initial Nf responses, and requires association with an active kinase for signal transduction due to the inactive kinase (Mulder et al., 2006; Rey et al., 2013; Arrighi et al., 2006). Functional analyses on HAIR CURLING (HCL), a gene that encodes MtLYK3, revealed that MtLYK3 recognizes structure-specific Nfs and functions at the later stage of the rhizobial infection thread formation (Smit et al., 2007). The perception of Nod factors in non-legume plants such as Arabidopsis is mediated by AtLYK3, which was found to suppress PTI (Liang et al., 2013).

Myc factors are also lipochitooligosaccharides (LCOs) similar to NFs, produced by mycorrhizal fungi and serve as signaling molecules for symbiosis (Maillet et al., 2011). The genes involved in Nfs or Myc factors perception were hypothesized to originate from the same ancestor, which underwent duplication followed by neofunctionalization to facilitate the establishment of rhizobial or mycorrhizal symbiosis (Buendia et al., 2016). An example is the homolog of *MtNFP* in *Parasponia andersoni*, *PaNFP*, which is involved in both rhizobial and mycorrhizal symbiosis (Den Camp et al., 2011). Whereas the homolog in *Solanum lycopersicum*, *SILYK10*, only regulates mycorrhization (Buendia et al., 2016). OsCERK1 is highly homologous to *LjNFR1*/*MtLYK3*, and was reported to have dual functions, being involved not only in immune signaling against fungal pathogen but also in symbiosis with mycorrhizal fungi (Zhang et al., 2015). OsNFR5, the homolog of LjNFR5/MtNFP, was characterized as a potential co-receptor of OsCERK1 in mediating this symbiotic signaling. However, OsNFR5 does not heterodimerize with OsCERK1 (Miyata et al., 2016). Analysis of a chimeric receptor containing the extracellular domain of *LjNFR5* and the intracellular domain of *OsNFR5* showed that the kinase domain of *OsNFR5* has capability to initiate symbiotic signaling in *L. japonicus* by complementing the *Ljnfr5* mutant for rhizobial symbiosis, suggesting a possible role of OsNFR5 in mycorrhization. However, the *Osnfr5* mutants showed a wildtype-like colonization by mycorrhizal fungi (Miyata et al., 2016).

2.2.4 LysM-RLKs/RLPs in Peptidoglycan (PGN) Perception

In Arabidopsis, AtCERK1 was reported to take also part in peptidoglycan (PGN) perception and downstream signaling pathways together with AtLYM1 and AtLYM3 (Willmann et al., 2011). PGN is the main component of bacterial cell walls composed of alternating β-1,4-linked N-acetylglucosamine (GlcNAc) and N-acetylmuramic acid (MurNAc) residues (Schleifer and Kandler, 1972). AtLYM1 and AtLYM3 are plasma membrane-localized GPI-anchored LysM-RLPs that directly bind structurally different PGN from both gram positive and negative bacteria (Willmann et al., 2011). The single and double knock-out mutants of these genes are highly susceptible to *Pseudomonas syringae* ptv tomato DC3000 (Willmann et al., 2011). AtLYM1 and AtLYM3 that lack intracellular kinase domains require additional proteins to activate downstream signaling after binding PGN. AtCERK1 is a proper candidate to fullfil this function since it is involved in both PGN sensitivity and immunity to bacterial infection (Willmann et al., 2011). The *Atcerk1-2* mutant is highly susceptible to infection by PtoDC3000 (Gimenez-Ibanez et al., 2009). In rice, OsCERK1 was reported to be involved in both fungal chitin and bacterial PGN signaling pathways by interacting with different LysM proteins (Kouzai et al., 2014; Ao et al., 2014). OsCERK1-disrupted lines have lowered responsiveness to PGN. According to data from Yeast two-hybrid assays, OsCERK1 interacts with LYP4 and LYP6, the AtLYM1 and AtLYM3 homologs in rice, which are responsible for binding PGN (Kouzai et al., 2014). LYP4 and LYP6 were reported to exhibit dual functions in PGN and chitin binding in rice innate immunity (Liu et al., 2012). The involvement of LysM-RLKs/RLPs in different ligand perception is visualized in **Figure 2.5**.

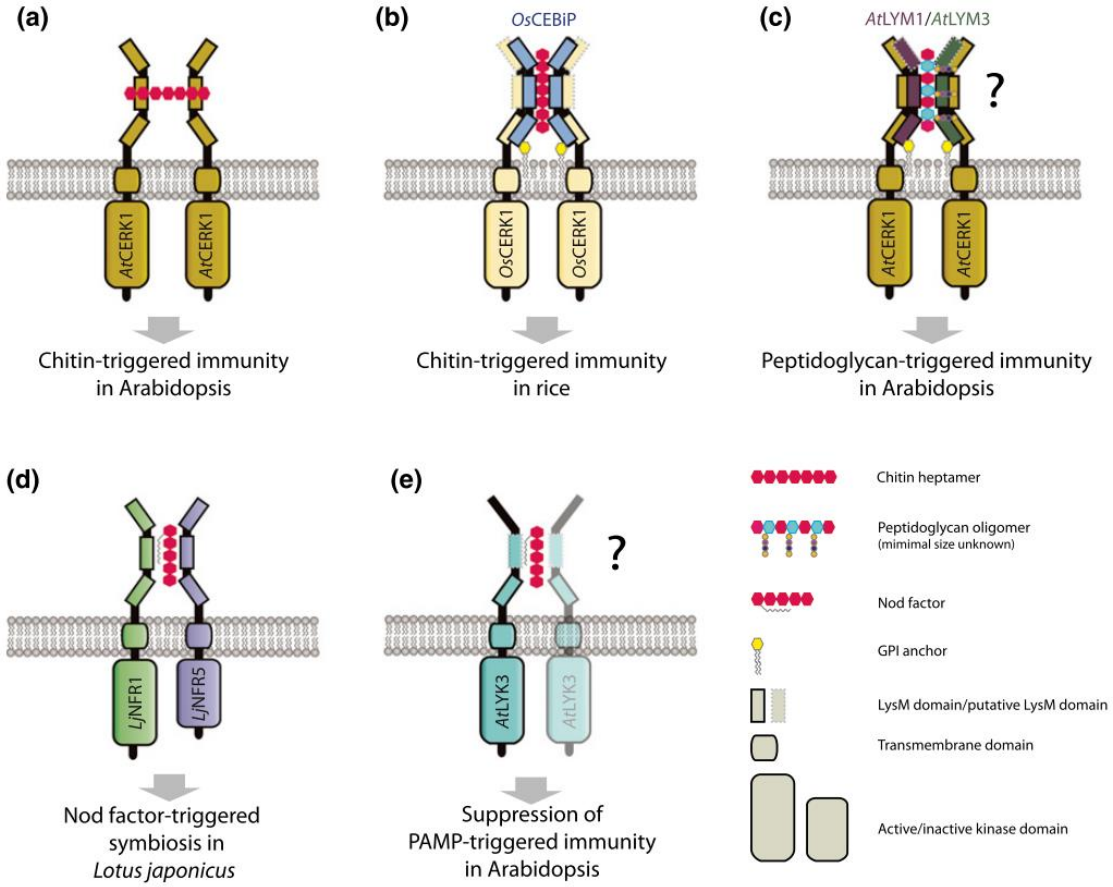

Figure 2.5. Perception of different ligands by LysM-RLKs/RLPs. (a) CERK1 mediates fungal chitin perception in Arabidopsis, leading to chitin-triggered plant responses. (b) In rice, CERK1 associates with a LysM-RLP, CEBiP, to facilitate the recognition of chitin and further initiate chitin responses. (c) In Arabidopsis, the association of CERK1 with LysM-RLPs, AtLYM1/AtLYM3, mediates bacterial peptidoglycan (PGN) perception. (d) In *Lotus japonicus*, Nod-factor recognition is mediated by Nod Factor Receptor 1 (NFR1) that associates with NFR5, leading to symbiosis signaling. (e) In Arabidopsis, the perception of Nod factor by a LysM-RLK, AtLYK3, suppresses PTI. Image from Antolín-Llovera et al. (2014).

2.3 Plasmodesmata

The homolog of rice CEBiP in Arabidopsis, AtLYM2, is responsible for mediating chitin-induced plasmodesmal closure independent of CERK1 (Faulkner et al., 2013). Plasmodesmata (PD) are plasma membrane-lined cytoplasmic channels that establish a supracellular network in plants by connecting the cytoplasm, endoplasmic reticulum (ER) and plasma membrane (PM) of adjacent cells (Burch-Smith and Zambryski, 2012; Sager and Lee, 2014; Faulkner, 2013). PD allow signal transfer for direct cell-cell communication and facilitate the symplastic transport of cellular components that are different in size and chemical composition, such as sugars, proteins and RNAs (Alberts et al., 2014; Sager and Lee, 2018). Based on the basis of their origins, PD are classified into primary and secondary PD. Primary PD are formed during cell division, while secondary PD are produced during

cell wall expansion, in the absence of cytokinesis (Ehlers and Kollmann, 2001). Both primary and secondary PD initially have simple morphology with a single channel (Burch-Smith et al., 2011; Faulkner et al., 2008; Roberts and Oparka, 2003), however, during plant growth and development they will undergo several steps of structural modifications and turn into a complex-branched primary PD (Ehlers and Kollmann, 2001).

2.3.1 Structure and Molecular Component of Plasmodesmata

A plasmodesmos (in plural plasmodesmata) is composed of a desmotubule, which is a fine tubular structure of compressed ER that traverses across the cell walls of adjacent cells (Alberts et al., 2014). This cylindrical structure spans the cell walls but allows the continuity of the plasma membrane of neighboring cells, thus establishing a cytoplasmic channel (referred to as *cytoplasmic sleeve*) between the continuous PM and the desmotubule (Sager and Lee, 2018) (**Figure 2.6**). Trafficking from cell to cell occurs through this cytoplasmic sleeve (Sager and Lee, 2018). Alternatively, trafficking can also happen via the desmotubule lumen (Cantrill et al., 1999) and along the desmotubule lipid bilayer-membrane (Guenoune-Gelbart et al., 2008). However, the evidence supporting these alternative transport routes is limited and remains an open question since the ER that runs through the pore of PD is constricted (Oparka et al., 1999). The constriction of the desmotubule is assumed to be modulated by unknown proteins that tightly compress the ER. However, certain PD show a desmotubule with an open lumen (Ehlers and Kollmann, 2001) which might explain the observation of alternative transport routes via the desmotubule lumen.

Actin and myosin, are localized and possibly helically arranged in a spoke-like structure along the pore, connecting the continuous plasma membrane and the desmotubule (White et al., 1994; Blackman and Overall, 1998). These cytoskeletal elements may be involved in controlling PD aperture through contractile mechanism that allows constriction and relaxation of the pore (Overall and Blackman, 1996; Zambryski and Crawford, 2000).

The continuous PM along the cytoplasmic sleeve of PD is called plasmodesmal-PM (PD-PM) (**Figure 2.6**). Despite the fact that PD-PM is a continuity of PM between neighboring cells, molecular composition of both membranes is highly different (Bayer et al., 2014; Grison et al., 2015; Sager and Lee, 2018). Similar to the PM, PD-PM is also divided into microdomain (Bayer et al., 2014), which is a specialized membrane compartment with different molecular composition, structure and biological function (Malinsky et al., 2013). Some proteins concentrate at PD-PM but some are excluded such as the PM proton pump ATPase (PMA2), aquaporin PIP2 and cellulose synthase subunit CesA3

(Grison et al., 2015). Immunolocalization, genetic and biochemical studies have been performed to elucidate residents of PD-PM which revealed the presence of proteins with various functions (Han et al., 2019). Han et al. (2019) classified proteins that are found in PD into: PD-associated structural proteins that include actin, myosin and tubulin; and PD-associated regulatory proteins that are mostly callose-related, either for synthesis, degradation or maintaining callose stability.

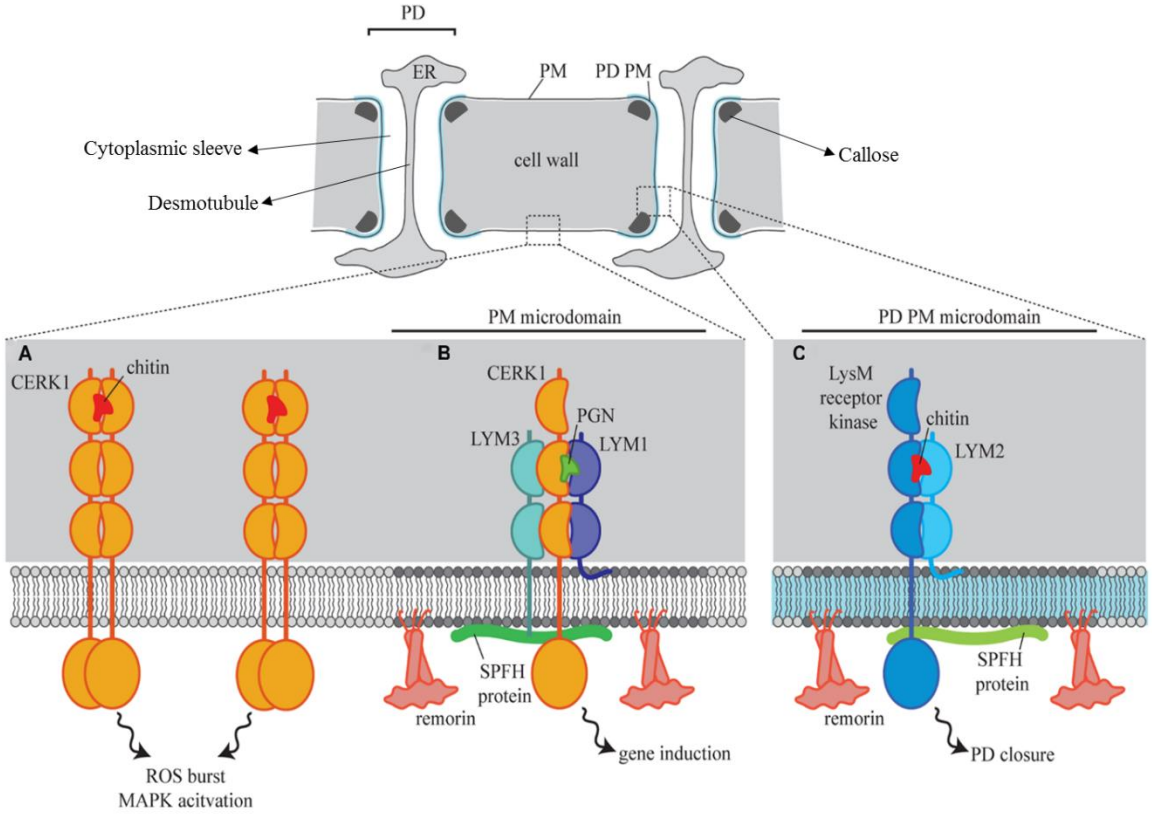

Figure 2.6. Schematic model of plasmodesmata including the molecular components of plasmodesmal-plasma membrane (PD-PM). The plasmodesmos contains a desmotubule, which is an ER continuity that lays across the cell walls thus forming a cytoplasmic sleeve between the desmotubule and the PD-PM. PD-PM is the continuous plasma membrane that is exposed to the cytoplasmic sleeve. The size of the cytoplasmic sleeve is highly affected by callose accumulation at the neck region of the plasmodesmata. The molecular components of PD-PM also differ from the PM. In the PM microdomain, surface-localized receptors perceive either fungal or bacterial PAMPs (chitin or PGN), leading to the induction of defense response (A and B). Meanwhile in the PD-PM microdomain, the perception of chitin by LYM2 in association with another unknown LysM-RLK was reported to mediate PD closure. Remorin and stomatin/prohibitin/flotillin/HflK/C (SPFH) are proteins at the lipid rafts of PD-PM. Modified schematic picture from Faulkner (2013).

PD-PM is also partitioned into lipid rafts, specialized plasma membrane nanodomains that are enriched in sterols and sphingolipids (Mongrand et al., 2010; Malinsky et al., 2013). The enrichment of lipid rafts at PD was suggested to be essential for modulating PD-PM flexibility, which in turn contributes to the plasticity of PD opening and closure (Iswanto and Kim, 2017; Sun et al., 2019). Remorin, a lipid nanodomain-binding protein

was reported to regulate viral movement through PD by establishing specialized subcompartmentalization of PD-PM and interacting with viral MPs to prevent them from increasing PD aperture (Gronnier et al., 2017; Raffaele et al., 2009). Some Glycosylphosphatidylinositol (GPI)-anchored proteins show preferential association with lipid rafts-associated compounds. As an example is PD localization of PDCB1, a protein important for callose deposition, is sterol dependent (Grison et al., 2015). AtBG_ppap, a protein involved in callose degradation, is another GPI-anchored protein that localizes at the PD-PM (Zavaliev et al., 2016). *Arabidopsis thaliana* plasmodesmata-located proteins (PDLPs) are another group of proteins that reside at the PD-PM, which do not contain GPI anchors. There are at least eight members of the PDLP family in *A. thaliana*, which contain two domains of unknown function26 (DUF26) at the N-terminus followed by a transmembrane domain and a short cytoplasmic tail at the C-terminus (Thomas et al., 2008). PDLP1 and PDLP5 were suggested to be important for systemic acquired resistance (SAR), and PDLP5 in particular is required for symplastic signal transport through PD by controlling PD callose accumulation in response to salicylic acid (SA) (Lim et al., 2016). *Arabidopsis thaliana* PDLP5 was also reported to mediate crosstalk between PD regulation and salicylic acid-dependent defense response (Lee et al., 2011).

2.3.2 Permeability of Plasmodesmata

The size of the plasmodesmal cytoplasmic sleeve is dynamically controlled and fine-tuned in response to endogenous factors or to environmental conditions, thus determining the size of the PD aperture. Control of PD pore size occurs spatially and temporally (Han et al., 2019). Moreover, PD gating is classified into several states: closed and open states, dilated state when a large molecule of more than 1 kDa can pass-through. The size exclusion limit (SEL) is the upper size limit of a molecule usually around 30-50 kDa that can pass through PD (Sevilem et al., 2013). The rate of cellular transport is greatly affected by plasmodesmal permeability in a callose-dependent or callose-independent manner (Zavaliev et al., 2011; Tilsner et al., 2016). Callose is a β-1,3-glucan cell wall polymer with β-1,6-ramifications/branches (Chen and Kim, 2009; Ellinger and Voigt, 2014) that is synthesized at the plasma membrane and deposited at the cell plates during cytokinesis, but it is removed from the new cell walls once the division process is completed. However, some portions of callose remain in the cell walls near by the plasmodesmata (Sager and Lee, 2018). Callose is involved in many plant processes including sieve pore regulation, pollen development, differentiation of vascular tissue, cell plate formation during cytokinesis, in response to

abiotic and biotic stress (Wu et al., 2018). Callose deposition at the neck and along the length of the plasmodesmal channel regulates plasmodesmal gating (Sager and Lee, 2018; Wu et al., 2018). Despite the fact that callose is a permanent structural PD component and naturally resides around PD in normal condition, the level of callose deposition is variable and fluctuating over the plant life cycle. Increase in callose level reduces the rate of molecular trafficking between neighboring cells (Sager and Lee, 2018) and *vice versa* (Wu et al., 2018). Balancing callose levels at PD is maintained through a mechanism called PD callose homeostasis (Wu et al., 2018).

Callose homeostasis highly depends on the ratio of synthesis and degradation that are regulated by two groups of antagonistic enzymes: β-1,3-glucan synthase and β-1,3-glucanase, respectively. There are 12 genes encoding β-1,3-glucan synthase referred to as callose synthase (CalS) also known as glucan synthase-like (GSL) (Verma and Hong, 2001) and some of them are well-characterized in *A. thaliana* such as *CalS1*/*GSL6* (Cui and Lee, 2016), *CalS3*/*GSL12* (Vatén et al., 2011), *CalS7* (Xie et al., 2011), *CalS8*/*GSL4* (Cui and Lee, 2016), *CalS10*/*GSL8*/*CHORUS* (Guseman et al., 2010; Cui and Lee, 2016) and *CalS12/GSL5* (Shi et al., 2014; Ellinger and Voigt, 2014). The level of callose accumulation is not only determined by the rate of its synthesis but also by the stability and location where callose is deposited. The aforementioned, GPI anchored, plasmodesmata callose-binding proteins (PDCBs) are regulators of callose deposition. PDCBs do not have catalytic activity, but they bind callose through carbohydrate-binding module 43 (CBM43). PDCBs overexpression results in an increased callose deposition and leads to reduction of SEL (Simpson et al., 2009). Due to the fact that PDCBs lack enzymatic activity, it is suggested that PDCBs stabilize callose deposition at the neck region of plasmodesmata, which is responsible for the regulation of PD permeability by altering the size of SEL (Roberts and Oparka, 2003; Levy et al., 2007; Guseman et al., 2010; Vatén et al., 2011; Liesche et al., 2019).

β-1,3-glucanases (BGs) or callose hydrolases that function in callose degradation catalyze the cleavage of 1,3-β-D-glucosidic linkages into single β-1,3- glucan units (Wu et al., 2018). In *A. thaliana*, BGs are encoded by around 50 genes containing a glucosyl hydrolase 17 family domain (Sager and Lee, 2014; Zavaliev et al., 2011), AtBG_ppap (Levy et al., 2007) and plasmodesmata β-1,3-glucanases (*PDBG*s) (Benitez-Alfonso et al., 2013) are some of the examples of the active BGs. Some BGs contain one or two repeats of CBM43 (Doxey et al., 2007) to bind callose in a way similar to PDCBs callose-binding mechanism. Callose accumulation is also influenced by abiotic stress. Abiotic stress such as wounding,

chilling, light and heavy metals can induce altered callose accumulation (Cui and Lee, 2016; Xie et al., 2011; Sivaguru et al., 2000; Rinne et al., 2001).

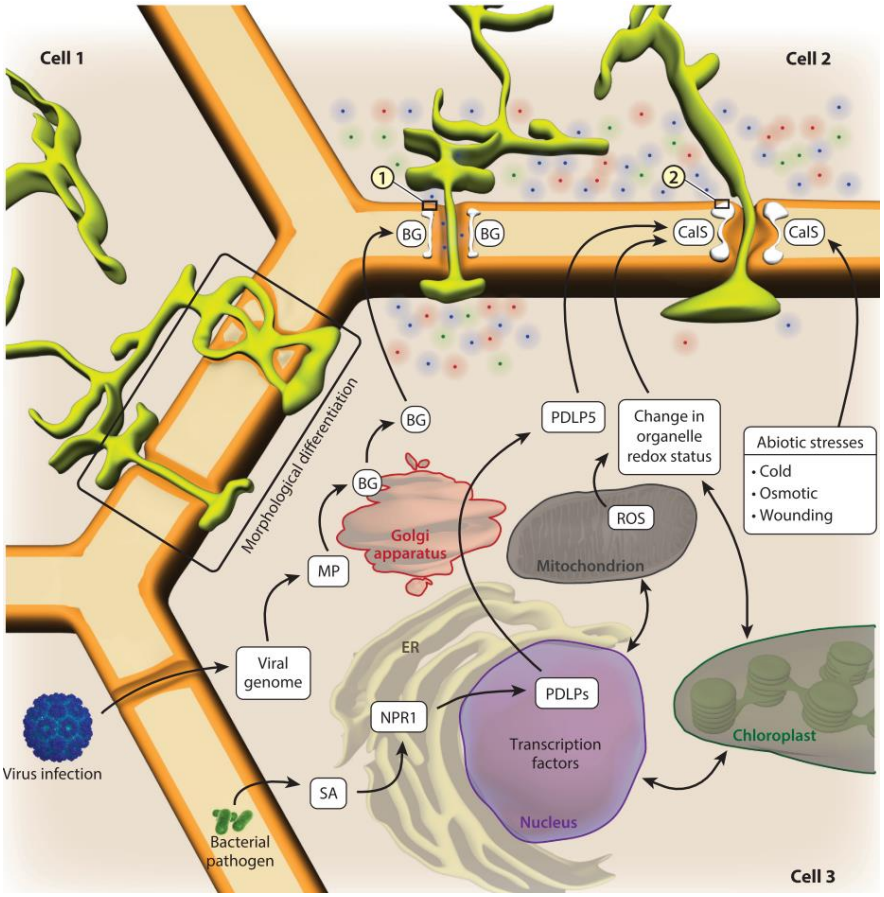

Figure 2.7. PD permeability is regulated by several factors, which affect callose homeostasis. Callose homeostasis is regulated by the activity of antagonistic enzymes: β-1,3-glucan synthase (CalS) and β-1,3-glucanase (BG), respectively. Beside abiotic stresses, pathogen infection also influences the activity of CalS and BG and, as a consequence PD are closed or opened. ER = endoplasmic reticulum, PDLP5 = PD-Located protein 5, SA = salicylic acid, NPR1 = NONEXPRESSOR OF PATHOGENESIS-RELATED GENE 1, ROS = reactive oxygen species. Image from Tilsner et al. (2016).

During callose-independent regulation of PD permeability, PD aperture is thought to be changed by several other factors including globular and spoke-like particles along the cytoplasmic sleeve that were identified as actin and myosin filaments. These cytoskeletons might affect PD gating by linking the desmotubule and the plasmodesmal-PM, thus regulating the contraction and relaxation of the cytoplasmic sleeve (Burch-Smith and Zambryski, 2012). Tilsner et al. (2016) also reported an effect of actin filament disruption on the cellular trafficking including the transport of viral movement proteins (MPs). Changes in PD permeability also depend on the architecture and the density of plasmodesmata, which are variable during plant development (Sager and Lee, 2018). The frequency of plasmodesmata is another factor influencing PD permeability. Even though the densities of primary PD in new division walls are evenly distributed (Faulkner et al., 2008), the number

of PD can change, decrease or increase, during cell development and differentiation, and can be also altered temporarily or permanently in mature plant tissues (Roberts and Oparka, 2003). Fuchs et al. (2010) observed massive increases in PD number of perennial plants in spring, which is necessary for cambial reactivation and the high amount is maintained during summer, and decreases during late summer until dormancy is reached in autumn.

2.3.3 Plasmodesmata in Plant Immunity

Plasmodesmata provide a conduit for both elicitors and the induced defense-related molecules. Movement proteins (MPs) from viral pathogens for instance, spread from cell to cell through PD channel (Guenoune-Gelbart et al., 2008; Dobnik et al., 2013; Yuan and Lazarowitz, 2016; Yuan et al., 2018; Epel, 2009). Diffusion gradients are established between the infected and non-infected adjacent cells, and MPs were suggested to facilitate mobilization of bound viral RNA (vRNA) through diffusion along the cytoplasmic sleeve (Epel, 2009). Dobnik et al. (2013) reported that the spreading of potato virus PVY^{NTN} is promoted by the activity of β-1,3-glucanase class III, a class of glucanases that is involved in callose degradation. Tobacco mosaic virus (TMV) spreads by lateral diffusion through the desmotubule facilitated by TMV replicase and MPs. MPs are recognized by synaptotagmin A (SYTA), a protein required to form ER-plasma membrane contact sites in plants, which interacts with the PD localization signal (PLS) of MPs (Guenoune-Gelbart et al., 2008; Yuan and Lazarowitz, 2016; Yuan et al., 2018). Even though PD functions as a conduit for viral spreading, this symplastic channel also facilitates systemic antiviral RNA silencing as a defense mechanism of plants against viral infection (Vogler et al., 2008).

Callose that is deposited around PD was suggested to act as a barrier to restrict or even stop the invading pathogens that grow intracellularly (Ellinger and Voigt, 2014). Callose synthases or callose glucanases act as gate-keepers for PD-mediated cell-cell communication. Viral MPs were also suggested to be involved in activating and directing virus-induced β-1,3-glucanases (BGs), which results in PD-callose degradation (Epel, 2009), leading to PD opening as a conduit for viral movement (**Figure 2.7**). However, the increase of BG expression could be also a defense mechanism of plants instead of a viral strategy to open PD. Another example for the role of PD in plant immunity is the induction of *PDLP5*-mediated callose deposition after bacterial infections (Lee et al., 2011). The bacterial PAMP flg22 was shown to induce the upregulation of a plasmodesmal-localized Ca^{2+}-binding protein CALMODULIN LIKE41 (CML41), which leads to callose deposition and, as a consequence, PD closure (Xu et al., 2017). This *CML41*-mediated pathway was suggested

to be independent from other flg22-triggered responses (ROS burst, MAPK activation). *CML41*-mediated Ca^{2+}-signaling specificity is required for plant resistance against *Pseudomonas syringae*.

Also, the perception of other PAMPs leads to the alteration of PD aperture (Faulkner et al., 2013). Cheval and Faulkner (2018) suggested that PD closure is a key mechanism of PTI and facilitates systemic defense signaling. Fungal chitin was shown to promote PD closure in a LYM2-dependent manner in *Arabidopsis thaliana* (Faulkner et al., 2013). AtLYM2 is a GPI-anchored protein that was suggested to associate with a LysM-RLK in order to induce PD-related downstream signaling (Cheval and Faulkner, 2018). Cheval et al. (2019) further suggested that the interaction partner of AtLYM2 in mediating chitin-triggered PD closure is LYK4, a LysM-RLK that harbors an inactive kinase domain. They analysed PD flux by performing microprojectile bombardment assays on *Atlyk4* and *Atlyk5-2* mutants, showing that there is no change in GFP spreading from the transformed to the neighboring cells of both mutants after chitin treatment. These results indicate that AtLYK4 and AtLYK5 are necessary for chitin-triggered PD closure. To check whether both proteins are present in PD, they conducted protein extraction of PD fractions and found that only AtLYK4 is present in these fractions. Association between AtLYK4 and AtLYM2 was observed by conducting co-immunoprecipitation (Co-IP) assays, which revealed that AtLYM2 associates with AtLYK4 in a chitin-dependent manner. To analyse the involvement of AtLYK5 in this chitin-triggered response, Cheval et al. (2019) characterized the association of AtLYK4 and AtLYK5 at the PM. They hypothesized that AtLYK5 is important for AtLYK4 function upstream of PD signaling. In their model, Cheval et al. (2019) proposed that the perception of chitin promotes changes in LYM2 and LYK4 localization and affects the interaction of the partners. In the absence of chitin, LYM2 localizes at the PM and PD-PM, while LYK4 resides at the PM and associates with LYK5. Upon chitin treatment, PM-localized LYM2 accumulates at PD and further interacts with LYK4 that also moves to PD after chitin-induced dissociation from the LYK4-LYK5 complex. The AtLYK2-AtLYK4 complex was suggested to recruit CALCIUM DEPENDENT PROTEIN KINASE 6 (CPK6), a protein involved in the phosphorylation of RBOHD, which activates this enzyme and triggers ROS production (Kadota et al., 2014).

Production of reactive oxygen species (ROS) is an early plant response to pathogen infection regulating PD connectivity. The application of exogenous ROS decreases PD permeability in a salicylic acid (SA)- and *PDLP5*-independent manner (Cui and Lee, 2016). *PDLP5* was previously shown to mediate cross-talk between PD regulation and SA-

dependent defense response (Lee et al., 2011). Overexpressing *PDLP5* gene induces spontaneous cell death and clorosis, which was suggested to be due to the hyperaccumulation of SA, since SA content in plants overexpressing *PDLP5* was 15-fold higher than the control plant. Moreover, introducing NahG, an SA-degrading bacterial salicylate hydroylase (Friedrich et al., 1995), suppresses the PDLP5-induced cell death (Lee et al., 2011).

2.4 Poplar as a Model System

Analysis of physiological and developmental processes in the herbaceous annual eudicot model plant, *Arabidopsis thaliana,* is not sufficient to get a comprehensive picture of the biology of perennial tree species. There are many tree-specific traits that cannot be investigated in *A. thaliana* such as wood formation, perennial growth, seasonality and interaction with other organisms like beneficial and pathogenic microbes during long life spans (Jansson and Douglas, 2007; Duplessis et al., 2009). Therefore, a perennial plant model that allows studies of these exclusive traits is necessary for tree research. Poplar (*Populus spp.*) was proposed as a model system for studying woody plant species (Bradshaw et al., 2000) due to several reasons. *Populus trichocarpa* Nisqually was the first tree to be sequenced. Poplar has a relatively small genome size of around 500 million bases, which is 4 times larger than Arabidopsis' but 50 times smaller than Pine's (Tuskan et al., 2006). Poplar shows rapid growth: the seeds germinate within 24h and the plantlets can grow up to 1-2 m in the first year of cultivation (Bradshaw et al., 2000). Poplar also has a high capacity for *in vitro* regeneration, which is a prerequisite for its genetic transformation (Han et al., 2013; García-Angulo et al., 2018). The genetic transformation of poplar can be done either through *Agrobacterium*-mediated stable transformation (Song et al., 2006; Movahedi et al., 2014; Li et al., 2015; Li et al., 2017) or *Agrobacterium*-mediated transient gene expression (Takata and Eriksson, 2014). The transgenic traits of stably-transformed plants have long-term stability (Fladung et al., 2013), which is important for the studies on transgenic perennial plants.

Tuskan et al. (2006) reported that the *Populus* genome contains more gene copies compared to the genome of *Arabidopsis*. For each homolog in *Arabidopsis*, there are at least 1.4 to 1.6 putative genes in poplar. The poplar genome also includes some exceptional genes associated with tree-specific traits such as lignocellulosic wall biosynthesis, meristem development, disease resistance and metabolite transport. Despite the conservation of basic cellular signaling pathways in plants, a single model organism like *Arabidopsis* cannot reflect those aspects of gene function that are exclusive to certain groups of plants.

CONSTANS (CO)/FLOWERING LOCUS T (FT) regulatory module, for instance, that functions in the photoperiod-dependent induction of flowering in the plant model *A. thaliana*, is also involved in bud set modulation during late season in poplar (Koornneef et al., 1998; Böhlenius et al., 2006).

Poplar has also widespread use such as in the pulp and paper industry, as well as for lowland reforestation (Movahedi et al., 2014), phytoremediation of contaminated soil (Song et al., 2007; Guerra et al., 2011; Castro-Rodríguez et al., 2016), large-scale carbon sequestration (Jansson et al., 2010) and as a bioenergy resource (Pereira et al., 2016; Manevski et al. 2019). Poplar is a fast growing tree that is cultivated on short-rotation coppices (SRCs) and was observed to use water more efficiently than willow based on the development and evaluation of SRCs (Tallis et al., 2013). These particular characteristics of poplar make it a promising feedstock for bioenergy resources to establish an environmentally and commercially viable alternative to avoid the negative effects of fossil fuels (Littlewood et al., 2014). Besides fuels for transportation, electricity and biogas are also produced through biomass conversion (Sannigrahi et al., 2009; Guo et al., 2015; Wang et al., 2014; Aghaalikhani et al., 2017). Since the productivity of biomass-bioenergy conversion highly depends on the availability of the biomass itself, external factors influencing the growth of bioenergy crops need to be controlled. One major biotic stressor affecting poplar biomass are rust diseases caused by biotrophic fungal pathogens. Understanding the reasons for poplar susceptibility to rust fungi is a key for improvement of poplar resistance.

2.5 Poplar-Melampsora as a Plant-Pathosystem

The availability of genomic information of the woody plant model *Populus* and *Melampsora larici-populina* (strain 98AG31), one of the major fungal leaf pathogens causing rust disease on *Populus*, is the basis for characterization of molecular components involved in pathogenicity, susceptibility and resistance (Duplessis et al., 2009). *Populus-Melampsora* interaction occurs in an incompatible or a compatible manner depending on the virulence carried by the fungal strain and the corresponding resistance in *Populus*. Incompatible interaction is caused by avirulent *Melampsora* strains that activate defense responses and fail to infect and colonize plant tissues. On the contrary, during a compatible interaction a virulent strain successfully colonizes and cause disease in plants (Hacquard et al., 2011). Infection by *Melampsora spp*. can cause severe damages resulting in decreased photosynthesis, early defoliation and increased susceptibility to other pathogens such as

Venturia spp. and *Septoria spp.*, which may finally lead to the death of plants (Duplessis et al., 2009).

Studies have been carried out to identify key genetic regulators that mediate molecular cross-talk between *Populus* and *Melampsora*. Plant interactions with biotrophic pathogens are determined via specific interactions between pathogen *avr* (avirulence) genes with the corresponding plant disease resistance (R) locus (Dangl and Jones, 2001). Disease-resistance (R) proteins are classified into several classes including intracellular kinases, extracellular receptors, extracellular receptors coupled to kinases, and intracellular receptors. One of the largest classes of R proteins are intracellular receptors that consist of either a coiled-coil (CC) or a Toll/interleukin-1 receptor (TIR) domain followed by nucleotide binding site (NBS) at the N-terminal and a series of leucine rich repeats (LRRs) at the C-terminal end of proteins (Dangl and Jones, 2001). Kohler et al. (2008) performed genome-wide analysis on the *Populus trichocarpa* genome and found genes encoding nucleotide-binding site/ leucine-rich repeat proteins (NBS-LRRs) that are classified into three groups based on their domain organizations: CC-NBS-LRR (119 genes), TIR-NBS-LRR (64 genes), and BED-finger-NBS-LRR (34 genes).

NBS-LRR type R-proteins are involved in the detection of effectors and mediate Effector-Triggered Immunity (ETI). Using available bioinformatic data and selection criteria which typically classify effectors, Petre et al. (2015) identified 20 effector candidates from *Melampsora larici-populina*. One of the candidates, CHLOROPLAST-TARGETED PROTEIN1 (CTP1), accumulated in the chloroplast and mitochondria in *N. benthamiana* transient assays (Petre et al., 2016). This effector carries a predicted transit peptide that mimics the host signal peptide and is necessary for its translocation to the stroma of chloroplast. *In silico* analysis of the signal peptides of all reported *Melampsora larici-populina* effector candidates revealed that 115 proteins, carry chloroplast transit peptides (Petre et al., 2016). These findings suggest that fungi evolved effector proteins that mimic host signal peptides, thus, allowing them to target specific organells.

Despite several researches done on Poplar-*Melampsora* interactions, information on the susceptibility and resistance of poplar to rust fungi is still limited. Most reports focus on the identification of R-proteins and effectors, but nothing is known on how poplar recognizes fungal pathogens. Hamel et al. (2005) reported that chitosan induces ROS-dependent mitogen-activated protein kinase (MAPK) activation in poplar (*Populus trichocarpa* x *Populus deltoides*). However, the perception of this elicitor in poplar has not been further

investigated. Hence, in this research, the mechanisms of fungal pathogen recognition and corresponding defense responses in the perennial tree species poplar will be analysed.

3. Research Objectives

Proteins involved in chitin perception have been well characterized in the plant models *A. thaliana* and *O. sativa*. In both plants, similar components are present but apparently they differ in complex formation and they are involved in different chitin mediated responses. These components include LysM-RLKs and/or LysM-RLPs. In Arabidopsis, the main component of the chitin receptor complex is CERK1, a LysM-RLK that associates with LYK4 and LYK5, two other LysM-RLKs that differ from CERK1 due to an inactive kinase domain. In rice, the homolog of CERK1 acts as a co-receptor of CEBiP, a LysM-RLP that was characterized as the main component of the chitin receptor complex in rice. Chitin perception has not been analysed in perennial plants. The aim of this study is to indentify and characterize the components involved in chitin perception and signaling in the model tree poplar.

3.1 Chapter 1

Three LysM-RLKs are involved in chitin recognition and signaling: CERK1, LYK4 and LYK5. This research focuses on the identification and functional characterization of poplar LYK4 and LYK5 homologs. In detail the objectives are:

1) Identification of candidate genes encoding LYK4 and LYK5 homologs in *P. x canescens*.
2) *In silico* analysis of the domain organization of proteins encoded by LYK4 and LYK5 homologs.
3) Subcellular localization studies of proteins encoded by LYK4 and LYK5 homologs.
4) Functional characterization of proteins encoded by LYK4 and LYK5 homologs.

3.2 Chapter 2

OsCEBiP is a LysM-RLP that has been characterized as the main chitin receptor in rice, which in association with OsCERK1 mediates chitin-induced ROS production and MAPK activation. AtLYM2, the homolog of OsCEBiP in Arabidopsis was also characterized as a chitin-binding protein, but, in contrast to rice, Arabidopsis LYM2 is involved in chitin-induced plasmodesmal closure independent of AtCERK1. This chapter focuses on the identification and functional characterization of LYM2 homologs in poplar with the detailed objectives below:

1) Identification of candidate genes encoding LYM2 homologs in *P. x canescens*.
2) *In silico* analysis of the domain organization of proteins encoded by LYM2 homologs.
3) Subcellular localization studies of proteins encoded by LYM2 homologs.
4) Functional characterization of proteins encoded by LYM2 homologs.

4. Chapter 1 The *Populus* x *canescens* LysM-RLKs PcLYK4 and PcLYK5 are involved in chitin perception and chitin-induced signaling

Mo Awwanah, Elena Petutschnig, Thomas Teichmann, Volker Lipka
Department of Plant Cell Biology, Geor-August Universität Göttingen, Germany

*This manuscript is not published and under preparation for submission.
Author contributions: TT and VL, designed research; MA, performed research; MA and TT, analysed data; MA, TT and EP, wrote the manuscript; TT, EP and VL, supervised and organized funding.
Email for correspondence: tteichm@gwdg.de

4.1 Abstract

CHITIN ELICITOR RECEPTOR KINASE 1 (CERK1) is the main component of the chitin receptor in *Arabidopsis thaliana* (*At*), which associates with LYK4 and LYK5 for a functional receptor complex. AtLYK4 and AtLYK5 are plasma membrane-localized lysin motif receptor-like kinases (LysM-RLKs) that differ from AtCERK1 in the absence of conserved amino acids essential for kinase activity. However, knock-out of both, *AtLYK4* and *AtLYK5*, abolishes the chitin induced ROS burst and MAPK activation of *Arabidopsis*. Four homologs of *LYK4* and two homologs of *LYK5* were found in the hybrid poplar *Populus x canescens* (*Pc*) (*P. tremula x P. alba*). Gene expression analysis showed that all-identified *PcLYK4*/*PcLYK5* genes are expressed in roots, wood, developing xylem, bark and leaves of *P. x canescens*. The coding sequences of two of the *LYK4* and one of the *LYK5* homologs contain internal stop codons. These homologs were classified as pseudogenes. Subcellular localization studies and *in silico* analyses of the domain organization of the remaining candidates (PcLYK4-1, PcLYK4-2 and PcLYK5-2) indicate that PcLYK4/PcLYK5 proteins are plasma membrane-localized LysM-RLKs that have a domain organization similar to AtLYK4/AtLYK5 proteins with three extracellular LysM domains, a transmembrane domain, and an intracellular kinase domain that lacks enzymatic activity. Functional characterization of the *PcLYK4*/*PcLYK5* genes was done by complementation analyses in an *Atlyk4*-1 *Atlyk5*-2 double knock-out mutant. *Atlyk4*-1 *Atlyk5*-2 lines expressing the poplar candidate genes under control of the Arabidopsis *LYK5* promoter were examined for re-constitution of the chitin responses by performing reactive oxygen species (ROS) burst analysis and mitogen-activated protein kinase (MAPK) assays. The results revealed that expression of *PcLYK4/PcLYK5* restores the chitin responses of *Atlyk4*-1 *Atlyk5*-2 with respect to ROS production and MAPK activation, suggesting that PcLYK4/PcLYK5 proteins are functional co-receptors for chitin perception and signaling in poplar. All identified PcLYK4/PcLYK5 proteins also undergo endocytosis after chitin treatment. The dependency of this endocytosis on CERK1 was characterized and confirmed for PcLYK5-2.

Key words: LysM-RLK, inactive kinase, endocytosis, chitin recognition and signaling.

4.2 Introduction

Chitin is a major component of fungal cell walls that is composed of β-1,4-linked N-acetylglucosamine and functions as a pathogen-associated molecular pattern (PAMP) capable of inducing defense signaling in plants (Kaku et al., 2006). N-acetylglucosamine-containing ligands like chitin are recognized by LysM-containing receptors that have been well-characterized in the model plants *Arabidopsis thaliana* (*At*) and *Oryza sativa* (*Os*). However, the chitin receptors in these plants differ (Buist et al., 2008; Antolín-Llovera et al., 2014). In rice, the major chitin binding component of the chitin receptor complex is CHITIN ELICITOR BINDING PROTEIN (CEBiP), a GPI-anchored lysin motif receptor-like protein (LysM-RLP), that associates with the lysin motif receptor-like kinase (LysM-RLK) CHITIN ELICITOR RECEPTOR KINASE 1 (CERK1) for chitin perception and signal transduction (Kaku et al., 2006; Shimizu et al., 2010; Kouzai et al., 2014; Hayafune et al., 2014; Gong et al., 2017). Rice CERK1 cannot bind chitin on its own. In contrast, *A. thaliana* CERK1 exhibits chitin binding capacity without the need for accessory proteins (Miya et al., 2007; Wan et al., 2008; Petutschnig et al., 2010; Shinya et al., 2012; Liu et al., 2012). After ligand binding, AtCERK1 homodimerizes and the kinase domain of AtCERK1 autophosphorylates, which leads to chitin-induced signal transduction (Petutschnig et al., 2010; Shinya et al., 2012). The homodimerization of AtCERK1 is essential for its autophosphorylation and activation (Liu et al., 2012). AtCERK1 loss-of-function mutations abolish chitin-induced responses such as mitogen-activated protein kinase (MAPK) activation, reactive oxygen species (ROS) production and chitin-related defense gene expression. Complementation of an *Atcerk1* mutant with WT AtCERK1 restores these chitin responses, confirming that CERK1 plays an essential role in chitin perception and signaling in *A. thaliana* (Miya et al., 2007; Wan et al., 2008; Petutschnig et al., 2010; Shinya et al., 2012; Liu et al., 2012).

In addition to AtCERK1, chitin perception and signaling in *A. thaliana* involves two other LysM-RLKs, AtLYK4 and AtLYK5, that also have the capability to bind chitin but differ from AtCERK1 due to the absence of an active kinase domain (Wan et al., 2012; Cao et al., 2014; Petutschnig et al., 2010). *Atlyk4* knock-out mutants show a reduction of both chitin-triggered gene expression (*WRKY53, MPK3, ZAT12*) and cytosolic calcium elevation as well as increased susceptibility to *Pseudomonas syringae* pv tomato DC3000 and *Alternaria brassicicola* (Wan et al., 2012). Meanwhile, the role of AtLYK5 in chitin perception is still under debate. Wan et al. (2012) analysed the response of plants carrying mutations in *AtLYK* genes that include a Ler *Atlyk5* mutant (*Atlyk5*-1 or CSHL_GT7089),

showing that loss-of-function mutations of *AtLYK5* have no significant effect on the expression of chitin-induced genes. However, Cao et al. (2014), analysing a Col-0 *Atlyk5* mutant (*Atlyk5*-2 or SALK_131911C), reported that AtLYK5 is the major chitin receptor and essential for the chitin-induced responses in *A. thaliana*. The *Atlyk5*-2 mutant has reduced chitin-triggered ROS production, MAPK activation, calcium influx, as well as expression of chitin responsive genes (*AtWRKY29*, *AtWRKY30*, *AtWRKY33*, and *AtWRKY53*). However, the observed defects in chitin-induced responses of the *Atlyk5*-2 mutant could not be reproduced by other groups (Gubaeva et al., 2018). Therefore, Desaki et al. (2018) suggests the need of further investigations on the chitin receptor model with regard to the role of AtLYK5.

In *Atlyk4*-1 *Atlyk5*-2 double knock-out mutants, chitin-induced ROS burst and MAPK activation are abolished (Cao et al., 2014). Thus, analyses of these mutants indicate redundancy of AtLYK4 and AtLYK5 function in chitin signaling. AtLYK5 was shown to associate with AtCERK1 after chitin treatment and this interaction is essential for chitin-induced AtCERK1 homodimerization and phosphorylation (Cao et al., 2014). However, Liu et al. (2012) reported that AtCERK1 autophosphorylation is promoted by its homodimerization upon chitin treatment, meaning that it does not need to associate with AtLYK5 to be activated. This indicates that association of AtCERK1 with AtLYK5 occurs after the activation of AtCERK1. Erwig et al. (2017) reported that AtLYK4 and AtLYK5 are direct phosphorylation targets of AtCERK1 and further suggested that interaction of AtCERK1 with AtLYK4 and AtLYK5 is required for chitin signaling in Arabidopsis. In addition, AtLYK5 showed AtCERK1-dependent endocytosis after chitin treatment while AtCERK1 stayed in the plasma membrane, which indicates that AtLYK5 dissociates from AtCERK1 after chitin perception (Erwig et al., 2017). However, endosomes containing AtLYK5 might not be capable of initiating intracellular signal transduction because AtLYK5 harbors an inactive kinase domain.

In this research, the homologs of *AtLYK4*/*AtLYK5* in the hybrid poplar *Populus x canescens* (*Pc*) (*P. tremula x P. alba*) were characterized. The potential use of poplar (*Populus spp.*) as an established model system for studying the regulation of physiological processes in tree species was proposed by Bradshaw et al., (2000) due to several reasons including the available genetic information, as well as robust *in vitro* regeneration capability (Tuskan et al., 2006; Song et al., 2006; Chen et al., 2013; Han et al., 2013; Fladung et al., 2013; Movahedi et al., 2014; Li et al., 2015; Li et al., 2017; García-Angulo et al., 2018). Poplar also shows promising commercial and environmental benefits as it has been used

widely in the pulp and paper industry and lowland reforestation (Movahedi et al., 2014), phytoremediation of contaminated soils by heavy metals (Song et al., 2007; Guerra et al., 2011; Castro-Rodríguez et al., 2016), large-scale carbon sequestration (Jansson et al., 2010), as well as a potential bioenergy resource for biofuel or biogas (Pereira et al., 2016; Tallis et al., 2013; Littlewood et al., 2014; Sannigrahi et al., 2009; Guo et al., 2015; Wang et al., 2014; Aghaalikhani et al., 2017). However, poplar plantations are facing severe problems due to prevalent infections by the fungal pathogen, *Melampsora larici-populina*, which is a major factor causing yield losses of poplar plantations (Duplessis et al., 2009; Hacquard et al., 2011). Hence, studies on pathogen perception in poplar are important in order to understand the initiation of immune responses in perennial tree species. Four homologs of *AtLYK4* and two homologs of *AtLYK5* were found in poplar (*P. x canescens*), in which two homologs of *AtLYK4* and one homolog of *AtLYK5* are designated as pseudogenes. Characterization of the putatively functional PcLYK4/PcLYK5 proteins indicates that they are components of the poplar chitin receptor.

4.3 Materials and Methods

4.3.1 Sequence analysis of genes encoding putative LysM-RLKs in Poplar

Protein sequences of LysM-RLKs from *A. thaliana*, *O. sativa*, *Lotus japonicus* and *Medicago truncatula* were used as references to perform a BLASTP search on Phytozome v12.1 (www.phytozome.org) to identify homologs in the *Populus trichocarpa* Nisqually genome. A phylogenetic tree of LysM-RLKs was generated based on sequence similarity of putative *P. trichocarpa* Nisqually proteins with well-characterized LysM-RLKs from the references. The phylogenetic analysis was done in phylogeny.fr (https://www.phylogeny.fr/, Dereeper et al., 2008; Dereeper et al., 2010) using MUSCLE for multiple alignment (default settings), Gblocks for alignment refinement (least stringent settings), PhyML for phylogenetic tree construction (for the maximum likelihood with bootstrapping of 500 replicates) and TreeDyn for the visualization of phylogenetic tree, displaying only branch support values of >90 %.

The sequence information from the putative *P. trichocarpa LysM-RLK* genes was used to design primers (Supplemental Table 4.1) for PCR amplification of candidate genes from leaf-derived cDNA of the hybrid *P. x canescens* (*P. tremula* x *P. alba*). In order to obtain allele-specific sequences of each gene, TA cloning of the amplicons was carried out and the clone-derived plasmids were further sequenced (TA cloning kit® K2020-20 from

Invitrogen and sequencing by Microsynth Seqlab, Germany). Open reading frame (ORF) length was predicted by mapping the obtained sequences to the published hypothetic *LysM-RLK* sequences of *P. x canescens* extracted from the Aspen data base (AspenDB, http://aspendb.uga.edu/). The AspenDB also provides the hypothetic transcript sequences of *P. tremula* and *P. alba* to assign whether the obtained sequencing result is the *P. tremula* or *P. alba* allele. Several online prediction tools were used to perform *in silico* domain prediction for the obtained sequences. SignalP 4.1 server (Petersen et al., 2011) was used to predict signal peptides (SP), InterPro Scan integrated in Geneious 8.1.8 (Quevillon et al., 2005) for LysM and kinase domain prediction, and TMHMM server v. 2.0 for prediction of transmembrane domains (Krogh et al., 2001). In order to predict a kinase activity, alignment with the PKA-Cα protein sequence was performed showing the presence or absence of conserved amino acids necessary for enzymatic activity (Hanks and Hunter, 1995).

4.3.2 Plant materials and growth conditions

For amplification and expression analyses of the candidate genes, the hybrid *P. x canescens* (*P. tremula* x *P. alba*) clone INRA 717-1B4 was used in this research. *In vitro* propagation of both wild type and transgenic plantlets was conducted on half-strength Murashige-Skoog (½ MS) medium (Duchefa Biochemie BV, Haarlem, The Netherlands) supplemented with 2% (w/v) sucrose. The plantlets were cultivated under long day conditions (light: 16h at 22 °C, dark: 8h at 18 °C, 60% relative humidity, light intensity at 70–80 µmol m^{-2} s^{-1}). Potting on soil was done on Fruhstorfer Erde Typ T25, Hawita Gruppe GmbH, Vechta, Germany supplemented with 5% (v/v) washed screed sand (0/8 mm). The potted plantlets were further cultivated in the same long day climate chamber or in the greenhouse (a minimum temperature of 22:14 °C for day:night was maintained by heating, natural daylight was supplemented by metal halide lamps (HQI-TS 400W/D; Osram) to maintain a 16 h photoperiod).

For complementation studies, transgenic as well as wild type *A. thaliana* (L.) Heynh. plants were cultivated under short day conditions (day/night: 8h at 22 °C /16h at 18 °C, 65% relative humidity, and light intensity at 150 µmol m^{-2} s^{-1}) and used for experiments 5-6 weeks after sowing. The *A. thaliana* ecoptype Col-0 was used in these studies, as well as the T-DNA insertion lines *Atlyk4*-1 (WiscDsLox297300_01C), *Atlyk5*-2 (SALK_131911C) (Cao et al., 2014), the T-DNA insertion double knock-out mutant *Atlyk4*-1 *Atlyk5*-2 (Cao et al., 2014), *Atcerk1*-2 (GABI-Kat 096F09) (Miya et al., 2007), *fls2c* (obtained from Cyril Zipfel,

Sainsbury Lab, Norwich, UK), and *pAtLYK4:AtLYK4_mCitrine* in Col-0 (lines 1-329, 1-337, 1-338 and 4-173 from Jan Erwig collections, Plant Cell Biology Department, Georg-August Universität Göttingen).

4.3.3 Expression analysis of PcLYK4/PcLYK5 genes

Expression analysis was conducted by doing PCR on cDNA synthesized from five different tissues (roots, wood, developing xylem, bark and leaves) of *P. x canescens* using a proofreading DNA polymerase (F-530L, Thermo Scientific) (primers listed in Supplemental Table 4.1). Additionally, qPCR was conducted using cDNA from water or chitin-treated samples for checking the expression level of *PcLYK4*/*PcLYK5* genes in leaves after chitin treatment. qPCR was performed using the SsoFast EvaGreen Supermix (#172-5204, Bio-Rad) with primers listed in Supplemental Table 4.2. The efficiency of the primers was determined on gDNA, showing amplification efficiency of 87-89%. Ubiquitin was used as a reference to calculate the relative expression levels. RNA samples were isolated from the five different tissues, which were harvested from soil-grown. *P. x canescens* grown in either long day climate chamber or in the greenhouse. The harvested plant materials were immediately frozen in liquid nitrogen before being ground and used for RNA isolation, which was conducted using the CTAB extraction protocol according to Chang et al. (1993). Plant material was ground under liquid nitrogen and ~100 mg of each tissue were added with a pre-heated mix of 750 µl extraction buffer (Supplemental Table 4.4.1) and 15 µl β-mercaptoethanol and further incubated in 65 °C for 15 minutes. After shaking for 15 minutes at 160 rpm, 750 µl of chloroform:Isoamyl alcohol (24:1) (A1935, AppliChem) was added, and the solution was shaken for another 15 minutes at the same speed. This step was repeated twice by adding the same amount of chloroform:Isoamyl alcohol (24:1) to the collected supernatant. For precipitation, the supernatant was added to an equal amount of pre-cooled (4 °C) 8 M LiCl and incubated on ice in the fridge (4 °C) overnight. The following day, the samples were centrifuged for 40 minutes at 4 °C and 13,300 rpm. The supernatant was discarded and the pellet was suspended in 100 µl preheated SSTE (Supplemental Table 4.4.2. Recipe of SSTE for RNA isolation) to 60 °C, followed by two times extraction with 100 µl chloroform:Isoamyl alcohol (24:1). The pellet was precipitated again by adding pre-cooled (4 °C) 96% EtOH and incubation at -20 °C for 2 hours. The RNA was collected by centrifugation at 4 °C and 13,300 rpm for 40 minutes. The precipitated RNA was washed once with 400 µl 70% EtOH, and dissolved in 20 µl nuclease-free/DEPC-treated water (T143,

Roth). The extracted RNA was reverse transcribed into cDNA (cDNA synthesis Kit #K1631, Thermo Scientific), and used as a template for RT-PCR.

4.3.4 Generation of stably transformed A. thaliana for complementation studies

The amplified coding sequences of poplar *LysM-RLK* homologs (*PcLYK4-1*, *PcLYK4-2* and *PcLYK5-2*) from the hybrid *P. x canescens* in fusion with the mCitrine fluorescent marker (*PcLYK4-1_mCitrine, PcLYK4-2_mCitrine, PcLYK5-2_mCitrine*) under control of the endogenous *AtLYK5* promoter were cloned into the modified pGreenII-0229 vector (referred to as pGreen-Sulfadiazine) (primers listed in Supplemental Table 4.3). The original pGreenII-0229 vector (Hellens et al., 2000) carries a Basta selectable marker for plant resistance. Since the *Atlyk4*-1 *Atlyk5*-2 mutant that would be transformed with the generated constructs carries Basta and kanamycin resistance markers, the pGreenII-0229 selectable marker was changed into sulfadiazine to allow selection of the transgenic lines. The generated constructs were then used for *Agrobacterium*-mediated transformation into the *Atlyk4*-1 *Atlyk5*-2 double knock-out mutant through floral dipping as described in Clough and Bent (1998), and further cultivated under short day conditions. For endocytosis experiments, the constructs were also transformed into Col-0 and *Atcerk1-2*. For *in vitro* screening of the transgenic plants expressing *PcLYK4-1_mCitrine*, *PcLYK4-2_mCitrine*, or *PcLYK5-2_mCitrine*, seeds from the transformation experiment were sown on ½ strength Murashige and Skoog (½ MS) medium supplemented with 0.5% sucrose and 7.5 µg/ml sulfadiazine (S8626-25G from SIGMA-ALDRICH) and cultivated for two weeks. Surviving plantlets were transferred to soil and further sorted under the confocal laser scanning microscope (CLSM) Leica TCS SP5 (Leica Microsystems, Wetzlar, Germany) equipped with argon laser by tracing the mCitrine fluorescence. CLSM-sorted plants were further screened via western blotting using an anti GFP antibody to check for the presence of the protein. For experiments using the transgenic plants, wild type *A. thaliana* (L.) Heynh. ecotype Columbia (Col-0) was used as a control as well as other corresponding ecotypes.

4.3.5 Subcellular localization studies of poplar LysM-RLKs in Nicotiana benthamiana

The generated constructs for expression of *LysM-RLKs* in fusion with the *mCitrine* fluorescent marker (from section 4.3.4) were infiltrated into *N. benthamiana* leaves for *Agrobacterium*-mediated transient gene expression. For subcellular localization studies, a construct expressing *pAtLYK5:AtLYK5-mCitrine* was used as a control. Microscopic

analysis was performed 72h post infiltration using the CLSM. Images shown in this work are the maximum projections of 10 Z-stack series taken ~1 µm apart using the 40x objective.

4.3.6 Endocytosis experiments

Analysis of chitin-induced endocytosis of poplar LysM-RLKs was carried out using lines expressing *pAtLYK5:PcLYK4-1_mCitrine, pAtLYK5:PcLYK4-2_mCitrine* and *pAtLYK5:PcLYK5-2_mCitrine* in Arabidopsis Col-0 or *Atlyk4*-1 *Atlyk5*-2 (Cao et al., 2014) background. *pAtLYK5:PcLYK5-2_mCitrine* was also transformed into *Atcerk1*-2 (Miya et al., 2007) to examine the dependence of endocytosis on CERK1. Leaf disks were vacuum-infiltrated using a syringe with either 100 µg/ml chitin or water for 30 min before CLSM analysis. *AtLYK5* carrying the same fluorescent tag (*pAtLYK5:AtLYK5-mCitrine* x *Atlyk4*-1 *Atlyk5*-2) was used as a positive control for chitin induced endocytosis.

4.3.7 ROS burst assay

Analysis of reactive oxygen species (ROS) was conducted by overnight incubation of leaf discs (4 mm diameter) in 100 µl normal tap water in a 96-well plate. The following day, water was removed and replaced with a mixture of 100 µM luminol L-012 (120-04891, Wako Chemicals) and 10 µg/ml horseradish peroxidase (P6782, SIGMA ALDRICH). For chitin-elicited ROS burst, 100 µg/ml chitin from shrimp shells (C9752-5G, SIGMA ALDRICH) was added to the reaction solution. In addition, reactions with 100 nM flg22 or ultrapure water were carried out as controls. The luminescence was detected every one minute using an Infinite M200 Tecan plate reader for 1h.

4.3.8 MAPK assay

One leaf per plant was detached and incubated in normal tap water overnight. The following day, leaf materials were vacuum infiltrated with either 10 µg/ml chitin (C9752-5G from SIGMA ALDRICH), 100 nM flg22 or water, and harvested 10 minutes post infiltration. Protein extraction was carried out based on protocol described in Petutschnig et al. (2010). Total protein was extracted from a pool of leaf materials from three soil grown plants. Frozen leaf materials were ground, 500 µl protein extraction buffer (Supplemental Table 4.4.3) supplemented with 1:100 protease inhibitor (Supplemental Table 4.4.4) was added and mixed thoroughly. After centrifugation (10 min, 13.000 rpm at 4 °C), the supernatant was collected. The same amount of total protein extract for each sample was

supplemented with 1x SDS loading buffer for western blotting on SDS-PAGE (Supplemental Table 4.4.5). Phosphorylated MAPK4/6 were detected using as primary antibody phospho-p44/42 (#9101, Cell Signaling Technology).

4.4 Results

4.4.1 Identification of genes encoding LysM-RLKs in poplar

Protein sequences of putative LysM-RLKs of poplar were obtained by performing a BLASTP search in the *Populus trichocarpa*-Nisqually genome (www.phytozome.org) using protein sequences of well-characterized LysM-RLKs from *Arabidopsis thaliana* (*At*), *Oryza sativa* (*Os*), *Lotus japonicus* (*Lj*), and *Medicago truncatula* (*Mt*) as queries. Phylogenetic tree was constructed based on sequence similarity of the obtained putative LysM-RLKs from *P. trichocarpa*-Nisqually with LysM-RLKs from the references (**Figure 4.1**). Four homologs of LYK4 and two homologs of LYK5 were identified in the *P. trichocarpa*-Nisqually proteome. To identify whether the genes encoding these proteins are expressed in *P. x canescens* (*P. tremula* x *P. alba*), PCR was conducted using cDNA derived from five different tissues including roots, wood, developing xylem, bark and leaves. All analyzed genes encoding LysM-RLKs are expressed in the investigated tissues of *P. x canescens* (**Figure 4.2**). Upon chitin treatment, the expression levels of *PcLYK4-1*, *PcLYK4-2* and *PcLYK5-2* in leaves showed a tendency to increase. However, the increase was not statistically significant (Supplemental Figure 4.1).

Cloning and sequencing of the amplified cDNAs revealed allele-specific SNPs for all analysed *LYK4* and *LYK5* homologs, except for *PcLYK5-1*. This shows that both alleles of these homologs are expressed in *P. x canescens* leaves. The second allele of *PcLYK5-1* is either not expressed or could not be amplified with the primers used (Supplemental Table 1 in the appendix). Moreover, the analysis of the coding sequences showed that among the four homologs of *LYK4*, only two homologs (*PcLYK4-1* and *PcLYK4-2*) are putatively functional, based on the presence of an open reading frame (ORF), while the other two homologs are pseudogenes due to the occurrence of premature stop codons. For *LYK5* genes, only one homolog (*PcLYK5-2*) is predicted to be functional (Summarized data in **Table 4.1** and sequences in Supplemental Table 4.5). A phylogenetic tree that accommodates the predicted protein sequences of *P.* x *canescens PcLYK4*/*PcLYK5* genes was generated, showing that they are in the same clade with the corresponding homologs from Arabidopsis as well as from *P. trichocarpa*-Nisqually (Supplemental Figure 4.2).

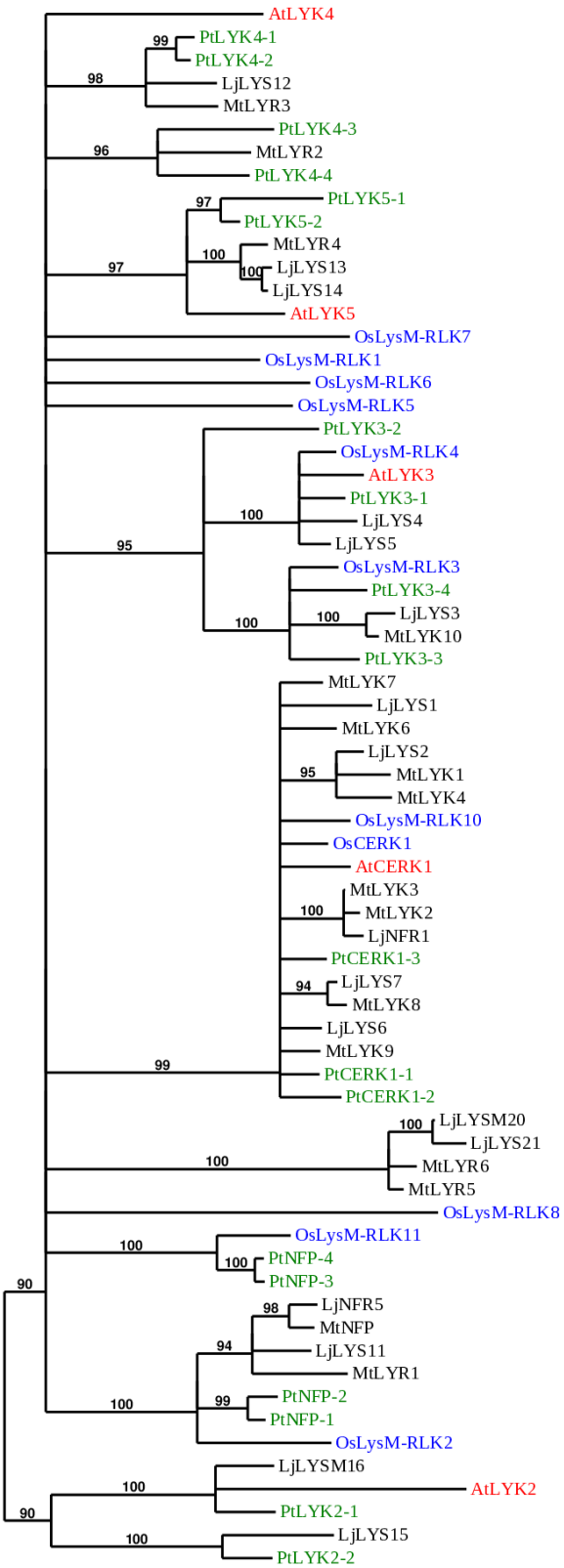

Figure 4.1. The poplar genome codes for several LYK4 and LYK5 homologs. A phylogenetic tree of LysM-RLKs was constructed based on sequence similarity of putative *P. trichocarpa*-Nisqually proteins (green) with well-characterized LysM-RLKs from *Arabidopsis thaliana* (red), *Oryza sativa* (blue), *Medicago truncatula* and *Lotus japonicus* (black). Three homologs of *AtCERK1*, four homologs of *AtLYK4*, and two homologs of *AtLYK5* are encoded by the *P. trichocarpa* genome. Numbers on the clade are branch support values (%) from bootstrapping of 500 replicates (analyzed with PhyML for maximum likelihood).

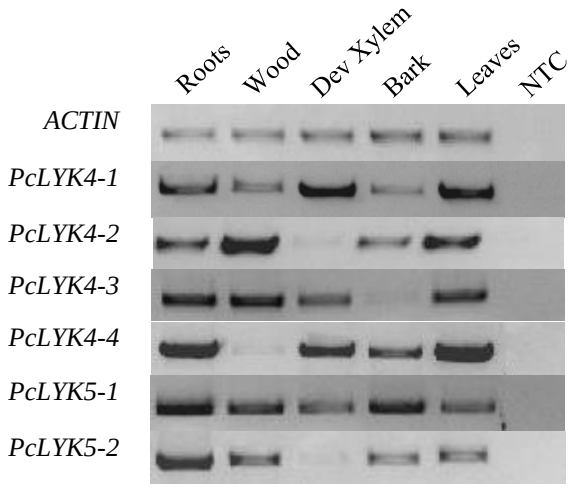

Figure 4.2. Expression pattern of *LysM-RLK* genes in *P. x canescens.* Semiquantitative RT-PCR analyses were conducted using cDNA synthesized from RNA isolated from roots, wood, developing xylem, bark and leaves. Expression of a house-keeping gene (Actin) was evaluated in all analysed tissues to determine cDNA quality. In addition, no template control (NTC) was performed as a negative control.

Table 4.1. Summary of cDNA sequencing data of genes encoding LysM-RLKs (PcLYK4/PcLYK5) in *P. x canescens*. The presence (✓) and absence (×) of alleles originating from the parental lines *P. alba* and *P. tremula* were determined in the hybrid *P. x canescens*. Open reading frames (ORF) and transcript sequences containing premature stop codons (pseudogenes) are indicated.

Name of Genes	*P. alba* allele	ORF	*P. tremula* allele	ORF
PcLYK4-1	✓	Yes	✓	Yes
PcLYK4-2	✓	Yes	✓	Yes
PcLYK4-3	✓	Pseudogene	✓	Pseudogene
PcLYK4-4	✓	Pseudogene	✓	Pseudogene
PcLYK5-1	×	×	✓	Pseudogene
PcLYK5-2	✓	Yes	✓	Yes

4.4.2 The cytoplasmic domains of PcLYK4/PcLYK5 proteins are most likely inactive kinases

Arabidopsis LYK4/LYK5 proteins are chitin-binding LysM-RLKs that harbor a cytoplasmic domain, which is kinase-inactive (Petutschnig et al., 2010; Wan et al., 2012; Cao et al., 2014). To determine whether PcLYK4/PcLYK5 proteins have a domain organization similar to AtLYK4/AtLYK5, domain prediction was performed on the obtained sequences using several online tools, which revealed that LysM-RLKs in poplar, in particular PcLYK4/PcLYK5 proteins, consist of three extracellular LysM domains, a transmembrane domain and an intracellular kinase domain (**Figure 4.3A**).

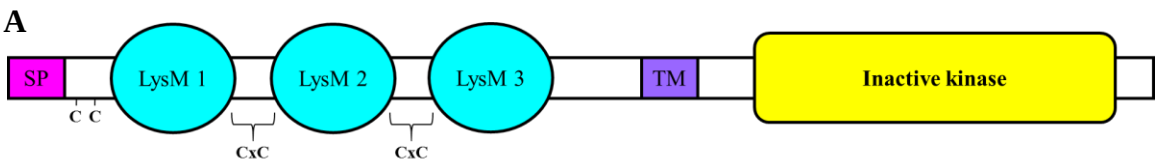

B

```
                 *        20        *        40        *        60        *        80        *       100
AtCERK1  : -MKLKISLIAPILLLFSFFFA-----------VESKCRTSCPLALASYYLENGTTLSVINQNLNSSIAPYDQIN-------FDP----ILRYNSNIKDK :  76
AtLYK4   : MISFSF----HLLVFILLSLSSFATAQQPYVGISTTDCSVSDNTTSVFGYSCNGLNKTCQAYVIFRSTPSFSTVTSISSLFSVDPS---LVSSLNDASPS :  93
AtLYK5   : MAACTLHALSVTLFLLLFFAVSPAKAQQPYVNNHQLACEVRVYDNITNGFTCNGP-PSCRSYLTFWSQPPYNTADSIAKLLNVS--AAEIQSINNLPTAT :  97
PcLYK4-1 : -MSCLS--AVSSFVLFIVCCSSLIQAQQPYVGKGTTNCSFTEN--SALGYSCNALNKSCQAYLIFRSQPPYNTVASISTLLGSDPS---QLSEGNSVSET :  92
PcLYK4-2 : -MSFRS--VVSPFALFVLYCCSLIQAQQPYVGKGTTKCSNTQN--SALGYSCNGLNKSCQAYLTFRSQPPYTTVASISTLLASDPS---QLSQMNSVSET :  92
PcLYK5-2 : -----MDFLILYLYVVLLLSPALVQGQQTYLANHQLDCYNNNFNETTKGFLCNGVQSSCQSYLTFRSMPPYNSPVYIAYLLGVPQSATLIASVNNLSSDT :  95

                 *       120        *       140        *       160        *       180        *       200
AtCERK1  : DRIQMGSRVLVFPFECQP--GDFLGHNFSYSVRQ---EDTYERVAISNYANLTTMESLQARNPFPA-TNIPLSATLNVLVNCSCGDESV--SKDFGLFV : 168
AtLYK4   : TSFPSGQQVIIPLTCSCT---GDDSQSNITYTIQP---NDSYFAIANDTLQGLSTCQALAKQNNVS-SQSLFPGMRIVVPIRCACPTAKQINEDGVKYLM : 186
AtLYK5   : TRIPTRELVVIPANCSCSSSSGGFYQHNATYNLSGNRGDETYFSVANDTYQALSTCQAMMSQNRYGE-RQLTPGLNLLVPLRCACPTAKQ-TTAGFKYLL : 195
PcLYK4-1 : ATFPSNQMVIVPVNCSCS---GEYSQANASYIVQQ---NDNLLLIANNTYQGLSTCQALRNQKSTRTNDIILSGETLTVPLRCACPTKNQ-SDLGIRYLL : 185
PcLYK4-2 : ASFPTNQLVLVPVNCSCS---GDYFQANASYIVQP---GNTPFLIANNTYQGLSTCQAIRNLKSTLTVDI-FAGETLTVPLRCACPTKNQ-SDLGIRYLL : 184
PcLYK5-2 : APIPTDFQVVVPVNCSCYD--RQYYQHNSSYLLKE--KSETYFTVANNTYQGLTTCQSLMSQNPYGD-RNLSIGLNLQIPLRCACPTSNQ-NASGINYLL : 189

                 *       220        *       240        *       260        *       280        *       300
AtCERK1  : TYPLRPEDSLSSIARSSGVSADILQRYNF------GVNF----------NSGNGIVYVPGRDPNGAFPP------------FKSSKQD--GVGAGVIAGI : 238
AtLYK4   : SYTVVFEDTIAIISDRFGVETSKTLKANEMSFENSEVFPFTTILIPLVNPPANTNSLIPPPPPPP---PQSVSPPPLSPDGRKSKKKTWVYALAGVLGGA : 283
AtLYK5   : TYLVAMGDSISGIAEMFNSTSAAITEGNELTS--DNIFFFTPVLVPLTTEPTKIVISPSPPPPPVVATPPQTP----VDPPGSSSSHKWIYIGIGIGAGL : 289
PcLYK4-1 : SYIVIPGDTVTVISEQFGADTGRIFEANGLPEQNPTIFPSTTLLIPLQSTPTSSQTVVPSPPPASSSPPSQ------SPNPEKRSKKTWLYVVVGVVGGI : 279
PcLYK4-2 : SYLVTQGDTVSRASVRFGADIGRALEANEISEKYPTIYPFTTLLIPLKNPPTSSQTVVPPPPPASPAPPPPPPPPPPSPNSVKSSNTTWVYVVVGVFGGI : 284
PcLYK5-2 : TYMVTFGDTISSIAELFGVDKQRVLDANKLSSS-DIIFPFTPILVPLPTNPTKIEKPSAAPPP--AAPSPQTP----NVSVGGSSDHKALYVGVGIGAAF : 282

                 *       320        *       340        *       360        *       380        *       400
AtCERK1  : VIGVIVALLLILFIVYYAYRKNKSKGDSFS--------------SSIPLSTKADHASSTSLQSGGLGGAGVSPGIAAISVDKSVEFSLEELAKATDNFNL : 324
AtLYK4   : LV----LSVIGAAIFCLSKKKTKTQTQEETGNLDSFMG------KKPPMS--D----------Q---EFDPLDGLSGMVVESLKVYKFHELQSATSDFTS : 358
AtLYK5   : LL----LLSI--LALCFYKRRSKKKSLPSSLPEENKLFDS-STKQSIPTTTTQWS-------IDLSNSSEAFG-LKSAIESLTLYRFNDLQSATSNFSD : 374
PcLYK4-1 : AL----TVVIGTIIFFMLSRRSKKQPGPVIE-SQSFEA------HEKPLN--KKLD-------E---ESQEFFESISAIAQSIKVYKFEDLKAATDNFSP : 356
PcLYK4-2 : VL----TLVIGTIIFFMFFRKSKKQPGPIIV-SQSFQA------HEKPLN--RKLD-------E---EPQDLLESVSIAQSIKVYNYEDLKAATDNFSP : 361
PcLYK5-2 : LV----LLSA-AFGFLFWHRKSRKQHKPVSTSETKTLPSDSTDFTVLPVSSNKSWS-------LSPN------D-ARYAIESLTVYKYEDLQVATGYFAQ : 363

                      I          II         III        IV          V                    VIA
                 *       420        *       440        *       460        *       480        *       500
AtCERK1  : SFKIGQGGFGAVYYAELRGEKAAIKKMDMEASKQFLAELKVLTRVHHVNLVRLIGYCV-EGSLFLVYEYVENGNLGQHLHGSG--REPLPWTKRVQIALD : 421
AtLYK4   : SSSIG-----GSGYIGKINGDGAMIKKIEGNAS----EEVNLLSKLNHLNIIRLSGFCFHEGDWYLVYEHASNGSLSEWIHTTK---SLLSLTQKLQIALD : 447
AtLYK5   : ENRIK----GSVYRATINGDDAAVKVIKGDVSS---SEINLLKKLNHSNIIRLSGFCIREGTSYLVFEYSENGSISDWLHSSG--KKSLTWKQRVEIARD : 465
PcLYK4-1 : SCWIK----GSVYRGLINGDFAAIKKMNGDVS----KEIELLNKINHSNLIRLSGVCFNGGQWYLVYEYAANGQLSDWIYDRSNEGKFLNWTKRIQIASD : 448
PcLYK4-2 : SCWIK----GSVFRGLINGDFAAIKKMNGDVS----KEIDLLNKISHSNLIRLSGVCFNDGHWYLVYEYAANGPLSDWIHVSSNEGKFLKWTQRIQIATD : 453
PcLYK5-2 : ANLIK----GSVYRGSFKGDTAAVKVVKGDVS----SEINILKMINHSNVIRLSGFCLHEGNTYLVYEYADNGSLTDWLHFNN-TYRILAWKQRVRIAYD : 454

                           VIB        VII                VIII                IX
                 *       520        *       540        *       560        *       580        *       600
AtCERK1  : SARGLEYIHEHTVPVYVHRDIKSANILIDQKFRAKVADFGLTKLTEV----GGSATRGAMGTFGYMAPETVY-GEVSAKVDVYAFGVVLYELISAKGAVV : 516
AtLYK4   : IATGLNYLHNFADPPYVHRDLNSNNVFLDLEFRAKIGSLGSARST----TEDFVLTKHVEGTRGYLAPEYLEHGLVSTKLDVYAFGVVLLEIVTGKEASE : 543
AtLYK5   : VAEALDYLHNYITPPHIHKNLESTNILLDSNFRAKIANFGVARILDE-GDLDLQLTRHVEGTQGYLAPEYVENGVITSKLDVFAFGVAVLELLSGREAVT : 564
PcLYK4-1 : VAMGLNYLHSFTNYPHVHKDITSSNILLDSDLRAKIANFSLARSTGD-LDGEFALTRHIVGTKGYMAPEYLENGVVSSKLDVYAFGILTLEIITGKEVAA : 547
PcLYK4-2 : VATGLNYLHCFTDYPHVHKDIKSSNILLDNDLRAKIANFSLARSTDG-PEGEFALTRHIVGTKGYMAPEYLENGIICTKLDVYAFGVLTLEIMTGKEVAA : 552
PcLYK5-2 : VADALNYLHNYTNPSYIHKNLKTSNILLDANLRAKVANFGLARTLENDQDGGLQLTRHVVGTQGYLAPEYIENGVITPKLDVFAFGVVMLELLSGKEAAA : 554

                           X                     XI
                 *       620        *       640        *       660        *       680        *       700
AtCERK1  : KMTEAVGE--FRGLVGVFEESF-KETDKEEALRKIIDPRLGDSYPFDSVYKMAELGKACTQENAQLRPSMRYIVVALSTLFSSTGNWDVGNFQNEDLVSL : 613
AtLYK4   : LKKEIDEG-----K------------AIDE---ILI---HGRLLPEGLTSFVERLVVDCLKKDHLNRPSMDENVMSLSKILAATQNWEESSY-------- : 612
AtLYK5   : IHKKKEGEEEVEMLCKVINSVL-GGENVREKLKEFMDPSLGNEYPLELAYTMAQLAKSCVATDLNSRPSVTQVLTTLSMIVSSSIDWEPSDDLLRSG-SL : 662
PcLYK4-1 : LHTEENRN-----LSDVLNGALSEEDGQEESLKQLIDPSLHENYPSGLAVLVVRLIDSCLNKNPGDRPTMDEIVQSLSRILTTSLAWELSSNVSGYH-IS : 641
PcLYK4-2 : LYGEENRE-----LSDVLNGVLSEEGGLEESPSQLIDPSMQGNYPSGLAVLMVRLIDSCLSKNPADRPAMDEIVQALSGILTTSLAWELSNNTSSYH-SS : 646
PcLYK5-2 : TAIDKSAG--DDLLSVMIMRVL-EGDNVREKLSAFLDPCLRDEYPLDLAFSMAQLAKSCVEHDLNTRPSMPQVFMMLSKILSSSLDWDPSDELNRSR-SI : 650


AtCERK1  : MSGR : 617
AtLYK4   : ---- :   -
AtLYK5   : GN-- : 664
PcLYK4-1 : S--- : 642
PcLYK4-2 : N--- : 647
PcLYK5-2 : DSGR : 654
```

Figure 4.3. The intracellular domains of PcLYK4/PcLYK5 proteins are most likely inactive kinases. A. The domain organization of LysM-RLKs in *P. x canescens* was analyzed by using online prediction tools, which predict signal peptides (SP), three extracellular LysM domain and a transmembrane domain (TM). Intracellular inactive kinase domain was predicted through alignment with *A. thaliana* LysM-RLKs **B.** Alignment of poplar LysM-RLKs with AtCERK1 (Miya et al., 2007) to assign the kinase subdomains (yellow I-XI). AtLYK4 and AtLYK5 sequences were included. LysM-RLKs with inactive kinases lack the ATP-binding loop (orange GxGxxGxV) in subdomain I and the conserved DFG motif (red) in subdomain VII that are present in AtCERK1. Three LysM domains (light blue), separated by a CxC motif (green), were predicted. Amino acids encoding a signal peptide are indicated in magenta color separated from LysM1 by two conserved cysteine residues (green). Putative transmembrane domains are marked in purple. LysM-RLKs from *P. x canescens* (PcLYK4-1, PcLYK4-2 and PcLYK5-2) in this alignment are the *P. tremula* allele.

The kinase domain is devided into twelve subdomains: The N-terminal domain (subdomains 1-IV) is involved in anchoring and orienting the nucleotide, the C-terminal domain (subdomains VI(A and B)-XI) is responsible for binding the peptide substrate and initiating phosphotransfer, while the subdomain V spans the N- and C-terminal lobes as sites of catalysis (Hanks and Hunter, 1995). Sequence alignment of PcLYK4/PcLYK5 proteins with *Arabidopsis thaliana* CERK1 as well as AtLYK4/AtLYK5 showed that PcLYK4 and PcLYK5 (both alleles) lack the consensus ATP-binding loop (GxGxxGxV motif) in subdomain I and amino acid residues (DFG motif) in subdomain VII that are necessary for enzymatic activity similar to the homologs AtLYK4/AtLYK5 in Arabidopsis (**Figure 4.3B**). Essential amino acids for kinase activity had been described by Hanks and Hunter (1995) using the PKA-Cα protein sequence that include Gly50 and Gly52 in kinase subdomain I, Lys72 in subdomain II, Glu91 in subdomain III, Asp166 and Asn171 in subdomain VIB, Asp184 and Gly186 in subdomain VII, Glu208 in subdomain VIII, Asp220 and Gly225 in subdomain IX and Arg280 in subdomain XI. Alignment of PcLYK4/PcLYK5 proteins with this sequence confirmed that PcLYK4/PcLYK5 proteins lack some of those amino acids (Supplemental Figure 4.3).

4.4.3 PcLYK4-1, PcLYK4-2 and PcLYK5-2 proteins are likely plasma membrane-localized LysM-RLKs

In Arabidopsis, LYK4 and LYK5 are plasma membrane-localized LysM-RLKs that act as partners of CERK1 for chitin perception and chitin-induced signaling (Petutschnig et al., 2010; Erwig et al., 2017). Localization of poplar PcLYK4/PcLYK5 proteins was investigated in a *Nicotiana benthamiana* transient expression system (Supplemental Figure 4.4) and in leaves of stably-transformed *A. thaliana* (**Figure 4.4**). All analysed PcLYK4/PcLYK5 proteins (PcLYK4-1, PcLYK4-2 and PcLYK5-2) of *P. x canescens* reside at the cell periphery similar to the localization of AtLYK5 that is known to reside at the plasma membrane, indicating that these proteins might play a similar role like the homologs in Arabidopsis that associate with CERK1 in the plasma membrane in order to mediate chitin perception and signal transduction.

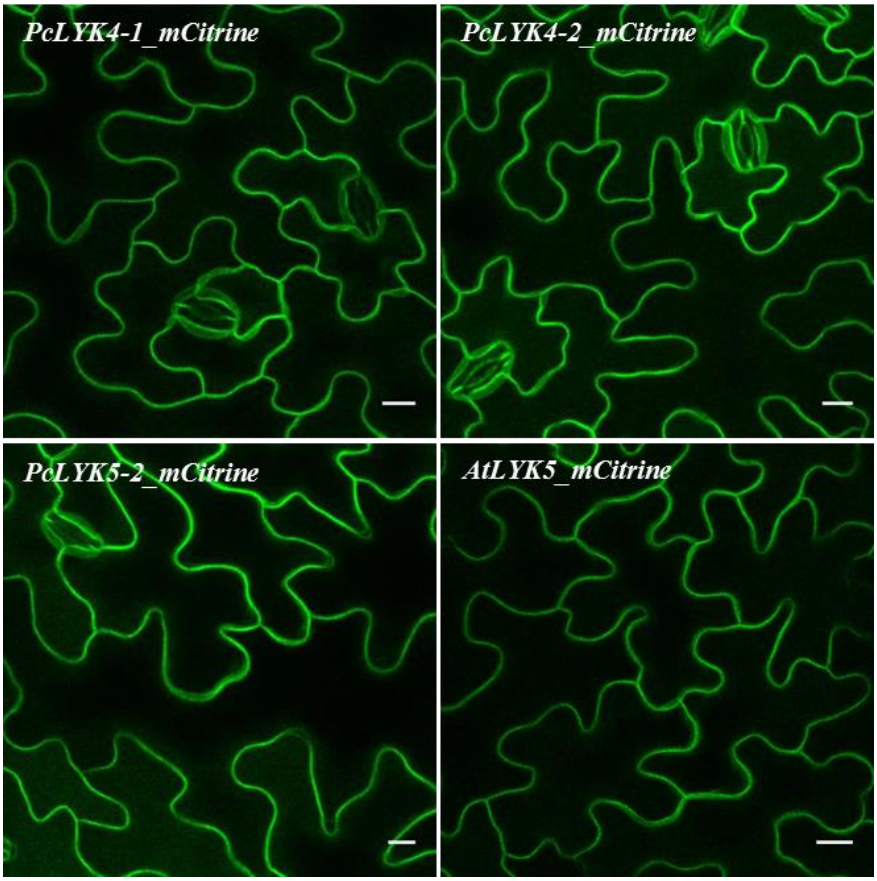

Figure 4.4. LYK4/LYK5 proteins of *P. x canescens* localize at the cell periphery. For subcellular localization studies, constructs for expression of poplar LysM-RLKs (*PcLYK4-1*, *PcLYK4-2* and *PcLYK5-2*) as well as *AtLYK5* under the promoter of *AtLYK5*, carrying the mCitrine fluorescent marker at the C-terminus were generated and stably transformed into the *A. thaliana* double knock-out mutant, *lyk4*-1 *lyk5*-2. A construct expressing *AtLYK5* was used as a control, further validating that the cell periphery localization likely represents plasma membrane localization. Observation under CLSM SP5 was conducted using a 40x objective, and the displayed images are maximum projections of 10 Z-stack series with ~1 µm per-stack. Scale bars = 10 µm.

4.4.4 Complementation assays in the Atlyk4-1 Atlyk5-2 *mutant using* PcLYK4/PcLYK5 *indicate a function of the poplar homologs in chitin perception and signaling*

Functional analyses of genes can be done by complementation assays. In this study, the capablility of a poplar *LYK* homolog to restore the chitin-sensitivity of the Arabidopsis *lyk4*-1 *lyk5*-2 mutant (Cao et al. 2014) was tested. However, before conducting these assays, complementation studies with the Arabidopsis homolog, *AtLYK5*, were carried out to evaluate if complementation is principally possible. Hence, *AtLYK5* was expressed in the *Atlyk4*-1 *Atlyk*5-2 background under control of the *AtLYK5* promoter. Additionally, *Atlyk4*-1 and *Atlyk5*-2 single knock out lines were analysed to evaluate the contribution of each LYK gene to chitin-induced responses, which was analysed by performing ROS burst and MAPK assays. The *Atlyk4*-1 single knock-out lines showed a reduced chitin-induced ROS burst in comparison to Col-0, while the *Atlyk5*-2 single knock-out lines exhibited a ROS production similar to Col-0 (Supplemental Figure 4.5A), and they have a wildtype-like

response to flg22 (Supplemental Figure 4.5B), indicating that *AtLYK4* might be the primary LYK protein involved in chitin-induced ROS production in Arabidopsis. This hypothesis is supported by ROS burst results obtained with Col-0 plants expressing AtLYK4 under the endogenous promoter in the wildtype background (*pAtLYK4:AtLYK4_mCitrine* in Col-0). These lines showed higher and extended ROS burst compared to Col-0 (Supplemental Figure 4.6A and Supplemental Figure 4.6B), but normal responses to flg22 (Supplemental Figure 4.7A and Supplemental Figure 4.7B). The *pAtLYK5:AtLYK5_mCitrine*-expressing *Atlyk4*-1 *Atlyk5*-2 lines show partial restoration of chitin-induced ROS production (Supplemental Figure 4.5) and MAPK activation (Supplemental Figure 4.8), while the response to flg22 is normal, indicating that complementation of the *Atlyk4*-1 *Atlyk5*-2 double mutant can be achieved.

The role of a poplar *LYK* homolog in chitin perception and signaling was then tested by conducting complementation studies using poplar genes. *PcLYK4*/*PcLYK5*-containing constructs *pAtLYK5:PcLYK4-1_mCitrine*, *pAtLYK5:PcLYK4-2_mCitrine* and *pAtLYK5:PcLYK5-2_mCitrine*, were transformed into the chitin-insensitive *Atlyk4-1lyk5-2* double knock-out mutant. The *AtLYK5* promoter was used for both constructs because it has a higher activity than the *AtLYK4* promoter. In these complementation studies, only one allele of each homolog was tested (indicated in Supplemental Table 4.4). The chitin responses of the generated lines were examined by performing ROS burst and MAPK assays. Expressing the *PcLYK4-1_mCitrine* or *PcLYK4-2_mCitrine* partially restores the sensitivity of *Atlyk4*-1 *Atlyk5*-2 mutants to chitin, as shown by the induction of ROS burst (**Figure 4.5**), while the lines do not respond to water (Supplemental Figure 4.9) and have a normal response to flg22 (Supplemental Figure 4.10 and Supplemental Figure 4.11). Partial restoration of chitin-induced ROS production was also observed in *pAtLYK5:PcLYK5-2_mCitrine*- lines (**Figure 4.6** and Supplemental Figure 4.12) which show Col-0 wildtype-like response to flg22 (Supplemental Figure 4.13). However, the restoration of the chitin response in *Atlyk4*-1 *lyk5*-2 expressing *PcLYK4*/*PcLYK5* genes is only partial compared with the wild type Col-0 response. Also, the complementation efficiency is line-dependent. To evaluate whether *PcLYK4-1*/*PcLYK4-2*/*PcLYK5-2* restores the chitin-induced ROS production of *Atlyk4*-1 *Atlyk5*-2 to a different extent, the ROS burst assay after chitin treatment was performed in the same assay (Supplemental Figure 4.14). This analysis showed that the complementation capacity of the analysed poplar LYK genes is similar. Moreover, all lines characterized in complementation assays exhibit wildtype-like responses to flg22 (Supplemental Figure 4.15).

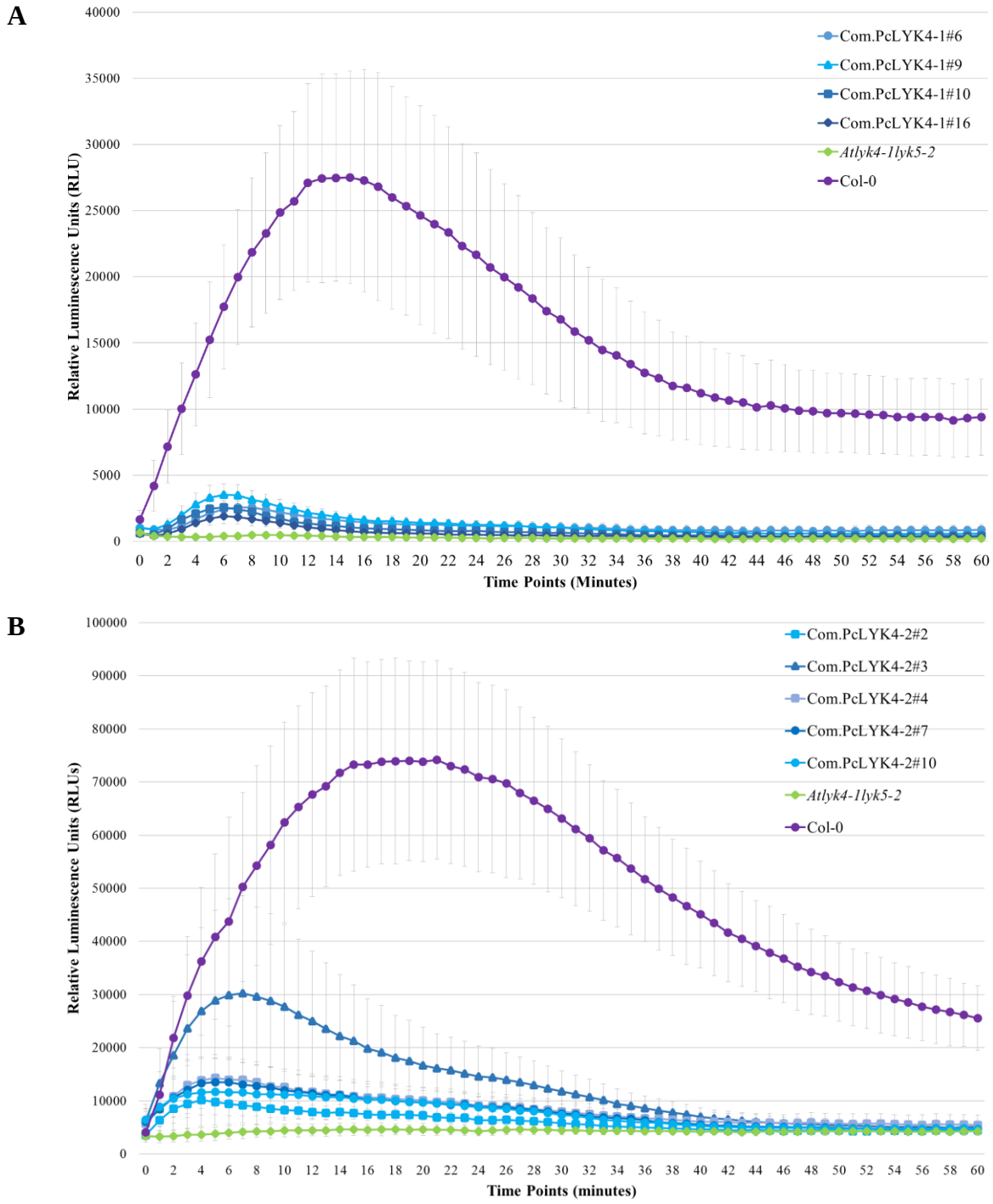

Figure 4.5. Expression of *PcLYK4-1* and *PcLYK4-2* partially restores the chitin induced ROS production of *Atlyk4-1 Atlyk5-2*. For complementation studies, constructs for expression of *pAtLYK5:PcLYK4-1_mCitrine* (Com.PcLYK4-1) or *pAtLYK5:PcLYK4-2_mCitrine* (Com.PcLYK4-2) were stably-transformed into the *A. thaliana* double knocked-out mutant *Atlyk4*-1 *Atlyk5*-2. Complementation of the chitin-induced ROS burst was analysed with the obtained lines by measuring the ROS production for 1h after treatment with 100 µg/mL chitin. *Atlyk4*-1 *Atlyk5*-2 and Col-0 were used as negative and positive controls respectively. A minimum of four individual lines was tested for each construct. Numbers after '#' designate individual lines. Data are means ± SD (n = 8 biological replicates). Technical repeats were performed for each sample. The experiment was repeated independently for 2-3 times with similar results. Representative results are shown.

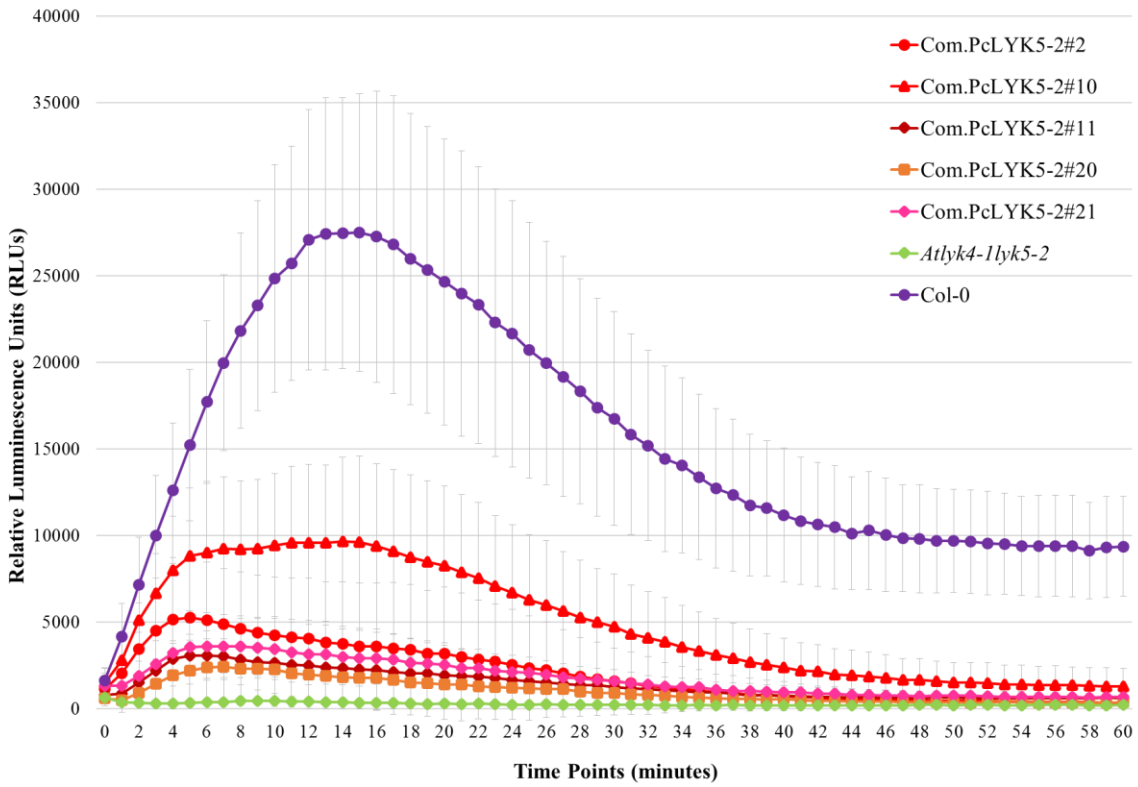

Figure 4.6. Expression of PcLYK5-2 partially complements the chitin induced ROS production of *Atlyk4*-1 *Atlyk5*-2. *pAtLYK5:PcLYK5-2_mCitrine* (Com.PcLYK5-2) was stably-transformed into the *A. thaliana* double knocked-out mutant *lyk4*-1 *lyk5*-2. Complementation of the chitin-induced ROS burst was analysed with the obtained lines by measuring the ROS production for 1h after treatment with 100 µg/mL chitin. *Atlyk4*-1 *lyk5*-2 and Col-0 were used as negative and positive controls respectively. Five individual lines were tested. Numbers after '#' designate individual lines. Data are means ± SD (n = 8 biological replicates). Technical repeats were performed for each sample. The experiment was repeated independently for four times with similar results. Representative results are shown.

Expressing *PcLYK4*/*PcLYK5* genes also partially restores MAPK activation that is abolished in the double knock-out mutant *Atlyk4*-1 *Atlyk5*-2 (**Figure 4.7** and **Figure 4.8**). MAPK activation is strongly induced by chitin in Col-0 and this response is completely abolished in *Atlyk4*-1 *Atlyk5*-2, while the *Atlyk4-1* and *Atlyk5-2* single knock-out mutants still show MAPK activation after chitin treatment (**Figure 4.7A** and **Figure 4.8**). These data indicate functional redundancy of *AtLYK4* and *AtLYK5* as it was already reported by Cao et al. (2014). Expressing *PcLYK4-1_mCitrine* or *PcLYK4-2_mCitrine* in the *Atlyk4*-1 *Atlyk5*-2 mutant partially restores the MAPK activation (**Figure 4.7**). Partial restoration of chitin-induced MAPK activation was also observed in *Atlyk4*-1 *Atlyk5*-2 plants expressing *PcLYK5-2_mCitrine* (**Figure 4.8**). In conclusion, the restoration of chitin responses in the *Atlyk4*-1 *Atlyk5*-2 double knock-out mutant by *PcLYK4*/*PcLYK5* as shown via chitin-induced ROS production and MAPK activation suggests that LYK4/LYK5 proteins from poplar play a role in mediating chitin signaling in the presence of CERK1. However, the role of

PcLYK4/*PcLYK5* also needs to be examined by generating knock-out lines in poplar, to do the analyses in a homologous system.

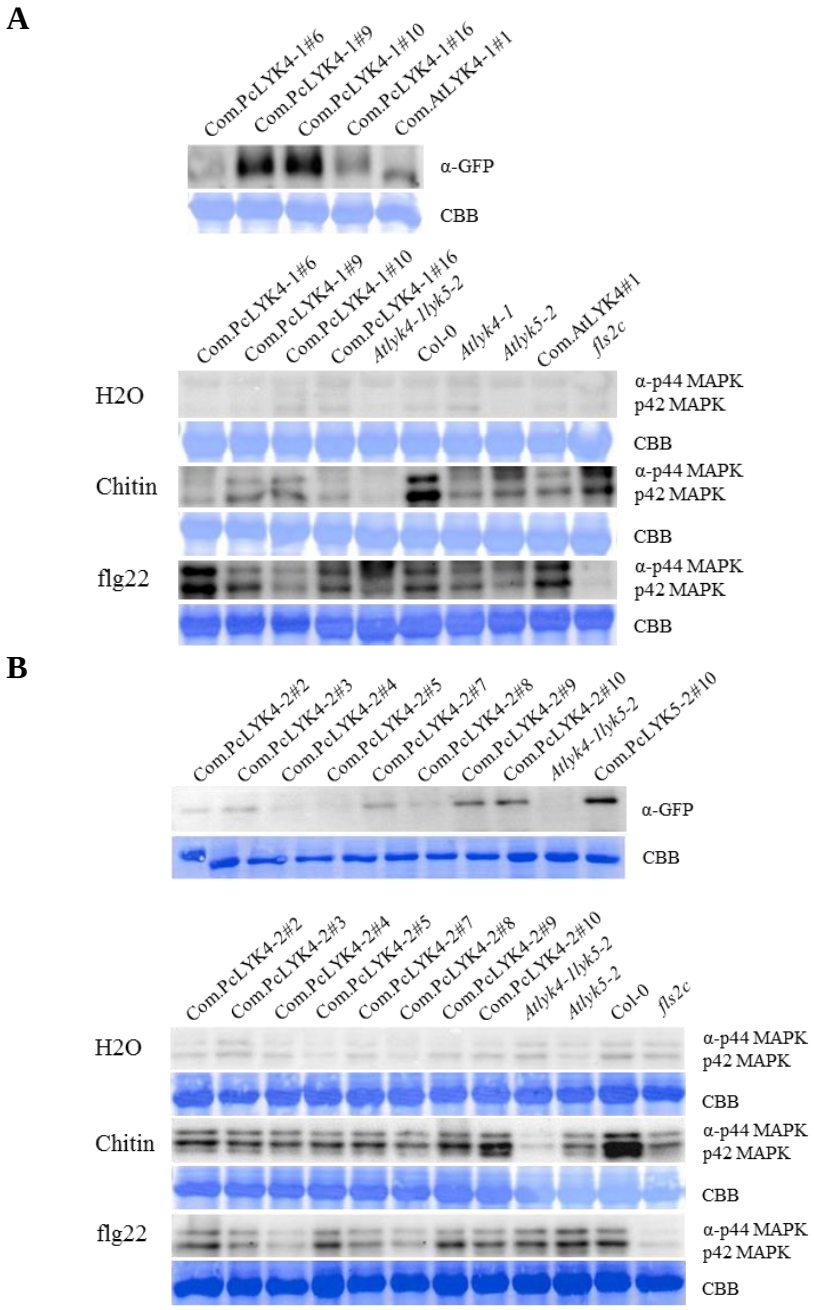

Figure 4.7. Expression of *PcLYK4-1* and *PcLYK4-2* genes partially restores the chitin induced MAPK activation of *Atlyk4*-1 *Atlyk5*-2. A. MAPK activation in the Com.PcLYK4-1 (*pAtLYK5:PcLYK4-1_mCitrine* in *Atlyk4*-1 *Atlyk5*-2). Upper panel of A shows protein levels of poplar LYK4-1_mCitrine in individual lines, Com.AtLYK4 line was used as a control. **B**. MAPK activation in the Com.PcLYK4-2 lines (*pAtLYK5:PcLYK4-2_mCitrine* in *Atlyk4*-1 *Atlyk5*-2). Upper panel of B shows protein levels of poplar LYK4-2_mCitrine in individual lines, Com.PcLYK5-2 was used as a control. Total proteins were extracted from a pool of leaves from three plants that were infiltrated with 10 µg/mL chitin, 10 nM flg22 or water (ddH2O) and harvested 10 minutes post infiltration. MAPK activation of plants after flg22 treatment shows that lines have a wildtype response to flg22. Numbers after '#' designate individual lines. *Atlyk4*-1 *Atlyk5*-2 and Col-0 were included as negative and positive controls for chitin-induced response, respectively. In addition, *Atlyk4*-1 or *Atlyk5*-2 single knock-out mutants, Com.AtLYK4 line (*pAtLYK5:AtLYK4_mCitrine* in *Atlyk4*-1 *Atlyk5*-2), as well as *fls2c* plants (for flg22 negative control) were also included. MAPK activation was detected by using the primary antibody phospho-p44/p42. Coomassie brilliant blue (CBB) staining was done to control that similar amounts of protein were loaded. Each experiment was independently repeated for at least twice showing similar results.

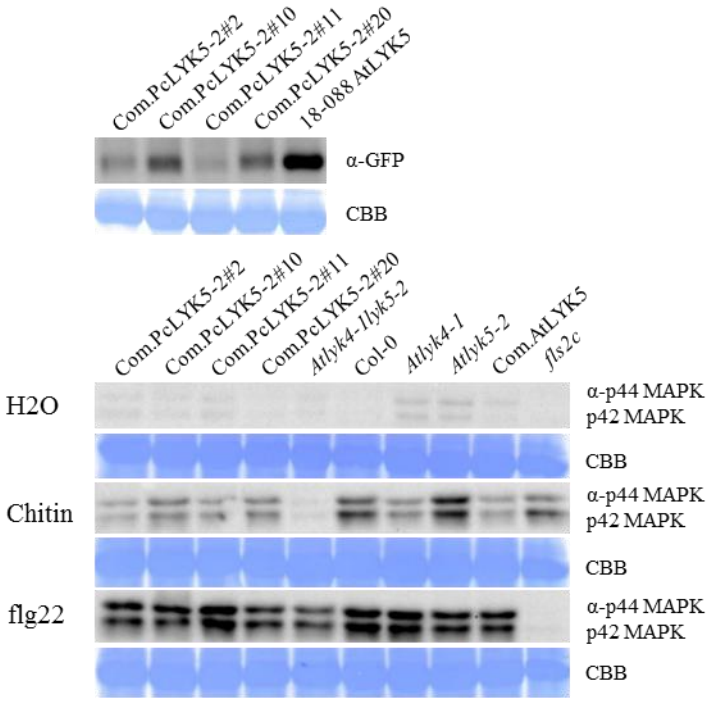

Figure 4.8. Expression of *PcLYK5-2* genes partially restores the chitin induced MAPK activation of *Atlyk4*-1 *Atlyk5*-2. Total proteins were extracted from a pool of leaves from three plants that were infiltrated with 10 µg/mL chitin, 10 nM flg22 or water (ddH_2O) and harvested 10 minutes post infiltration. MAPK activation of Com.PcLYK4-2 lines (*pAtLYK5:PcLYK5-2_mCitrine* in *Atlyk4*-1 *Atlyk5*-2) was tested after flg22 treatment, showing that the lines have a wildtype response to flg22. Four independent lines were evaluated. Numbers after '#' designate individual lines. Upper panel shows protein levels of poplar LYK5-2_mCitrine in individual lines, *Atlyk4*-1 *Atlyk5*-2 and Col-0 were included as negative and positive controls for chitin-induced response, respectively. In addition, *Atlyk4-1* or *Atlyk5-2* single knock-out mutants, Com.AtLYK5 line (*pAtLYK5:AtLYK5_mCitrine* in *Atlyk4-1lyk5-2*), as well as *fls2c* plants (for flg22 negative control) were also included. MAPK activation was detected by using the primary antibody phospho-p44/p42. Coomassie brilliant blue (CBB) staining was done to control that similar amounts of protein were loaded. Each experiment was independently repeated for at least twice showing similar results.

4.4.5 Chitin induces the endocytosis of PcLYK4/PcLYK5 proteins

AtLYK5 undergoes endocytosis after chitin treatment in a CERK1 dependent manner (Erwig et al., 2017). To analyse whether PcLYK4/PcLYK5 proteins are also endocytosed after chitin perception, leaves from Col-0 or *Atlyk4-1 Atlyk5-2* plants expressing *PcLYK4*/*PcLYK5* carrying a mCitrine fluorescent marker under the promoter of AtLYK5 were treated with chitin for 30 minutes. Endosomes containing PcLYK4-1, PcLYK4-2 or PcLYK5-2 were observed in the chitin-treated samples but not in the water controls (**Figure 4.9**). The dependency of this endocytosis on CERK1 was determined only for PcLYK5-2 by transforming the same construct into the *Atcerk1-2* mutant, resulting in the absence of vesicle formation after chitin treatment (**Figure 4.10**). This further suggests that PcLYK5-2 is likely a phosphorylation target of CERK1 as is also indicated by the chitin-induced mobility shift of PcLYK5-2 after chitin treatment (Supplemental Figure 4.16).

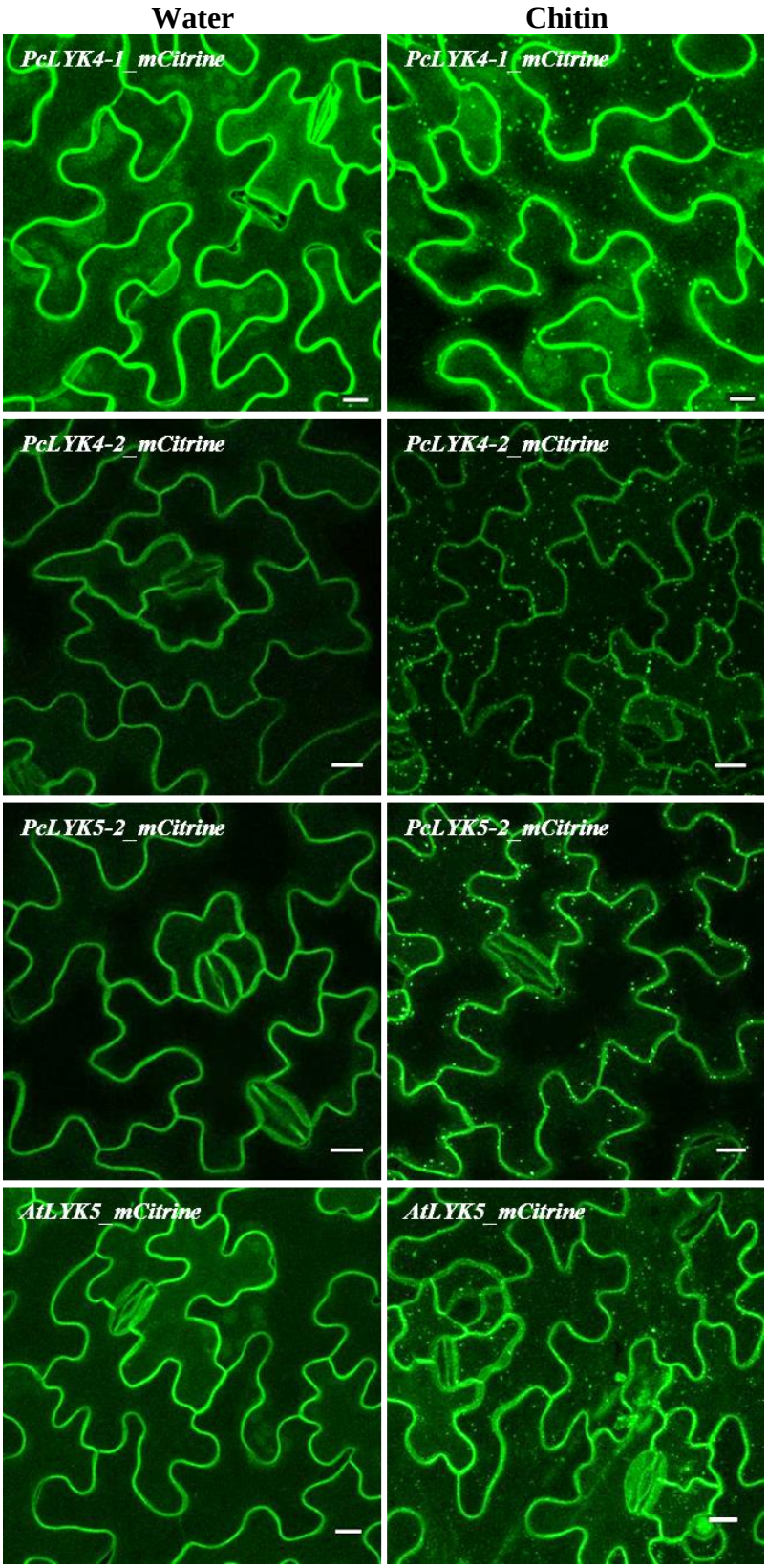

Figure 4.9. Chitin triggers the endocytosis of PcLYK4-1, PcLYK4-2 and PcLYK5-2. Leaves of Arabidopsis Col-0 or *Atlyk4*-1 *Atlyk5*-2 plants expressing *pAtLYK5:PcLYK4-1_mCitrine*, *pAtLYK5:PcLYK4-2_mCitrine*, or *pAtLYK5:PcLYK5-2_mCitrine* were infiltrated with chitin or water as a negative control. A plant expressing *pAtLYK5:AtLYK5_mCitrine* in the *Atlyk4*-1 *Atlyk5*-2 background was used as a control for chitin induced endocytosis. mCitrine-tagged vesicles were formed indicating endocytosis after 30 minutes of 100 µg/mL chitin treatment. CLSM images are maximum projections of 10 focal planes taken 1 µm apart under 40x objective. Similar results were obtained with two independent lines for each set-up. Scale bars = 10 µm.

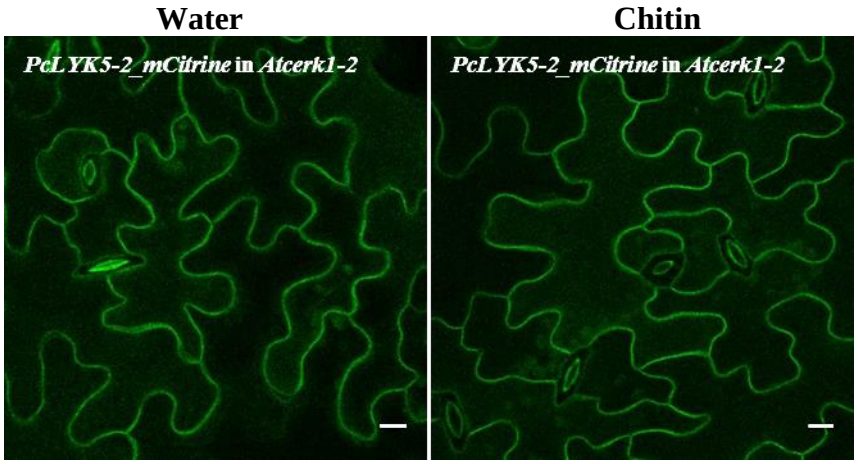

Figure 4.10. PcLYK5-2 endocytosis after chitin treatment is CERK1-dependent. A *pAtLYK5:PcLYK5-2_mCitrine*-containing construct was transformed into the *Atcerk1*-2 mutant. The mCitrine tag was added at the C-terminus of the construct to trace the protein localization and vesicle formation. For endocytosis experiments, leaf samples were infiltrated with 100 µg/mL chitin or water as a negative control. No vesicle formation was observed after 30 minutes of chitin treatment, indicating that PcLYK5-2 endocytosis is CERK1-dependent. CLSM images are maximum projections of 10 focal planes taken 1 µm apart under 40x objective. Similar results were obtained with two independent lines. Scale bars = 10 µm.

4.5 Discussion

4.5.1 PcLYK4/PcLYK5 proteins have a domain organization similar to the homologs in Arabidopsis

During evolution, single gene- or whole genome duplications can occur that result in the presence of more than one copy of a gene. On a statistical average, there are at least 1.4 to 1.6 putative genes in the *Populus* genome per homolog in the *Arabidopsis* genome (Tuskan et al., 2006). Accordingly, four homologs of *LYK4* and two homologs of *LYK5* were predicted to be present in the poplar genome (*P. trichocarpa* Nisqually) (**Figure 4.1**). For this research, *P. x canescens*, a hybrid of *P. tremula* and *P. alba*, was used. The genome of the hybrid contains alleles, which originated either from *P. tremula* or from *P. alba*. During the sequence analysis of *PcLYK4*- and *PcLYK5*-cDNAs, two alleles representing the *P. tremula* and *P. alba* parents, respectively, were identified. The two alleles were characterized based on single nucleotide polymorphisms (SNPs) detected in the cDNA sequences, which had been individually cloned. The sequence analysis of the predicted LysM-RLK homologs in *P. x canescens* also revealed that only two homologs of *LYK4* (referred to as *PcLYK4-1* and *PcLYK4-2*) and one homolog of *LYK5* (*PcLYK5-2*) are putatively functional (**Table 4.1** and sequences in Supplemental Table 4.4). The other predicted homologs (*PcLYK4-3*, *PcLYK4-4* and *PcLYK5-1*) are pseudogenes containing premature stop codons in the coding region. The occurence of pseudogenes is a typical phenomenon observed in genomes that underwent a duplication. One of the paralogs, that orginated from the duplication, is free

from functional constraints and may accumulate mutations resulting in either deletion/inactivation or modification of the genes (Mach, 2014; Vanneste et al., 2014). A well characterized example are poplar *PRX* genes, encoding a class of peroxidases in *Populus*. Some members of this family of paralogous genes turned into pseudogenes, while other members most likely underwent neofunctionalization, indicated by a change in subcellular localization (Ren et al., 2014).

Domain prediction with the protein sequences of PcLYK4-1, PcLYK4-2 and PcLYK5-2 proteins revealed that these proteins are putative LysM-RLKs composed of three extracellular LysM domains, a transmembrane domain and an intracellular kinase domain that lacks subdomains necessary for the enzymatic activity (**Figure 4.3** and Supplemental Figure 4.3). Hence, PcLYK4/PcLYK5 proteins are inactive kinases similar to Arabidopsis LYK4 and LYK5 (Wan et al., 2012; Cao et al., 2014; Erwig et al., 2017). AtLYK4 and AtLYK5 were reported as chitin-binding proteins (Petutschnig et al., 2010). Also, mass spectrometry analysis of proteins extracted from leaves of soil grown *P. x canescens* showed that PcLYK4-1, PcLYK4-2 and PcLYK5-2 proteins are present in the protein extracts enriched for chitin binding proteins (Muhr, unpublished). This indicates that PcLYK4/PcLYK5 proteins are also chitin-binding. Subcellular localization studies in *N. benthamiana* as well as in Arabidopsis, showed that PcLYK4-1, PcLYK4-2 and PcLYK5-2 proteins localize at the cell periphery (**Figure 4.4** and Supplemental Figure 4.4). Thus, the poplar proteins are most likely also plasma membrane (PM)-residents similar to their homologs AtLYK4 and AtLYK5 (Erwig et al., 2017). Taken together, the data suggests that PcLYK4/PcLYK5 proteins are PM-localized LysM-RLKs involved in chitin perception.

4.5.2 PcLYK4/PcLYK5 proteins are involved in mediating chitin-induced defense signaling

In *A. thaliana, AtLYK4* and *AtLYK5* were reported to be involved in chitin perception and signaling. Loss-of-function mutations of *AtLYK4* or *AtLYK5* reduce the chitin-triggered responses such as ROS production, calcium influx, MAPK activation as well as the induction of chitin-responsive genes (Wan et al., 2012; Cao et al., 2014). The *Atlyk4* mutant also has an increased susceptibility to the bacterial pathogen *Pseudomonas syringae* pv tomato DC3000 as well as fungal pathogen *Alternaria brassicicola*, even though the effects on plant immunity are not as drastic as it was observed in the *Atcerk1* mutants (Wan et al., 2012). AtLYK5 was shown to bind chitin with a much higher affinity than AtCERK1, and chitin-binding to AtLYK5 was considered to be indispensable for chitin-triggered AtCERK1 phosphorylation (Cao et al., 2014). However, keeping in mind that AtLYK5 harbors an

inactive kinase, the data suggests that AtLYK5 might be the main component of the receptor complex for binding chitin, but for a proper chitin signal transduction, it requires heterodimerization with AtCERK1. Furthermore, the insensitivity of *Atlyk4*-1 *Atlyk5*-2 mutants to chitin indicate that the two mutated genes are functionally redundant. To evaluate if complementation of the Arabidopsis knockout lines using heterologous poplar genes is feasible, complementation with the homologous Arabidopsis gene, *AtLYK5*, was also tested. Complementing *Atlyk4*-1 *Atlyk5*-2 with *AtLYK5* only partially restores ROS production compared to wildtype Col-0 (Supplemental Figure 4.5). The MAPK activation in the *pAtLYK5:AtLYK5_mCitrine*-expressing *Atlyk4*-1 *Atlyk5*-2 leaves is also restored after chitin treatment (Supplemental Figure 4.8).

Functional characterization to analyse the role of PcLYK4/PcLYK5 proteins in chitin signaling was addressed by conducting the complementation studies using *PcLYK4*/*PcLYK5* genes. *pAtLYK5:PcLYK4-1_mCitrine*, *pAtLYK5:PcLYK4-2_mCitrine*, and *pAtLYK5:PcLYK5-2_mCitrine*-expressing constructs were transformed into *Atlyk4*-1 *Atlyk5*-2 mutants, and the chitin responses of the generated lines were further tested by performing chitin-induced ROS burst and MAPK assays. The *Atlyk4*-1 *Atlyk5*-2 double knock-out mutant is chitin insensitive (Cao et al., 2014), and expressing *PcLYK4*/*PcLYK5* partially restores the responses of this mutant to chitin as shown via the production of ROS (**Figure 4.5**, **Figure 4.6**, and Supplemental Figure 4.14) and the activation of the MAPK cascade (**Figure 4.7** and **Figure 4.8**). These results indicate that PcLYK4-1, PcLYK4-2 and PcLYK5-2 are involved in chitin perception and signaling, in particular with respect to ROS production and MAPK activation. The presence of more than one copy of LYK4 homologs in poplar might allow a possible fine-tuning interaction of components of chitin receptors, depending on *PcLYK4-1* or *PcLYK4-2* presence in the complex. However, the role of these proteins has to be further studied in poplar *Pclyk4*/*Pclyk5* knock-out lines.

The role of the poplar genes *PcLYK4*/*PcLYK5* in chitin-induced signaling was examined in a heterologous system (*Atlyk4*-1 *Atlyk5*-2 background) in which the functional AtCERK1 is still present, providing the interacting partner. PcLYK4/PcLYK5 alignment with the homologs from Arabidopsis as well as AtCERK1 revealed that PcLYK4/PcLYK5 proteins harbor inactive kinases (**Figure 4.3** and Supplemental Figure 4.3), indicating that a LysM-RLK with an active kinase is needed as a partner in the receptor complex to allow chitin-triggered defense signaling. In Arabidopsis, AtLYK5 was indeed shown to associate with AtCERK1 upon chitin treatment and the interaction is essential for chitin-induced AtCERK1 homodimerization and phosphorylation (Cao et al., 2014). The activity of the

kinase domain was confirmed by *in vitro* kinase assays in *E. coli* using the intracellular kinase domains (IDs) of AtLYK4, AtLYK5 and AtCERK1. Conclusions from these *in vitro* studies are that AtCERK1-ID exhibits autophosphorylation and that AtLYK4-ID and AtLYK5-ID are direct phosphorylation targets of AtCERK1-ID (Erwig et al. (2017). The importance of AtCERK1 kinase activity for AtLYK5 phosphorylation was also characterized *in planta* by co-expression of *AtLYK5* with *AtCERK1* in the *Atcerk1*-2 background. In these studies the protein mobility shift of AtLYK5 in western blots indicating phosphorylation, was dependent on the presence of functional AtCERK1. Moreover, AtCERK1 association with AtLYK4 and AtLYK5 is required for effective chitin signaling. To examine the dependence of PcLYK4/PcLYK5-mediated chitin-induced signaling on CERK1 in poplar, *in vitro* kinase assay and investigation of kinase activity *in planta* have to be done in future studies.

4.5.3 PcLYK4/PcLYK5 proteins undergo endocytosis

Ligand-induced endocytosis of receptors plays a crucial role in plant defense responses against pathogens, e.g. it was shown that the bacterial flagellin receptor FLS2 is transferred into intracellular mobile vesicles and targeted for degradation upon perception of flg22 (Robatzek et al., 2006). In Arabidopsis, AtLYK5 dissociates from the chitin receptor complex after chitin perception and undergoes AtCERK1-dependent endocytosis, while AtCERK1 stays in the plasma membrane. In this study, it was shown that poplar PcLYK5-2 also undergoes chitin-induced endocytosis comparable to Arabidopsis LYK5 (**Figure 4.9**). Receptor signaling from endosomes is possible as it was shown that plant defense-related FLS2 receptor and the brassinosteroid receptor BRI1 have the capability to signal from endosomes (Robatzek et al., 2006; Geldner et al., 2007). However, signaling from receptor-containing endosomes is possible if the endocytosed receptor components have signaling capacity on their own, e.g. an active kinase domain, or establishes association with other proteins capable of initiating signal transduction. Thus, the internalized endosomes that contain PcLYK5 with an inactive kinase might be unable to initiate chitin-triggered signal transduction similar to AtLYK5-containing endosomes, unless it interacts with other signaling proteins in the endosomes. AtLYK4 is functionally redundant with AtLYK5 and is also a phosphorylation target of AtCERK1 *in vitro* (Wan et al., 2012; Erwig et al., 2017). However, the endocytosis of LYK4 was not well studied due to its weak expression in leaves (Erwig et al., 2017). Here, we showed that the two putatively functional homologs of PcLYK4 (PcLYK4-1 and PcLYK4-2) are found in vesicles after elicitation by chitin (**Fig.**

9). According to *in silico* analysis, the kinase domain of PcLYK4 most likely also has no enzymatic activity (**Figure 4.3** and Supplemental Figure 4.3). To confirm that the observed vesicles are endosomes, a line expressing *pAtLYK5:AtLYK5_mCitrine* in the *Atlyk4*-1 *Atlyk5*-2 background was included as control. This line shows endocytosis after chitin treatment (**Figure 4.9**). However, co-localization experiments with endocytic tracers like FM4-64, filipin-labeled 3-β-hydroxysterols, and fluorescently-labeled Rab guanosine triphosphatases (GTPases) have to be done in order to validate that the internalized vesicles are indeed endosomes (Otegui and Spitzer, 2008).

4.5.4 Endocytosis of PcLYK5 is CERK1-dependent

AtLYK5 is a phosphorylation target of AtCERK1 and undergoes endocytosis after chitin treatment in a CERK1-dependent manner (Erwig et al., 2017). The chitin-induced vesicle formation of PcLYK5 was shown to also depend on CERK1. PcLYK5 undergoes endocytosis after chitin treatment in the *Atlyk4*-1 *Atlyk5*-2 background where endogenous AtCERK1 is present (**Figure 4.9**), but the endocytosis of PcLYK5 does not occur in the *Atcerk1-2* background (**Figure 4.10**). These results also indicate that LYK5 from poplar interacts with CERK1 from Arabidopsis, suggesting conserved mechanisms in these different species. In Arabidopsis, the endocytosis of AtLYK5 occurs through the phosphorylation of AtLYK5 by AtCERK1. Hence, the absence of PcLYK5 endocytosis when the gene is expressed in the *Atcerk1*-2 background confirms conservation of this mechanism. Data from chitin-induced mobility shift showed the phosphorylation of PcLYK5 by AtCERK1 in *Atlyk4*-1 *Atlyk5*-2 background (Supplemental fig. 15). However, the chitin-induced band-shift of PcLYK5-2 in the *Atcerk1*-2 background was not tested. The dependence of PcLYK4 endocytosis on functional CERK1 was not analysed. However, the complementation studies showed that PcLYK4 and PcLYK5 perform similar functions, indicating that PcLYK4 endocytosis might also depend on CERK1 similar to PcLYK5. The requirement of CERK1 for AtLYK5 and PcLYK5 endocytosis is in line with other investigations showing that endocytosis of receptor components depends on the presence of a functional receptor complex. Leucine-rich repeat receptor-like kinases (LRR-RLKs) such as FLS2, EFR and BRI1 also show dependence on BRI1-associated receptor kinase 1 (BAK1) for a proper ligand-induced signaling that includes vesicle formation and internalization (Chinchilla et al., 2007; Beck et al., 2012; Yan et al., 2012; Mbengue et al., 2016; Paez Valencia et al., 2016).

4.6 Conclusion

The homologs of LysM-RLKs that are chitin receptor components in *A. thaliana* were also found in the hybrid poplar *P. x canescens*. These components include two homologs of *AtCERK1*, *PcCERK1-1* and *PcCERK1-2* (personal communication with Mascha Muhr), four homologs of *AtLYK4* and two homologs of *AtLYK5*. Only two homologs of *AtLYK4*, *PcLYK4-1* and *PcLYK4-2*, and one homolog of *AtLYK5*, *PcLYK5-2*, were predicted to be functional based on the presence of an open reading frame (ORF). Complementation studies showed that *PcLYK4* and *PcLYK5* paralogs contribute to the chitin-induced responses, since expressing the genes in *Atlyk4*-1 *Atlyk5*-2 restores the chitin-induced ROS production and MAPK activation of this double knock-out mutant. All identified PcLYK4/PcLYK5 proteins undergo endocytosis upon chitin treatment, and the dependency of this endocytosis on CERK1 was observed for *PcLYK5-2*. These data also indicate that AtCERK1 phosphorylates PcLYK5-2, suggesting functional conservation of chitin signaling in Arabidopsis and poplar. However, there are two functional, paralogous copies of *LYK4* genes in poplar that have comparably similar function in mediating chitin-induced responses, making it conceivable that chitin receptor complexes are formed that include either PcLYK4-1 or PcLYK4-2. It is hypothesized that the presence of different paralogs in the receptor complex may affect the receptor characteristics in regard to the signaling efficiency.

4.7 Appendix

Supplemental Table 4.1. Primer pairs to amplify genes encoding LYK4/LYK5 from *P. x canescens*

Genes	Homologs in *P. trichocarpa* Nisqually	Primer sequences (5'->3')	AT* (°C)	Length (bp)
PcLYK4-1	Potri.005G128200.1	Fw_388: GTCTTAGTTGGAAGGTGAAGGG Rv_393: GGTGGTGAATCTGATGGATCTC	63.1	2531
PcLYK4-2	Potri.007G032100.1	Universal primers for both alleles (designed on CDS) Fw_355: GAGCTTCCGTTCTGTTGTTTCTCC Rv_356: GTGTTGTTTGACAATTCCCAGGC	61	1905
		Primers for full length of *P. tremula* allele Fw_680: ATGAGCTTCCGTTCTGTTG Rv_681: GATAATAGAAGTTCTAGATTAATGATTTC	56.8	2037
		Primers for full length of *P. alba* allele Fw_680: ATGAGCTTCCGTTCTGTTG Rv_682: CTGCATTCTATAACCATTAGATG	57.5	2088
PcLYK4-3	Potri.005G128300.1	Fw_316: GATAAGCTTCAGTGAAGCTGAGTTTCAAAG Rv_398: GGGCTGACAAGTCCAAGTAG	59.8	2198
PcLYK4-4	Potri.014G040000.1	Universal primers for both alleles (designed on CDS) Fw_407: CGCGCTTATTGATAGCCC Rv_412: CCATAGTTGGGCTGCTTC	61.4	1977
		Primers for full length of *P. tremula* allele Fw_740: GCCCTAACATGAGTCCATCTATTC Rv_741: GAGTGAAGTTTAATAATTATGATTTCTGTG	57.2	1915
PcLYK5-1	Potri.002G001600.1	Fw_306: GTCGAATTCGTGTGCAACGGAGTAAAATC Rv_340: CTAGAATTCTACTGTTGGTAATGGGGATCC	60.1	1661
PcLYK5-2	Potri.005G259600.1	Fw_320: GTCGAATTCCCAATCAACATCCTCCAC Rv_321: GACGAATTCACAATGACACTCTTGGGAAC	59.4	2305

*AT = annealing temperature for protocol using a proofreading DNA polymerase (Phusion Hot Start II, Thermo Fisher Scientific Inc., Waltham, U.S.A.). Restriction sites designated in red.

Supplemental Table 4.2. Primer pairs for qPCR of PcLYK4/PcLYK5 genes

Genes	Sequences (5'->3')	Efficiency (%)
PcLYK4-1	Fw: ATCGTTCCCGATTCGACATGAG Rv: CTTTCCCTACATATGGTTGCTGAGC	87
PcLYK4-2	Fw: GAGCTTCCGTTCTGTTGTTTCTCC Rv: CACTTTGTTGTACCTTTCCCCACG	87
PcLYK5-2	Fw: GAGCTCCTGTTCCATGGACTTTC Rv: GTAGCAGTCCAGTTGGTGGTTG	89

Supplemental Table 4.3. Primers for generating *PcLYK4/PcLYK5*-constructs

Fragments	Primer pairs (5'->3')
pAtLYK5:PcLYK4-1_mCitrine	
pAtLYK5	Fw: CTATAGGGCGAATTGGGTACCCCACCTCTGTTTTTTGTTGTG Rv: GTTTTGTGGTGTTCTGATCTG
PcLYK4-1 CDS	Fw: CAGATCAGAACACCACAAAACATGAGCTGCCTTTCTGCTG Rv: ACTGGAGATATGGTAGCCAGATAC
mCitrine	Fw: GTATCTGGCTACCATATCTCCAGTTACGCTGGAGCGATGGTGAGCAAGGGCG Rv: GCGGACTCTAGAACTAGTGGATCCTACTTGTACAGCTCGTCCATG
t35S	*
Destination Vector**	Fw: GGTACCCAATTCGCCCTATAG Rv: GATCCACTAGTTCTAGAGTCCGC
pAtLYK5:PcLYK4-2_mCitrine	
pAtLYK5	Fw: GCGGACTCTAGAACTAGTGGATCCCACCTCTGTTTTTTGTTGTG Rv: GTTTTGTGGTGTTCTGATCTG
PcLYK4-2 CDS	Fw: CAGATCAGAACACCACAAAACATGAGCTTCCGTTCTGTTG Rv: ATTCGAACTATGGTAGCTAGATG
mCitrine	Fw: CATCTAGCTACCATAGTTCGAATTACGCTGGAGCGATGGTGAGCAAGGGCG Rv: CTATAGGGCGAATTGGGTACCCTACTTGTACAGCTCGTCCATG
t35S	*
Destination vector**	Fw: GGTACCCAATTCGCCCTATAG Rv: GATCCACTAGTTCTAGAGTCCGC
pAtLYK5:PcLYK5-2_mCitrine	
pAtLYK5	Fw: CTATAGGGCGAATTGGGTACCCCACCTCTGTTTTTTGTTGTG

	Rv: GTTTTGTGGTGTTCTGATCTG
PcLYK5-2 CDS	Fw: CAGATCAGAACACCACAAAACATGGACTTTCTTATACTGTATCTGTATG Rv: CCTGCCACTGTCTATAGACC
mCitrine	Fw: GGTCTATAGACAGTGGCAGGTACGCTGGAGCGATGGTGAGCAAGGGCG Rv: GCGGACTCTAGAACTAGTGGATCCTACTTGTACAGCTCGTCCATG
t35S	*
Destination vector**	Fw: GGTACCCAATTCGCCCTATAG Rv: GATCCACTAGTTCTAGAGTCCGC

*On the vector backbone

**primer used for Inverse PCR

Blue =linkers

Red = overlapping sites to assemble the fragments trhough Gibson Assembly

Supplemental Table 4.4. Recipes

Supplemental Table 4.4.1. CTAB RNA extraction buffer

Chemicals	Final concentration
CTAB (Hexadecyltrimethylammoniumbromid)	2%
Tris HCl	100 mM
EDTA	25 mM
NaCl	2 M
PVP K30	2%

Supplemental Table 4.4.2. Recipe of SSTE for RNA isolation

Chemicals	Final concentration
SDS	0.5 %
Tris HCl	10 mM
EDTA	1 mM
NaCl	1 M

Supplemental Table 4.4.3. Extraction buffer solution for total protein extract

Materials	Final concentration
Sucrose	250 mM
HEPES-KOH pH 7.5	100 mM
Glycerol	5%
Na2MoO4 + 2H2O	1 mM
NaF	25 mM
EDTA	10 mM
DTT	1 mM
Triton X-100	0.50%
Protease inhibitor cocktail (see table 12.8)	1:100

Supplemental Table 4.4.4. Recipe of protease inhibitor cocktail for total protein extraction buffer

Protease inhibitor cocktail (200 ml, 100x)	
4-(2-aminoethyl) benzenesulfonyl fluoride hydrochloride (AEBSF)	1 g
Bestatin hydrochloride	5 mg
Leupeptin hemisulfate	100 mg
Pepstatin A	10 mg
E-64 (trans-epoxysuccinyl-L-leucylamido-(4-guanidino)butane)	10 mg
Phenanthroline (1, 10-phenanthroline monohydrate)	10 g
All components were dissolved separately in a small amount of DMSO, combined and filled up with DMSO to a total volume of 200 ml. 2 ml aliquots were prepared and stored at -20°C.	

Supplemental Table 4.4.5. Recipes for Western Blotting

SDS-PAGE gel buffer (250 ml)		
10% running gel buffer	1 M Tris-HCl, pH 8.8	143.6 ml
	10% SDS	3.79 ml
	ddH_2O	102.61 ml
Stacking gel buffer	1 M Tris-HCl, pH 6.8	38.58 ml
	SDS (10%)	3.06 ml
	ddH_2O	208.36 ml
SDS-PAGE gel (10 ml)		
10% running gel	10% running gel buffer	6.6 ml
	30% acrylamide	3.3 ml
	10% APS	0.1 ml
	TEMED	0.004 ml
Stacking gel	Stacking gel buffer	8.16 ml
	30% acrylamide	1.66 ml
	10% APS	0.05 ml
	TEMED	0.005 ml
SDS-PAGE and Immunoblot analysis		
10x SDS running buffer (1 l)	Glycine	144.2 g
	Tris-base	30.4 g
	10% SDS	100 ml
20x transfer buffer, pH 8.3 (1 l)	Tris-base	121.14 g
	Boric acid	61.83 g
20x TBS-T (1 l)	NaCl	175.32 g
	1M Tris-HCl, pH 8	200 ml
	Tween-20	10 ml
3% Milk solution	Milk powder (Roth)	3 g
	1x TBS-T	100 ml
AP buffer (1 l)	1 M Tris-HCl, pH 9.5	100 ml
	5 M NaCl	20 ml
	1 M $MgCl_2$	50 ml
4x SDS loading buffer (50 ml)	1 M Tris-HCl, pH 6.8	10 ml
	DTT	3.085 g
	SDS	4 g
	Gycerin	20 ml
	Bromphenolblue	50 mg
CBB staining solution (700 ml)	EtOH	300 ml
	ddH_2O	300 ml
	Acetic acid (10%)	100 ml
	Coomassie Brilliant Blue R-250	0.35 mg
Destaining solution for CBB	EtOH	300 ml
	ddH_2O	300 ml
	Acetic acid (10%)	100 ml

Supplemental Table 4.5. Transcript and protein sequences of genes encoding LysM-RLKs (PcLYK4/PcLYK5) in *P. x canescens*. * = premature stop codons.

PcLYK4-1
***P. tremula* allele** (used for generating the construct of *pAtLYK5:PcLYK4-1_mCitrine*)
ATGAGCTGCCTTTCTGCTGTTTCTTCTTTTGTTCTCTTTATTGTTTGTTGCAGTTCTTTGATTCAAGCTCAGCAACCATAT GTAGGGAAAGGTACGACAAATTGTTCCTTCACAGAAAATTCTGCTCTCGGGTATTCTTGCAACGCCCTAAACAAGAGC TGCCAAGCTTATCTCATCTTCAGATCCCAGCCTCCTTACAACACTGTTGCCTCCATATCTACCCTTTTGGGATCTGACCC ATCTCAGCTCTCTGAAGGAAATTCAGTTTCTGAGACCGCAACATTCCCATCAAACCAGATGGTGATAGTTCCAGTAAA CTGCTCATGTTCAGGCGAGTACTCTCAGGCAAACGCATCTTATATTGTTCAACAGAACGATAATCTTTTGTTGATTGCT AATAACACCTATCAAGGCCTCTCAACCTGTCAAGCTCTCCGGAATCAAAAAAGTACGCGAACTAACGATATTATACTT AGCGGTGAAACACTCACTGTTCCTCTTAGATGTGCCTGTCCCACAAAGAACCAGAGTGATTTAGGTATAAGGTATCTC TTAAGTTACATAGTCATACCGGGAGATACAGTTACAGTTATTAGTGAACAATTTGGCGCAGATACTGGGAGAATTTTC GAGGCTAATGGACTCCCTGAGCAAAATCCCACCATTTTTCCCTCCACAACACTCCTAATTCCTTTACAAAGCACGCCAA

CAAGTTCTCAAACTGTAGTGCCATCACCACCTCCAGCTTCATCTTCACCACCATCACAATCTCCAAACCCTGAAAAAA
GGTCAAAGAAAACATGGCTTTATGTTGTGGTTGGGGTTGTTGGAGGAATTGCTCTTACAGTAGTCATTGGAACCATTA
TTTTCTTCATGTTGTCCCGTAGAAGTAAGAAGCAACCCGGTCCAGTTATCGAATCGCAAAGCTTTGAGGCACATGAGA
AACCACTCAACAAGAAGTTGGATGAAGAATCTCAGGAGTTTTTCGAGAGTATATCCGCTATAGCTCAATCCATCAAAG
TCTACAAGTTTGAAGATCTGAAAGCTGCAACTGATAACTTCAGTCCTAGCTGTTGGATCAAAGGGTCTGTTTATCGTGG
TCTAATCAATGGTGACTTTGCTGCCATTAAGAAGATGAATGGAGACGTGTCTAAAGAGATAGAATTGTTGAATAAGAT
CAACCATTCTAATCTAATTCGCCTCTCCGGTGTTTGTTTCAATGGTGGTCAATGGTACCTGGTTTACGAGTATGCTGCT
AATGGGCAATTGAGTGATTGGATTTATGATAGAAGCAATGAAGGAAAGTTTTTAAACTGGACAAAAAGAATACAGAT
TGCTTCCGATGTCGCCATGGGACTTAATTATCTACATAGTTTCACTAACTATCCGCATGTCCACAAGGATATAACGAGC
AGCAACATTCTTCTTGACAGTGATTTAAGGGCTAAAATTGCAAACTTTTCCCTGGCAAGGTCAACAGGTGACCTGGAT
GGTGAATTTGCTTTGACAAGGCACATTGTTGGGACAAAAGGTTACATGGCTCCTGAGTACTTGGAAAATGGAGTTGTC
TCCTCAAAGCTTGATGTCTATGCATTTGGGATTCTCACTCTGGAGATAATTACCGGGAAAGAAGTTGCTGCTTTACACA
CTGAGGAAAACAGGAACTTATCAGATGTTTTAAATGGTGCTCTATCTGAGGAAGATGGGCAGGAGGAGAGTTTGAAG
CAACTCATTGATCCTTCACTGCATGAGAACTATCCTTCAGGACTTGCTGTTTTAGTGGTCAGATTGATTGATAGTTGCT
TAAACAAAAACCCAGGAGATCGCCCGACCATGGATGAAATCGTGCAGTCTCTCTCAAGAATTTTGACTACTTCTCTAG
CCTGGGAATTGTCTAGCAATGTATCTGGCTACCATATCTCCAGTTAG

MSCLSAVSSFVLFIVCCSSLIQAQQPYVGKGTTNCSFTENSALGYSCNALNKSCQAYLIFRSQPPYNTVASISTLLGSDPSQLS
EGNSVSETATFPSNQMVIVPVNCSCSGEYSQANASYIVQQNDNLLLIANNTYQGLSTCQALRNQKSTRTNDIILSGETLTVPL
RCACPTKNQSDLGIRYLLSYIVIPGDTVTVISEQFGADTGRIFEANGLPEQNPTIFPSTTLLIPLQSTPTSSQTVVPSPPPASSSPP
SQSPNPEKRSKKTWLYVVVGVVGGIALTVVIGTIIFFMLSRRSKKQPGPVIESQSFEAHEKPLNKKLDEESQEFFESISAIAQSI
KVYKFEDLKAATDNFSPSCWIKGSVYRGLINGDFAAIKKMNGDVSKEIELLNKINHSNLIRLSGVCFNGGQWYLVYEYAAN
GQLSDWIYDRSNEGKFLNWTKRIQIASDVAMGLNYLHSFTNYPHVHKDITSSNILLDSDLRAKIANFSLARSTGDLDGEFAL
TRHIVGTKGYMAPEYLENGVVSSKLDVYAFGILTLEIITGKEVAALHTEENRNLSDVLNGALSEEDGQEESLKQLIDPSLHE
NYPSGLAVLVVRLIDSCLNKNPGDRPTMDEIVQSLSRILTTSLAWELSSNVSGYHISS

***P. alba* allele**

ATGAGCTGCCTTTCTGTTGTTTCTTCTTTTGTTCTCTTTATTGTTTGTTGCAGTTCTTTGATTCAAGCTCAGCAACCATAT
GTAGGGAAAGGTACGACAAATTGTGACAACACAGAAAATTCTGCTCTTGGGTATTCTTGCAACGCCCTAAACAAGAG
CTGCCAAGCTTATCTCATCTTCAGATCCCAGCCTCCTTACAACACTGTTGCCTCCATATCTACCCTTTTAGGATCTGACC
CATCTCAGCTCTCTGAAGTAAATTCAGTTTCTGAGACCACATCATTCCCATCAAACCAGATGGTGATAGTTCCAGTAAA
CTGCTCATGTTCAGGCGAGTACTCTCAGGCAAACGCATCTTATATTGCTCAACCGAACGATTATCTTTTGTTGATTGCT
AATAACACCTATCAAGGCCTCTCAACCTGTCAAGCTCTCCGGAATCAAAAAAGTACGCGAACTAACGGTATACTTAGC
GGTGAAACACTCACTGTTCCTCTTAGATGTGCCTGTCCCACAAAGAACCAGAGTGATTTAGGTATAAGGTATCTCTTA
AGTTACATAATCATACCGGGAGATACAGTTACAGTTATTAGTGAACAATTTGGCGCAGATACTGGGAGAATTTTCGAG
GCTAATGGACTCCCTGAGCAAAATCCCACCATTTTTCCCTCCACAACACTCCTAATTCCTTTACAAAGCACGCCAACAA
GTTCTCAAACTGTAGTGCCACCACCACCTCCAGCTTCATCTTCACCACCATCACCATCTCCAAACCCTGAAAAAAGCTC
AAAGAAAACATGGCTTTATGTTGTGGTTGGGGTTGTTGGAGGAATTGCTCTTACAATAGTCATTGGAACCATTATTTTC
TTCATGTTGTCCCGTAAAAGTAAGAAGCAACCCGGTCCAGTTATCGAATCGCAAAGCTTTGAGGCACATGAGAAACCA
CTCAACAAGAAGTTGGATGAAGAATCTCAGGAGCTTTCCGAGAGTATATCCGCTATAGCTCAATCCATCAAAGTCTAC
AAGTTTGAAGATCTGAAAGCTGCAACTGATAACTTCAGTCCTAGCTGTTGGATCAAAGGGTCTGTTTATCGTGGCCTA
ATCAATGGTGACTTTGCTGCCATTAAGAAGATGAATGGAGACGTGTCTAAAGAGATAGAATTATTGAATAAGATCAAC
CATTCTAATCTAATTCGCCTCTCCGGGGTTTGTTTCAATGGTGGTCAATGGTACCTGGTTTACGAGTATGCTGCTAATG
GACAATTGAGTGATTGGATTTATGATAGAAGCAATGAAGGGAAGTTTTTAAGTTGGACAAAAAGAATACAGATTGCTT
CCGATGTCGCCATGGGACTTAATTATCTACATAGTTTCACTAACTATCCGCATGTCCACAAGGATATAAAGAGCAGCA
ACATTCTTCTTGACAGTGATTTAAGGGCTAAAATTGCAAACTTTTCCCTGGCAAGGTCAACAGGTGGCCTGGATGGTG
AATTTGCTTTGACAAGGCACATTGTTGGGACAAAAGGTTACATGGCTCCTGAGTACTTGGAAAATGGAGTTGTCTCCT
CAAAGCTTGATGTCTATGCATTTGGGATTCTCACTCTGGAGATAATTACCGGGAAAGAAGTTGCTGCTTTACACACTG
AGGAAAACGGGAACTTATCAGATGTTTTAAATGGTGCTCTATCTGAGGAAGATAGGCAGGAGGAGAGTTTGAAGCAA
CTCATTGATCCTTCACTGCATGAGAGCTATCCTTCAGGACTTGCTGTTTTAGTGGTCAGATTGATTGATAGTTGCTTAA
ACAAAAACCCAGGAGATCGCCCGACCATGGATGAAATCGTGCAGTCTCTCTCAAGAATTTTAACTACTTCGCTAGCCT
GGGAGTTGTCTAGCAATGTATCTGGCTATCATATCTCTAGTTAG

MSCLSVVSSFVLFIVCCSSLIQAQQPYVGKGTTNCDNTENSALGYSCNALNKSCQAYLIFRSQPPYNTVASISTLLGSDPSQL
SEVNSVSETTSFPSNQMVIVPVNCSCSGEYSQANASYIAQPNDYLLLIANNTYQGLSTCQALRNQKSTRTNGILSGETLTVPL
RCACPTKNQSDLGIRYLLSYIIIPGDTVTVISEQFGADTGRIFEANGLPEQNPTIFPSTTLLIPLQSTPTSSQTVVPPPPPASSSPPS
PSPNPEKSSKKTWLYVVVGVVGGIALTIVIGTIIFFMLSRKSKKQPGPVIESQSFEAHEKPLNKKLDEESQELSESISAIAQSIK
VYKFEDLKAATDNFSPSCWIKGSVYRGLINGDFAAIKKMNGDVSKEIELLNKINHSNLIRLSGVCFNGGQWYLVYEYAANG
QLSDWIYDRSNEGKFLSWTKRIQIASDVAMGLNYLHSFTNYPHVHKDIKSSNILLDSDLRAKIANFSLARSTGGLDGEFALT
RHIVGTKGYMAPEYLENGVVSSKLDVYAFGILTLEIITGKEVAALHTEENGNLSDVLNGALSEEDRQEESLKQLIDPSLHESY
PSGLAVLVVRLIDSCLNKNPGDRPTMDEIVQSLSRILTTSLAWELSSNVSGYHISS

PcLYK4-2

***P. tremula* allele** (used for generating the construct of *pAtLYK5:PcLYK4-2_mCitrine*)

ATGAGCTTCCGTTCTGTTGTTTCTCCTTTCGCTCTCTTCGTTCTTTATTGCTGTTCTTTGATTCAAGCTCAGCAGCCTTAC
GTGGGGAAAGGTACAACAAAGTGTTCAAACACACAGAATTCCGCTCTGGGATATTCTTGCAATGGCCTGAACAAGAG
TTGCCAAGCTTATCTGACCTTCAGATCCCAACCTCCTTACACTACTGTTGCCTCCATATCTACTCTTTTGGCTTCAGACC
CATCTCAGCTCTCTCAAATGAATTCAGTTTCCGAGACTGCATCATTTCCAACAAACCAGTTGGTGCTGGTTCCCGTCAA
CTGCTCATGTTCAGGCGATTATTTTCAGGCAAACGCATCTTACATTGTTCAACCAGGTAACACTCCTTTCTTGATTGCT
AATAACACTTATCAAGGCCTCTCAACCTGTCAAGCTATCCGGAATCTAAAAAGTACACTCACTGTCGATATATTTGCTG
GTGAGACACTCACTGTTCCTCTTAGATGTGCCTGTCCTACAAAGAACCAGAGTGATTTAGGTATCAGGTATCTGTTAAG
TTACTTAGTCACACAGGGCGATACAGTTTCAAGAGCTAGTGTACGATTTGGTGCAGATATCGGGAGAGCTCTTGAAGC
AAATGAAATCAGTGAGAAATATCCCACGATTTACCCCTTCACAACACTCCTAATTCCTCTAAAAAACCCACCAACAAG
TTCACAAACTGTAGTGCCACCTCCACCTCCAGCTTCACCTGCACCTCCACCTCCACCTCCACCTCCACCACCGTCACCA

AACTCCGTCAAAAGCTCAAACACAACATGGGTCTATGTTGTCGTTGGGGTTTTTGGAGGAATTGTTCTTACACTAGTCA
TTGGAACCATTATTTTCTTCATGTTCTTCCGAAAAAGTAAGAAGCAACCGGGTCCAATTATCGTGTCACAAAGCTTTCA
GGCACATGAGAAACCACTCAACAGGAAGTTGGATGAAGAACCTCAGGATTTGTTAGAGAGTGTTTATAGCATAGCTC
AATCCATCAAAGTCTACAACTATGAAGATCTGAAAGCTGCAACAGATAACTTCAGTCCCAGTTGTTGGATCAAAGGGT
CTGTTTTTCGTGGCCTAATCAATGGTGATTTCGCTGCCATTAAGAAGATGAACGGAGACGTGTCTAAGGAGATAGATT
TATTGAATAAGATCAGCCACTCTAATCTAATTCGCCTCTCTGGTGTTTGTTTCAATGACGGGCATTGGTACCTGGTTTA
CGAGTATGCTGCCAATGGACCTCTGAGTGATTGGATTCATGTTAGCAGCAACGAAGGAAAGTTCTTGAAATGGACACA
AAGGATACAGATTGCTACGGATGTAGCTACAGGGCTTAACTACCTGCATTGTTTTACTGACTATCCTCATGTCCACAAG
GATATAAAGAGCAGCAACATACTTCTTGATAATGATTTAAGGGCTAAGATTGCAAACTTTTCCCTGGCAAGGTCAACA
GATGGGCCGGAAGGTGAATTCGCATTGACAAGGCACATCGTTGGGACTAAAGGTTACATGGCTCCTGAGTACCTGGA
AAATGGTATTATCTGTACAAAACTTGATGTCTATGCATTTGGAGTTCTCACACTGGAGATAATGACTGGGAAAGAAGT
TGCTGCTCTTTACGGAGAGGAAAACAGGGAGCTATCTGATGTTTTAAATGGTGTTCTTTCAGAGGAAGGTGGGCTGGA
GGAGAGTCCGAGTCAGCTTATTGATCCTTCAATGCAAGGGAATTATCCTTCAGGACTCGCCGTTTTAATGGTCAGATTG
ATTGATAGTTGCTTGAGTAAAAATCCAGCAGATCGCCCGGCCATGGATGAAATCGTGCAGGCTCTCTCAGGAATTTTG
ACTACTTCTCTGGCCTGGGAATTGTCAAACAACACATCTAGCTACCATAGTTCGAATTAG

MSFRSVVSPFALFVLYCCSLIQAQQPYVGKGTTKCSNTQNSALGYSCNGLNKSCQAYLTFRSQPPYTTVASISTLLASDPSQ
LSQMNSVSETASFPTNQLVLVPVNCSCSGDYFQANASYIVQPGNTPFLIANNTYQGLSTCQAIRNLKSTLTVDIFAGETLTVP
LRCACPTKNQSDLGIRYLLSYLVTQGDTVSRASVRFGADIGRALEANEISEKYPTIYPFTTLLIPLKNPPTSSQTVVPPPPPASP
APPPPPPPPPPSPNSVKSSNTTWVYVVVGVFGGIVLTLVIGTIIFFMFFRKSKKQPGPIIVSQSFQAHEKPLNRKLDEEPQDLLE
SVYSIAQSIKVYNYEDLKAATDNFSPSCWIKGSVFRGLINGDFAAIKKMNGDVSKEIDLLNKISHSNLIRLSGVCFNDGHWY
LVYEYAANGPLSDWIHVSSNEGKFLKWTQRIQIATDVATGLNYLHCFTDYPHVHKDIKSSNILLDNDLRAKIANFSLARSTD
GPEGEFALTRHIVGTKGYMAPEYLENGIICTKLDVYAFGVLTLEIMTGKEVAALYGEENRELSDVLNGVLSEEGGLEESPSQ
LIDPSMQGNYPSGLAVLMVRLIDSCLSKNPADRPAMDEIVQALSGILTTSLAWELSNNTSSYHSSN

***P. alba* allele**

ATGAGCTTCCGTTCTGTTGTTTCTCCTTTCGCTCTCTTCGTTCTTTATTGCTGTTCTTTGATTCAAGCTCAGCAGCCTTAC
GTGGGGAAAGGTACAACAAAGTGTTCAAACACAGAGAATTCCGCTCTGGGGTATTCTTGCAATGGCCTGAACAAGAG
TTGCCAAGCTTATCTGACCTTCAGATCCCAACCTCCTTACACTACTGTTGCCTCCATATCTACTCTTTTGGCTTCAGACC
CATCTCAGCTCTCTCAAATGAATTCAGTTTCCGAGACTGCACCATTTCCAACAAACCAGTTGGTGCTGGTTCCTGTCAA
CTGCTCATGTTCCGGCGATTATTTTCAGGCAAACGCATCTTATATTGTTCAACCAGGTAACACTCCGTTCTTGATTGCT
AACAACACTTATCAAGGCCTCTCAACCTGTCAAGCTATCCGGAATCTAAAAAGTACACTCACTGTCGATATATTTGCT
GGTGAGACACTCACTGTTCCTCTTAGATGTGCCTGTCCTACAAAGAACCAGAGTGATTTAGGTATCAGGTATCTGTTAA
GTTACTTAGTCACACAGGGCGATACAGTTTCAATTGCTAGTGTACGATTTGGTGCAGATATCGGGAGAGCTCTTGAAG
CAAATGAAATCAGTGAGAAATATCCCACGATTTACCCCTYCACAACACTCCTAATTCCTCTAAAAAACCCACCAAGAA
GTTCACAAACTGTAGTGCCACCTCCACCTCCAGCTTCACCTTCACCTTCACCTCCACCACCGTCACCAAACTCCGTCAA
AAGCTCAAACACAACATGGGTTTATGTTGTCGTTGGGGTTTTTGGAGGAATTGTTCTTACACTAGTCATTGGAACCATT
ATTTTCTTCATGTTCTTCCGAAAAAGTAAGAAGCAACCGGGTCCAATTATCGTGTCACAAAGCTTTGAGGCACATGAG
AAACCACTCAACAGGAAGTTGGATGAAGAACCTCAGGATTTGTTAGAGAGTGTTTATAGCATAGCTCAATCCATCAAA
GTCTACAACTATGAAGATCTGAAAGCTGCAACAGATAACTTCAGTCCCAGTTTTTGGATCAAAGGGTCTGTTTTTCGTG
GCCTAATCAATGGTGATTTCGCTGCCATTAAGAAGATGAACGGAGACGTGTCCAAGGAGATAGATTTATTGAATAAGA
TCAACCACTGTAATCTAATTCGCCTCTCTGGTGTTTGTTTCAATGATGGGCATTGGTACCTGGTTTACGAGTATGCTGC
CAATGNACCTTTGAGTGATTGGATTCATGTTAGCAGCAACGAAGGAAAGTTCTTGAAATGGACACAAAGGATACAGA
TTGCTACGGATGTAGCTACAGGGCTTAACTATCTGCATAGTTTTACTGACTATCCTCATGTCCACAAGGATATAAAAAG
CAGCAACATACTTCTTGATAATGATTTAAGGGCTAAGATTGCAAACTTTTCCCTGGCAAGGTCAACAGATGGGCCGGA
AGGTGAATTCGCATTGACAAGGCACATCGTTGGGACTAAAGGTTACATGGCTCCTGAGTACCTGGAAAATGGTATTAT
CTGTACAAAACTTGATGTCTATGCATTTGGAGTTCTCACACTGGAGATAATGACTGGGAAAGAAGTTGCTGCTCTATA
CAGAGAGGAAAACAGGGAGCTATCTGATGTTTTAAATGGTGTTCTTTCTGAGGAAGGTGGGCTGGAGGAGAGTCTGA
GTCAGATTATTGATCCTTCAATGCATGGGAATTATCCTTCAGGACTCGCCGTTTTAATGTTCAGATTGATTGACAGTTG
CTTGAGTAAAAATCCAGCAGATCGCCCGGCCATGGATGAAATCGTGCAGGCTCTCTCAGGAATTTTGACTACTTCTCT
GGCCTGGGAATTGTCAAACAACACATCTAGCTACCATAGTTCGAATTAG

MSFRSVVSPFALFVLYCCSLIQAQQPYVGKGTTKCSNTENSALGYSCNGLNKSCQAYLTFRSQPPYTTVASISTLLASDPSQL
SQMNSVSETAPFPTNQLVLVPVNCSCSGDYFQANASYIVQPGNTPFLIANNTYQGLSTCQAIRNLKSTLTVDIFAGETLTVPL
RCACPTKNQSDLGIRYLLSYLVTQGDTVSIASVRFGADIGRALEANEISEKYPTIYPXTTLLIPLKNPPRSSQTVVPPPPPASPS
PSPPPPSPNSVKSSNTTWVYVVVGVFGGIVLTLVIGTIIFFMFFRKSKKQPGPIIVSQSFEAHEKPLNRKLDEEPQDLLESVYSI
AQSIKVYNYEDLKAATDNFSPSFWIKGSVFRGLINGDFAAIKKMNGDVSKEIDLLNKINHCNLIRLSGVCFNDGHWYLVYE
YAANXPLSDWIHVSSNEGKFLKWTQRIQIATDVATGLNYLHSFTDYPHVHKDIKSSNILLDNDLRAKIANFSLARSTDGPEG
EFALTRHIVGTKGYMAPEYLENGIICTKLDVYAFGVLTLEIMTGKEVAALYREENRELSDVLNGVLSEEGGLEESLSQIIDPS
MHGNYPSGLAVLMFRLIDSCLSKNPADRPAMDEIVQALSGILTTSLAWELSNNTSSYHSSN

PcLYK4-3

***P. tremula* allele**

ATGAATCAGCTTCTTCTGAGTCTCCTATTTTTGTTCTATTTATCTCCAAATCTCCATGCCCAACAAAATTATTCAGGAAA
CGCAGTGTTACGTACCTGGAGGAAAAGAAGAAGAATGCAGGAAGTGCAAGATTAATAACGTCTACTGTTAGTTAGTT
AGCATTAAGTCAGTTAACAGAGTTTGTTACAACAGTTAGAGCTAGTTAGAGTAATCAGTTAGTAGTTATTACAATGAC
TATAAAAGCAGATGGCAGGAATCACATTAGACACGAAATATATAGAATACAGAAAATTCAGTCTCAACTCTTCTCTTT
CGAATCCTCTCTAACAATTCCTCTGTTCTTTGCCTCCTTTCTTCTTCACTTGTTAAGCAACCTTAACACGCAGTCATGGA
TTGTGATAACAGCGATGCAACGGGTCCATCTCCAGCTTTTCTCTACACCTGCAACGTCAAGAATCGATCATGCCAAGC
CTTTCTCATCTACAAATCTCAGCCTCCTTATAACACAATCTCTAGTTTTTCAAACCTCCTGTCTGCAGACCGACTTGAGC
TTGCTCGCATCAACAATTTCTCAAGCTCAGCTGTCTTCCCAACAGATAAAGAGGTAATAGTTCCTATACTTTGCTCCTG
CTCAGGGAAATACTATCAGGCCAACACCTCTTACACAATTCCAAGTAATTATGATACATATTTTACAATTGCCAACTAC
ACTTATGAGGGTTTAGCAACTTGTAGCTCTCTTATTCACGAAAACAATTACAGCGAATTTGGCTTGGATATTGGTATGA
AACTGCAGGTGCCACTTAGATGTGCTTGTCCTACAAGCAATCAAACCAAAAATGGCACAAAGTATCTATTAAGTTACT

TGGTCAGTTGGGGTGATGAAGTTCGTAATGTCAGTAGGAGATTCAATGCGAGCACAAACAGTGTAACCTATGCAAATG
TGTTCACTGAAGATAATCCAACTGTTTTTCCTTTTACCACTACTCTTATTCCACTGTCAAATGAACCTTCAAGCTCTCAA
ACCATAATTCACTATCCACTACCGCCCAATTCTTCTCCTTCCAATCCACTTCATCGGATCGAGAGACCAAGTAAGGGAT
CTCAAAGAACAATCACAATTGGAATTTCCTTGCTAGTCATATCCTTCATTTTATCTATGGTCTTGTTGCTTTACAAAAA
AAACTATGTGGAGCTCGGAAGGATGGAAAGGAGAAAAAGATATTATCTATGTCAGAAGAATTCCGACATCACGTTGC
TGAGATAGATCAGGGGTTGAAAATCTACAAATTTGAGGAGCTAAGGGTGGCTACCAAAGATTTCAGCACTGAAAATA
GATTGAGTTGTTCCGTCTATCAAGGGGTACTCGGTGGACAAGTAGTAGCGATAAAAAAGATGAGCAAAGATGTATCT
AATGAGGTGATTTTTCTGAGAAAGATTAACCACTTCAATTTAATAAGGCTTTATGCTGCGTGTGAGCATCAGGAGGGT
TTCTACCTTATCTATGAGTTTATGGAGAATGGTTCTTTGAGAGATTGGCCCTGCAGAAAGGATTGTCTTGAAGTTCAAA
GTTGGAATTTTAGGATTCAGATTGGCTTGGATGTTGCTAATGGGCTGAACTATCTTCACAACTTCACTGATCCTATATG
TGTGCACAAGCGCATCTGTAGTAGCAATGTTCTACTCAACAGACATTTAAGGGCTCAAATTGCTAACTTCAGCTGTGC
ACATTCAGCAAAGCAAGAAGAATACATGAATTCTTCAATGAGGTTGGCGTTGGGGGAAAAGGTTGTCTGGCTCCTGA
GTACATAGAATATGGCTTGGTGGCTCCTGAGATTGATGTATATGCTTTCGGGGTTGTTCTGCTGGAATTAATAACCGGA
AAGGAAGCAGTTTTTATACAGGATGAAGAAGAAATGAAATTATCGGAAGCAATAATTTCAATTATGGAGGAAGATGA
TGGAGAAGCTGAACTTGGTGGCCTTATAGATCCTTGTCTGATGGAGAAGTGTAGTATGAAACTTGTCCTGCGACTGGT
GAAGTTGAGTCTAGACTGCTTGGAACAAGAACCAGAAAGTAGACCAGGTATGGGTGAAATAGTCTCCTCACTTTAGA
AGATTCAAGTTGATGTACAGAAACCAGAACCATATTTGTGGAGGGGGGTCAATTTCTGA

MNQLLLSLLFLFYLSPNLHAQQNYSGNAVLRTWRKRRRMQEVQD**RLLLVS*H*VS*QSLLQQLELVRVIS**LLQ*L*KQ
MAGITLDTKYIEYRKFSLNSSLSNPL*QFLCSLPPFFFTC*ATLTRSHGL**QRCNGSISSFSLHLQRQESIMPSLSHLQISASL*H
NL*FFKPPVCRPT*ACSHQQFLKLSCLPNR*RGNSSYTLLLLREILSGQHLLHNSK*L*YIFYNCQLHL*GFSNL*LSYSRKQLQ
RIWLGYWYETAGAT*MCLSYKQSNQKWHKVSIKLLGQLG**SS*CQ*EIQCEHKQCNLCKCVH*R*SNCFSFYHYSYSTVK*
TFKLSNHNSLSTTAQFFSFQSTSSDRETK*GISKNNHNWNFLASHILHFIYGLVALQKKLCGARKDGKEKKILSMSEEFRHHV
AEIDQGLKIYKFEELRVATKDFSTENRLSCSVYQGVLGGQVVAIKKMSKDVSNEVIFLRKINHFNLIRLYAACEHQEGFYLIY
EFMENGSLRDWPCRKDCLEVQSWNFRIQIGLDVANGLNYLHNFTDPICVHKRICSSNVLLNRHLRAQIANFSCAHSAKQEE
YMNSSMRLALGEKVVWLLST*NMAWWLLRLMYMLSGLFCWN**PERKQFLYRMKKK*NYRKQ*FQLWRKMMEKLNLV
AL*ILV*WRSVV*NLSCDW*S*V*TAWNKNQKVDQVWVK*SPHFRRFKLMYRNQNHICGGGSIS

***P. alba* allele**

ATGAATCAGCTTCTTCTGAGTCTCCTATTTTTGTTCTATTTATCTCCAAATCTCCATGCCCAACAAAATTATTCAGGAAA
CGCAGTGTTACGTACCTGGAGGAAAAGAAGAAGAATGCAGGAAGTGCAAGATTAATAACGTCTACTGTTAGTTAGTT
AGCATTAAGTCAGTTAACAGAGTTTGTTACAACAGTTAGAGCTAGTTAGAGTAATCAGTTAGTAGTTATTACAATGAC
TATAAAAGCAGATGGCAGGAATCACATTAGACACGAAATATATAGAATACAGAAAATTCAGTCTCAACTCTTCTCTTT
CGAATCCTCTCTAACAATTCCTCTGTTCTTTGCCTCCTTTCTTCTTCACTTGTTAAGCAACCTTAACACGCAGTCATGGA
TTGTGATAACAGCGATGCAACGGGTCCATCTCCAGCTTTTCTCTACACCTGCAACGTCAAGAATCGATCATGCCAAGC
CTTTCTCATCTACAAATCTCAGCCTCCTTATAACACAATCTCTAGTTTTTCAAACCTCCTGTCTGCAGACCGACTTGAGC
TTGCTCGCATCAACAATTTCTCAAGCTCAGCTGTCTTCCCAACAGATAAAGAGGTAATAGTTCCTATACTTTGCTCCTG
CTCAGGGAAATACTATCAGGCCAACACCTCTTACACAATTCCAAGTAATTATGATACATATTTTACAATTGCCAACTAC
ACTTATGAGGGTTTAGCAACTTGTAGCTCTCTTATTCACGAAAACAATTACAGCGAATTTGGCTTGGATATTGGTATGA
AACTGCAGGTGCCACTTAGATGTGCTTGTCCTACAAGCAATCAAACCAAAAATGGCACAAAGTATCTATTAAGTTACT
TGGTCAGTTGGGGTGATGAAGTTCGTAATGTCAGTAGGAGATTCAATGCGAGCACAAACAGTGTAACCTATGCAAATG
GGTTCACTGAAGATAATCCAACTGTTTTTCCTTTTACCACTATTCTTATTCCACTGTCAAATGAACCTTCAAGCTCTCAA
ACCATAATTCACTATCCACTACCGCCCAATTCTTCTCCTTCCAATCCACTTCATCGGATCGAGAGACCAAGTAAGGGAT
CTCAAAGAACAATCACAATTGGAATTTCCTTGCTAGTCATATCCTTCATTTTATCTATGGTCTTGTTGCTTTACAAAAA
AAACTATGTGGAGCTCGGAGGGATGGAAAGGAGAAAAAGATATTATCTATGTCAGAAGAATTCCGACATCACGTTGC
TGAGATAGATCAGGGGTTGAAAATCTACAAATTTGAGGAGCTAAGGGTGGCTACCAAAGATTTCAGCACTGAAAATA
GATTGAGTTGTTCCGTCTATCAAGGGGTACTCGGTGGACAAGTAGTAGCGATAAAAAAGATGAGCAAAGATGTATCT
AATGAGGTGATTTTTCTGAGAAAGATTAACCACTTCAATTTAATAAGGCTTTATGCTGCGTGTGAGCATCAGGAGGGT
TTCTACCTTATCTATGAGTTTATGGAGAATGGTTCTTTGAGAGATTGGCCCTGCAGAAAGGATTGTCTTGAAGTTCAAA
GTTGGAATTTTAGGATTCAGATTGGCTTGGATGTTGCTAATGGGCTGAACTATCTTCACAACTTCACTGATCCTATATG
TGTGCACAAGCGCATCTGTAGTAGCAATGTTCTACTCAACAGACATTTAAGGGCTCAAATTGCTAACTTCAGCTGTGC
ACATTCAGCAAAGCAAGAAGAATACATGAATTCTTCAATGAGGTTGGCGTTGGGGGAAAAGGTTGTCTGGCTCCTGA
GTACATAGAATATGGCTTGGTGGCTCCTGAGATTGATGTATATGCTTTCGGGGTTGTTCTGCTGGAATTAATAACCGGA
AAGGAAGCAGTTTTTATACAGGATGAAGAAGAAATGAAATTATCGGAAGCAATAATTTCAATTATGGAGGAAGATGA
TGGAGAAGCTGAACTTGGTGGCCTTATAGATCCTTGTCTGATGGAGAAGTGTAGTATGAAACTTGTCCTGCGACTGGT
GAAGTTGAGTCTAGACTGCTTGGAACAAGAACCAGAAAGTAGACCAGGTATGGGTGAAATAGTCTCCTCACTTTAGA
AGATTCAAGTTGATGTACAGAAACCAGAACCATATTTGTGGAGGGGGGTCAATTTCTGA

MNQLLLSLLFLFYLSPNLHAQQNYSGNAVLRTWRKRRRMQEVQD**RLLLVS*H*VS*QSLLQQLELVRVIS**LLQ*L*KQ
MAGITLDTKYIEYRKFSLNSSLSNPL*QFLCSLPPFFFTC*ATLTRSHGL**QRCNGSISSFSLHLQRQESIMPSLSHLQISASL*H
NL*FFKPPVCRPT*ACSHQQFLKLSCLPNR*RGNSSYTLLLLREILSGQHLLHNSK*L*YIFYNCQLHL*GFSNL*LSYSRKQLQ
RIWLGYWYETAGAT*MCLSYKQSNQKWHKVSIKLLGQLG**SS*CQ*EIQCEHKQCNLCKWVH*R*SNCFSFYHYSYSTVK
*TFKLSNHNSLSTTAQFFSFQSTSSDRETK*GISKNNHNWNFLASHILHFIYGLVALQKKLCGARRDGKEKKILSMSEEFRHH
VAEIDQGLKIYKFEELRVATKDFSTENRLSCSVYQGVLGGQVVAIKKMSKDVSNEVIFLRKINHFNLIRLYAACEHQEGFYLI
YEFMENGSLRDWPCRKDCLEVQSWNFRIQIGLDVANGLNYLHNFTDPICVHKRICSSNVLLNRHLRAQIANFSCAHSAKQE
EYMNSSMRLALGEKVVWLLST*NMAWWLLRLMYMLSGLFCWN**PERKQFLYRMKKK*NYRKQ*FQLWRKMMEKLNL
VAL*ILV*WRSVV*NLSCDW*S*V*TAWNKNQKVDQVWVK*SPHFRRFKLMYRNQNHICGGGSIS

PcLYK4-4

***P. tremula* allele**

ATGGCAAACTTCTTTCTCAGTTTGCTCACTCTCAGTTTTCTCATTTCATATGCTAATGCTCAACAAAACCACTCGAAGG
ATTCAGCACTAGACTGCAACGCCAATGATGATGCAGGACCATCCTCTGCATTTCTTTACACCTGCACTGGCCAGGACC
AATCTTGCCAGGCCTTTCTGATCTTCAAATCTCAACCTTCTTTTAACTCGGTGCCTTCAATCTCAGCCCTTACGTCGGCA
AACCAAGAAGAGCTGGCAAGAATCAACAATGTTACAAGGCTATCAGAGTTCCCTGCCAACAATGAGGTGATTGTTCC
CGTAAATTGTTTTTGTTTTGGCCAATATTATCAGGCCAACACTACAGTTCAGGTCACGACTACTCGTGGAACCTACTAT

GTCATAGCGAATGAAACTTACGAGGGATTGTCTACTTGTTCTGCGCTTAAGCATTTGAATATACATGGTGAATATGATT
TGTTGCCTGGTGAGGAACTGCAAGTAGCCCTTCGATGTGCTTGCCCTACAACGAATCAAATGATAAGAGGAACAGAGT
ATCTAGTGACTTACCCTCTTAGCTCAAATCATAACATTCCTGATATTGCTGACAGATTCAAAGTAAGCACCAAGGATAT
ACTTGATGCAAATGGCATGGAAGAAAATCCAACTCTTTATCCTGATACAACATTTCTCATACCTCTGCCTACTCAACCT
ACAAAACAATAATTCACAGCAACCCAGACATTTCTCCTCCATCAGCTTTGAGTCCTGGAAATAGAGGATCAAAGAAAA
GACTTTATGAGTCTGCTGGGCTTGCTGCAGCCTGCTCTTTGCTAGTCATCAGTATCATTACAGCTGTCGTTTTTCTCTCT
TGCAAAAAGACAAGAGAAAAAGGTTTCTTGGAGAGGTAGAGAAAGAAAACAGGTAGTGCCAGAAGACATTCGTGTC
GAAATTGCAAGCTATGAGCAAGTTTTGAAAGTCTTCAAATTCGAAGAGGTAAGGAAAACTACTGAAAATCTCAGTTCA
GAAAGTAGAATAAATGGCTCTGTGTATCGTAGAGAGTTTGGTGGGGAGATCTTAGCTGTCAAGAAGATGAGTAGAGA
TGTAACAAAGGAAGTGGACATTTTGAAGAGGATCAACCACTTCAATTTGATTAAGCTTGAAGGTGTATGCGAAAACCG
TGGCTGTTTCTACCTTGTTTTGGAGTATATGGAAAATGGGTCCGTTAGAGAGTGGCTGTCCTGTAAAAAGTTCGAAGA
AACTGGAAATTGGGCACAGAGAATTCAGATTGCTCTGGATGTTGCTAATGGACTTTACTATCTTCACAGCTTCACCGA
ACCTGCCTATGTGCACAAGGACATCAAAAGCAGCAATGTTCTGTTAAACAGCAATCTAAGGGCCAAGATTGCAAATTT
CAGTCTTGCGAGAGCAGCGACAAACGCTGACAAAACATGTTGTGGGCTCTATAGGTTACATGGCGCCTGAGTACGTAC
GGGAAGGACAAGTGACTCCCAAGATTGATGTTTATGCTTTTGGAGTCATTTTGCTGGAACTGATCACAGGGAAAGATG
CTGTTTTCACACAGGATGGCAGGGAAGCCCTCCTTTCAACGGAAATAGTTTCTATCATGGAGAATAAAAACCCTGAAG
TTGAGCTGGATTTCTTTGTCGATCCTGCTCTGAAAGGAAGTTGTGGGACAAACTTCGCATTATGCTTGGCTAAAGTAAG
CGTAGCCTGCTTGATCAAAGAACCAGCAAGGAGACCTAGTATGGAGGAAGTGGTATCAATTCTGTTGAAAATTCAGG
CAAATGCACAGAAATCATAA

MANFFLSLLTLSFLISYANAQQNHSKDSALDCNANDDAGPSSAFLYTCTGQDQSCQAFLIFKSQPSFNSVPSISALTSANQEE
LARINNVTRLSEFPANNEVIVPVNCFCFGQYYQANTTVQVTTTRGTYYVIANETYEGLSTCSALKHLNIHGEYDLLPGEELQ
VALRCACPTTNQMIRGTEYLVTYPLSSNHNIPDIADRFKVSTKDILDANGMEENPTLYPDTTFLIPLPTQPTKQ*FTATQTFLL
HQL*VLEIEDQRKDFMSLLGLLQPALC*SSVSLQLSFFSLAKRQEKKVSWRGRERKQVVPEDIRVEIASYEQVLKVFKFEEV
RKTTENLSSESRINGSVYRREFGGEILAVKKMSRDVTKEVDILKRINHFNLIKLEGVCENRGCFYLVLEYMENGSVREWLSC
KKFEETGNWAQRIQIALDVANGLYYLHSFTEPAYVHKDIKSSNVLLNSNLRAKIANFSLARAATNADKTCCGLYRLHGA*V
RTGRTSDSQD*CLCFWSHFAGTDHRERCCFHTGWQGSPPFNGNSFYHGE*KP*S*AGFLCRSCSERKLWDKLRIMLG*SKRS
LLDQRTSKET*YGGSGINSVENSGKCTEII

***P. alba* allele**

ATGGCAAACTTCTTTCTCAGTTTGCTCACTCTCAGTTTTCTCACTTCATATGCTAATGCTCAACAAAACTACTCGAAGG
ATTCAGCACTAGACTGCAACGCTAATGATGATGCAGGACCATCCTCTGCATTTCTTTACACCTGCAATGGCCAGGACC
AATCTTGCCAGGCCTTTCTGATCTTCAAATCTCAAACTTGTTTTAACTCGGTGCCTTCAATCTCAGCCCTTACGTCGGCA
AACCAAGGAGAGCTGGCAAGAATCAACAATGTTACAAGGCTATCAGAGTTCCCTGCCAACAATGAGGTGATTTTTCCT
GTAAATTGTTTTTGTTTCGACCAATATTATCAGGCCAACACTACAATTCAGGTCACGACTACTCGTGGAACCTACCATG
TCATAGCGAATGAAACTTACGAGGGATTGTCTACTTGTGCTGCGCTTAAGCGTTTGAAATATACATGGTGAATATGATTT
GTTGCCTGGTGAGGAACTGCAAGTAGCACTTCGATGTGCTTGCCCTACAACGAATCAAATGATAAGAGGAACAGAGT
ATCTAGTGACTTACCCTCTTAGCTCAGATGATATCATTCCTGATATTGCTGACAGATTCAAAGTAAGCACCAAGGATAT
ACTTGATGCAAATGGTATGGAAGAAAATCCAACTCTTTATCCTGATACAACAATTCTCATACCTCTGCCTACTCAACCT
ACAAGTTCACAAACAATAATTCACAGCAACCCAGACATTTCTCCTCCATCAGCTTTGAGTCCTAGAAATAGAGGATCA
AAGAAAAGATTTTATGAGTCTTCAGGGCTTGCTGCAGCCTGCTCTTTGCTAGTCATCAGTATCATTACAGCTGTCGTTT
TTCTCTCTTGCAAAAAGACAAGAGAAAAGGTTTCTGGGAGAGGTAGAGAAAGAAAACAGGTAGTGCCAGAAGACATT
CGTGTCGAAATTGCAAGCTATGAGCAAGTTTTGAAAGTCTTCAAATTCGAAGAGGTAAGGAAAGCTACTGAAAATCTC
AGTTCAGAAAGTAGAATAAATGGCTGTGTGTATCGTAGAGAGTTTGGTGGGGAGATCTTAGCTGTCAAGAAGATGAG
TAGAGATGTAACAAAGGAAGTGAACATTTTGAAGAGGATCAACCACTTCAATTTGATTAAGCTTGAAGGTGTATACGA
AAATCGTGGCTGTTTCTACCTTGTTTTGGAGTATATGGAAAATGGGTCCCTTAGAGAGTGGCTGTCCTGTAAATAGTTC
GAAGAAACTGGAAATTGGGCACAGAGAATTCAGATTGCTCTGGATGTTGCTAATGGACTTTACTATCTTGACAGCTTC
ACCGAACCTGCCTATGTGCACAAGGACATCAAAAGCAGCAATGTTCTGTTAAACGGCAATCTAAGGGCCAAGATTGC
AAATTTCAGTCTTGCGAGAGCAGCGACAAACGCTGACAAAACATGTTGTGGGCTCTATAGGTTACATGGCGCCTGAGT
ACGTACGGGAAGGACAAGTGACTCCCAAGATTGATGTTTATGCTTTTGGAGTTATTTTGCTGGAACTGATCACAGGGA
AAGATGCTGTTTTCACACAGGATGGCAGGGAAGCCCTCCTTTCAACGGAAATAGTTTCTATCGTGGAGAATAAAAACC
CTGAAGTTGAGTTGGATTTCTTTGTCGATCCTGCTCAAAAAGGAAGTTGTGGGACAAACTTCGCATTATGCTTGGCTAA
AGTAAGCGTAGCCTGCTTGATGAAAGAACCAGCAAGGAGACCTAGCATGGAGGAAGTGGTATCAATTCTGTTGAAAA
TTCAGGCAAATGTACAGAAATCATAA

MANFFLSLLTLSFLTSYANAQQNYSKDSALDCNANDDAGPSSAFLYTCNGQDQSCQAFLIFKSQTCFNSVPSISALTSANQG
ELARINNVTRLSEFPANNEVIFPVNCFCFDQYYQANTTIQVTTTRGTYHVIANETYEGLSTCAALKRLNIHGEYDLLPGEELQ
VALRCACPTTNQMIRGTEYLVTYPLSSDDIIPDIADRFKVSTKDILDANGMEENPTLYPDTTILIPLPTQPTSSQTIIHSNPDISPP
SALSPRNRGSKKRFYESSGLAAACSLLVISIITAVVFLSCKKTREKVSGRGRERKQVVPEDIRVEIASYEQVLKVFKFEEVRK
ATENLSSESRINGCVYRREFGGEILAVKKMSRDVTKEVNILKRINHFNLIKLEGVYENRGCFYLVLEYMENGSLREWLSCK*
FEETGNWAQRIQIALDVANGLYYLDSFTEPAYVHKDIKSSNVLLNGNLRAKIANFSLARAATNADKTCCGLYRLHGA*VRT
GRTSDSQD*CLCFWSYFAGTDHRERCCFHTGWQGSPPFNGNSFYRGE*KP*S*VGFLCRSCSKRKLWDKLRIMLG*SKRSLL
DERTSKET*HGGSGINSVENSGKCTEII

PcLYK5-1

***P. tremula* allele**

ATGATTCCCTATGACTCTCCTTCCCTTATTGCCAAACTTTTAGGCGCAGCCACTCTTATCGCCTCCATCAATCACATCTC
CTCTGAAAATGCCTCCATTCCCACCACCTCCCAGGTCGTGGTTCCCGTCAACTGCTCCTGTTATGCCCGTCAATATTAC
CAGCACAAAGTCAACTACACACTCAAGCACGGATACGAAACTTCACGGTGGCCAACAACACCTACCAGCTACCAAGG
CCTCACCACTTGCCAGTCCTCGATATCTCAGAACCCCTATGTTTTTCTGAATATGACCGCGGGACTCATTCCCCAGATA
CCCCTGAGGTGTGCTAGCTCACCTACATGGTCAACTGGGCCAATTCCATCTCTTACAAGTGACAAACCCCGGTTGTTCG
GTGTTGACCATCAGAGGCTGTTTGACGCAAACATGCTGTCGTCCTCCAGTGTCATTTTCCCCTTCACTTCTGGTTCCTTT
GACCACTGAGACCACCAAAACTGAACATATCGGCAGTCCCTCCGCTTGCCCAACCTCGCGCAGACCCCCATTGCCCCC
CCCCCCACCCTACTCCCAGCTCTTCCGATCACAATCGGGTGCATGCGGGTGTTGGGATAGGTGCTGATTTGCTCGTTCT

TGTATTTGCGATCTTTGGATTTCTGTTTTGGTACCGCAAATCTCTCAGTACAAGCCTGTCTCCACTTCAAAACCCAACA
CACTGCCAATCTTTTAAGGGCAATACAGCTGCTGTCAAGGTCATGAAAGGGGATGTCTCTAACGAGATTGACATTTTT
TGAAGATGATCAATAACTCCAACGTCATTAGGCTCTCTGGTTTCTGCGTACATGAGGGCAACACTCACCTTGTTTATCA
TTTCACAGAGAATGGCTCTCTCGCTGATTGGCTTCTATCTAACAACAAATACCGAAGCCTTGCATGGATGCAGATAATT
CAGATTGCCCACGACGTGGCTGATGCCCTCAATTGCCTTCTCAACTACACCAACCCTCTCTATATCCACAAAAACTTGA
AGAGCAGCAATATTCTTTTGGATGCCAATTTGAGAGCCAAGCTTGCTGATTTCGGGTTGGCAATAACTCTGGAAAATG
ACCAAGATGGTGGATTTCAATCGACAAGGCACGATAGTGGCTACTCAAAGTTATTTGGCCCCTTGAATACATATAAAA
TGGAGTCTGCCCCGAGATTGGCATCTGGGGTTGTTATGTTGGAGCTCTTATCTGGGAAGGAAGCAGCTGCAGCGGCTA
TTGAAAAGAGTTCAGGTGATGAGTTGCTCTCCGTAATGATAGTGCGTGTGCTTGAGGTAGACAACGTGAGAGAGACTC
TCTGGCTTCCTATACCCCTTGGATCTAGCCTTCCCAATGGCCCAGCAGGCTAAAAGCTGTGTCTATCATGATCTCAATA
CAAGAGCTTCAATGACTCAAGTTTTCATGATATTGTCCAGGTTCCTCTCGTCTTCATTCGACTGGGATCCATCCGATGA
GCTTGATCGCTCTACGTGTCTTTAGGCTAG

MIPYDSPSLIAKLLGAATLIASINHISSENASIPTTSQVVVPVNCSCYARQYYQHKVNYTLKHGYETSRWPTTPTSYQGLTTC
QSSISQNPYVFLNMTAGLIPQIPLRCASSPTWSTGPIPSLTSDKPRLFGVDHQRLFDANMLSSSSVIFPFTSGSFDH*DHQN*TY
RQSLRLPNLAQTPIAPPPTLLPALPITIGCMRVLG*VLICSFLYLRSLDFCFGTANLSVQACLHFKTQHTANLLRAIQLLSRS*K
GMSLTRLTFFEDDQ*LQRH*ALWFLRT*GQHSPCLSFHREWLSR*LASI*QQIPKPCMDADNSDCPRRG*CPQLPSQLHQPSL
YPQKLEEQQYSFGCQFESQAC*FRVGNNSGK*PRWWISIDKAR*WLLKVIWPLEYI*NGVCPEIGIWGCYVGALIWEGSSCS
GY*KEFR**VALRNDSACA*GRQRERDSLASYTPWI*PSQWPSRLKAVSIMISIQELQ*LKFS*YCPGSSRLHSTGIHPMSLIAL
RVFRL

PcLYK5-2

***P. tremula* allele**

ATGGACTTTCTTATACTGTATCTGTATGTGGTGCTTCTGCTCTCACCAGCACTAGTACAAGGGCAACAAACCTATTTAG
CCAACCACCAACTGGACTGCTACAACAATAACTTCAATGAAACGACCAAAGGATTTCTGTGCAACGGAGTTCAGTCAT
CATGCCAATCCTACCTCACCTTCCGATCTATGCCTCCCTACAATTCTCCTGTCTATATTGCGTATCTCTTAGGCGTCCCG
CAATCCGCCACTCTCATCGCCTCCGTCAATAACCTCTCCTCTGACACTGCCCCTATTCCCACCGACTTCCAGGTCGTGG
TTCCAGTCAACTGCTCCTGTTATGACCGTCAATATTACCAGCACAATTCCAGCTATCTGCTCAAGGAAAAATCCGAAA
CCTACTTCACCGTGGCCAACAACACCTACCAAGGCCTCACCACATGCCAGTCCTTGATGTCTCAGAATCCCTACGGCG
ATCGGAATCTGTCAATCGGTCTCAATCTCCAAATACCCCTGAGGTGTGCTTGCCCAACTTCCAACCAGAATGCTTCAGG
GATCAACTACTTGCTCACCTACATGGTCACTTTTGGCGATACCATCTCTTCCATTGCCGAGCTGTTTGGCGTTGACAAG
CAGAGGGTACTTGATGCAAACAAGCTGTCTTCCTCCGATATCATTTTCCCCTTCACTCCGATTCTGGTTCCTCTGCCCAC
TAACCCCACCAAAATCGAAAAGCCATCGGCAGCCCCTCCGCCGGCCGCACCATCTCCGCAGACTCCCAATGTTTCCGT
TGGGGGCTCTTCCGATCACAAAGCCTTGTATGTGGGTGTTGGGATAGGAGCTGCTTTCCTCGTTCTTCTATCTGCTGCT
TTTGGATTTCTGTTTTGGCACCGCAAATCTCGTAAGCAACACAAGCCTGTCTCCACTTCAGAAACCAAAACACTGCCAT
CAGACTCTACTGATTTCACTGTACTCCCAGTCTCCAGCAACAAATCGTGGTCTCTCTCTCCTAATGACGCCCGATATGC
TATTGAGTCCTTGACTGTCTACAAATACGAGGACTTACAAGTGGCCACCGGGTACTTCGCCCAAGCTAATCTGATCAA
GGGCTCGGTTTATAGGGGATCTTTCAAGGGTGACACAGCCGCAGTCAAGGTCGTGAAAGGAGATGTCTCCAGCGAGA
TCAACATTTTGAAGATGATCAATCACTCCAACGTCATCAGGCTCTCTGGTTTCTGCTTACATGAGGGCAACACTTACCT
TGTTTATGAGTACGCCGACAATGGCTCTCTCACTGATTGGCTTCACTTTAACAACACATACCGAATTCTTGCTTGGAAG
CAGAGAGTTCGGATTGCCTACGATGTGGCTGATGCCCTCAATTACCTTCACAACTACACCAACCCGTCCTATATCCATA
AGAACTTGAAGACCAGCAACATTCTTTTGGATGCCAACTTGAGAGCCAAGGTTGCTAATTTCGGCTTGGCAAGAACAC
TGGAAAATGACCAAGATGGTGGACTGCAACTGACAAGACATGTGGTAGGCACTCAAGGTTATTTGGCCCCCGAGTAC
ATCGAGAATGGAGTTATCACCCCGAAATTAGATGTTTTTGCTTTCGGGGTTGTGATGTTGGAGCTCTTATCTGGGAAGG
AAGCAGCTGCTACAGCTATTGACAAGAGTGCAGGAGACGACTTGCTCTCTGTAATGATAATGCGTGTGCTTGAGGGGG
ACAATGTGAGAGAGAAACTCTCTGCCTTCCTGGACCCTTGCCTAAGAGACGAGTACCCCTTGGATCTAGCTTTCTCAAT
GGCCCAACTGGCTAAAAGCTGTGTCGAGCATGATCTCAATACACGACCTTCAATGCCTCAAGTTTTCATGATGTTGTCC
AAGATCCTCTCGTCTTCGTTGGACTGGGATCCATCCGATGAGCTCAATCGATCTAGGTCTATAGACAGTGGCAGGTAG

MDFLILYLYVVLLLSPALVQGQQTYLANHQLDCYNNNFNETTKGFLCNGVQSSCQSYLTFRSMPPYNSPVYIAYLLGVPQS
ATLIASVNNLSSDTAPIPTDFQVVVPVNCSCYDRQYYQHNSSYLLKEKSETYFTVANNTYQGLTTCQSLMSQNPYGDRNLSI
GLNLQIPLRCACPTSNQNASGINYLLTYMVTFGDTISSIAELFGVDKQRVLDANKLSSSDIIFPFTPILVPLPTNPTKIEKPSAAP
PPAAPSPQTPNVSVGGSSDHKALYVGVGIGAAFLVLLSAAFGFLFWHRKSRKQHKPVSTSETKTLPSDSTDFTVLPVSSNKS
WSLSPNDARYAIESLTVYKYEDLQVATGYFAQANLIKGSVYRGSFKGDTAAVKVVKGDVSSEINILKMINHSNVIRLSGFCL
HEGNTYLVYEYADNGSLTDWLHFNNTYRILAWKQRVRIAYDVADALNYLHNYTNPSYIHKNLKTSNILLDANLRAKVAN
FGLARTLENDQDGGLQLTRHVVGTQGYLAPEYIENGVITPKLDVFAFGVVMLELLSGKEAAATAIDKSAGDDLLSVMIMR
VLEGDNVREKLSAFLDPCLRDEYPLDLAFSMAQLAKSCVEHDLNTRPSMPQVFMMLSKILSSSLDWDPSDELNRSRSIDSG
R

***P. alba* allele** (used for generating the construct of *pAtLYK5:PcLYK5-2_mCitrine*)

ATGGACTTTCTTATACTGTATCTGTATGTGGTGCTTCTGCTCTCACCAGCACTAGTACAAGGGCAACAAACCTATTTAG
CCAACCACCAACTGGACTGCTACAACAATAACTTCAATGAAACGACCAAAGGATTTCTGTGCAACGGAGTTCAGTCAT
CATGCCAATCCTACCTCACCTTCCGATCTATGCCTCCCTACAATACTCCTGTCTATATTGCGTATCTCTTAGGCGTCCCG
CAATCCGCCACTCTCATCGCCTCCGTCAATAACCTCTCCTCTGACACTGCCACTATTCCCACCGACTTCCAGGTCGTGG
TTCCAGTCAACTGCTCCTGTTATGACCGTCAATATTACCAGCACAATTCCACCTATCAGCTCAAGGACGAAACCGAAA
ACTACTTCACCGTGGCCAACAACACCTACCAAGGCCTCACCACATGCCAGTCCTTGATGTCTCAGAATCCCTACGGCG
ATCGGAATCTGTCAAAGGGTCTCAATCTCCAAATACCCCTGAGGTGTGCTTGCCCAACTTCCAACCAGAATGCTTCAG
GGATCAACTACTTGCTCACCTACATGGTCACTTGGGGCGATACCATCTCTTCCATTGCCGAGCTGTTTGGCGTTGACGT
GCAGAGGGTACTTGATGCAAACAAGCTGTCTTCCTCCGATATCATTTTCCCCTTCACTCCGATTCTGGTTCCTCTGCCC
ACTAACCCCACCAAAATCGAAAAGCCATCGGCAGCCCCTCCGCCGGCCTCACCATCTCCGCAGACTCCCAATGTTTCC
GTTGGGGGCTCTTCCGATCACAAAGCCTTGTATGTCGGTGTTGGGATAGGAGCTGCTTTCCTCATTCTTCTATCTGCTG
CTTTTGGATTTCTGTTTTGGCACCGCAAATCTCGTAAGCAACACAAGCCTGTCTCCACTTCAGAAACCAAAACACTGCC
ATCAGACTCTACTGATTTCACTGTACTCCCAGTCTCCAGCAACAAATCGTGGTCTCTCTCTCCTAATGACGCCCGATAT
GCTATTGAGTCCTTGACTGTCTACAAATACGAGGACTTACAAGTGGCCACCGGGTACTTCGCCCAAGCTAATCTGATC

AAGGGCTCGGTTTATAGGGGATCTTTCAAGGGTGACACAGCCGCAGTCAAGGTCGTGAAAGGAGATGTCTCCAGCGA
GATCAACATTTTGAAGATGATCAATCACTCCAACGTCATCAGGCTCTCTGGTTTCTGCTTACATGAGGGCAACACTTAC
CTTGTTTATGAGTACGCCGACAATGGCTCTCTCACTGATTGGCTTCACTTTAACAACACATACCGAATTCTTGCTTGGA
AGCAGAGAGTTCGGATTGCCTACGATGTGGCTGATGCCCTCAATTACCTTCACAACTACACCAACCCGTCCTATATCC
ATAAGAACTTGAAGACCAGCAACATTCTTTTGGATGCCAACTTGAGAGCCAAGGTTGCTAATTTCGGTTTGGCAAGAA
CACTGGAAAATGACCAAGATGGTGGACTGCAACTGACAAGACATGTGGTAGGCACTCAAGGTTATTTGGCCCCCGAG
TACATCGAGAATGGAGTTATCACCCCGAAATTAGATGTTTTTGCTTTCGGGGTTGTGATGTTGGAGCTCTTATCTGGGA
AGGAAGCAGCTGCTACAGCTATTGACAAGAGTGCAGGAGACGACTTGCTCTCTGTAATGATAATGCGTGTGCTTGAGG
GGGACAATGTGAGAGAGAAACTCTCTGCCTTCCTGGACCCTTGCCTAAGAGACGAGTACCCCTTGGATCTAGCTTTCT
CAATGGCCCAACTGGCTAAAAGCTGTGTCGAGCATGATCTCAATACACGACCTTCAATGCCTCAAGTTTTCATGATGTT
GTCCAAGATCCTCTCGTCTTCGTTGGACTGGGATCCATCCGATGAGCTCAATCGATCTAGGTCTATAGACAGTGGCAG
GTAG

MDFLILYLYVVLLLSPALVQGQQTYLANHQLDCYNNNFNETTKGFLCNGVQSSCQSYLTFRSMPPYNTPVYIAYLLGVPQS
ATLIASVNNLSSDTATIPTDFQVVVPVNCSCYDRQYYQHNSTYQLKDETENYFTVANNTYQGLTTCQSLMSQNPYGDRNLS
KGLNLQIPLRCACPTSNQNASGINYLLTYMVTWGDTISSIAELFGVDVQRVLDANKLSSSDIIFPFTPILVPLPTNPTKIEKPSA
APPPASPSPQTPNVSVGGSSDHKALYVGVGIGAAFLILLSAAFGFLFWHRKSRKQHKPVSTSETKTLPSDSTDFTVLPVSSNK
SWSLSPNDARYAIESLTVYKYEDLQVATGYFAQANLIKGSVYRGSFKGDTAAVKVVKGDVSSEINILKMINHSNVIRLSGFC
LHEGNTYLVYEYADNGSLTDWLHFNNTYRILAWKQRVRIAYDVADALNYLHNYTNPSYIHKNLKTSNILLDANLRAKVA
NFGLARTLENDQDGGLQLTRHVVGTQGYLAPEYIENGVITPKLDVFAFGVVMLELLSGKEAAATAIDKSAGDDLLSVMIM
RVLEGDNVREKLSAFLDPCLRDEYPLDLAFSMAQLAKSCVEHDLNTRPSMPQVFMMLSKILSSSLDWDPSDELNRSRSIDS
GR

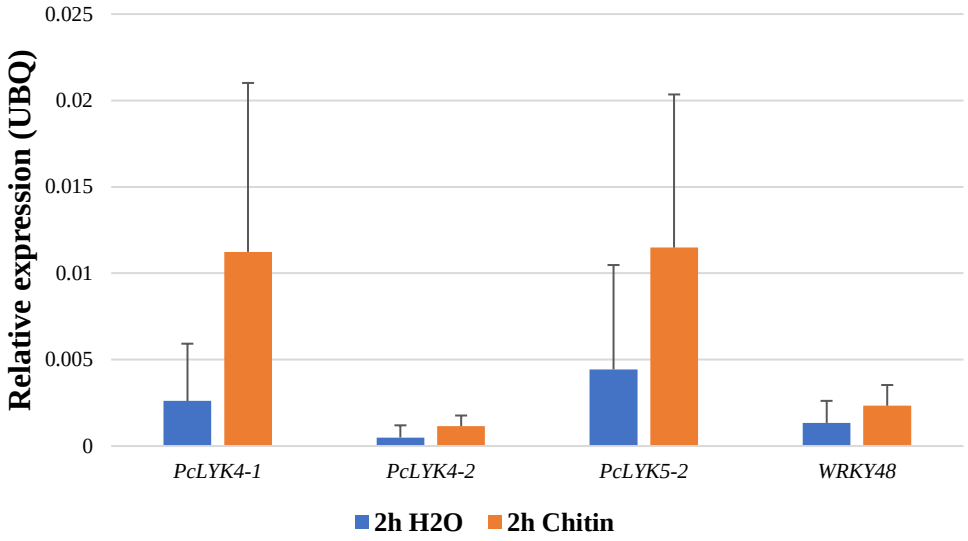

Supplemental Figure 4.1. Expression levels of genes encoding LysM-RLKs (*PcLYK4-1*, *PcLYK4-2* and *PcLYK5-2*) in leaves of *P. x canescens* show a tendency to increase after chitin treatment . Chitin responsive gene *WRKY48* was included as a control. qRT-PCR was repeated independently twice and results showed the same tendency. Statistical analysis did not show significant differences among the tested groups. Data are means ± standard deviation (n = 3 biological replicates). For statistical analysis, two-way anova ($P \leq 0.05$) was performed.

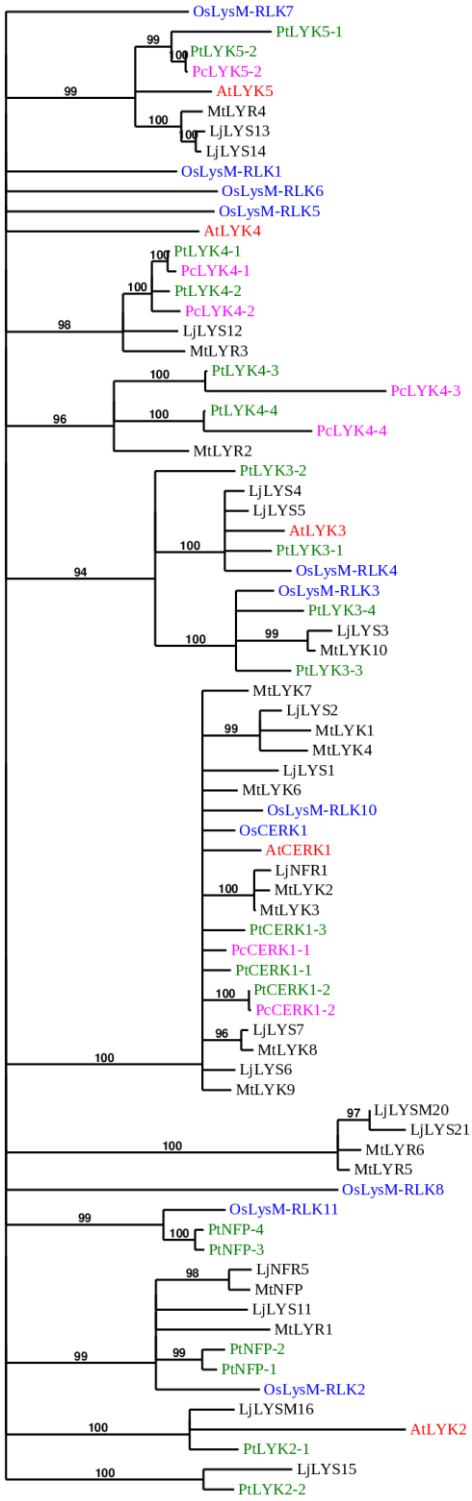

Supplemental Figure 4.2. The genomes of *P. trichocarpa* and *P.* x *canescens* code for several LYK4 and LYK5 paralogs. A phylogenetic tree of LysM-RLKs was constructed based on sequence similarity of putative *P. trichocarpa*-Nisqually proteins (green) and sequencing results of LysM-RLKs from *P. x canescens* (*P. tremula* allele in magenta) with well-characterized LysM-RLKs from *Arabidopsis thaliana* (red), *Oryza sativa* (blue), *Medicago truncatula* and *Lotus japonicus* (black). Two homologs of *AtCERK1*, four homologs of *AtLYK4*, and two homologs of *AtLYK5* are encoded by the *P. x canescens* genome. The phylogenetic analysis was done with phylogeny.fr (Dereeper et al., 2008; Dereeper et al., 2010) using MUSCLE for multiple alignment (default settings), Gblocks for alignment curation (least stringent settings), PhyML for phylogenetic tree construction (for the maximum likelihood) and TreeDyn for the visualization of phylogenetic tree, displaying only branch support values of >90 % (boostrapping of 500 replicates).

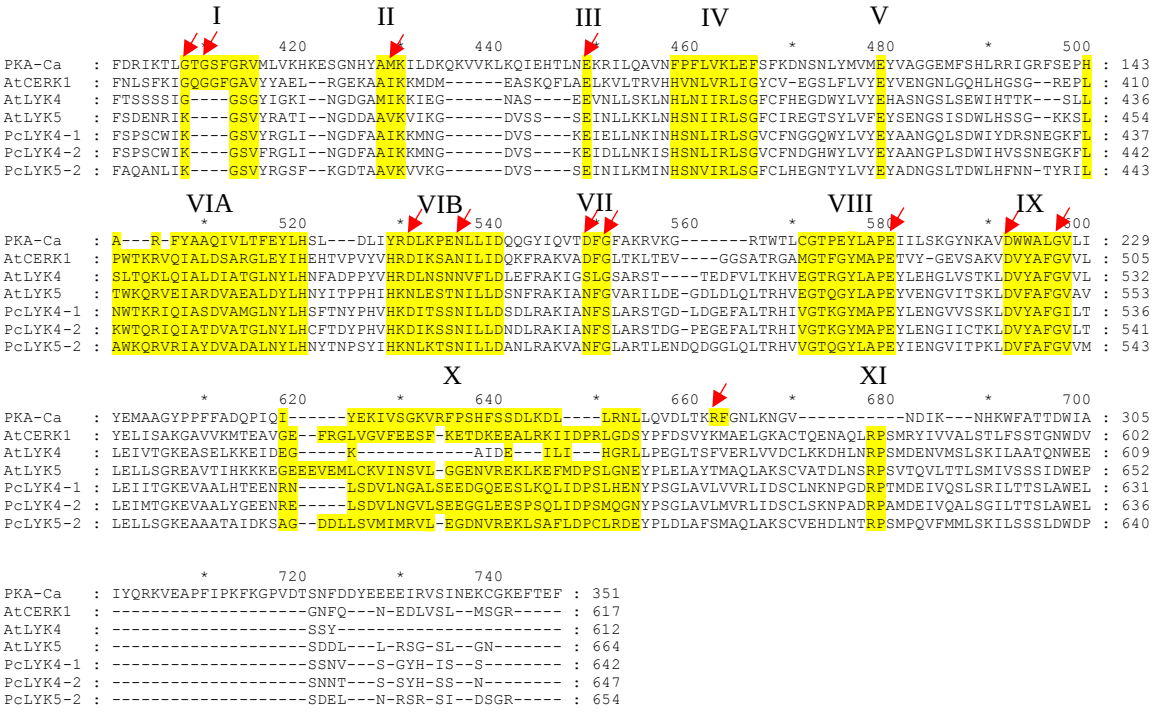

Supplemental Figure 4.3. PcLYK4/PcLYK5 proteins are LysM-RLKs that likely harbor an inactive kinase. Poplar LysM-RLKs were aligned with PKA-Cα to analyse the presence/absence of invariant amino acids in the kinase domain (indicated by red arrows) (Hanks and Hunter, 1995). Sequences of LysM-RLKs from Arabidopsis that harbor active and inactive kinasea, AtCERK1 and AtLYK4/AtLYK5 respectively, are included.

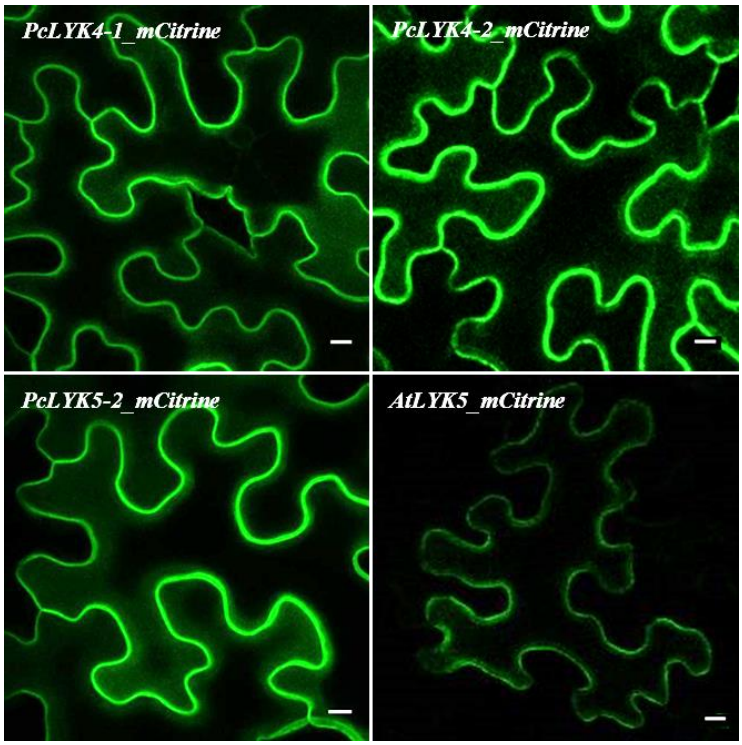

Supplemental Figure 4.4. LYK4/LYK5 proteins of *P. x canescens* are plasma membrane-localized proteins. For subcellular localization studies, constructs expressing genes encoding poplar LysM-RLKs (*PcLYK4-1*, *PcLYK4-2* and *PcLYK5-2*) under the promoter of AtLYK5, carrying a mCitrine fluorescent marker at the C-terminus were generated and infiltrated into the leaves of *N. benthamiana* for transient expression assays. A construct expressing the AtLYK5 gene carrying the same fluorescent marker was included as a control. Observation under CLSM SP5 was conducted with 40x objective, and the displayed images are maximum projections of ten Z-stack series with ~1 µm per-stack. Bars = 10 µm.

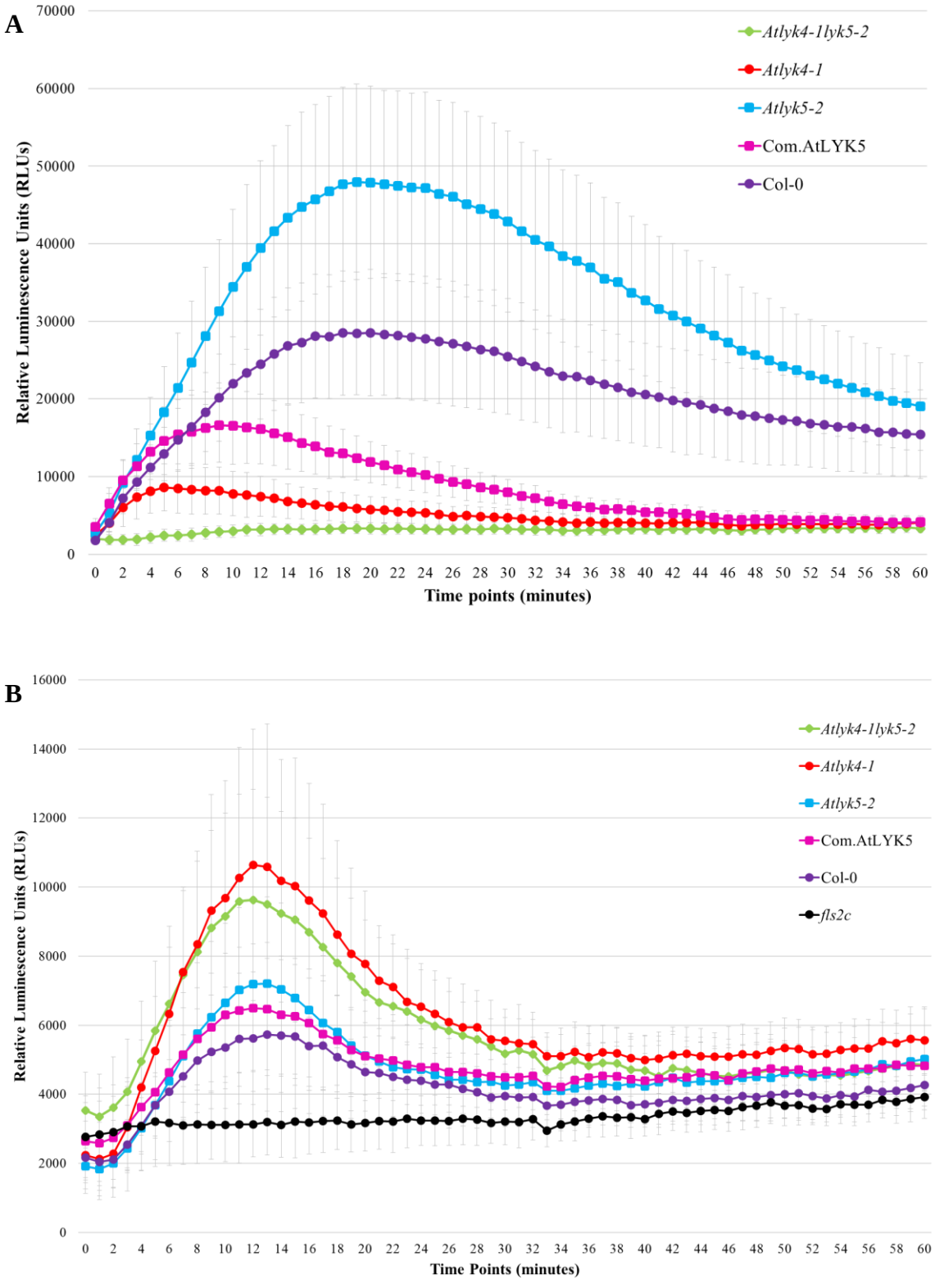

Supplemental Figure 4.5. Expression of AtLYK5 partially restores the chitin-induced ROS production of *Atlyk4*-1 *Atlyk5*-2. A. ROS burst of Com.AtLYK5 (*pAtLYK5:AtLYK5_mCitrine* in *Atlyk4*-1 *Atlyk5*-2) after 100 µg/ml chitin treatment, B. ROS burst of Com.AtLYK5 after 100 nM flg22 treatment ROS production was measured for 1h after treatment. *Atlyk4*-1 *Atlyk5*-2 and Col-0 were used as negative and positive controls respectively, and in addition, the *Atlyk4*-1 and *Atlyk5*-2 single knock-out lines were included. Data are means ± SD (n = 8 biological replicates). Technical repeats were performed for each sample. The experiment was repeated independently for three times with similar results. Representative results are shown.

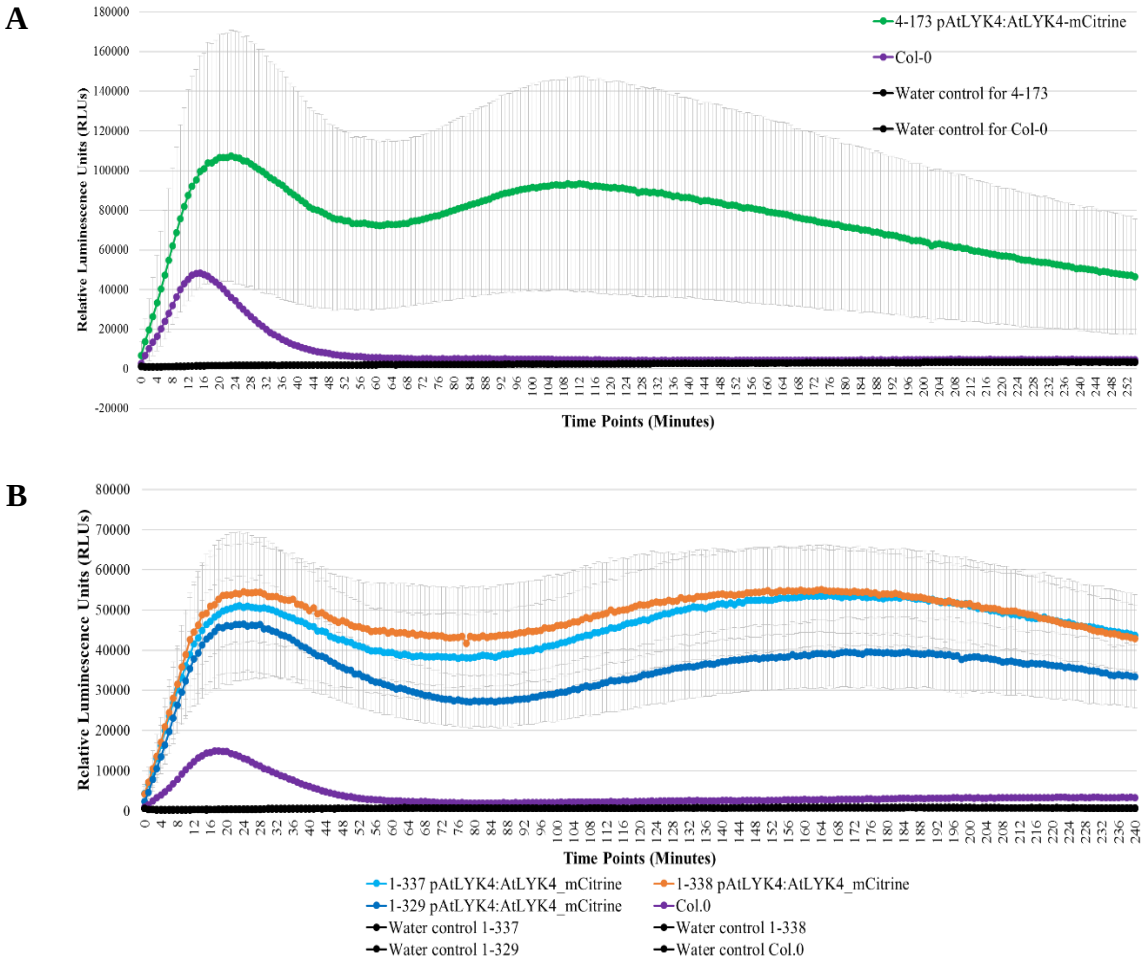

Supplemental Figure 4.6. Overexpression of *AtLYK4* induces higher and extended ROS burst in comparison to the wildtype Col-0. The assay was performed with Col-0 plants expressing *AtLYK4* under the endogenous promoter (*pAtLYK4:AtLYK4_mCitrine* in Col-0). ROS production was measured for ~4h after treatment with either 100 µg/ml chitin or water. One independent line (4-173 T2 generation in fig. A) and three independent lines (1-337, 1-338 and 1-329 T1 generations in fig. B) were tested. Col-0 plants were included as a control for the lines. Data are means ± SD (n = 8 biological replicates). Technical repeats were performed for each sample. The experiment was repeated independently for two times with similar results. Representative results are shown.

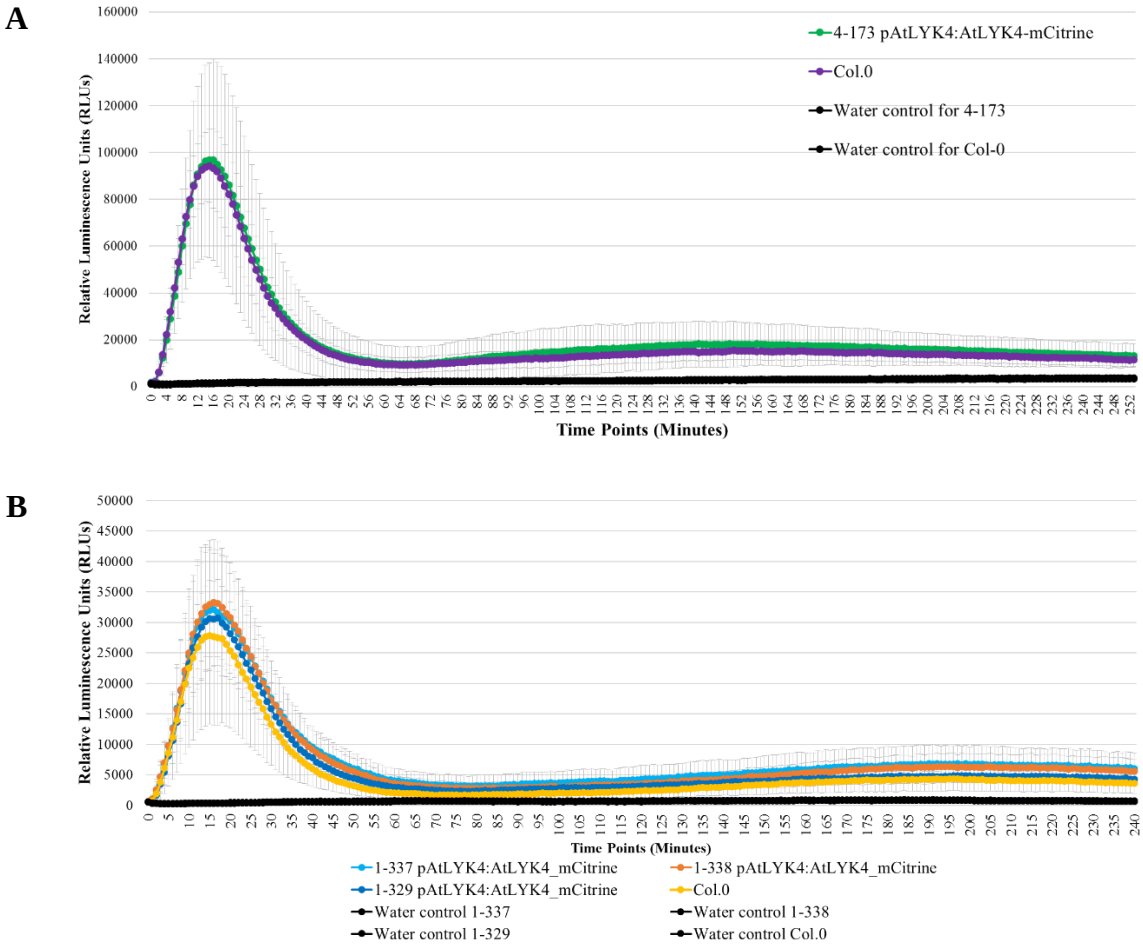

Supplemental Figure 4.7. Overexpressing *AtLYK4* under the endogenous promoter induces higher and extended ROS burst in comparison to the wildtype Col-0. These ROS burst assays were performed using plants tested in supplemental figure 6A and 6B for analyzing the response of plants to flg22 treatment (100 nM). Col-0 plants were included as controls. ROS production was measured for ~4h after treatment with either flg22 or water. Data are means ± SD (n = 8 biological replicates). Technical repeats were performed for each sample. The experiment was repeated independently for two times with similar results. Representative results are shown.

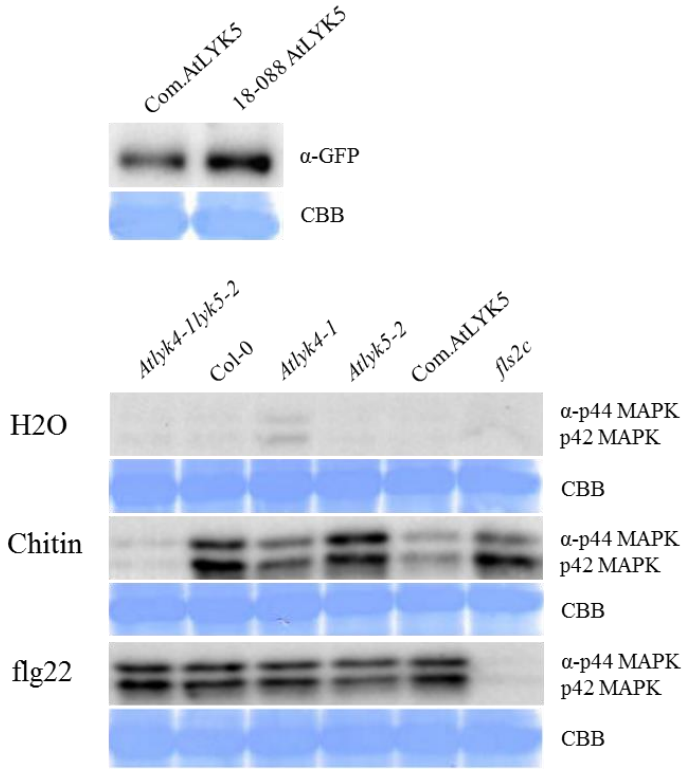

Supplemental Figure 4.8. Expression of *AtLYK5* genes partially restores the chitin induced MAPK activation of *Atlyk4*-1 *Atlyk5*-2. Total proteins were extracted from a pool of leaves from three plants that were infiltrated with 10 µg/ml chitin, 10 nM flg22 or water (ddH_2O) and harvested 10 minutes post infiltration. MAPK activation of plants after flg22 treatment shows that lines have a wildtype response to flg22. Comp.AtLYK5-2 = *pAtLYK5:PcLYK5-2_mCitrine* in *Atlyk4*-1 *Atlyk5*-2. *Atlyk4*-1 *Atlyk5*-2 and Col-0 were included as negative and positive controls, respectively. In addition, *Atlyk4*-1 or *Atlyk5*-2 single knock-out mutants, as well as *fls2c* plants (for flg22 negative control) were also included. MAPK activation was detected by using the primary antibody phospho-p44/p42. Technical repeats were performed for each sample. The experiment was repeated independently at least twice with similar results. Upper panel shows protein levels of AtLYK5 in individual lines the Com.AtLYK5 line A 18-088 AtLYK5 = *pAtLYK5:AtLYK5_mCitrine*-expressing plant crossed with *Atlyk4*-1 *Atlyk5*-2 was used as a positive control.

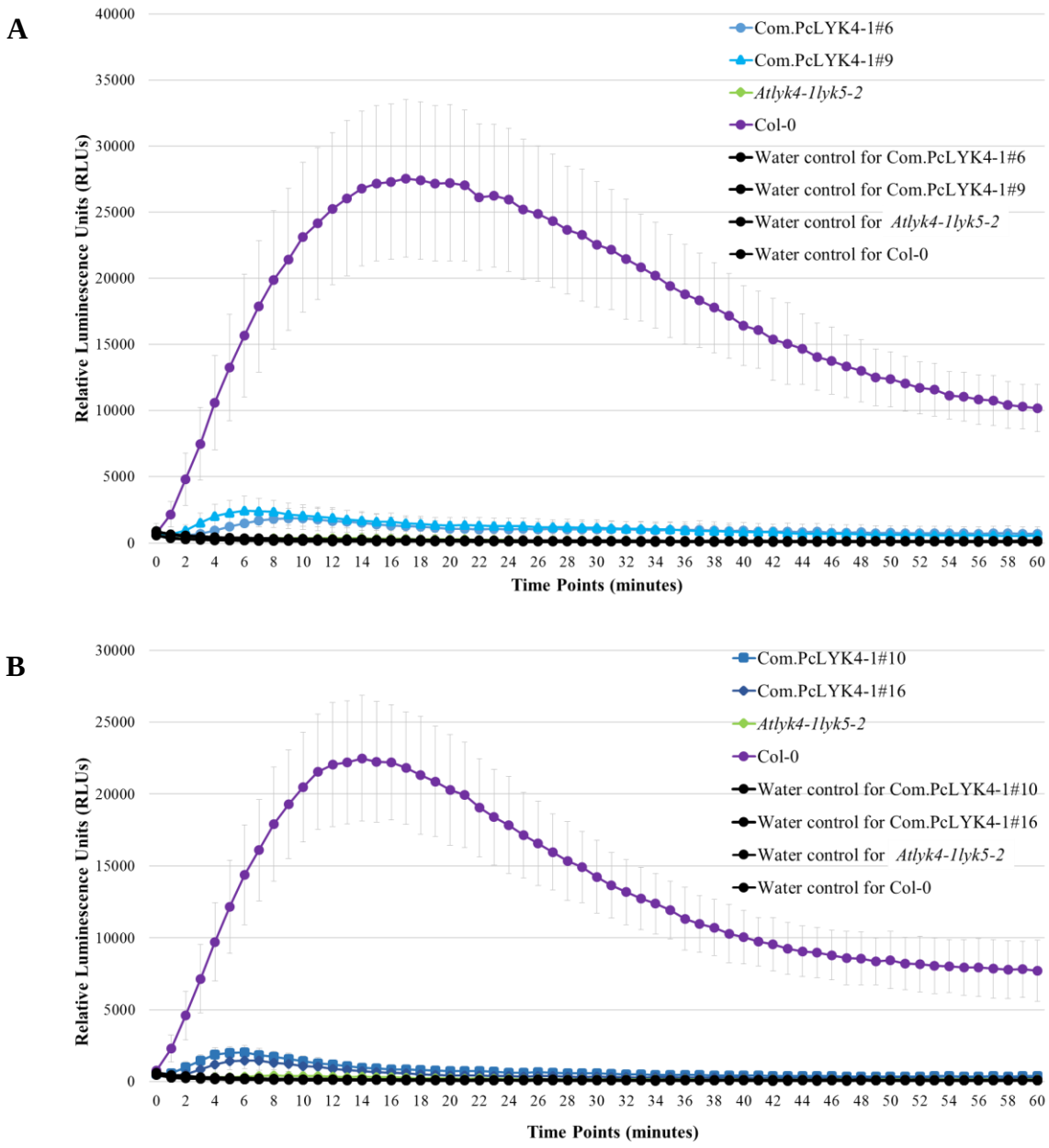

Supplemental Figure 4.9. Expressing *PcLYK4-1* patially restores the chitin-triggered ROS production of *Atlyk4-1 lyk5-2*. Two individual lines of Com.PcLYK4-1 (*pAtLYK5:PcLYK4-1_mCitrine* in *Atlyk4-1lyk5-2*) designated as numbers after '#' were tested in each set up (A and B) for their response to chitin (100 µg/ml). *Atlyk4-1lyk5-2* and Col-0 were used as negative and positive controls respectively. ROS production was measured for 1h after treatment with either chitin or water. Data are means ± SD (n = 8 biological replicates). Technical repeats were performed for each sample. The experiment was repeated independently for three times with similar results. Representative results are shown.

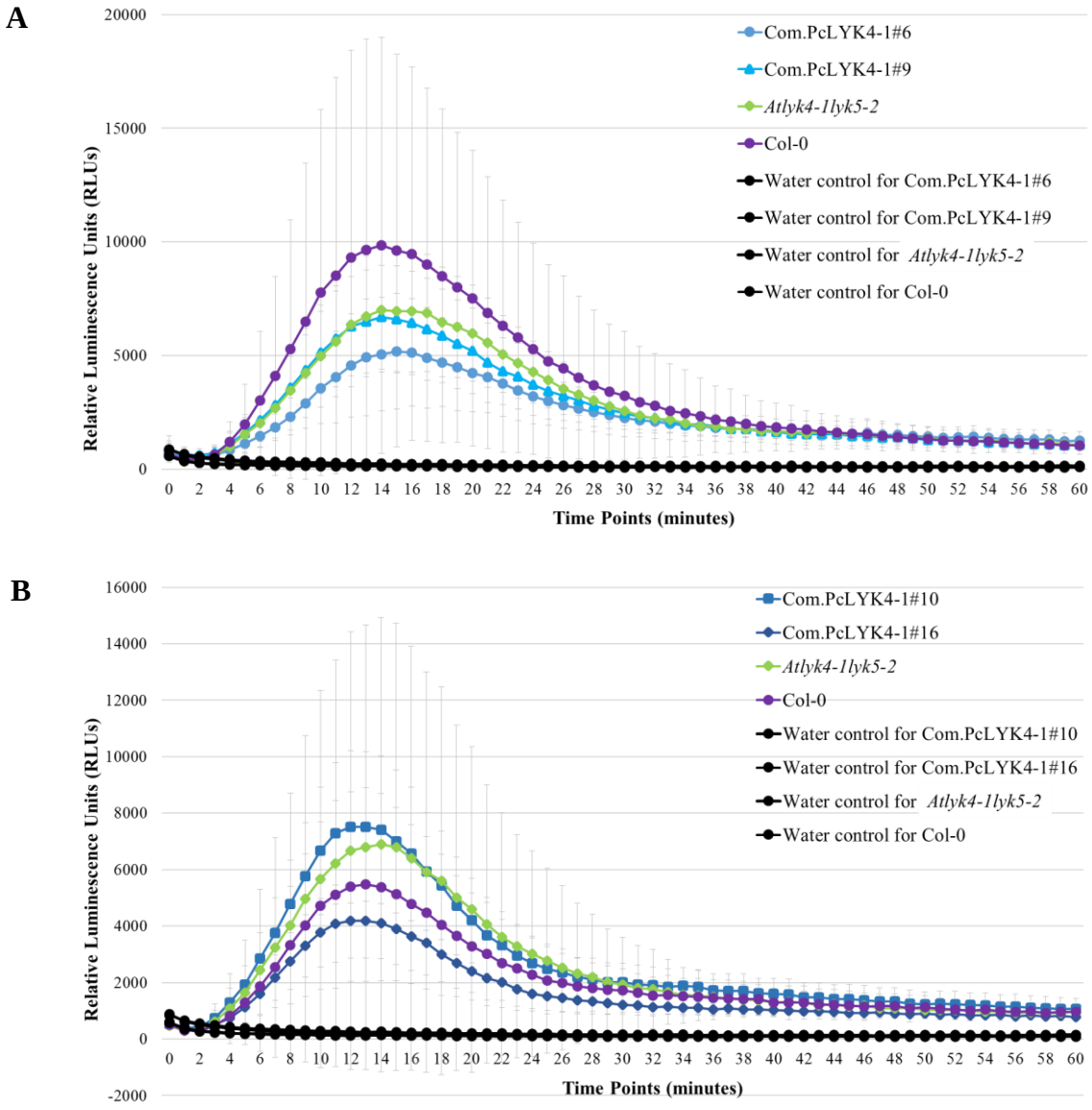

Supplemental Figure 4.10. *Atlyk4-1 Atlyk5-2* plants expressing *PcLYK4-1* show normal response to flg22 in comparison to the wildtype Col-0. Two individual lines of Com.PcLYK4-1 (*pAtLYK5:PcLYK4-1_mCitrine* in *Atlyk4-1lyk5-2*) designated as numbers after '#' were tested in each set up (A and B) for their response to flg22 (100 nM). *Atlyk4-1 lyk5-2* and Col-0 were included as controls. ROS production was measured for 1h after treatment with either flg22 or water. Data are means ± SD (n = 8 biological replicates). Technical repeats were performed for each sample. The experiment was repeated independently for three times with similar results. Representative results are shown.

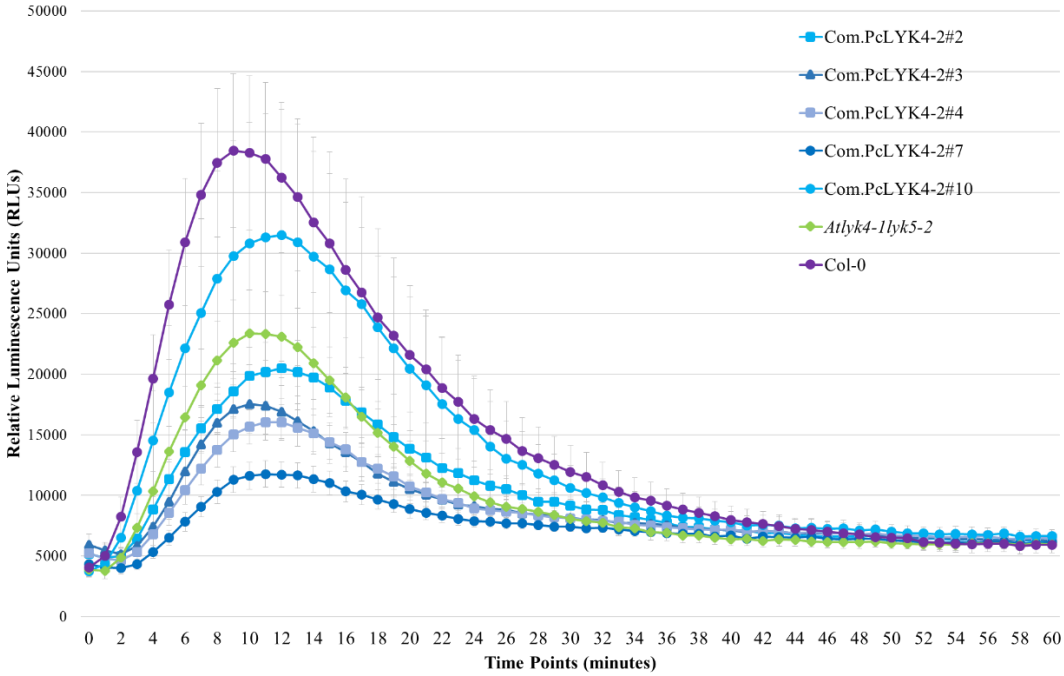

Supplemental Figure 4.11. *Atlyk4-1 lyk5-2* plants expressing *PcLYK4-2* show normal response to flg22 in comparison to the wildtype Col-0. These ROS burst assays were performed using plants tested in Figure 4B for analyzing the response of plants to flg22 treatment (100 nM). Com.PcLYK4-2 = *pAtLYK5:PcLYK4-1_mCitrine* in *Atlyk4-1 lyk5-2*, and numbers after '#' designate individual lines. *Atlyk4-1 lyk5-2* and Col-0 were included as controls. ROS production was measured for 1h after 100 nM flg22 treatment (water treatment was not performed due to the limited plant material, since these generated lines are T1 generation). Data are means ± SD (n = 8 technical replicates). Technical repeats were performed for each sample. The experiment was repeated for two times with similar results. Representative results are shown.

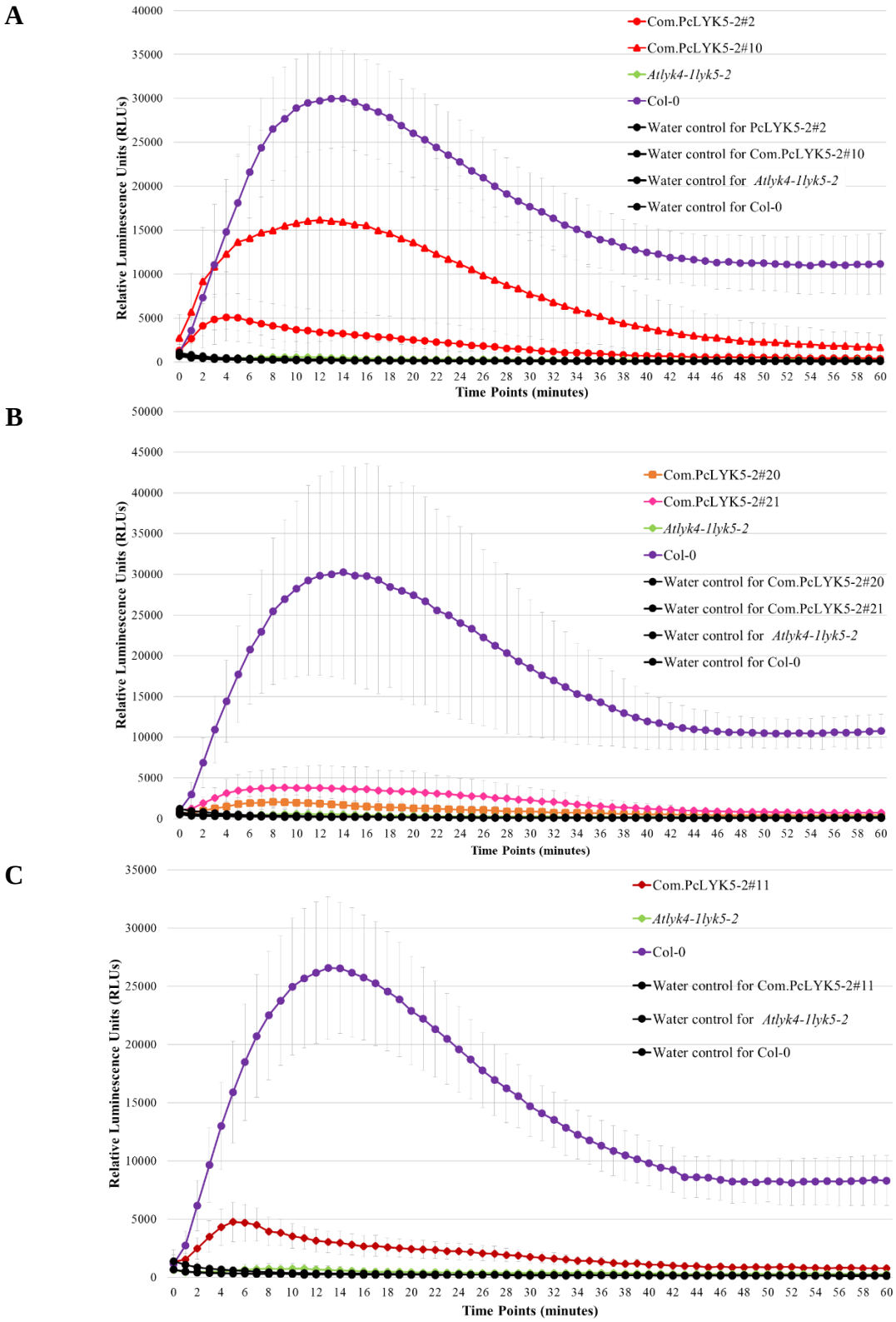

Supplemental Figure 4.12. Expressing *PcLYK5-2* partially restores the chitin-triggered ROS production of *Atlyk4-1 lyk5-2*. One or two individual lines of Com.PcLYK5-2 (*pAtLYK5:PcLYK5-2_mCitrine* in *Atlyk4-1lyk5-2*) designated as numbers after '#' were tested in each set up (A-C) for their response to chitin (100 µg/ml). *Atlyk4-1 lyk5-2* and Col-0 were used as negative and positive controls respectively. ROS production was measured for 1h after treatment with either chitin or water. Data are means ± SD (n = 8 biological replicates). Technical repeats were performed for each sample. The experiment was repeated independently for four times with similar results. Representative results are shown.

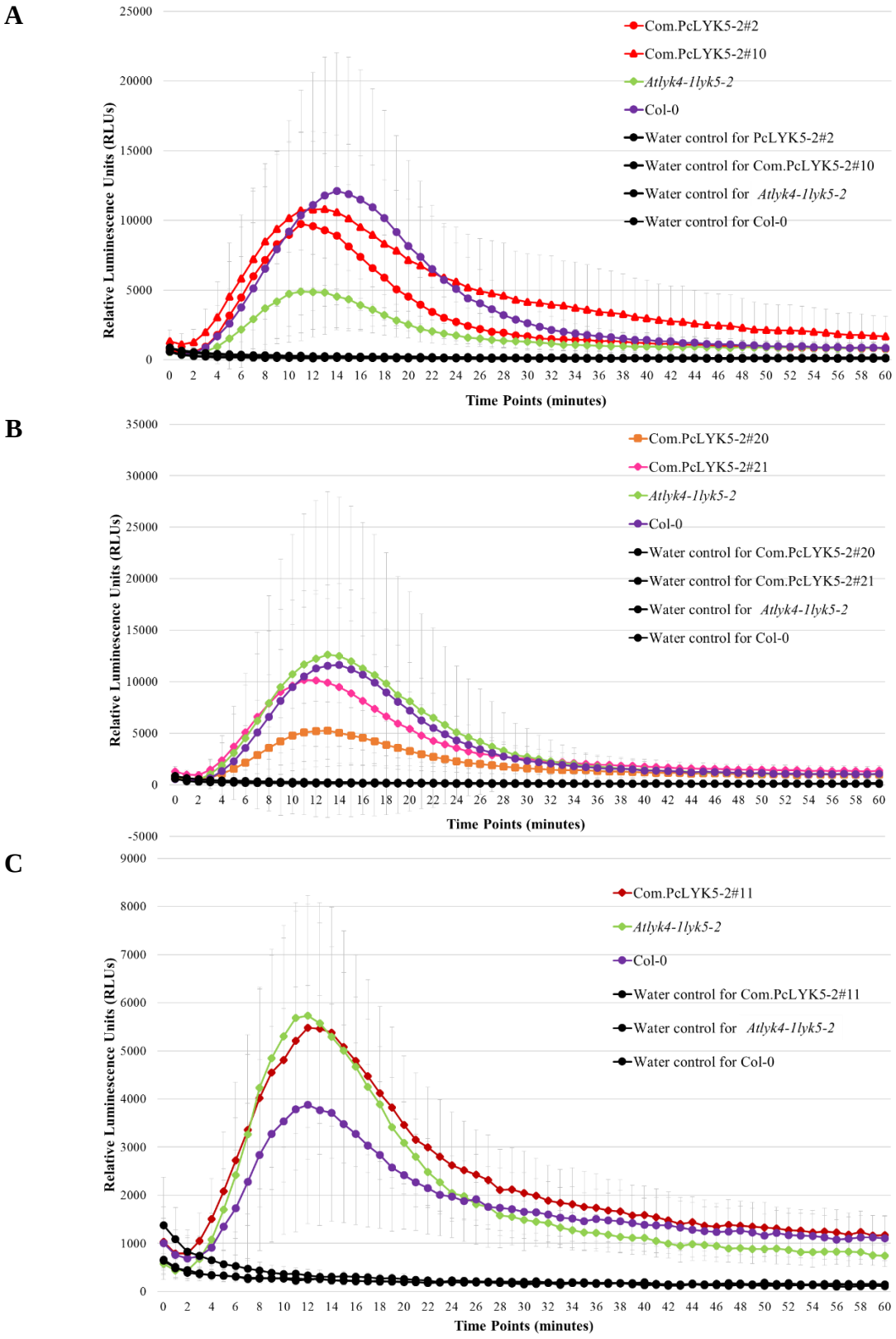

Supplemental Figure 4.13. *Atlyk4-1 lyk5-2* plants expressing *PcLYK5-2* show normal response to flg22 in comparison to the wildtype Col-0. These ROS burst assays were performed using plants tested in Figure 5 for analyzing the response of plants to flg22 treatment. One or two individual lines of Com.PcLYK5-2 (*pAtLYK5:PcLYK5-2_mCitrine* in *Atlyk4-1lyk5-2*) designated as numbers after '#' sign were tested in each set up (A-C) for their response to flg22 (100 nM). *Atlyk4-1lyk5-2* and Col-0 were included as controls. ROS production was measured for 1h after treatment with either flg22 or water. Data are means ± SD (n = 8 biological replicates). Technical repeats were performed for each sample. The experiment was repeated independently for four times with similar results. Representative results are shown.

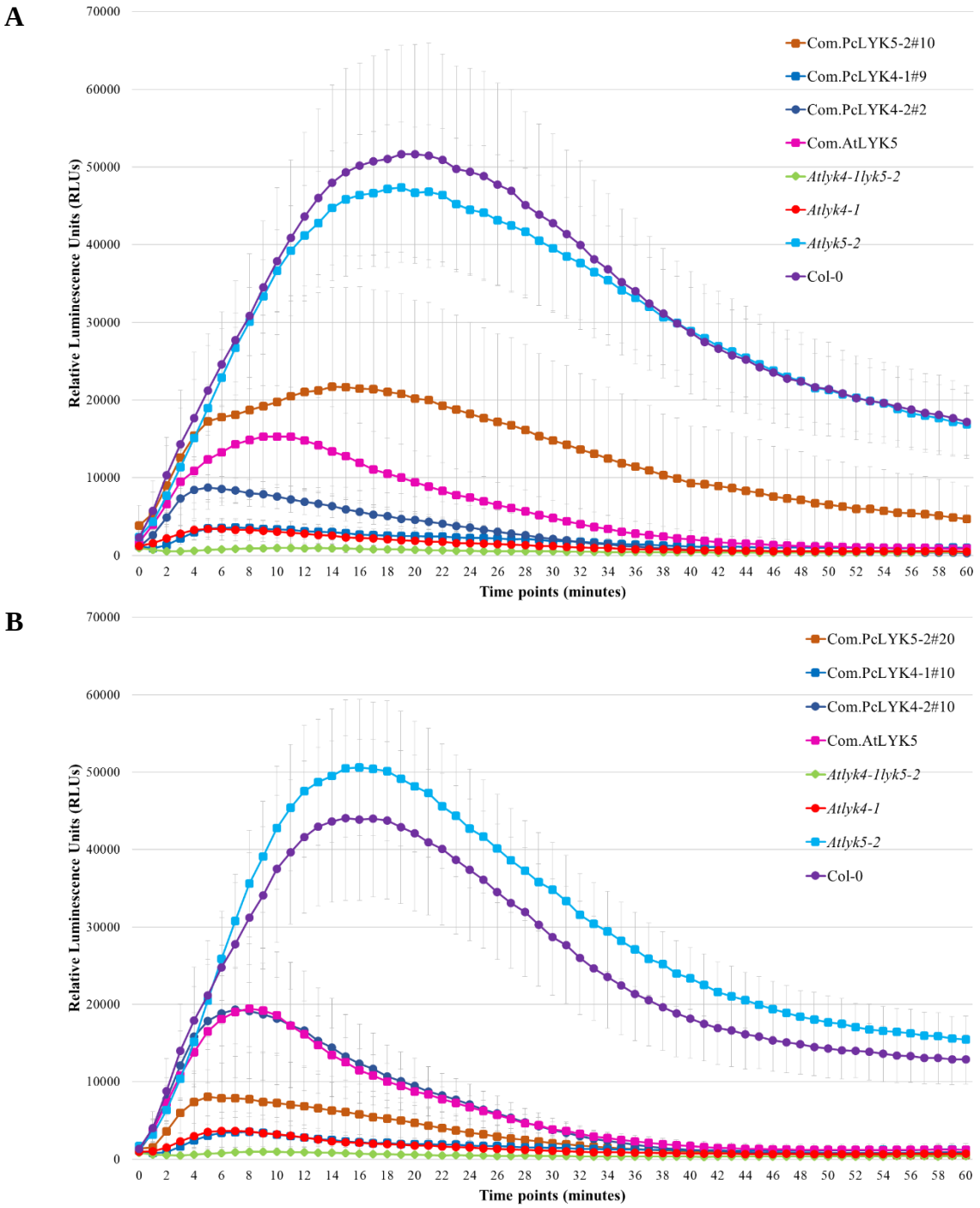

Supplemental Figure 4.14. The restoration of ROS production in the *Atlyk4-1 lyk5-2* plants expressing *PcLYK4-1*/*PcLYK4-2*/*PcLYK5-2* is line-dependent. For complementation studies, constructs for expression of poplar LysM-RLKs under the endogenous promoter of AtLYK5 were stable-transformed into the *A. thaliana* double knocked-out mutant *Atlyk4-1lyk5-2*. Complementation of the chitin induced ROS burst was analysed with the obtained lines by measuring the ROS production for 1h after treatment with 100 µg/ml chitin. *Atlyk4-1lyk5-2* and Col-0 were used as negative and positive controls respectively. Comp.PcLYK5-2 = *pAtLYK5:PcLYK5-2_mCitrine*, Comp.PcLYK4-1 = *pAtLYK5:PcLYK4-1_mCitrine*, Com.PcLYK4-2 = *pAtLYK5:PcLYK4-2_mCitrine*, all constructs were expressed in *Atlyk4-1lyk5-2* background and numbers after '#' designate the individual lines. Data are means ± SD (n = 8 biological replicates). Technical repeats were performed for each sample. The experiment was repeated independently for two times with similar results. Representative results are shown.

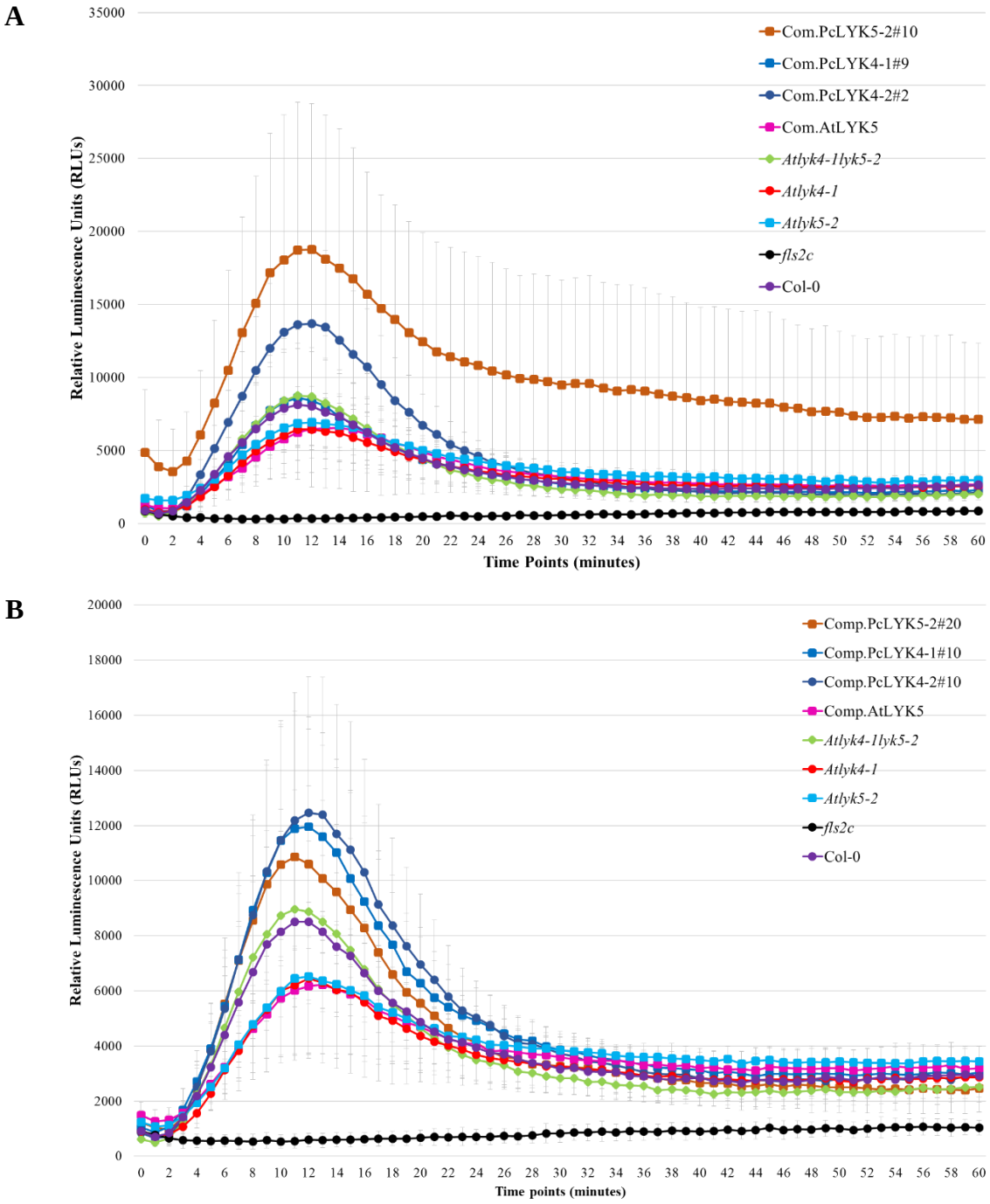

Supplemental Figure 4.15. *Atlyk4*-1 *Atlyk5*-2 plants expressing *PcLYK5-2* show normal response to flg22 in comparison to the wildtype Col-0. These ROS burst assays were performed using plants tested in supplemental figure 11 for analyzing the response of plants to flg22 treatment. Two independent lines of each construct was tested separately (A and B) for their response to flg22 (100 nM). *Atlyk4*-1 *Atlyk5*-2 and Col-0 were included as controls. ROS production was measured for 1h after treatment with either flg22. Comp.PcLYK5-2 = *pAtLYK5:PcLYK5-2_mCitrine*, Comp.PcLYK4-1 = *pAtLYK5:PcLYK4-1_mCitrine*, Comp.PcLYK4-2 = *pAtLYK5:PcLYK4-2_mCitrine*, all constructs were expressed in *Atlyk4*-1 *Atlyk5*-2 background and numbers after '#' designate individual lines. Col-0, *Atlyk4*-1 *Atlyk5*-2 and *fls2c* mutant were included as controls. *fls2c* is insensitive to flg22. Data are means ± SD (n = 8 biological replicates). Technical repeats were performed for each sample. The experiment was repeated independently for two times with similar results. Representative results are shown.

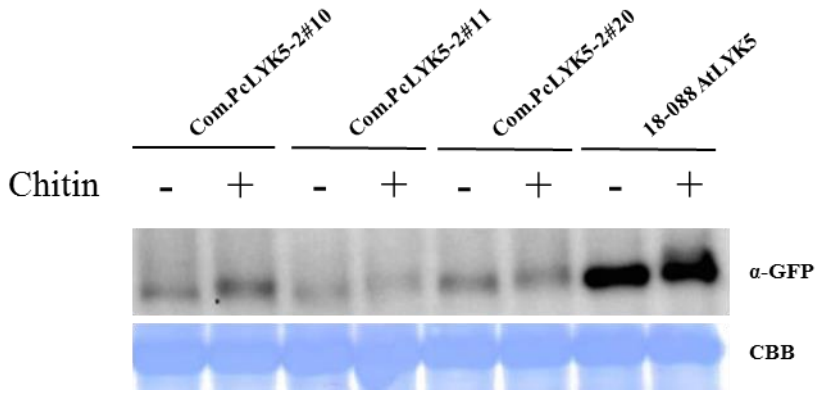

Supplemental Figure 4.16. PcLYK5 is likely phosphorylated by AtCERK1. Western blotting was conducted using total protein extract of *Atlyk4*-1 *Atlyk*5-2 lines expressing *pAtLYK5:PcLYK5-2_mCitrine* that were treated by either chitin or water. Three independent lines were evaluated (Com.PcLYK5-2#10, #11, #20), and protein extract from *pAtLYK5:AtLYK5_mCitrine*-expressing leaves (18-088 AtLYK5, complementation line that was generated through crossing with *Atlyk4*-1 *Atlyk5*-2) was used as a positive control. The Com.PcLYK5-2 lines show a band-shift after chitin treatment similar to the control 18-088 AtLYK5, indicating phosphorylation. The mCitrine fusion protein was detected by using the primary antibody GFP. Coomassie brilliant blue (CBB) staining was done to control that similar amounts of protein were loaded. The experiment was repeated twice with similar results. Representative results are shown.

4.8 References

Aghaalikhani, A., Savuto, E., Di Carlo, A., & Borello, D. (2017). Poplar from phytoremediation as a renewable energy source: Gasification properties and pollution analysis. *Energy Procedia*, *142*, 924–931. https://doi.org/10.1016/j.egypro.2017.12.148

Antolín-Llovera, M., Petutsching, E. K., Ried, M. K., Lipka, V., Nürnberger, T., Robatzek, S., & Parniske, M. (2014). Knowing your friends and foes - plant receptor-like kinases as initiators of symbiosis or defence. *New Phytologist*, *204*(4), 791–802. https://doi.org/10.1111/nph.13117

Beck, M., Zhou, J., Faulkner, C., Mac, D. L., & Robatzek, S. (2012). Spatio-temporal cellular dynamics of the Arabidopsis flagellin receptor reveal activation status-dependent endosomal sorting. *Plant Cell*, *24*(10), 4205–4219. https://doi.org/10.1105/tpc.112.100263

Bradshaw, H. D., Ceulemans, R., Davis, J., & Stettler, R. (2000). Emerging model systems in plant biology: Poplar (Populus) as a model forest tree. *Journal of Plant Growth Regulation*, *19*(3), 306–313. https://doi.org/10.1007/s003440000030

Buist, G., Steen, A., Kok, J., & Kuipers, O. P. (2008). LysM, a widely distributed protein motif for binding to (peptido)glycans. *Molecular Microbiology*, *68*(4), 838–847. https://doi.org/10.1111/j.1365-2958.2008.06211.x

Cao, Y., Liang, Y., Tanaka, K., Nguyen, C. T., Jedrzejczak, R. P., Joachimiak, A., & Stacey, G. (2014). The kinase LYK5 is a major chitin receptor in Arabidopsis and forms a chitin-induced complex with related kinase CERK1. *ELife*, *3*(October). https://doi.org/10.7554/eLife.03766

Castro-Rodríguez, V., García-Gutiérrez, A., Canales, J., Cañas, R. A., Kirby, E. G., Avila, C., & Cánovas, F. M. (2016). Poplar trees for phytoremediation of high levels of nitrate and applications in bioenergy. *Plant Biotechnology Journal*, *14*(1), 299–312. https://doi.org/10.1111/pbi.12384

Chen, Z., Wang, J., Ye, M. X., Li, H., Ji, L. X., Li, Y., … An, X. M. (2013). A novel moderate constitutive promoter derived from poplar (Populus tomentosa carrière). *International Journal of Molecular Sciences*, *14*(3), 6187–6204. https://doi.org/10.3390/ijms14036187

Chinchilla, D., Zipfel, C., Robatzek, S., Kemmerling, B., Nürnberger, T., Jones, J. D. G., … Boller, T. (2007). A flagellin-induced complex of the receptor FLS2 and BAK1 initiates plant defence. *Nature*, *448*(7152), 497–500. https://doi.org/10.1038/nature05999

Clough, S. J., & Bent, A. F. (1998). Floral dip: A simplified method for Agrobacterium-mediated transformation of Arabidopsis thaliana. *Plant Journal*, *16*(6), 735–743. https://doi.org/10.1046/j.1365-313X.1998.00343.x

Dereeper, A., Guignon, V., Blanc, G., Audic, S., Buffet, S., Chevenet, F., … Gascuel, O. (2008). Phylogeny.fr: robust phylogenetic analysis for the non-specialist. *Nucleic Acids Research*, *36*(Web Server issue), 465–469. https://doi.org/10.1093/nar/gkn180

Dereeper, Alexis, Audic, S., Claverie, J. M., & Blanc, G. (2010). BLAST-EXPLORER helps you building datasets for phylogenetic analysis. *BMC Evolutionary Biology*, *10*(1), 8–13. https://doi.org/10.1186/1471-2148-10-8

Desaki, Y., Miyata, K., Suzuki, M., Shibuya, N., & Kaku, H. (2018). Plant immunity and symbiosis signaling mediated by LysM receptors. *Innate Immunity*, *24*(2), 92–100. https://doi.org/10.1177/1753425917738885

Duplessis, S., Major, I., Martin, F., & Séguin, A. (2009). Poplar and pathogen interactions: Insights from populus genome-wide analyses of resistance and defense gene families and gene expression profiling. *Critical Reviews in Plant Sciences*, *28*(5), 309–334. https://doi.org/10.1080/07352680903241063

Erwig, J., Ghareeb, H., Kopischke, M., Hacke, R., Matei, A., Petutschnig, E., & Lipka, V. (2017). Chitin-induced and CHITIN ELICITOR RECEPTOR KINASE1 (CERK1) phosphorylation-dependent endocytosis of Arabidopsis thaliana LYSIN MOTIF-CONTAINING RECEPTOR-LIKE KINASE5 (LYK5). *New Phytologist*, *215*(1), 382–396. https://doi.org/10.1111/nph.14592

Fladung, M., Hoenicka, H., & Raj Ahuja, M. (2013). Genomic stability and long-term transgene expression in poplar. *Transgenic Research*, *22*(6), 1167–1178. https://doi.org/10.1007/s11248-013-9719-2

García-Angulo, P., Villar, I., Giner-Robles, L., & Centeno, M. L. (2018). In vitro regeneration of two Populus hybrid clones. The role of pectin domains in cell processes underlying shoot organogenesis induction. *Biologia Plantarum*, *62*(4), 763–774. https://doi.org/10.1007/s10535-018-0819-y

Geldner, N., Hyman, D. L., Wang, X., Schumacher, K., & Chory, J. (2007). Endosomal signaling of plant steroid receptor kinase BRI1. *Genes and Development*, *21*(13), 1598–1602. https://doi.org/10.1101/gad.1561307

Gong, B. Q., Xue, J., Zhang, N., Xu, L., Yao, X., Yang, Q. J., … Li, J. F. (2017). Rice Chitin Receptor OsCEBiP Is Not a Transmembrane Protein but Targets the Plasma Membrane via a GPI Anchor. *Molecular Plant*, *10*(5), 767–770. https://doi.org/10.1016/j.molp.2016.12.005

Gubaeva, E., Gubaev, A., Melcher, R. L. J., Cord-Landwehr, S., Singh, R., Gueddari, N. E. El, & Moerschbacher, B. M. (2018). Slipped sandwich' model for chitin and chitosan perception in arabidopsis. *Molecular Plant-Microbe Interactions*, *31*(11), 1145–1153. https://doi.org/10.1094/MPMI-04-18-0098-R

Guerra, F., Gainza, F., Perez, R., & Zamudio, F. (2011). Phytoremidiation of heavy metals using poplars (Populus spp): a glimpse of the plant responses to copper, cadmium and zinc stress. *Nova Science Publishers, Inc.*, *ISBN: 978-*, 387–413.

Guo, M., Li, C., Facciotto, G., Bergante, S., Bhatia, R., Comolli, R., … Murphy, R. (2015). Bioethanol from poplar clone Imola: an environmentally viable alternative to fossil fuel? *Biotechnology for Biofuels*, *8*(1), 1–21. https://doi.org/10.1186/s13068-015-0318-8

Hacquard, S., Petre, B., Frey, P., Hecker, A., Rouhier, N., & Duplessis, S. (2011). The Poplar-Poplar Rust Interaction: Insights from Genomics and Transcriptomics. *Journal of Pathogens*, *2011*, 1–11. https://doi.org/10.4061/2011/716041

Han, Xue, Ma, S., Kong, X., Takano, T., & Liu, S. (2013). Efficient Agrobacterium-mediated transformation of hybrid poplar Populus davidiana Dode × Populus bollena lauche. *International Journal of Molecular Sciences*, *14*(2), 2515–2528. https://doi.org/10.3390/ijms14022515

Hanks, S. K., & Hunter, T. (1995). The eukaryotic protein kinase superfamily: Kinase (catalytic) domain structure and classification. *FASEB Journal*, *9*(8), 576–596.

Hayafune, M., Berisio, R., Marchetti, R., Silipo, A., Kayama, M., Desaki, Y., … Shibuya, N. (2014). Chitin-induced activation of immune signaling by the rice receptor CEBiP relies on a unique sandwich-type dimerization. *Proceedings of the National Academy of Sciences of the United States of America*, *111*(3). https://doi.org/10.1073/pnas.1312099111

Hellens, R. P., Edwards, E. A., Leyland, N. R., Bean, S., & Mullineaux, P. M. (2000). Biotechnology resources for arable crop transformation (bract)\npGreen: a versatile and flexible binary Ti vector for Agrobacterium-mediated plant transformation. *Plant Mol Biol*, *42*, 819–832. Retrieved from http://www.bract.org

Jansson, C., Wullschleger, S. D., Kalluri, U. C., & Tuskan, G. A. (2010). Phytosequestration: Carbon Biosequestration by Plants and the Prospects of Genetic Engineering. *BioScience*, *60*(9), 685–696. https://doi.org/10.1525/bio.2010.60.9.6

Kaku, H., Nishizawa, Y., Ishii-Minami, N., Akimoto-Tomiyama, C., Dohmae, N., Takio, K., Minami, E., Shibuya, N. (2006). Plant cells recognize chitin fragments for defense signaling through a plasma membrane receptor. *Proceedings of the National Academy of Sciences of the United States of America*, *103*(29), 11086–11091. https://doi.org/10.1073/pnas.79.20.6304

Kouzai, Y., Mochizuki, S., Nakajima, K., Desaki, Y., Hayafune, M., Miyazaki, H., … Nishizawa, Y. (2014). Targeted gene disruption of OsCERK1 reveals its indispensable role in chitin perception and involvement in the peptidoglycan response and immunity in rice. *Molecular Plant-Microbe Interactions*, *27*(9), 975–982. https://doi.org/10.1094/MPMI-03-14-0068-R

Krogh, A., Larsson, B., Von Heijne, G., & Sonnhammer, E. L. L. (2001). Predicting transmembrane protein topology with a hidden Markov model: Application to complete genomes. *Journal of Molecular Biology*, *305*(3), 567–580. https://doi.org/10.1006/jmbi.2000.4315

Li, Q, Yeh, T., Yang, C., Song, J., Chen, Z., Sederoff, R., & Chiang, V. (2015). Populus trichocarpa. *Methods in Molecular Biology*, *1224*, 357–363. https://doi.org/10.1007/978-1-4939-1658-0

Li, S., Zhen, C., Xu, W., Wang, C., & Cheng, Y. (2017). Simple, rapid and efficient transformation of genotype Nisqually-1: A basic tool for the first sequenced model tree. *Scientific Reports*, *7*(1), 1–10. https://doi.org/10.1038/s41598-017-02651-x

Littlewood, J., Guo, M., Boerjan, W., & Murphy, R. J. (2014). Bioethanol from poplar: A commercially viable alternative to fossil fuel in the European Union. *Biotechnology for Biofuels*, *7*(1), 1–12. https://doi.org/10.1186/1754-6834-7-113

Liu, T., Liu, Z., Song, C., Hu, Y., Han, Z., She, J., … Chai, J. (2012). Chitin-induced dimerization activates a plant immune receptor. *Science*, *336*(6085), 1160–1164. https://doi.org/10.1126/science.1218867

Lu, D., Lin, W., Gao, X., Wu, S., Cheng, C., Avila, J., … Shan, L. (2011). Direct ubiquitination of pattern recognition receptor FLS2 attenuates plant innate immunity. *Science*, *332*(June), 1439–1442. https://doi.org/10.1126/science.1204903

Mach, J. (2014). When to hold them: Retention of duplicate genes in poplar. *Plant Cell*, *26*(6), 2283. https://doi.org/10.1105/tpc.114.128827

Martins, S., Dohmann, E. M. N., Cayrel, A., Johnson, A., Fischer, W., Pojer, F., … Vert, G. (2015). Internalization and vacuolar targeting of the brassinosteroid hormone receptor BRI1 are regulated by ubiquitination. *Nature Communications*, *6*. https://doi.org/10.1038/ncomms7151

Mbengue, M., Bourdais, G., Gervasi, F., Beck, M., Zhou, J., Spallek, T., … Robatzek, S. (2016). Clathrin-dependent endocytosis is required for immunity mediated by pattern recognition receptor kinases. *Proceedings of the National Academy of Sciences of the United States of America*, *113*(39), 11034–11039. https://doi.org/10.1073/pnas.1606004113

Miya, A., Albert, P., Shinya, T., Desaki, Y., Ichimura, K., Shirasu, K., … Shibuya, N. (2007). CERK1, a LysM receptor kinase, is essential for chitin elicitor signaling in Arabidopsis. *Proceedings of the National Academy of Sciences of the United States of America*, *104*(49), 19613–19618. https://doi.org/10.1073/pnas.0705147104

Movahedi, A., Zhang, J., Amirian, R., & Zhuge, Q. (2014). An efficient agrobacterium-mediated transformation system for poplar. *International Journal of Molecular Sciences*, *15*(6), 10780–10793. https://doi.org/10.3390/ijms150610780

Otegui, M. S., & Spitzer, C. (2008). Endosomal functions in plants. *Traffic*, *9*(10), 1589–1598. https://doi.org/10.1111/j.1600-0854.2008.00787.x

Paez Valensia, J., Goodman, K., Otegui, M.S. 2016. Endocytosis and endosomal trafficking in plants. Annu. Rev. Plant Biol. 2016. 67:309–35

Pereira, S., Costa, M., Carvalho, M., & Rodrigues, A. (2016). Potential of poplar short rotation coppice cultivation for bioenergy in Southern Portugal. *Energy Conversion and Management*, *125*. https://doi.org/10.1016/j.enconman.2016.03.068

Petersen, T. N., Brunak, S., Von Heijne, G., & Nielsen, H. (2011). SignalP 4.0: Discriminating signal peptides from transmembrane regions. *Nature Methods*, *8*(10), 785–786. https://doi.org/10.1038/nmeth.1701

Petutschnig, E. K., Jones, A. M. E., Serazetdinova, L., Lipka, U., & Lipka, V. (2010). The Lysin Motif Receptor-like Kinase (LysM-RLK) CERK1 is a major chitin-binding protein in Arabidopsis thaliana and subject to chitin-induced phosphorylation. *Journal of Biological Chemistry*, *285*(37), 28902–28911. https://doi.org/10.1074/jbc.M110.116657

Quevillon, E., Silventoinen, V., Pillai, S., Harte, N., Mulder, N., Apweiler, R., & Lopez, R. (2005). InterProScan: Protein domains identifier. *Nucleic Acids Research*, *33*(SUPPL. 2), 116–120. https://doi.org/10.1093/nar/gki442

Ren, L. L., Liu, Y. J., Liu, H. J., Qian, T. T., Qi, L. W., Wang, X. R., & Zeng, Q. Y. (2014). Subcellular relocalization and positive selection play key roles in the retention of duplicate genes of Populus class III peroxidase family. *Plant Cell*, *26*(6), 2404–2419. https://doi.org/10.1105/tpc.114.124750

Robatzek, S., Chinchilla, D., & Boller, T. (2006). Ligan-induced endocytosis of the pattern recognition receptor FLS2 in Arabidopsis. *Reserach Communication: Genes & Development*, *20*, 537–542. https://doi.org/10.1101/gad.366506.nized

Sannigrahi, P., Ragauskas, A., & Tuskan, G. (2009). Poplar as a feedstock for biofuels: a review of compositional characteristics. *Biofuels, Bioproducts and Biorefining*, *4*, 209–226. https://doi.org/10.1002/bbb

Shimizu, T., Nakano, T., Takamizawa, D., Desaki, Y., Ishii-Minami, N., Nishizawa, Y., … Shibuya, N. (2010). Two LysM receptor molecules, CEBiP and OsCERK1, cooperatively regulate chitin elicitor signaling in rice. *Plant Journal*, *64*(2), 204–214. https://doi.org/10.1111/j.1365-313X.2010.04324.x

Shinya, T., Motoyama, N., Ikeda, A., Wada, M., Kamiya, K., Hayafune, M., … Shibuya, N. (2012). Functional characterization of CEBiP and CERK1 homologs in arabidopsis and rice reveals the presence of different chitin receptor systems in plants. *Plant and Cell Physiology*, *53*(10), 1696–1706. https://doi.org/10.1093/pcp/pcs113

Song, J., Lu, S., Chen, Z. Z., Lourenco, R., & Chiang, V. L. (2006). Genetic transformation of Populus trichocarpa genotype Nisqually-1: A functional genomic tool for woody plants. *Plant and Cell Physiology*, *47*(11), 1582–1589. https://doi.org/10.1093/pcp/pcl018

Song, W.-Y., Choi, Y.-I., Shim, D., Kim, D.-Y., Noh, E.-W., Martinoia, E., & Lee, Y. (2007). Transgenic Poplar for Phytoremediation. *Biotechnology and Sustainable Agriculture 2006 and Beyond*, 265–271. https://doi.org/10.1007/978-1-4020-6635-1_40

Tallis, M. J., Casella, E., Henshall, P. A., Aylott, M. J., Randle, T. J., Morison, J. I. L., & Taylor, G. (2013). Development and evaluation of ForestGrowth-SRC a process-based model for short rotation coppice yield and spatial supply reveals poplar uses water more efficiently than willow. *GCB Bioenergy*, *5*(1), 53–66. https://doi.org/10.1111/j.1757-1707.2012.01191.x

Tuskan, G., DiFazio, S., Jansson, S., & Al., E. (2006). The Genome of Black Cottonwood Populus trichocarpa (Torr. & Gray). *Science*, *313*(September), 1596–1604.

Vanneste, K., Maere, S., & Van de Peer, Y. (2014). Tangled up in two: A burst of genome duplications at the end of the Cretaceous and the consequences for plant evolution. *Philosophical Transactions of the Royal Society B: Biological Sciences*, *369*(1648). https://doi.org/10.1098/rstb.2013.0353

Wan, J., Tanaka, K., Zhang, X. C., Son, G. H., Brechenmacher, L., Nguyen, T. H. N., & Stacey, G. (2012). LYK4, a lysin motif receptor-like kinase, is important for chitin signaling and plant innate immunity in Arabidopsis. *Plant Physiology*, *160*(1), 396–406. https://doi.org/10.1104/pp.112.201699

Wan, J., Zhang, X. C., Neece, D., Ramonell, K. M., Clough, S., Kim, S. Y., … Stacey, G. (2008). A LysM receptor-like kinase plays a critical role in chitin signaling and fungal resistance in Arabidopsis. *Plant Cell*, *20*(2), 471–481. https://doi.org/10.1105/tpc.107.056754

Wang, S., Hastings, A., Wang, S., Sunnenberg, G., Tallis, M. J., Casella, E., … Smith, P. (2014). The potential for bioenergy crops to contribute to meeting GB heat and electricity demands. *GCB Bioenergy*, *6*(2), 136–141. https://doi.org/10.1111/gcbb.12123

Yan, L., Ma, Y., Liu, D., Wei, X., Sun, Y., Chen, X., … Lou, Z. (2012). Structural basis for the impact of phosphorylation on the activation of plant receptor-like kinase BAK1.

Cell Research, *22*(8), 1304–1308. https://doi.org/10.1038/cr.2012.74

Zhou, J., Liu, D., Wang, P., Ma, X., Lin, W., Chen, S., … Shan, L. (2018). Regulation of Arabidopsis brassinosteroid receptor BRI1 endocytosis and degradation by plant U-box PUB12/PUB13-mediated ubiquitination. *Proceedings of the National Academy of Sciences of the United States of America*, *115*(8), E1906–E1915. https://doi.org/10.1073/pnas.1712251115

5. Chapter 2 LYM2 mediates chitin-induced plasmodesmal closure in *Populus* x *canescens*

Mo Awwanah, Merle Münier, Greta Niemann, Elena Petutschnig, Volker Lipka, Thomas Teichmann
Department of Plant Cell Biology, Georg-August Universität Göttingen, Germany

*This manuscript is not published and under preparation for submission.
Author contributions: TT and VL designed research; MA, MM and GN performed research; MA and TT analysed data; MA, TT and EP wrote the manuscript; TT, EP and VL supervised and organized funding.
Email for correspondence: tteichm@gwdg.de

5.1 Abstract

LYSIN MOTIF DOMAIN-CONTAINING GLYCOSYLPHOSPHATIDYL INOSITOL-ANCHORED PROTEIN 2 (LYM2) is a GPI-anchored LysM receptor-like protein (LysM-RLP) that harbors three extracellular LysM-domains and a GPI moiety at the C- terminus. LYM2 in *Arabidopsis thaliana* (*At*) is involved in chitin-triggered plasmodesmata (PD) closure. Two poplar homologs of *LYM2*, *PcLYM2-1* and *PcLYM2-2*, were identified and characterized in this study. Gene expression analysis showed that both genes are expressed in roots, wood, developing xylem, bark and leaves of *P. x canescens* (*Pc*) (*P. tremula* x *P. alba*). Genomic and transcriptomic analyses revealed that the second poplar homolog, *PcLYM2-2*, has two alternative splicing variants, *PcLYM2-2.1* and *PcLYM2-2.2*, which differ exclusively at the first exon encoding the three LysM domains. Chitin-binding assays showed that all identified PcLYM2 proteins bind chitin, with PcLYM2-1 exhibiting the highest binding capacity. Knocking out all *PcLYM2* genes does not abolish the chitin-induced production of reactive oxygen species (ROS) as well as MAPK activation, suggesting that poplar LYM2 proteins are not involved in these chitin-induced induced responses. Subcellular localization studies in *Nicotiana benthamiana* indicated that all identified PcLYM2 proteins localize at both plasma membrane (PM) and plasmodesmata (PD), suggesting a role of these proteins in PD-related functions. Plasmodesmal flux analysis using a mobile and immobile marker was performed on *Pclym2-1 Pclym2-2* double knock-out lines, which showed that PcLYM2 proteins mediate chitin-triggered PD closure. Moreover, loss-of-function of *PcLYM2-1* is sufficient to abolish chitin-induced PD closure, indicating that *PcLYM2-1* is the primary LysM-RLP in poplar involved in this process. However, the individual functions of the splicing variants of the *PcLYM2-2* paralog in chitin-induced PD-closure have not been analysed yet by generating *Pclym2-2.1* and *Pclym2-2.2* single knock-out lines. Analysis of *PcLYM2* transcript abundances in different tissues indicates that PcLYM2 proteins might have the potential to form tissue-specific complexes through homo- or heterodimerization, which remains to be examined.

Key words: LysM-RLP, GPI anchor, alternative splicing, chitin-binding affinity, plasmodesmal flux.

5.2 Introduction

Poplar (*Populus spp.*) is an established model system for studying tree species due to the available genetic information (of *P. trichocarpa* Nisqually), a small genome size of around 500 Mbp, simplicity of genetic transformation and high capacity for *in vitro* regeneration (Bradshaw et al., 2000; Tuskan et al., 2006; Song et al., 2006; Chen et al., 2013; Han et al., 2013; Fladung et al., 2013; Movahedi et al., 2014; Li et al., 2015; Li et al., 2017; García-Angulo et al., 2018). Poplar is also widely used in the pulp and paper industry as well as for lowland reforestation (Movahedi et al., 2014), phytoremediation of contaminated soils (Song et al., 2007; Guerra et al., 2011; Castro-Rodríguez et al., 2016), and large-scale carbon sequestration (Jansson et al., 2010). Moreover, poplar is considered as a potential bioenergy resource (Pereira et al., 2016; Tallis et al., 2013; Littlewood et al., 2014; Sannigrahi et al., 2009; Guo et al., 2015; Wang et al., 2014; Aghaalikhani et al., 2017). However, many poplar plantations are facing a severe problem due to infections caused by the rust fungus, *Melampsora larici-populina*, leading to huge losses of poplar biomass (Duplessis et al., 2009; Hacquard et al., 2011).

To initiate defense reactions against the threat, poplar plants have to detect the pathogen. Fungal pathogens can be recognized by plants through the perception of chitin, the main component of fungal cell walls that is a homopolymer of β-1,4-linked N-acetylglucosamine (GlcNAc) and serves as a pathogen-associated molecular pattern (PAMP) (Kaku et al., 2006), which can be recognized by LysM-containing receptors (Buist et al., 2008; Antolín-Llovera et al., 2014). In the model plants *Arabidopsis thaliana* and *Oryza sativa*, the components of the chitin receptor complex have been well characterized. Chitin recognition in Arabidopsis is mediated by CHITIN ELICITOR RECEPTOR KINASE1 (CERK1), a plasma membrane-localized Lysin motif receptor-like kinase (LysM-RLK) that is considered as the major component of the Arabidopsis chitin receptor complex (Miya et al., 2007; Petutschnig et al., 2010). CERK1 associates with two additional LysM-RLKs, LYK4 and LYK5, in order to facilitate proper chitin-induced signaling (Wan et al., 2012; Cao et al., 2014; Erwig et al., 2017). In rice, the major component of the chitin receptor complex is CHITIN ELICITOR BINDING PROTEIN (CEBiP), a GPI-anchored LysM-RLP that does not have a kinase domain and therefore requires association with OsCERK1 in order to trigger chitin-induced plant defenses (Kaku et al., 2006; Miya et al., 2007; Shimizu et al., 2010; Hayafune et al., 2014; Kouzai et al., 2014). OsCEBiP employs three extracellular LysM domains, and the central LysM domain is important for binding to chitin due to the presence of hydrophobic residues, especially Ile122, that act as chitin-binding site

(Hayafune et al., 2014). OsCEBiP homodimerizes upon binding to chitin hexamers, in which three GlcNAcs bind to the central LysM of each OsCEBiP molecule (Liu et al., 2016). Simultaneous binding of one chitin oligosaccharide to the mirrored-sites of two OsCEBiP molecules was described as sandwich-type dimerization by Hayafune et al. (2014). There are three homologs of OsCEBiP in Arabidopsis, LYSIN MOTIF DOMAIN-CONTAINING GLYCOSYLPHOSPHATIDYL INOSITOL-ANCHORED PROTEIN (LYM) 1, LYM2, and LYM3. Only LYM2 was shown to bind chitin (Shinya et al., 2012), while the other two homologs, LYM1 and LYM3, were reported to bind peptidoglycan (PGN) and in association with CERK1 mediate PGN-induced signaling (Willmann et al., 2011). Hayafune et al., (2014) found that Ile122, which is necessary for chitin binding, is conserved in the chitin binding homologs, OsCEBiP and LYM2, but it is replaced by Leu in LYM1 and LYM3. The chitin binding homolog in Arabidopsis, LYM2, is not involved in CERK1-mediated chitin responses (Shinya et al., 2012), but is essential for chitin-induced suppression of plasmodesmal flux independently of CERK1 (Faulkner et al., 2013).

Plasmodesmata (PD) are plasma membrane-lined cytoplasmic channels that connect cytoplasm, endoplasmic reticulum (ER) and plasma membrane (PM) of adjacent cells, establishing a supracellular network within plant cells (Burch-Smith and Zambryski, 2012; Sager and Lee, 2014; Alberts et al., 2014). The continuity of ER elements that traverses across the walls of adjacent cells is called desmotubule, which spans the cell walls but allows the continuity of the PM of neighboring cells (Alberts et al., 2014), thus establishing a cytoplasmic channel (also referred to as *cytoplasmic sleeve*) delineated by PM externally and by the desmotubule internally (Sager and Lee, 2018). Cellular trafficking occurs through this cytoplasmic sleeve and the flux is controlled by callose deposition (Zavaliev et al., 2011), which regulates the size exclusion limit of the pore. Callose accumulation around PD is regulated by the activity of two groups of antagonistic enzymes, β-1,3-glucan synthases (CalS) and β-1,3-glucanases (BGs) (Verma and Hong, 2001; Guseman et al., 2010; Vatén et al., 2011; Xie et al., 2011; Han et al., 2014; Ellinger and Voigt, 2014; Cui and Lee, 2016; Zavaliev et al., 2011; Sager and Lee, 2014; Wu et al., 2018). Some proteins that reside at the PD-PM, the continuous PM along the cytoplasmic sleeve that is exposed to the desmotubule, were reported to be also involved in the regulation of PD permeability. PD-PM contains lipid components that are highly different to those found in the PM (Grison et al., 2015; Sager and Lee, 2018), and some glycosylphosphatidyl inositol (GPI)-anchored proteins showed preferential association with sterols and sphingolipids that are abundant at the PD-PM (Galian et al., 2012; Zavaliev et al., 2016). An example is sterol-dependent PD targeting of

PDCB1, a GPI-anchored protein important for callose deposition (Grison et al., 2015). *Arabidopsis thaliana* LYM2 (AtLYM2) is another GPI-anchored protein that localizes to both PM and PD-PM. The perception of fungal chitin was shown to promote PD-closure in an AtLYM2 dependent manner (Faulkner et al., 2013). This LysM-RLP was hypothesized to associate with a LysM-RLK in order to induce PD-related downstream signaling (Cheval and Faulkner, 2018). Cheval et al. (2019) suggested AtLYK4 as a co-receptor of AtLYM2 in mediating chitin-induced PD closure since it was also found to accumulate at PD upon chitin treatment. However, AtLYK4 is a LysM-RLK that employs an inactive kinase (Wan et al., 2012; Petutschnig et al., 2010), hence, the proposed AtLYM2-AtLYK4 complex requires another component to initiate the downstream signaling. CALCIUM DEPENDENT PROTEIN KINASE 6 (CPK6), a protein involved in the phosphorylation of RBOHD for ROS production (Kadota et al., 2014), was found to associate with AtLYK4 (Cheval et al., 2019). Since ROS was reported to induce callose accumulation that leads to a reduced PD permeability (Cui and Lee, 2016), Cheval et al. (2019) suggested CPK6 as a signal transducer for the downstream signaling in PD-closure.

This research aimed at the identification of LYM2 homologs in poplar and characterization whether they are involved in chitin-triggered defense signaling and plasmodesmal flux. Two LYM2 homologs were found in poplar. One of the paralogs exhibits tissue-specific, alternative splicing, resulting in two LYM2 variants, which differ in their LysM domains. Both poplar LYM2 paralogs, including the splicing variants, are chitin-binding proteins that reside in both PM and PD-PM, pointing to a role in controlling PD function after chitin perception. The poplar LYM2 proteins may form homo- and heterodimers and differential LYM2 protein complex formation may enable tissue-specific modulation of chitin perception and signaling.

5.3 Materials and Methods

5.3.1 Phylogenetic analysis of poplar LysM-RLPs

Protein sequences of putative LysM-RLPs from *Populus trichocarpa* Nisqually were obtained by performing BLASTP searches on Phytozome (www.phytozome.org) using the *A. thaliana* LYM1, LYM2 and LYM3 sequences as queries. For phylogenetic tree construction, the protein sequences of LysM-RLPs from rice were included. The phylogenetic tree of LysM-RLPs was generated based on sequence similarity of putative *P. trichocarpa* Nisqually proteins with well-characterized LysM-RLPs from *Arabidopsis*

thaliana and *Oryza sativa*. The phylogenetic analysis was done in phylogeny.fr (https://www.phylogeny.fr/, Dereeper et al., 2008; Dereeper et al., 2010) using MUSCLE for multiple alignment (default settings), Gblocks for alignment refinement (least stringent settings), PhyML for phylogenetic tree construction (for the maximum likelihood with bootstrapping of 500 replicates) and TreeDyn for the visualization of phylogenetic trees, displaying only branch support values of >80%.

5.3.2 Plant materials and growth condition

The hybrid *P. x canescens* (*P. tremula* x *P. alba*) clone INRA 717-1B4 was used in this research. *In vitro* propagation of both wild type and transgenic plantlets was conducted on half-strength Murashige-Skoog (½ MS) medium (Duchefa Biochemie BV, Haarlem, The Netherlands) supplemented with 2% (w/v) sucrose. The plantlets were cultivated under long day conditions (light: 16h at 22 °C, dark: 8h at 18 °C, 60% relative humidity, light intensity at 70–80 µmol m^{-2} s^{-1}). Potting on soil was done on Fruhstorfer Erde Typ T25, Hawita Gruppe GmbH, Vechta, Germany supplemented with 5% (v/v) washed screed sand (0/8 mm). The potted plantlets were further cultivated in the same long day climate chamber or in the greenhouse (a minimum temperature of 22:14 °C for day:night was maintained by heating, natural daylight was supplemented by metal halide lamps (HQI-TS 400W/D; Osram) to maintain a 16 h photoperiod).

5.3.3 cDNA cloning and sequence analysis of poplar LYM2 homologs

The information on genes encoding putative LysM-RLPs that is available from the annotated genome of *P. trichocarpa* Nisqually was used to design primers (Supplemental Table 5.1) for sequence amplification of candidate genes encoding the homologs in the hybrid *P. x canescens* (*P. tremula* x *P. alba*). RT-PCR to amplify the candidate genes was conducted using phusion DNA polymerase (F-530L, Thermo Scientific) and cDNA from leaf tissue as a template. The PCR product was run on a 1% agarose gel (Biozym LE Agarose 840004, Bioyzm Scientific GmbH, Hessisch Oldendorf, Germany) supplemented with HDGreen plus DNA stain (INTAS). TA cloning (TA cloning KIT 45-0046, Invitrogen) of the purified amplicon was done to obtain allele-specific sequences of each gene (PCR purification using NucleoSpin Gel and PCR clean-up 740609.250, Macherey-Nagel). The clone-derived plasmids (Plasmid isolation using NucleoSpin Plasmid 740588.250, Macherey-Nagel) were sequenced (Seqlab, GmBH Göttingen, Germany) and further

analysed using Geneious 8.1.8 software. Predicted open reading frames (ORFs) of the obtained sequences were compared with the *PcLYM2* sequences of *P. x canescens* extracted from AspenDB (http://aspendb.uga.edu/index.php). Domain prediction was conducted on the obtained sequences by using several online prediction tools. The SignalP 4.1 server (Petersen et al., 2011) was used for assignment of signal peptides (SP), InterPro Scan integrated in Geneious 8.1.8 (Quevillon et al., 2005) for LysM domain prediction, KohGPI (Fankhauser and Mäser, 2005) and PredGPI (Pierleoni et al., 2008) for identification of a putative omega site (ω) as GPI attachment signal. The presence/absence of conserved hydrophobic residues, especially isoleucine122 that is essential for chitin binding, was determined based on sequence alignment of poplar LysM-RLPs with the sequence of the well-characterized OsCEBiP (Hayafune et al., 2014). Verification of alternative splicing of *PcLYM2-2* was done not only on the transcriptomic but also on the genomic level by amplifying the full length cDNA and genomic sequences from *P. x canescens* (Supplemental Table 5.2) and mapping the obtained nucleotide sequences to the scaffold of *PcLYM2-2* in the URGI database (https://urgi.versailles.inra.fr/Species/Forest-trees/Populus/Clone-INRA-717-1B4, Mader et al., 2018).

5.3.4 Expression analysis of PcLYM2 genes

RNA was isolated from five different tissues (roots, wood, developing xylem, bark and leaves) of soil-grown *P. x canescens* that were cultivated in either a long day climate chamber or in the greenhouse. The harvested plant materials were immediately frozen in liquid nitrogen before being ground and used for RNA isolation using the CTAB extraction protocol according to Chang et al. (1993). Plant material was ground under liquid nitrogen and ~100 mg of each tissue were added with a pre-heated mix of 750 µl extraction buffer (Supplemental Table 5.8.1. CTAB RNA extraction buffer) and 15 µl β-mercaptoethanol and further incubated in 65 °C for 15 minutes. After shaking for 15 minutes at 160 rpm, 750 µl of chloroform:Isoamyl alcohol (24:1) (A1935, AppliChem) was added, and the solution was shaken for another 15 minutes at the same speed. This step was repeated twice by adding the same amount of chloroform:Isoamyl alcohol (24:1) to the collected supernatant. For precipitation, the supernatant was added to an equal amount of pre-cooled (4 °C) 8 M LiCl and incubated on ice in the fridge (4 °C) overnight. The following day, the samples were centrifuged for 40 minutes at 4 °C and 13,300 rpm. The supernatant was discarded and the pellet was suspended in 100 µl preheated SSTE (Supplemental Table 5.8.2) to 60 °C, followed by two times extraction with 100 µl chloroform:Isoamyl alcohol (24:1). The pellet

was precipitated again by adding pre-cooled (4 °C) 96% EtOH and incubation at -20 °C for 2 hours. The RNA was collected by centrifugation at 4 °C and 13,300 rpm for 40 minutes. The precipitated RNA was washed once with 400 µl 70% EtOH, and dissolved in 20 µl nuclease-free/DEPC-treated water (T143, Roth). The extracted RNA was reverse transcribed into cDNA (cDNA synthesis Kit #K1631, Thermo Scientific), and used as a template for qPCR to measure the transcript abundance of genes encoding PcLYM2, using primers listed in the appendix Table 4. qPCR was performed using the SsoFast EvaGreen Supermix (#172-5204, Bio-Rad) and ubiquitin was used as a reference to calculate the relative expression levels. The efficiency of primers used for qPCR (Supplemental Table 5.3) were checked on gDNA, showing amplification efficiency of 89-95%.

5.3.5 Generating knock-out lines of PcLYM2 through CRISPR/Cas9

Single guide RNA (sgRNA) expression cassettes carrying the target sequences were generated according to the required parameters described in Ma et al. (2015) and Ma et al., (2016). In total, four sgRNAs were designed using primers listed in the Supplemental Table 5.4 to simultaneously modify target sites located after the LysM domains and before the omega (ω) site of all PcLYM2 homologs (both alleles including the variants) in order to disrupt the function of the omega (ω) site, which is crucial for the attachment of the GPI anchor to the proteins. The promoters of each expression cassette were amplified from intermediate vectors (AtU3d, AtU3b, AtU6-1 and AtU6-29) obtained from Addgene (Cambridge, MA, USA). These multiple sgRNA expression cassettes encoding the sgRNAs, AtU3d-sgRNA1_AtU3b-sgRNA2_AtU6-1-sgRNA3_AtU6-29-sgRNA4 in this respective order, were then cloned into pYLCRISPR/Cas9P_{35S}-N (Addgene, MA, USA) through Gibson assembly reactions at 50 °C for 1h (#E5520S, New England Biolabs, 2014; Gibson et al., 2009), using additional primers listed in the Supplemental Table 5.5. The assembled product was transformed into *E. coli* DH5-α competent cells and transformants were grown overnight at 37 °C. Plasmids isolated from the positively selected clones were sequenced to check for the proper inserts and further transformed into *Agrobacterium tumefaciens* (Plasmid isolation using NucleoSpin Plasmid 740588.250, Macherey-Nagel).

Agrobacterium-mediated plant transformation was carried out according to a protocol adopted from Matthias Fladung, Thünen Institute of Forest Genetics, Großhansdorf, Germany. Stems of *in vitro* cultivated *P. x canescens* were cut into pieces of about 3-8 mm, and then squeezed to create additional wounding as an entry site for Agrobacteria. The stem pieces were incubated in an *Agrobacterium* suspension (OD_{600} = 0.25-0.8) supplemented

with 20 µM acetosyringone (Sigma-Aldrich) for 30 minutes at 28 °C and 120 rpm shaking in the dark. Stems were then transferred onto co-incubation medium (Supplemental Table 5.8.3. Co-incubation medium (pH 5.8)) and incubated in the dark at 22 °C for 2-3 days. Subsequently, the explants were washed several times using sterile ddH_2O supplemented with 400 µg/ml timentin before transfer onto selection medium containing 50 µg/ml kanamycin (Supplemental Table 5.8.5). Some of the cut stems were also transferred onto regeneration medium as controls (Supplemental Table 5.8.4). After 2-4 weeks regenerates (explants with callus and shoot) were transferred to ½ MS media supplemented with 2% (w/v) sucrose, 150 mg/l cefotaxime, 200 mg/l timentin and 50 mg/l kanamycin for rooting (rooting medium in Supplemental Table 8.6). Rooting on selective media is an indication of transgenic plants. Leaf samples of the rooting plants were collected to isolate the gDNA for checking the editing of the target site using primers listed in Supplemental Table 5.6.

5.3.6 Transient gene expression in Nicotiana benthamiana

Coding sequences of LysM-RLPs (*PcLYM2-1*, *PcLYM2-2.1* and *PcLYM2-2.2*) were amplified from cDNA of *P. x canescens* (primers listed in the Supplemental Table 5.7). Constructs for expression of *PcLYM2* genes in fusion with the mVenus fluorescent tag under control of the 35S promoter were generated by assembling the 35S fragment and the respective coding sequence of *PcLYM2* paralogs and splicing variants as well as the mVenus coding sequence into the pGreenII-0229 vector (Hellens et al., 2000) via Gibson assembly (#E5520S, New England Biolabs, 2014; Gibson et al., 2009). The generated constructs were then transiently expressed in *Nicotiana benthamiana* leaves after leaf infiltration using a syringe. The transient assays were used for subcellular localization studies and chitin-binding assays.

5.3.7 Confocal microscopy

Microscopy analysis was conducted with the confocal laser scanning microscope (CLSM) Leica TCS SP5 system (Leica Microsystems, Wetzlar, Germany) equipped with an argon laser. mVenus was excited at 514 nm and the emitted light was captured in the range of 530-569 nm. For plasmodesmal flux analysis, the eGFP cytoplasmic marker and mKate nuclear marker were excited at 488 nm and 561 nm, respectively, and the emitted lights were collected at a range of 500-540 nm for eGFP and 620-640 nm for mKate. Images shown in this work are maximum projections of 10 Z-stack series taken ~1 µm apart under 40x

objective for imaging subcellular localization of PcLYM2 proteins and under 20x objective for plasmodesmal flux analysis.

5.3.8 Chitin-binding assay

Chitin-binding affinity assay was performed by isolation of proteins from *N. benthamiana* leaves transiently transformed with the constructs described in section 5.3.6. Total protein extract was collected by grinding 100 mg leaf materials in 1 ml protein extraction buffer (Supplemental Table 5.8.6) supplemented with 1:100 protease inhibitor cocktail (Supplemental Table 5.8.7) using a glass pistil. For chitin-binding assays, total protein extracts of around 500-1000 µg were incubated with 25 µl chitin magnetic beads (New England BioLabs *Inc*. #E8036L) at 4 °C for 1h to isolate chitin-binding protein. The chitin magnetic beads-bound protein was separated from the supernatant using a magnet, and then subsequently washed with pre-cooled 1x TBS-T and water. Water from the last washing step was removed by pelleting the chitin magnetic beads-bound protein using magnet, and the beads were mixed with 25 uL of 1.5x SDS-loading dye (diluted from 4x SDS loading dye in Supplemental Table 5.8.8). Following this assay, western blotting was carried out on SDS-PAGE (Supplemental Table 5.8.8) to detect mVenus-tagged PcLYM2 in the total protein extract (added with 1x SDS loading dye) and in the protein fraction which exhibits chitin binding, using α-GFP antibody (3h9-100, Chromotek). Quantification of western blot signals was performed in Bio-Rad Image Lab 5.2.1 software by manual lane and band detection. Signals from chitin binding proteins were normalized to total protein extract signals.

5.3.9 Microprojectile/particle bombardment assay for plasmodesmal flux analysis

A plasmid encoding a mobile eGFP cytoplasmic marker and immobile mKate nuclear marker was used for particle bombardment with a Biolistic® PDS-1000/He particle delivery system from Bio-Rad (plasmid isolation using #12945 plasmid plus midi kit (100), Qiagen). 1.0 µm gold microcarriers (#1652263 from Bio-Rad) were coated with the plasmid DNA based on a modified protocol from Robert Hänsch, Department of Plant Biology, Technische Universität Braunschweig, Germany. For coating, 3 mg gold particles were pre-washed with 100 µl of 70% EtOH and vortexed for 20 s until they are finely dispersed and the solution looks brownish. Pipetting up and down disperses the gold particles evenly. Then, centrifugation at 6000 rpm for 1 min was performed to discard the supernatant. The pelleted

gold particles were washed with 50 µl ddH_2O, and centrifugation at 2000 rpm for 1 min was done to remove the supernatant. 50 µl of pre-cooled 50% glycerin was added and the solution was vortexed for 20 s before being incubated in ultrasonic water bath for 10 s. A maximum of 15 µg plasmid DNA was added to the solution that was immediately pipetted up and down before being incubated on ice for 15 min. The suspension was added dropwise to 50 µl 2,5 M $CaCl_2$ and then to 20 µl of 0,1 M spermidine (S2626-5G, Sigma-Aldrich), and directly pipetted up and down before being incubated on ice for 10 min. To remove the supernatant, centrifugation at 700 rpm was performed for 1 min. The pellets of DNA-coated gold particles were subsequently washed two times with 100 µl of 70% EtOH and 100 µl of 96-100% EtOH. Centrifugation at 700 rpm for 1 min was performed between the washing steps. The DNA-coated gold particles were finally added to 50 µl of 96-100% EtOH. For bombardment using a hepta-adapter, 7 µl of DNA-coated particles were loaded evenly on each macrocarrier (#1652335, Bio-Rad). The third leaves of *in vitro* grown wild type *P. x canescens* as well as *PcLYM2* knock-out lines were detached from the plants and placed on a wet filter paper in a petri dish. The petri dish was positioned at a distance of 11 cm from the hepta-adapter and bombarded with DNA-coated gold particle using 900 psi rupture disks (#1652328 from Bio-Rad) that resulted in a final bombardment pressure of ~650-700 psi. The detached leaves were further infiltrated with 500 µg/ml chitin (C9752-5G from Sigma-Aldrich) or ddH_2O 2h post bombardment and further placed on a wet filter paper in a petri dish, which was then closed with parafilm and stored in the long day climate chamber. Imaging was done 48h post bombardment. For bombardment experiments with *A. thaliana*, 3-4-week-old plants were bombarded using the same plasmid DNA at a distance of about 4 cm from the macrocarrier using 1350 psi rupture disks (#1652330 from Bio-Rad) which resulted in a bombardment pressure of ~900-1000 psi.

5.3.10 ROS burst assay

Reactive oxygen species (ROS) burst was measured according to the protocol described in Petutschnig et al. (2010). Leaf discs with a diameter of 4 mm were incubated overnight in 100 µl normal tap water using 96-well plates. The following day, water from each well was replaced with 100 µl solution containing 100 µM L-012 (120-04891, Wako Chemicals) and 10 µg/ml horseradish peroxidase (P6782, Sigma-Aldrich). For analysis of chitin-elicited ROS burst, 100 µg/ml chitin from shrimp shells (C9752-5G from Sigma-Aldrich) was added to the wells. In addition, assays with 100 nM flg22 or ultrapure water

were carried out as controls. The kinetic luminescence was detected every minute using Infinite M200 Tecan plate reader for 1 hour.

5.3.11 MAP Kinase assay

The leaves of *in vitro* cultivated wild type *P. x canescens* as well as *Pclym2* knock-out mutants (*Pclym2-1* and *Pclym2-1 Pclym2-2*) were cut at the petiole and then incubated in normal tap water for overnight to allow the decline of wounding effects. The following day, leaves were vacuum infiltrated with either 10 µg/ml chitin (C9752-5G from Sigma-Aldrich), 100 nM flg22 or water and harvested after 10 minutes incubation. Total protein extraction was carried out based on the protocol described in Petutschnig et al. (2010). Frozen leaf materials were ground and 500 µl extraction solution (Supplemental Table 5.8.6) supplemented with 1:100 protease inhibitor cocktail (Supplemental Table 5.8.7) was added and the suspension was mixed thoroughly. Following 10 minutes centrifugation at 13000 rpm, the supernatant containing the total protein extract was collected. Protein concentrations were equalized and the same amount of total protein for each sample was mixed with 1x SDS loading buffer (from 4x SDS loading dye in Supplemental Table 5.8.8) for SDS-PAGE. Western blotting was carried out on SDS-PAGE (Supplemental Table 5.8.8) using an antibody against phospho-p44/42 (#9101, Cell Signaling Technology).

5.3.12 Statistical Analysis

Statistical analysis for chitin-binding was done by performing One-way Anova followed by Tukey's test. qPCR data were analyzed with Student's t-test or One-way Anova followed by Tukey's test. For bombardment experiments, statistical analyses of counts of cells showing an eGFP signal was conducted in R version 3.6.1 (R Core Team 2019). A generalized linear mixed-effects model using a negative binomial distribution was fitted to the data using the function 'glmer' from the package 'lme4' (Bates et al., 2015), applying the lines and the chitin treatment as factors and the separate plants as random effect to account for pseudoreplication effects (Harrison et al., 2018). An Analysis of Deviance (ANODE) was applied to the model to test for significant interaction effects using the function 'Anova' from the 'car' package (Fox and Weisberg, 2019). Subsequently, a post-hoc test was conducted to determine homogeneous subsets, applying Tukey's honest significance test using the function 'glht' from the package 'multcomp' (Hothorn et al., 2008).

5.4 Results

5.4.1 Identification of genes encoding LysM-RLPs in poplar

BLASTP search was carried out in the *Populus trichocarpa* (*Pt*) Nisqually genome using Phytozome v12.1 (www.phytozome.org), a plant comparative genomics portal provided by the Joint Genome Institute (JGI), to search for putative LysM-RLPs in poplar using the protein sequences of LysM-RLPs from *Arabidopsis thaliana* (AtLYM1, AtLYM2 and AtLYM3) as queries. Well-annotated protein sequences from *Populus trichocarpa*-Nisqually, that gave the highest BLAST score (representing sequence identity) with the query were extracted from the database and used for phylogenetic analysis. Phylogenetic trees were constructed based on sequence similarity of putative LysM-RLPs from *P. trichocarpa*-Nisqually with LysM-RLP sequences from the model plants *Arabidopsis thaliana* and *Oryza sativa* (**Figure 5.1**). Two homologs of LysM-RLPs, PtLYM2-1 and PtLYM2-2, were assigned to a cluster with AtLYM2, a GPI-anchored LysM RLP that binds chitin and mediates chitin-induced plasmodesmal (PD) closure (Faulkner et al., 2013). In addition, putative LysM-RLPs that are closely related with AtLYM1 and AtLYM3, LysM-RLPs involved in bacterial peptidoglycan perception (Willmann et al., 2011), were also predicted to be present in poplar. The annotation of the poplar genome (Phytozome v12.1) also indicates that the second homolog, *PtLYM2-2*, has two splicing variants designated in the Phytozome database as Potri.009G143300.1 and Potri.009G143300.2.

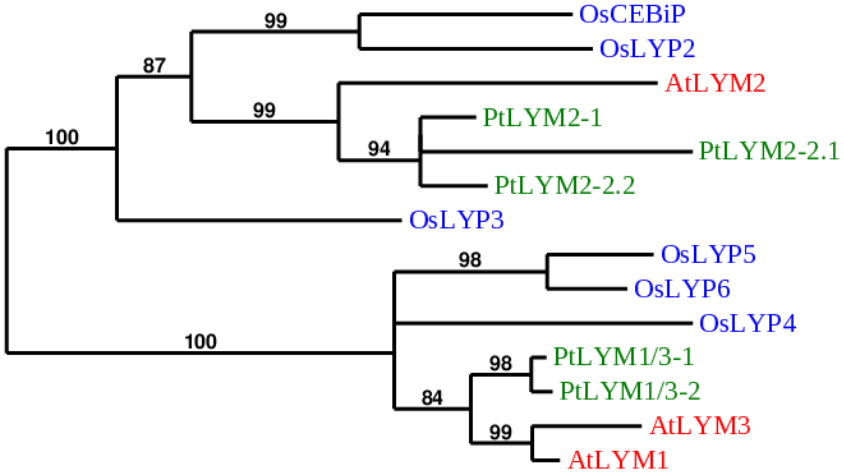

Figure 5.1. Two homologs of poplar *LYM2* are assigned to a cluster with *AtLYM2*. A phylogenetic tree of LysM-RLPs was constructed based on sequence similarity of putative *P. trichocarpa* Nisqually proteins (green) with well-characterized LysM-RLPs from *Arabidopsis thaliana* (red) and *Oryza sativa* (blue). Two poplar homologs of *AtLYM2*, a GPI-anchored protein that is involved in chitin-binding in *A. thaliana*, were assigned to a cluster with the Arabidopsis protein. Numbers on the clade are branch support values (%) from bootstrapping of 500 replicates (analyzed with PhyML for maximum likelihood).

To determine whether the candidate genes encoding putative LysM-RLPs are expressed in poplar, sequences of the putative LysM-RLP genes that are annotated in the *P. trichocarpa* Nisqually genome were used to design primers for full-length amplification of the two homologs, termed as *PcLYM2-1* and *PcLYM2-2*, as well as the predicted splicing variants from the hybrid *P. x canescens* using cDNA synthesized from leaf-derived RNA. The *PcLYM2* amplicons were sequenced and mapped to the hypothetic *LYM2* sequences of *P. x canescens* extracted from the Aspen data base (http://aspendb.uga.edu/index.php, AspenDB), which predicts allele-specific SNPs typical for a hybrid genome. To assign the SNPs to alleles, the amplified sequences were cloned and sequenced (Summarized data in **Table 5.1** and sequences in Supplemental Table 5.9).

Table 5.1. Summary of cDNA sequencing data of genes-encoding LysM-RLPs (PcLYM2) in *P. x canescens*. The presence (✓) and absence (×) of alleles originating from the parental lines *P. alba* and *P. tremula* were determined in the hybrid *P. x canescens*. Open reading frames (ORF) are indicated.

Name of Genes	*P. alba* allele	ORF	*P. tremula* allele	ORF
PcLYM2-1	✓	NA*	✓	Yes
PcLYM2-2.1	✓	Yes	✓	Yes
PcLYM2-2.2	✓	Yes	✓	Yes

***NA** = the full-length cDNA sequence of the *P. alba* allele was not obtained. The hypothetic sequence in the AspenDB indicates that this allele has an ORF. The sequence of the *PcLYM2-1 P. alba* allele is provided from the sequencing result of the URGI database instead, indicating *P. alba* allele has an ORF. (https://urgi.versailles.inra.fr/Species/Forest-trees/Populus/Clone-INRA-717-1B4).

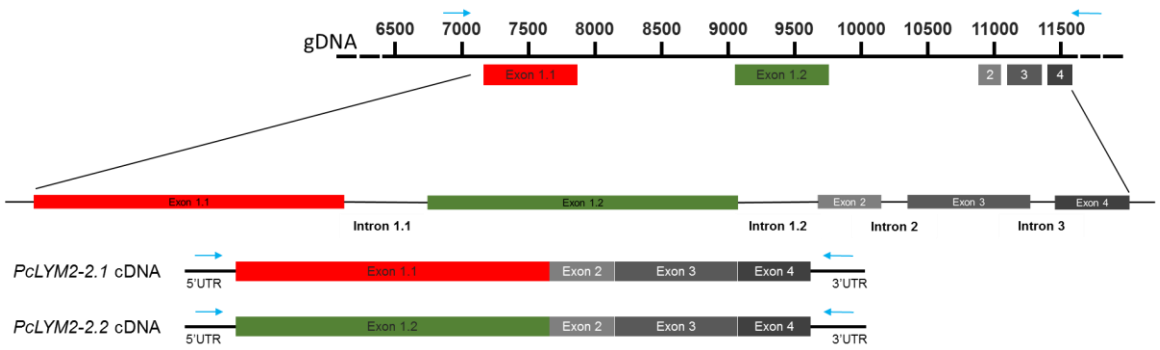

Figure 5.2. *PcLYM2-2* transcription generates two splicing variants, *PcLYM2-2.1* and *PcLYM2-2.2*, which only differ in the first exon encoding the LysM-domains. A. Genomic arrangement of *PcLYM2-2* mapped to the scaffold of *P. x canescens* from the URGI database (Mader et al., 2018), illustrating the splicing event of this homolog that results in distinct first exons (highlighted in red for *PcLYM2-2.1* and green for *PcLYM2-2.2*), giving different transcript variants. Blue arrows indicate the primer positions for amplification of the sequence from gDNA or cDNA.

The sequencing of cDNAs revealed that the predicted splicing variants of *PcLYM2-2* are present on the mRNA-level in *P. x* canescens, designated as *PcLYM2-2.1* and *PcLYM2-2.2*. The corresponding exon-intron structure of the *PcLYM2-2* gene was also verified by amplifying the full sequence of *PcLYM2-2* from the genome. The schematic mapping of the

obtained full-length *PcLYM2-2* genomic sequence to the scaffold of *PcLYM2* in the URGI database (https://urgi.versailles.inra.fr/Species/Forest-trees/Populus/Clone-INRA-717-1B4, Mader et al., 2018) indicated that the alternative splicing occurs through mutually exclusive alternative splicing, giving a different exon 1 for each variant (**Figure 5.2**) while the rest of the sequence is identical. Mass spectrometry analyses of chitin pulled-down proteins extracted from leaves also showed that PcLYM2-2 splicing variants are synthesized in leaves of *P. x canescens* (personal communication with Mascha Muhr). A phylogenetic tree that accommodates the predicted protein sequences of *P.* x *canescens LYM2* genes including the PcLYM2-2 splicing variants was generated, showing that they are in the same clade with the corresponding homologs from Arabidopsis as well as from *P. trichocarpa*-Nisqually (Supplemental Figure 5.1).

Domain prediction was performed on the obtained allele-specific protein sequences using several online tools, indicating that LYM2 homologs in poplar are GPI-anchored proteins with three extracellular LysM domains (**Figure 5.3A-B** and Supplemental Table 5.10). The predicted protein sequences were also aligned to the well-characterized LysM-RLP in rice, OsCEBiP, to provide additional *in silico* support for the predicted protein domains and the presence of conserved hydrophobic amino acid residues, in particular isoleucine122, that is essential for chitin-binding (Hayafune et al., 2014). The applied prediction tools only identified two putative LysM domains (2 and 3). However, the alignment with OsCEBiP indicated the presence of the first LysM domain, which is separated by a CxC motif from the second LysM domain. The sequence differences between the alternative exons 1 of *PcLYM2-2* splicing variants result in different amino acid compositions of the LysM domains of the two splicing variants (**Figure 5.3C**). PcLYM2-1 is highly similar to PcLYM2-2.2 with sequence identity of 86.8%, and PcLYM2-2.1 is the least similar one with sequence identity of 57.9%.

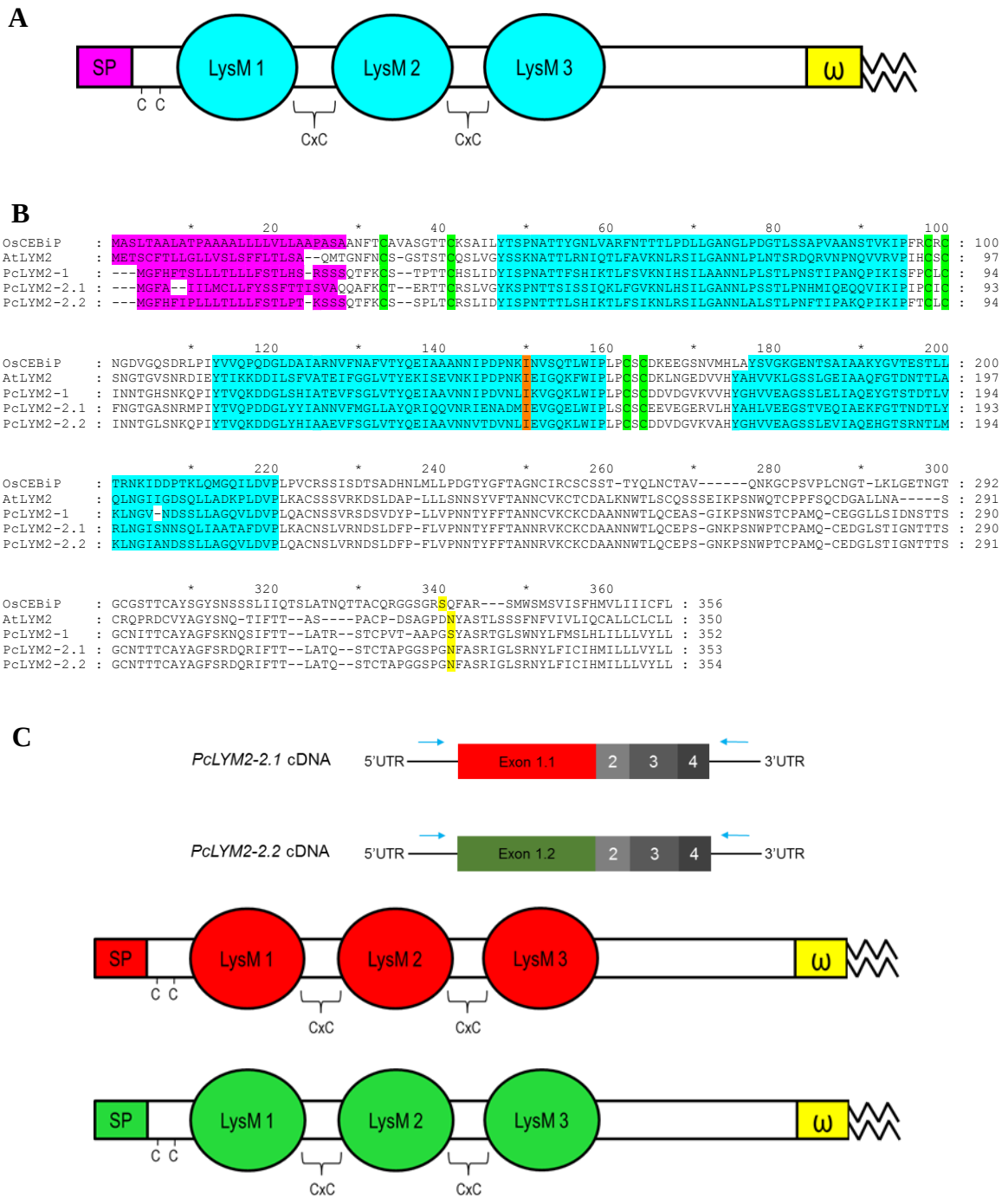

Figure 5.3. Putative LysM-RLPs in *P. x canescens* are GPI-anchored proteins with three extracellular LysM domains. A. The domain organization was predicted by using the following prediction tools: The SignalP 4.1 server (Petersen et al., 2011) was used for assignment of signal peptides (SP), InterPro Scan integrated in Geneious 8.1.8 (Quevillon et al., 2005) for LysM domain prediction, KohGPI (Fankhauser and Mäser, 2005) and PredGPI (Pierleoni et al., 2008) for identification of a putative omega site (ω) as GPI attachment signal. **B.** Alignment of Poplar LysM-RLPs with OsCEBiP (Hayafune et al., 2014), a major component of the chitin receptor complex in rice, was done to indicate the conserved isoleucine122 (highlighted in orange, numbering refers to the mature protein without SP) that is essential for chitin-binding. The AtLYM2 sequence was included in the alignment. The amino acids encoding SP are indicated in magenta, LysM-domains in light blue, separated by a CxC motif (green), and the omega site is indicated in yellow. Conserved two cysteine residues are also indicated in green. **C.** Alternative first exons in *PcLYM2-2* splicing variants result in different amino acid compositions of the N-termini comprising the three LysM domains. Blue arrows are primers used for full-length amplification of *PcLYM2-2* from leaf-derived cDNA of *P. x canescens*.

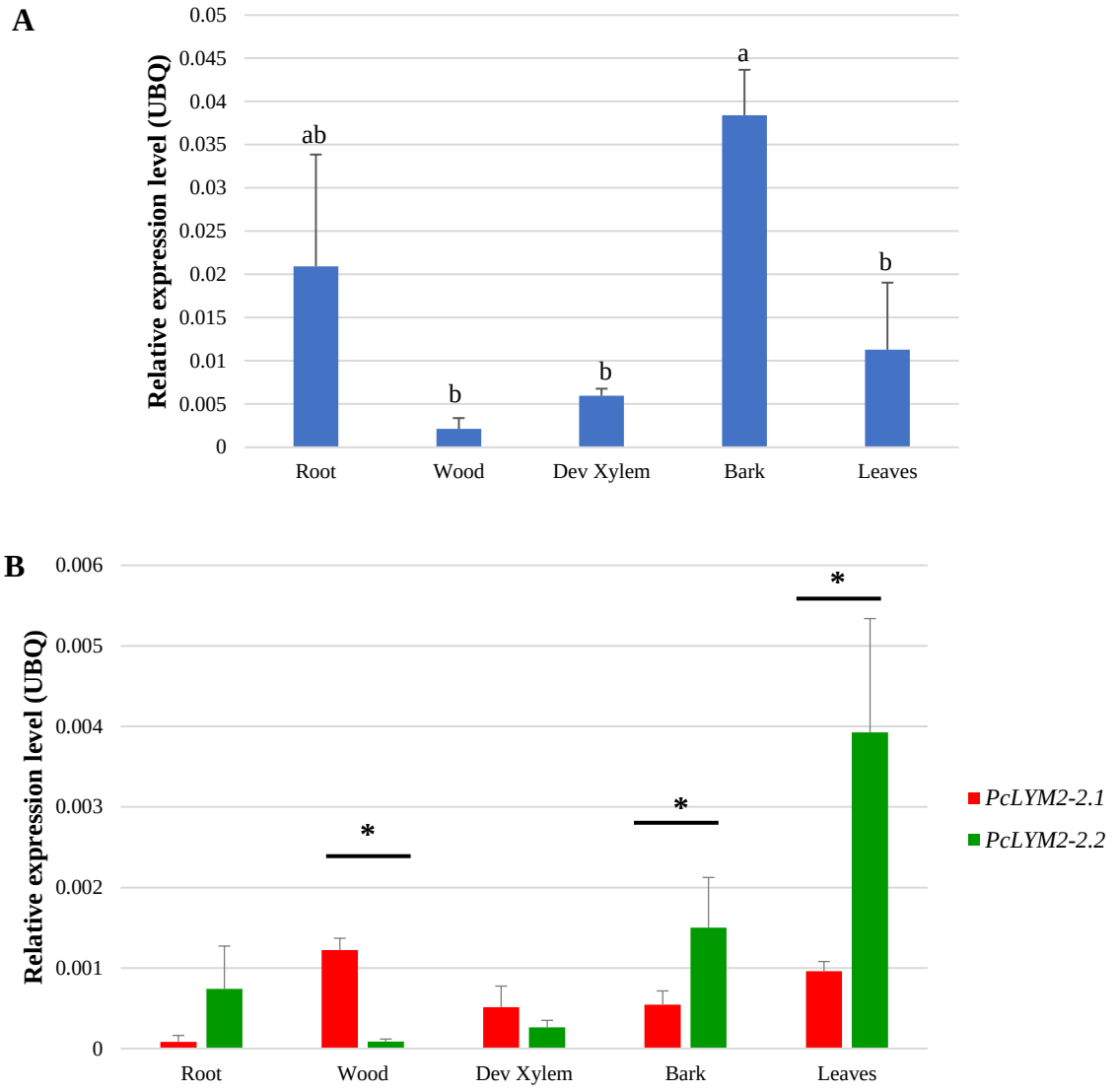

Figure 5.4. *PcLYM2* paralogs show tissue-specific expression level. cDNA synthesized from RNA from different tissues of *P. x canescens* was used as a template to perform qPCR. The transcript abundance was determined relative to UBQ as a reference. (A) Expression level of *PcLYM2-1*. Statistical analysis was conducted by one-way anova followed by Tukey's posthoc test. Different letters indicate statistical significant differences ($P \leq 0.05$), (B) Expression level of *PcLYM2-2* splicing variants. Statistical analysis was performed with unpaired student's t-test ($P \leq 0.05$), statistical significancy is designated as * . Data are means + SD (n = 3 biological replicates).

The obtained sequences of all *PcLYM2* candidate genes from *P. x canescens* were utilized to design species-specific primers for quantitative PCR (qPCR) to measure the transcript levels of *PcLYM2* genes in different tissues using cDNAs synthesized from RNA isolated from root, wood, developing xylem, bark and leaf as templates. The expression analysis shows that the two homologs as well as the splicing variants of *PcLYM2-2* are expressed in all investigated tissues of *P. x canescens* (**Figure 5.4**). *PcLYM2-1* expression is significantly higher in the bark compared to the other analysed tissues. The transcript levels of *PcLYM2-2* splicing variants (*PcLYM2-2.1* and *PcLYM2-2.1*) are lower compared

to *PcLYM2-1*. Splicing of *PcLYM2-2* is tissue specific. The splicing variant *PcLYM2-2.1* exhibits higher transcript abundances in wood compared to splicing variant 2 while *PcLYM2-2.2* shows significantly higher transcript levels in bark with the same tendency in leaves. Upon 2h chitin treatment, the expression levels of all identified *PcLYM2* genes in leaves showed a tendency to increase. However, the increase was not statistically significant (Supplemental Figure 5.2).

5.4.2 PcLYM2 proteins localize at PM and PD-PM

Subcellular localization of PcLYM2 proteins was analysed in leaves of *N. benthamiana* by *Agrobacterium*-mediated transient expression of *35S:PcLYM2-1_mVenus*, *35S:PcLYM2-2.1_mVenus* and *35S:PcLYM2-2.2_mVenus*. The generated translational fusion of PcLYM2 to mVenus allows the visualization of PcLYM2 proteins, showing PcLYM2-associated green fluorescence is unevenly distributed along the plasma membrane (PM) (**Figure 5.5A**). Bright green fluorescent dots are visible, indicating the enrichment of PcLYM2 proteins at plasmodesmal-PM (PD-PM). The number of PD-signals may be higher than the number of bright green fluorescent dots visible on the images. In PD where PcLYM2 protein level is comparable to PcLYM2 abundance at the PM, the PD-signals may be masked by the PM-signals, and therefore the bright green fluorescent dots indicating PD are not visible.

To further confirm that the bright green fluorescent dots are PD, *PcLYM2* constructs were also co-infiltrated with a plasmid expressing *PDLP5*, a PD-localized protein, tagged with mKate as fluorescent marker. The results of this observation show that the bright green fluorescent dots co-localize with the mKate-associated PDLP5 (**Figure 5.5B-D**), thus validating the PD localization. Additionally, transient expression of PM-localized *AtLYK5-mVenus* that does not show PD localization (Erwig et al., 2017) was performed, which did not result in point-shaped fluorescent signals typical for PD (Supplemental Fig. 3). This control experiment further supports the conclusion that mVenus-tagged PcLYM2 proteins localize at PD. Altogether, the data suggest that all identified PcLYM2 proteins localize at both PM and PD-PM similar to the AtLYM2 localization.

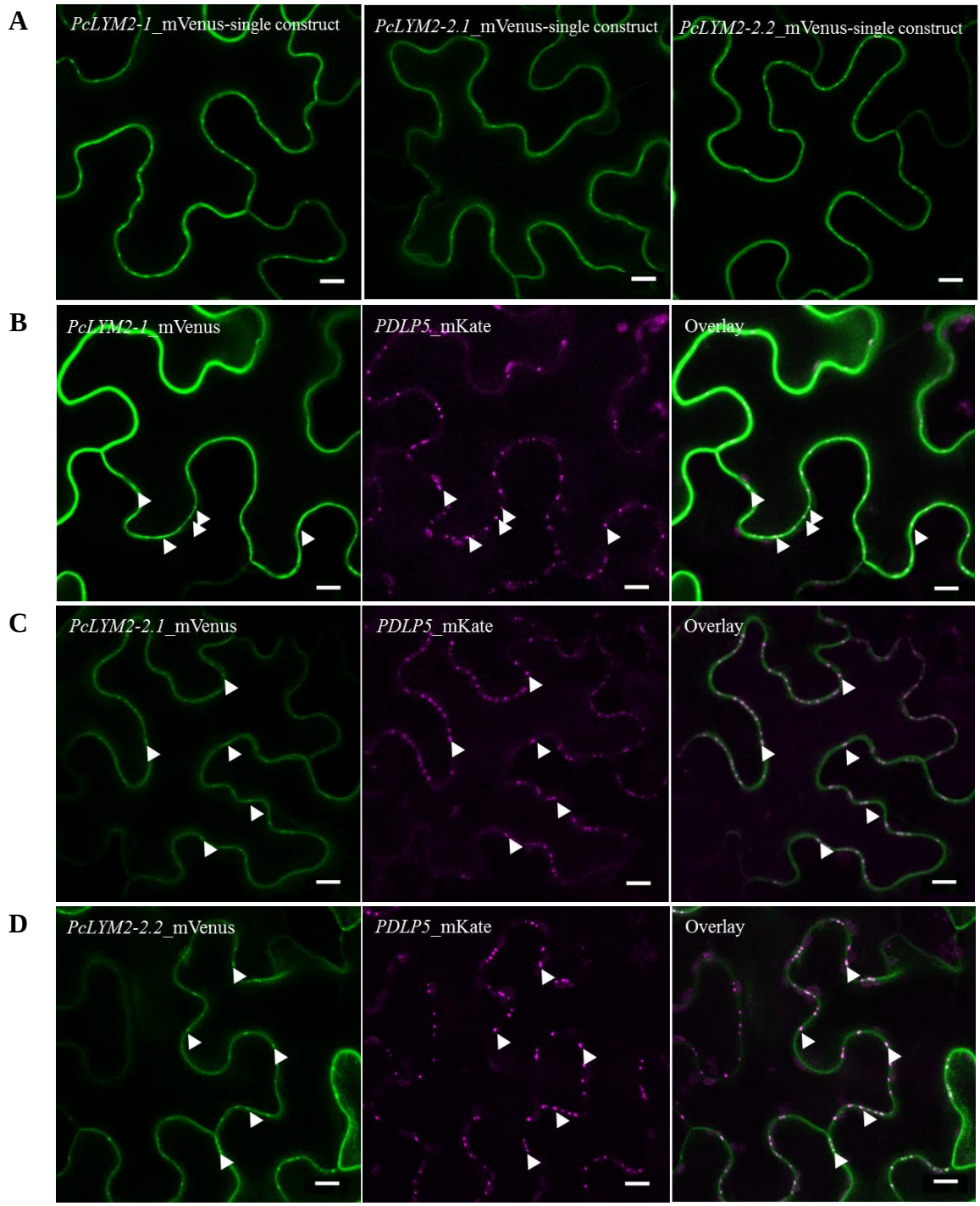

Figure 5.5. PcLYM2 proteins reside at both PM and PD-PM. A. Constructs for expression of PcLYM2 (PcLYM2-1, PcLYM2-2.1 and PcLYM2-2.2) in fusion with mVenus were infiltrated into the abaxial side of *N. benthamiana* leaves, showing uneven distribution of mVenus fluorescence, and bright green fluorescent dots are visible, indicating PcLYM2 localize at both PM and PD-PM. **B-D** Co-infiltration of PcLYM2-1_mVenus, PcLYM2-2.1_mVenus and PcLYM2-2.2_mVenus-expressing constructs with PDLP5_mKate in *N. benthamiana* leaves. In the left panel, images from the individual expression of each PcLYM2 construct show the PD-PM and PM localization of PcLYM2 proteins. The central panel are images of PDLP5-mKate as a marker for PD-localization visible as magenta dots. In the right panel, overlay images of mVenus and mKate channels confirm that all identified PcLYM2 proteins co-localize with the PD-marker PDLP5 in PD-PM (exemplarily shown by arrow heads). The protein localization was observed 72 hours post infiltration under CLSM SP5, and the displayed images are maximum projections of 10 Z-stack series taken ~1 µm apart under 40x objective. Scale bars indicate 10 µm.

5.4.3 PcLYM2 proteins are chitin-binding proteins

In Arabidopsis, AtLYM2 is involved in chitin-induced PD closure (Faulkner et al., 2013: Cheval et al., 2019). To characterize the proposed role of poplar LYM2 homologs in chitin perception, chitin-binding assays were performed by incubating total protein extracts from *N. benthamiana* leaves transiently expressing *35S:SP_mVenus:PcLYM2-1*, *35S:SP_mVenus:PcLYM2-2.1* or *35S:SP_mVenus:PcLYM2-2.2* (SP = signal peptide from the corresponding protein) with chitin magnetic beads. The amount of PcLYM2-mVenus protein was determined via western blotting using an antibody against GFP. Western blot signals of PcLYM2 in chitin magnetic bead pull-downs were normalized to signals from total protein extracts. The results show that all analysed PcLYM2 proteins can bind to chitin. PcLYM2-1 has a higher capacity to bind chitin compared with the PcLYM2-2 proteins. There is no difference in chitin-binding capacity between the two splicing variants of PcLYM2-2 (**Figure 5.6**).

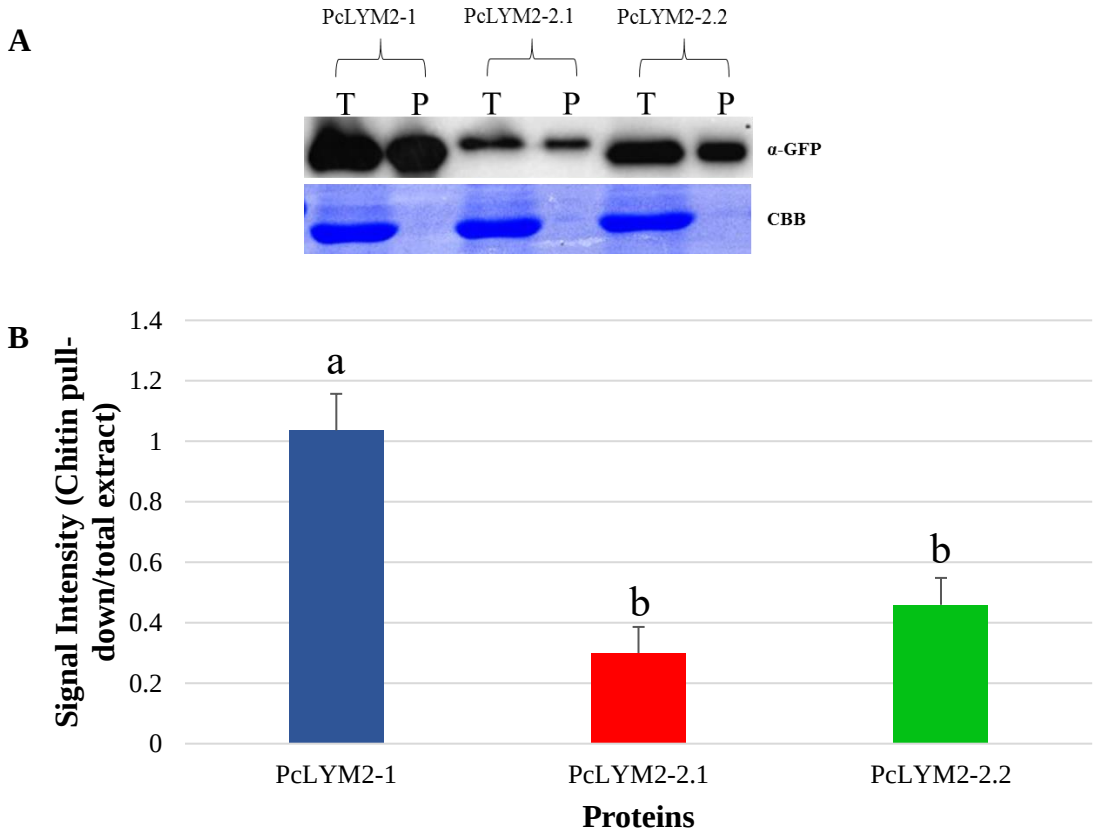

Figure 5.6. PcLYM2 proteins bind to chitin. *PcLYM2-1-mVenus*, *PcLYM2-2.1-mVenus* and *PcLYM2-2.2–mVenus* were transiently expressed in *N. benthamiana* leaves. **A.** Western blot analysis shows the comparison of total protein extracts (T) and the chitin-binding fraction purified by chitin pull-down (P) of the LYM2 homolog PcLYM2-1, as well as the splicing variants of PcLYM2-2: PcLYM2-2.1 and PcLYM2-2.2. An antibody against GFP was used to detect the mVenus-tagged proteins. Coomassie brilliant blue staining (CBB) was done on the membrane to control equal protein loading. **B.** The signals from chitin binding proteins were normalized to the signals from total protein extracts. Statistical analysis was performed by one-way anova followed by Tukey's posthoc test ($P \leq 0.05$). Data are means ± SD (n=4 technical repeats). The experiment was repeated twice with similar results.

5.4.4 PcLYM2 proteins are not involved in chitin-induced ROS burst and MAPK activation but mediate chitin-triggered PD closure

To characterize a role of PcLYM2 proteins in chitin induced ROS burst and MAPK activation, knock-out lines were generated through CRISPR/Cas9. sgRNAs were designed to simultaneously edit both alleles of *PcLYM2-1* and *PcLYM2-2* including the splicing variants (**Figure 5.7**). Two double knock-out mutants of *PcLYM2-1* and *-2* and four single knock-out lines of *PcLYM2-1* were obtained (**Table 5.2** and **Table 5.3**, Chromatogram in Supplemental Figure 5.4). In these loss-of-function mutants, editing introduced a premature stop codon or a frame shift in the coding sequence. ROS burst and MAPK assays were performed with the knock-out lines, showing that loss of LYM2 function in poplar does not abolish these plant responses to chitin treatment (**Figure 5.8**), while the lines respond like wildtype to flg22 (Supplemental Figure 5.5). These results indicate that LYM2 in poplar is not involved in canonical chitin-induced defense signaling like OsCEBiP in rice.

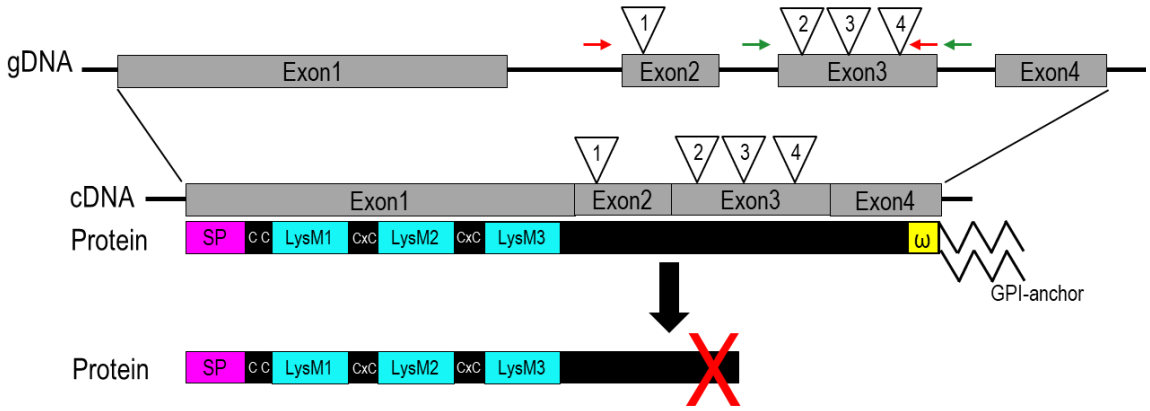

Figure 5.7. Position of target sites for CRISPR/Cas9 mediated mutagenesis of *PcLYM2* genes. Knock-out lines of *PcLYM2* were obtained by designing four sgRNAs (triangles 1-4) for knocking out all alleles of all *PcLYM2* homologs including the variants of *PcLYM2-2* simultaneously by disrupting the function of the omega site (yellow) important for GPI-anchoring. Arrows indicate primer positions for checking the editing on *PcLYM2-1* (green) on *PcLYM2-2* splicing variants (red).

Table 5.2. Summary of editing on *PcLYM2* targeted by CRISPR/Cas9

Transgenic Lines	*PcLYM2-1*				*PcLYM2-2*			
	P. alba		*P. tremula*		*P. alba*		*P. tremula*	
	T1	T2	T1	T2	T1	T2	T1	T2
T6#29	+ 1 bp		+ 1 bp		- 1 bp	+ 1 bp		+ 1 bp
T6#34b	+ 1 bp		+ 1 bp			+ 1 bp, G→A		+ 1 bp
T6#10	+ 1 bp		+ 1 bp					
T6#14	- 7 bp		- 7 bp					
T6#22c	+ 1 bp		+ 1 bp					
T6#41a	+ 1 bp		- 13 bp					

***P. alba*/*P. tremula*:** alleles of parental lines
T1/T2: sgRNA target sites

Table 5.3. Summary of CRISPR/Cas9 mediated editing on PcLYM2 protein level

Transgenic Lines	*PcLYM2-1*		*PcLYM2-2*			
	P. alba	*P. tremula*	*P. alba*		*P. tremula*	
			PcLYM2-2.1	*PcLYM2-2.2*	*PcLYM2-2.1*	*PcLYM2-2.2*
T6#29	*	*	*	*	*	*
T6#34b	→	→	*	*	*	*
T6#10	→	*				
T6#14	*	*				
T6#22c	→	*				
T6#41a	*	*				

***Premature stop** **→aa shift**

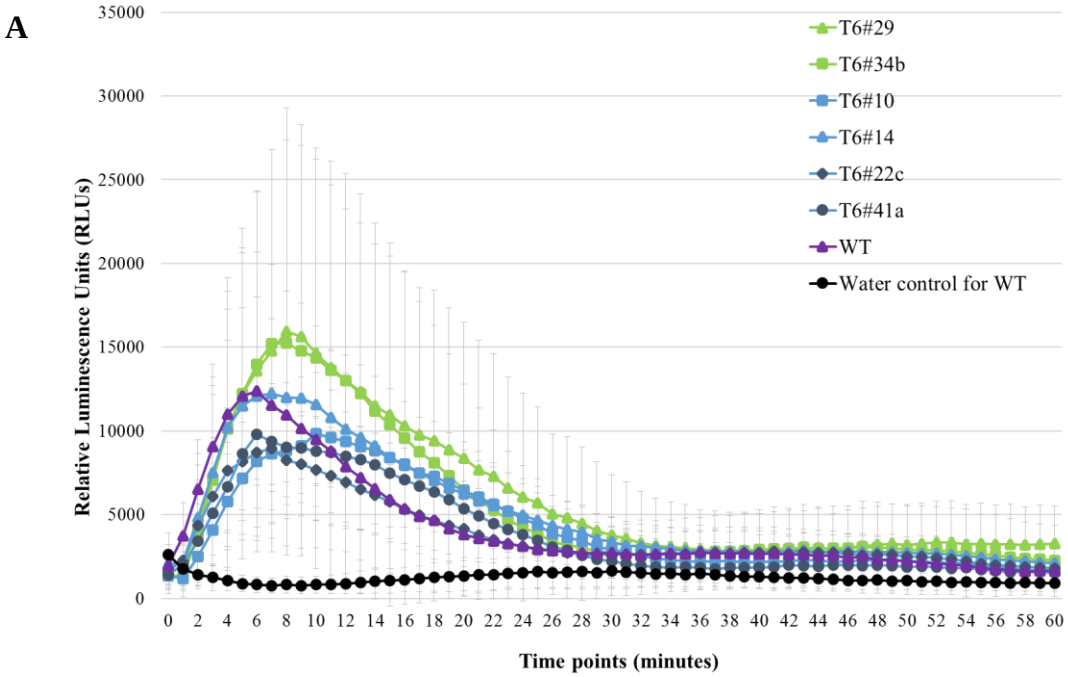

Figure 5.8. Knock-out of *LYM2* in *P. x canescens* does not impair the chitin response resulting in (A) ROS burst and (B) MAPK activation. *LYM2* knock-out lines were generated through a CRISPR/Cas9 approach in *P. x canescens*. For ROS burst assays leaf discs were treated with 100 µg/ml chitin. Data are means ± SD (n = 8 biological replicates). The ROS burst of plants after flg22 treatment is similar to wildtype plants (supplemental Figure 4). For MAPK assays, leaves were infiltrated with 10 µg/ml chitin and harvested 10 minutes post infiltration. Two independent *Pclym2-1 Pclym2-2* double knock-out lines (green) and four independent *Pclym2-1* single knock-out lines (blue) were tested. Protein samples were extracted from a pool of three plants. Coomassie brilliant blue (CBB) staining was done to check that similar amounts of protein were loaded. Each experiment was independently repeated twice showing similar results.

To examine whether *PcLYM2* has a similar function like *AtLYM2* in mediating chitin-induced PD closure, microprojectile bombardment using a plasmid for expression of a mobile cytosolic eGFP and an immobile nuclear mKate marker was carried out with the leaf discs of *PcLYM2* double knock-out mutants and wildtype plants as a control. A reduced number of neighboring cells showing the mobile eGFP marker was observed in the WT *P. x canescens* after chitin treatment, but not in the double knock-out mutants T6#29 and T6#34b (**Figure 5.9** and **Figure 5.10**), indicating that *PcLYM2* mediates chitin-induced PD closure similar to *AtLYM2*. Moreover, the single knock-out lines of *PcLYM2-1* (T6#10 and T6#22c) also showed the same response as the double knock-out lines following chitin treatment (**Figure 5.10**), indicating that PcLYM2-1 is the primary LysM-RLP in poplar involved in this process, since knocking out *PcLYM2-1* is sufficient to abolish the chitin-induced PD closure.

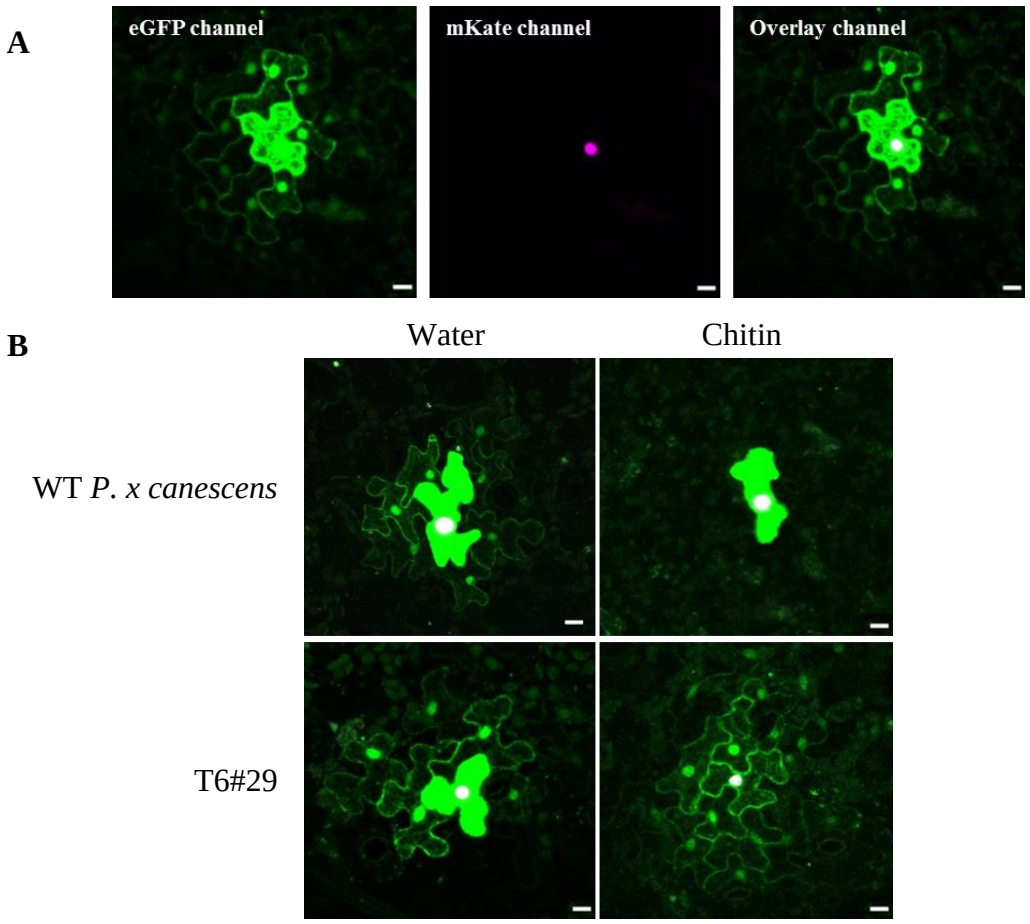

Figure 5.9. PcLYM2 mediates chitin-triggered PD closure. A. a plasmid encoding a mobile eGFP cytosolic marker (green) and an immobile mKate nuclear marker (magenta) was used to analyse PD flux by performing microprojectile bombardment on poplar leaf discs. **B.** Chitin treatment triggers PcLYM2-mediated PD closure, resulting in a reduced number (or absence) of cells showing the transferred mobile eGFP marker adjacent to the bombarded cell in WT *P. x canescens*, but not in *Pclym2-1 Pclym2-2* double knock-out mutant T6#29. The displayed images are a maximum projection of 10 Z-stack series taken ~1 µm apart, and in B only overlay channels are displayed.

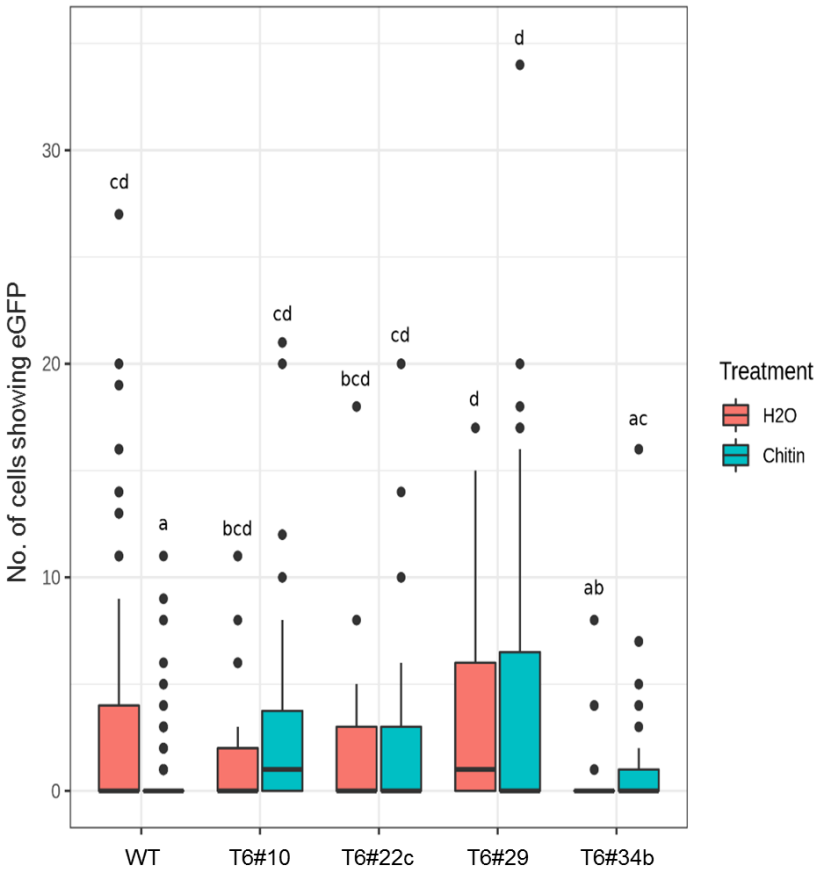

Figure 5.10. PcLYM2 mediates chitin-triggered PD closure. Two *Pclym2-1 Pclym2-2* double knock-out lines (T6#29 and T6#34b) and two *Pclym2-1* single knock-out lines (T6#10 and T6#22c) were characterized for chitin-induced PD closure by performing microprojectile bombardment assays. WT *P. x canescens* was included as a control. The number of adjacent cells showing transferred eGFP from the bombarded cell was counted. The boxplot displays the median of the dataset (central bar), the range between the first and third quartile (box) and the highest and lowest values still within the 1.5 interquartile range (IQR) of the higher and lower quartile, respectively (whiskers). Values outside of this range are depicted as circles. Statistical analyses of counts was conducted with a generalized linear mixed-effects model using a negative binomial distribution. An Analysis of Deviance (ANODE) was applied to the model to test for significant interaction effects. The ANODE results reveal a significant interaction between the treatment and the lines ($p = 5.132 \times 10^{-12}$,), *i.e.* at least one line reacts differently to the chitin treatment. Subsequently, a post-hoc test was conducted to determine homogeneous subsets, applying Tukey's honest significance test. The Tukey's test shows that the treatment has a significant effect in wildtype plants, but that none of the *PcLYM2* knockout lines exhibit significant differences in count numbers. Characters designate homogenous subsets.

5.4.5 PcLYM2 transcripts show differential expression after bud break

The presence of two homologs of LYM2 as well as two splicing variants of the second homolog in poplar raises the question whether these proteins perform different functions. Expression analysis in different tissues showed that the transcript of the first *PcLYM2-2* splicing variant, *PcLYM2-2.1*, has a higher abundance in wood compared to *PcLYM2-2.2*. Wood is built from the vascular cambium. The activity of this meristem changes upon the shift from winter dormancy to the active growth period. To analyse if *PcLYM2-2.1* transcript abundance correlates with cambial activity, expression of the two splicing variants in different seasons was analysed. RNA samples were isolated from wood and bark of wild type *P. x canescens* before and after bud break. During this time, the vascular cambium shifts from dormancy to active growth. In this analysis, the first homolog (*PcLYM2-1*) and the second splicing variant of *PcLYM2-2* (*PcLYM2-2.2*) were also included. In general, all *PcLYM2* genes exhibit higher expression in bark and wood after bud break (**Figure 5.11**), and consistent with the expression data in different tissues (**Figure 5.4**), *PcLYM2-1* expression is higher than both splicing variants of *PcLYM2-2*. In wood, the expressions of all *PcLYM2* genes show a statistically significant increase after bud break. However, the transcript abundance of the splicing variant *PcLYM2-2.1* is ten times higher after bud break compared to *PcLYM2-2.2*. On the contrary, in bark only the other paralog, *PcLYM2-1*, is significantly up-regulated after bud-break.

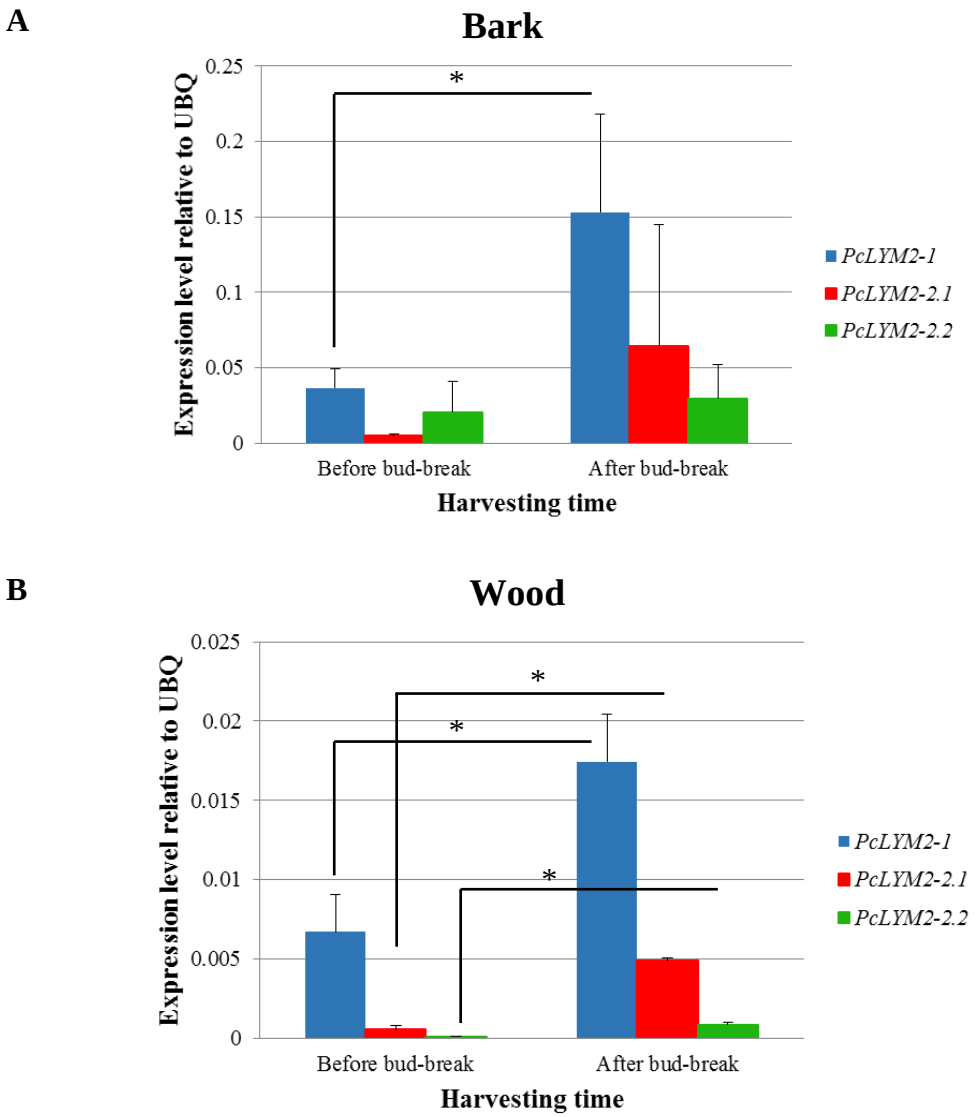

Figure 5.11. Expression of *PcLYM2* genes is induced in wood after bud break. A. In bark, expression level of *PcLYM2-1* significantly increases after bud break. **B.** In wood, higher expression levels of all identified *PcLYM2* genes after bud-break were observed. qPCR was conducted by using cDNA samples synthesized from bark or wood-derived RNAs of *P. x canescens* harvested before and after bud break. The expression level was calculated relative to UBQ as a reference. Statistical analysis was conducted by unpaired student t-test ($P \leq 0.05$) to check significant differences between samples before and after bud break. Data are means ± SD (n = 3 biological replicates). Asterisks represent significant differences, and bars indicate standard deviation.

5.5 Discussion

5.5.1 PcLYM2 proteins are GPI-anchored proteins with unique splicing variants

Tuskan et al. (2006) reported that the poplar genome contains on a statistical average at least 1.4 to 1.6 putative genes per homolog in the *Arabidopsis* genome. In line with this statement, two genes, *PcLYM2-1* and *PcLYM2-2* were identified as *LYM2* homologs in *P. x canescens*. The presence of more gene copies in poplar is due to a whole genome-duplication that occurred in poplar during evolution (Hou et al., 2019). After a duplication event, one of

the paralogs lost or kept and possibly acquire a new function. The reason is, that over time mutations may accumulate in one of the paralogs, which can result in either gene deletion/inactivation or functional modification (Mach, 2014; Vanneste et al., 2014). For instance, *PRX* genes, encoding a class of peroxidases in *Populus*, originated from gene duplication events. This gene class then lost some members during evolution (Ren et al., 2014), in which the persistent genes are mostly in clusters (37 out of 93 genes) due to tandem duplication. This is not the case for *LYM2* homologs in poplar that reside in different chromosomes, *PcLYM2-1* in chromosome 4 and *PcLYM2-2* in chromosome 9. However, both *PcLYM2* paralogs persist in the poplar genome and most likely, functionality of these paralogs is conserved. In *P. x canescens*, a hybrid poplar used in this study, not only two paralogs exist, but each gene has two alleles representing the parental lines *P.tremula* and *P. alba*.

Genomic and transcriptomic analysis revealed that the second homolog of *PcLYM2*, *PcLYM2-2*, is subject to alternative splicing which generates the protein variants PcLYM2-2.1 and PcLYM2-2.2. Alternative splicing (AS) is a mechanism of gene regulation that can increase protein diversity or play a role in regulation of protein activity (Chaudhary et al., 2019). For instance, four of *SECONDARY WALL-ASSOCIATED NAC DOMAIN 1* (*SND1*) gene family members in *P. trichocarpa*, *PtrSND1-A1*, *-A2*, *-B1* and *-B2*, undergo AS (Li et al., 2012). *SND1*s are transcription factors (TFs) that affect secondary cell wall biosynthesis by activating a cascade of TFs and gene pathways in Arabidopsis and poplar. *PtrSND1-A2*^{IR}, a non full-size alternative splicing variant of *PtrSND1-A2*, lacks DNA binding and transactivation ability, but was shown to have dimerization capability. For translocation of SND1 from the cytoplasm into the nucleus, the presence of any other full-size *PtrSND1* member as a heterodimeric partner is required. Thus, PtrSND1-A2^{IR} acts as a dominant negative regulator by disrupting the function of the interacting partner. Full-size *PtrSND1* members usually activate their own genes and a common *MYB* gene (*PtrMYB021*), but that is not the case for *PtrSND1-A2*^{IR} due to the loss of the crucial protein domains.

There are five modes of AS, exon skipping, intron-retention, mutually exclusive exons, alternative donor site, alternative acceptor site and alternative polyadenylation can occur (Zhang et al., 2015; Chaudhary et al., 2019). Comparative evaluation of the AS events that was conducted in four different fruit plants including *Malus domestica*, *Vitis vinifera*, *Citrus sinensis*, and *Fragaria vesca*, showed that splicing through intron retention occurs at a higher frequency in these four assessed plant species than the other alternative splicing modes (Sablok et al., 2017). Clark et.al. (2019) analysed AS in tomato, and also reported

that AS through intron retention is more dominant (18.9%) compared to the other modes of AS that were identified in tomato such as alternative donor site (12.9%), alternative acceptor site (7.3%) and exon skipping (6%). Usually, splicing events that occur through intron retention or exon skipping result in the loss of a protein domain as reported for *PtrSND1-A2*^{IR} for instance, which underwent AS through intron retention (Ner-Gaon et al., 2007; Li et al., 2012). Comparably, the primary transcript of *MdCesA8-A*, a cellulose synthase gene in *Malus x domestica* is differentially spliced, which results in the loss of the zinc-binding domain in one of the splicing variants (Greco et al., 2012). The pre-mRNA of *REVOLUTA* (*REV*), a poplar gene involved in regulating the architecture of leaf and vascular tissues, was also shown to undergo alternative splicing at the 3' end, resulting in splicing variants with putatively functional polymorphisms associated with resistance to *Melampsora x columbiana* rust fungus. This indicates pleiotropic functions of *REV* across different phenotypic traits, e.g. leaf morphology and pathogen resistance (Porth et al., 2014).

Comparison of gene structure and cDNA sequences of *PcLYM2-2* splicing variants shows that the splicing in *PcLYM2-2* occurs through mutually exclusive splicing of exon 1. This AS mode is not common in plants compared to intron retention and exon skipping (Zhang et al., 2015). This splicing mechanism commonly produces transcripts with identical ORF length (Zhang et al., 2015; Chen et.al., 2007). Chen et.al. (2007) analysed mutually exclusive exon splicing events in plants and found 84 and 79 in rice and Arabidopsis, respectively. Mutually exclusive splicing results in proteins with identical domain composition, but differences of amino acid sequence in one of the domains (Chen et.al., 2007). A *CALCIUM-DEPENDENT CALMODULIN-INDEPENDENT PROTEIN KINASE* (*CDPK*) gene of *Marchantia polymorpha* is subject to mutually exclusive alternative splicing. The *CDPK* gene consists of 9 exons and 8 introns, and the 6th and 7th exon are almost identical encoding the *EF-hands* of the calcium-binding domain (Nishiyama et al., 1999). Two transcript variants of *CDPK* were identified in *M. polymorpha* each containing only one of the two exons, and mRNA containing both exons was not detected. Also *PcLYM2-2* is subject to mutually exclusive alternative splicing. Two transcripts containing either exon 1.1 or exon 1.2 were detected. The alternative stranscripts are translated into two full-size splicing variants that have a similar protein domain organization, but different LysM-domains at the N-terminus (**Figure 5.3C**). Mass spectrometry analyses of total protein extracts showed that both splicing variants are present in poplar leaves (Muhr, personal communication).

Domain organization of the putative PcLYM2 protein sequences revealed that PcLYM2 proteins are GPI-anchored LysM-RLPs that have three extracellular LysM-domains but lack an intracellular kinase domain and employ a GPI-anchor at the C terminal region instead (**Figure 5.3A-B**). This domain organization is typical for LysM-RLPs such as rice OsCEBiP and Arabidopsis AtLYM2 (Hayafune et al., 2014; Gong et al., 2017; Shinya et al., 2012; Faulkner et al., 2013). GPI-anchored proteins have a GPI attachment signal (GPI signal peptide) at the C terminus that consists of a hydrophobic domain, an omega cleavage site and a short strand of hydrophilic residues (Galian et al., 2012). The GPI moiety is added to the C-terminus of the protein following the detection and cleavage of the GPI signal peptide by a multisubunit transamidase in the ER lumen. Concerning *PcLYM2-2* splicing, the two generated splicing variants differ only at the first exon that encode the LysM domains with distinct amino acid compositions of the variants. LysM domain alignment of all three identified PcLYM2 proteins, PcLYM2-1, PcLYM2-2.1 and PcLYM2-2.2, showed that PcLYM2-2.1 shares sequence identity of only 57.9% with the LysM domains of the other PcLYM2 proteins. On the contrary, LysM domains of the second splicing variant (PcLYM2-2.2) and the first homolog (PcLYM2-1) are highly similar with sequence identity of 86.8%. These alignment data indicate that PcLYM2-1 and PcLYM2-2.2 might perform redundant functions, while a distinct role of PcLYM2-2.1 is possible.

5.5.2 PcLYM2 proteins are chitin-binding, PD-PM-localized LysM-RLPs

Mutations that occur following gene duplication might lead to neofunctionalization of one of the paralogs. Therefore, the proteins encoded by the gene duplicates can exhibit redundant or different functions, and a functional divergence can be tissue- or stage-specific (Mach, 2014). Subcellular localization studies of two paralogous clusters of *PRXs* revealed that some of the paralogous *PRX*s underwent changes in subcellular localization resulting in two groups of PRXs, cell wall and vacuolar PRXs. Functional characterization of these two PRX clusters, also, showed that paralogous PRXs exhibit different substrate specificities. These results suggest that beside positive selection during evolution, alteration of subcellular localization is also important for retention of duplicate genes such as *PRXs* in poplar, and that the persistent duplicates could subsequently undergo functional specification (Ren et al., 2014). Subcellular localization studies in *N. benthamiana* of the two poplar *LYM2* homologs including the *PcLYM2-2* splicing variants revealed that despite different amino acid compositions of the LysM domains, all identified PcLYM2 proteins resided at the same location, at both PM and PD-PM (**Figure 5.5**). Since all identified PcLYM2 proteins reside

at the same location at the PD-PM, the different amino acid compositions of the LysM domains do not affect the subcellular localization. However, this study was conducted in a heterologous system in *N. benthamiana.* Thus, the localization in poplar remains to be investigated.

LYM2 in Arabidopsis (*AtLYM2*) and in rice (*OsCEBiP*) were shown to be involved in chitin perception but mediate different chitin-induced pathways (Kaku et al., 2006; Faulkner et al., 2013). This indicates that LYM2 proteins can work in different signaling pathways. Since *PcLYM2* gene duplicates, which were retained during evolution, can gain a new function, different roles of PcLYM2 proteins are conceivable. This hypothesis was addressed by performing chitin-binding assays to determine if the PcLYM2 LysM domains of the paralogs exhibit different chitin binding capacities (**Figure 5.6**). Mass spectrometry analysis of proteins extracted from leaves of soil grown *P. x canescens* showed that all characterized PcLYM2 proteins are present in the protein extracts enriched for chitin binding proteins (Muhr, unpublished), and chitin-binding capacity assays confirmed that they are capable of binding chitin (**Figure 5.6A)**. Based on the quantitative chitin-binding data (**Figure 5.6B**), the first homolog (PcLYM2-1) shows about 4 and 5 times higher capacity to bind chitin than PcLYM2-2.2 and PcLYM2-2.1 respectively, while the chitin-binding capacities of these two splicing variants of PcLYM2-2 are similar. These data indicate that the different amino acid compositions of the LysM domains, are not the determinants for affinity to the ligand chitin. The LysM domains of PcLYM2-2.1 and PcLYM2-2.2 are different, but show similar levels of chitin binding. Hayafune et al. (2014) in their work on OsCEBiP found that hydrophobic amino acid residues especially Ile122 at the central LysM domain are responsible for ligand-binding in particular to chitin. Ile122 is conserved in all identified PcLYM2 proteins (**Figure 5.3B**). However, more specific assays to examine ligand-binding affinity of the component of a receptor complex need to be performed. There are several approaches to examine interaction between ligand and protein receptor, such as labeled, label-free, structure-based, thermodynamic, and whole cell ligand-binding assays (Yakimchuk, 2011). According to the chitin-binding capacity assays and subcellular localization studies, all identified PcLYM2 proteins are chitin-binding LysM-RLPs that localize at PD-PM. However, the higher chitin-binding capacity of PcLYM2-1 compared to the other identified PcLYM2 proteins indicates that there might be functional divergence between the paralogs.

5.5.3 PD-localized PcLYM2 proteins mediate chitin-triggered PD closure and may form tissue-specific homo- or heterodimers

All identified PcLYM2 proteins are involved in chitin binding with the first homolog, PcLYM2-1, showing a higher binding capacity. To analyse whether chitin perception by PcLYM2 proteins mediates primary chitin-triggered defense signaling (involving ROS burst and MAPK activation in **Figure 5.8**) or controls plasmodesmal flux, functional characterizations of these two pathways were performed (**Figure 5.9** and **Figure 5.10**). Information on PD localization of PcLYM2 proteins is a hint that they might be involved in PD-related functions similar to AtLYM2, a well characterized PD-localized LysM-RLP that mediates chitin-triggered PD closure in *A. thaliana* (Faulkner et al., 2013: Cheval et al., 2019). This hypothesis is supported by the fact that knocking out PcLYM2 genes does not abolish chitin triggered ROS burst and MAPK activation. This suggests that PcLYM2 proteins are not crucial components of the canonical poplar chitin receptor complex as shown for OsCEBiP in rice (Kaku et al., 2006; Miya et al., 2007; Shimizu et al., 2010; Hayafune et al., 2014; Kouzai et al., 2014), but might be responsible for PD flux regulation like Arabidopsis LYM2. PD flux analysis on *PcLYM2* double and single knock-out lines revealed that PcLYM2 proteins are indeed indispensable for chitin-triggered PD closure, since plasmodesmal flux in this line does not respond to chitin treatment in contrast to chitin induced PD-closure in wild type *P. x canescens*.

Among all identified PcLYM2 proteins, PcLYM2-1 has the highest capacity to bind chitin and is, thus, suggested to be a component of a chitin receptor complex that plays a major role in mediating chitin-triggered PD closure in poplar. On the other hand, the two splicing variants that both have similar chitin-binding capacities might act as co-receptors of PcLYM2-1 in mediating chitin-induced responses in poplar. The molecular binding mechanism of LysM-RLP to chitin was described in rice CEBiP, showing that OsCEBiP homodimerizes in a sandwich-type dimerization upon binding to chitin (Liu et al., 2016; Hayafune et al., 2014). Hence, dimerization between poplar LYM2 proteins may also be necessary for chitin perception, which can occur in a homo- or heterodimerization mode that include interaction between the same or different PcLYM2 paralogs respectively.

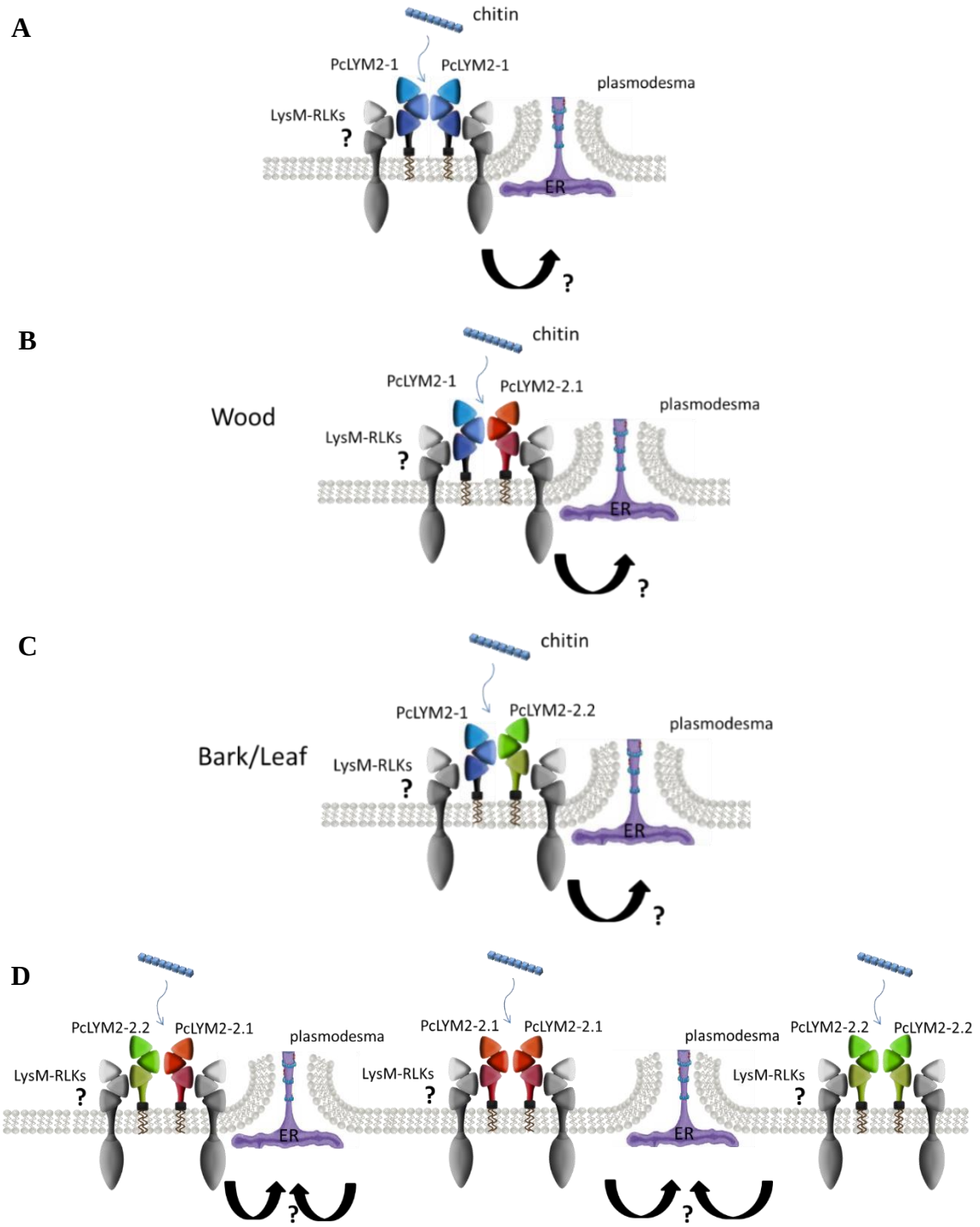

Figure 5.12. PcLYM2 proteins may establish tissue-specific complexes through homo- or heterodimerization. PcLYM2-1 is more abundant in all analysed tissues than the splicing variants of the second homolog and may be able to homodimerize upon chitin perception (A). In wood, where the transcript of PcLYM2-2.1 was found to be higher than in the other tissues, PcLYM2-1 might heterodimerize with this protein (B). In bark/leaf, PcLYM2-2.2 transcript was found to be more abundant than in the other tissues, therefore this protein might form a heterodimer with PcLYM2-1 (C). In addition, homo- or heterodimerization of PcLYM2-2.1 and PcLYM2-2.2 is also possible in any tissues since the number of PD varies in different tissues throughout different seasons and following developmental stage of the plants (D).

PcLYM2-1, which is generally expressed at a higher level compared to *PcLYM2-2*, might homodimerize in all identified tissues upon chitin perception. However, heterodimerization with PcLYM2-2 is also possible. The splicing variants of PcLYM2-2 show tissue-specific transcript abundances (**Figure 5.4**). Thus, it is conceivable that the associations of PcLYM2-2 variants with PcLYM2-1 might be tissue-specific. In wood, PcLYM2-2.1 could be the predominant interaction partner of PcLYM2-1, while in bark and leaves the splicing variant PcLYM2-2.2 prevails as a heterodimerization component. The two possible PcLYM2-1/PcLYM2-2 heterodimers may have a different chitin affinity or even bind ligands other than chitin. In addition, also homo- or heterodimerization of the two splicing variants of PcLYM2-2 is possible, eg. when the first paralog is less abundant. **Figure 5.12 A-D** illustrates a model on the hypothesized tissue-specific PcLYM2 complex formation. Keeping in mind that the amount of PD also varies over plant growth and development, which can be altered temporarily or permanently in different plant tissues (Roberts and Oparka, 2003), the abundance of PD-residents like PcLYM2 can be also change in correlation with PD frequency. Changes in the transcript abundances of *PcLYM2* for instance, were observed in wood and bark after bud-break (**Figure 5.11**), presumably due to the increasing number of plasmodesmata. A sharp rise of PD number is observed in spring and the high amount is maintained during summer, which is then decreasing toward the dormant state in autumn (Fuchs et al., 2010). Thus, the composition of PcLYM2 complexes in wood and bark may change during the year.

For initiating chitin-induced downstream signaling of PD closure, PcLYM2 proteins that do not have an intracellular signalling domain require association with a LysM-RLK as proposed for AtLYM2-mediated chitin-triggered PD closure in Arabidopsis (Cheval and Faulkner, 2018). Interaction between a LysM-RLP and a LysM-RLK was shown for OsCEBiP and OsCERK1 in mediating chitin-induced defense signaling related to ROS burst and MAPK activation in rice (Shimizu et al., 2010; Kouzai et al., 2014), as well as association between AtLYM1/AtLYM3 and AtCERK1 in mediating the recognition of peptidoglycan (PGN) in Arabidopsis (Willmann et al., 2011). AtLYM2 that mediates chitin-triggered PD closure was suggested to interact with AtLYK4, a PM-localized LysM-RLK. AtLYK4 was hypothesized to alter its localization from PM to PD-PM following its dissociation from a complex with AtLYK5 upon chitin perception (Faulkner et al., 2013: Cheval et al., 2019). However, this hypothesis can be questioned, since AtLYK4 is a LysM-RLK with an inactive kinase, unlike CERK1, which makes it unlikely that LYK4 mediates downstream signaling pathways. CALCIUM DEPENDENT PROTEIN KINASE 6 (CPK6),

protein involved in the phosphorylation of RBOHD for ROS production (Kadota et al., 2014), interacts with AtLYK4 (Cheval et al., 2019). Application of exogenous ROS induces callose accumulation that further reduces PD permeability (Cui and Lee, 2016). Thus, CPK6 that interacts with the inactive kinase domain of AtLYK4 in the AtLYM2-AtLYK4 association was suggested to function as signal transducer for the downstream signaling in PD closure (Cheval et al., 2019). The formation of a receptor complex that includes LYK4 as well as CPK6 in association with PcLYM2 for chitin-induced PD closure in poplar remains to be characterized.

5.5.4 Tissue specific splicing may provide poplar with receptor complexes against fungal pathogens with different infection strategies

PcLYM2-1 shows considerable expression in all tissues of poplar and may be involved in recognition of PAMPs from different fungal pathogens infecting roots, bark or leaves. However, transcript abundance of *PcLYM2-2* splicing variants is tissue-specific. *PcLYM2-2.2* that is highly expressed in leaves, may play a role in detection of pathogens like *Melampsora larici-populina*, the major fungal pathogen of poplar, which mainly infects leaves (Hacquard et al., 2011). *PcLYM2-2.1* that is highly abundant in wood might be involved in recognition of fungal pathogens that proliferate in wood (Singh and Chen, 2008).

5.5.5 PcLYM2-2 proteins might be receptors of other PAMPs beside chitin

Knocking out *PcLYM2-1* is sufficient to abolish chitin induced PD closure in poplar (**Figure 5.10**). This shows that the PcLYM2 paralogs are not functionally redundant and indicates functional divergence of the two paralogs. PcLYM2-2 splicing variants that were shown to bind chitin with lower capacity than PcLYM2-1 might bind other ligands than chitin. Lysin motifs containing proteins are involved in binding bacterial peptidoglycan (PGN) or symbiosis-related signals such as lipo-chitooligosaccharides (LCOs) (Buist et al., 2008; Antolín-Llovera et al., 2014; Buendia et al., 2018). Therefore, the possible different roles of PcLYM2 proteins remain to be explored by testing different ligands. Fungal cell walls consist of mannoproteins, β-1,3 or β-1,6 glucans and chitin, and the composition varies between different fungal species (Fesel and Zuccaro, 2016). In addition to chitin, β-1,3 glucan is another major component of fungal cell walls, which is synthesized by a PM-bound glucan synthase complex (Gow et al., 2003). Mélida et al. (2018) identified cell wall components of the ascomycete *Plectosphaerella cucumerina*, a pathogenic fungus. The cell wall of this fungus is mostly composed of glucans with a glucan to chitin ratio of 3:1. The

non-branched 1,3-β-D-(Glc) hexasaccharide of the *Plectosphaerella cucumerina* mycelial cell wall was characterized as the major fungal PAMP that can induce CERK1-mediated PTI responses in Arabidopsis (Mélida et al., 2018). The strength of the response is highly dependent on the degree of polymerization of the glucan. CERK1 was suggested to be a co-receptor for linear 1,3-β-D-glucans that are present in the walls of fungi and oomycetes, which works in a similar mechanism to the perception of fungal chitin-oligosaccharides and bacterial PGN. For the perception of PGN, CERK1 in Arabidopsis was suggested to associate with LYM1 and LYM3 (Willmann et al., 2011). PcLYM2 proteins in particular PcLYM2-2 might be involved as co-receptor for binding linear 1,3- β-D-glucans.

5.6 Conclusion

Two homologs of LYM2 were found in the hybrid poplar *P. x canescens*, *PcLYM2-1* and *PcLYM2-2*. Genomic and transcriptomic analysis revealed that the second homolog generates two splicing variants, *PcLYM2-2.1* and *PcLYM2-2.2*, which differ only at the first exon encoding the LysM domains. All identified *PcLYM2* genes are expressed in roots, wood, developing xylem, bark and leaves. Domain prediction on the protein sequences showed that PcLYM2 proteins have similar domain organization like Arabidopsis LYM2, which has three extracellular LysM domains and a GPI-anchor at the C-terminus. All identified PcLYM2 proteins have the capacity to bind chitin with PcLYM2-1 showing higher chitin-binding capacity than the others. Knocking out *PcLYM2* genes does not impair the chitin-induced ROS production and MAPK activation, suggesting that LYM2 homologs in poplar are not invoved in mediating these chitin-induced responses. Subcellular localization studies showed that all identified PcLYM2 proteins localize at the plasma membrane (PM) and plasmodesmata (PD), indicating that PcLYM2 proteins might have a PD-related function. Plasmodesmal flux analysis on the double knock-out lines of *PcLYM2* genes as well as on the single knock-out lines of *PcLYM2-1* suggest that PcLYM2 genes mediate chitin-induced PD closure, and that *PcLYM2-1* might play a more prominent role among *PcLYM2* genes in mediating this function. However, the individual functions of *PcLYM2-2* splicing variants remain to be tested. Expression levels in different tissues suggest that PcLYM2 proteins may have a potential to form tissue-specific complexes through homo- or heterodimerization depending on their abundance in the corresponding tissues. The composition of these complexes may affect ligand affinity or ligand specificity.

5.7 Appendix

Supplemental Table 5.1. Primer pairs to amplify genes encoding LYM2 from leaf-derived cDNA of *P. x canescens*

Genes	Homologs in *P. trichocarpa*-Nisqually	Primer sequences (5'->3')	AT* (°C)	Length (bp)
PcLYM2-1	Potri.004G183500.1	Fw_369: GCAAACGACCCAGGAATC Rv_372: GCCCCAACATCAAGAAACAG	64.5	1314
PcLYM2-2	Potri.009G143300.1	Primer pairs 1 Fw_373: GGAAAGCCGACATCTCTCCG Rv_325: GACGAATTCCACCCAGAGAGAAGCACC Primer pairs 2 Fw_742: CAAAGCCCAACTTTTCCCAG Rv_665: GAGAAGCACCGTTTCTTACTAG	61.1 59	1348 1213
	Potri.009G143300.2	Primer pairs 1 Fw_421: GTAATAACACAACAGCCAACC Rv_325: GACGAATTCCACCCAGAGAGAAGCACC Primer pairs 2 Fw_691: GAATTCCCCAGTTTATCCC Rv_692: GATTTCTCATATGACCCAATATC	61.4 58.3	1267 1248

*AT = Annealing temperature for protocol using a proofreading DNA polymerase (Phusion Hot Start II, Thermo Fisher Scientific Inc., Waltham, U.S.A.).

Supplemental Table 5.2. Primer pairs to analyse the exon-intron structure of the *PcLYM2* gene on gDNA level

Primer sequences	AT* (°C)	Length
Primer pairs for amplification of PcLYM2-2		
Fw: ATGGGGTTTGCCATAATTCTAATG Rv: CCAATCCTTGAAGCGAAATTGC	59	~ 4 kbp
Primers used for sequencing the full length of PcLYM2-2 in gDNA (5'->3')		
Fw_22: CGTTGTAAAACGACGGCCAGT	Designed on PCR 2.1 TA cloning vector (Invitrogen)	
Rv_23: CAGGAAACAGCTATGACCATG	Designed on PCR 2.1 TA cloning vector (Invitrogen)	
Fw_428: GTGGAAGAAGGGAGCACCG	Designed on the exon1 of PcLYM2-2.1	
Fw_864: GCTCTAAAGCTTACGAAGATTTAAGAG	Designed on the intron	
Rv_865: GCACATTGCCTAGCACTATC	Designed on the intron	

*AT = Annealing temperature using a proofreading DNA polymerase (Phusion Hot Start II, Thermo Fisher Scientific Inc., Waltham, U.S.A.).

Supplemental Table 5.3. Primer pairs for qPCR of PcLYM2 genes

Genes	Sequences (5'->3')	Efficiency (%)
PcLYM2-1	Fw: CTCCCAAGGAATCACACCATAGC Rv: GATCTTGAGTGGAGCGTGGAG	89
PcLYM2-2.1	Fw: CAAGCACGACACACCTCCAC Rv: GCTGGGCTACTGATATGGTGG	95
PcLYM2-2.2	Fw: GAAATCACACCAGAGCCAAAATGG Rv: GGATGAAGATTTTGTGGGCAGTG	89

Supplemental Table 5.4. Primers for amplifying fragments coding for sgRNA to generate *PcLYM2* knock-out lines

Primer names	Sequences (5'->3')
gRNA_LYM2-2_T1_F	TCGGTGAGAAGTGACTCTGGTTTTAGAGCTAGAAATAGCAAGTTAAA
U3d_LYM2-2_T1_R	CAGAGTCACTTCTCACCGATGACCAATGGTGCTTTGTAG
gRNA_LYM2_T2_F	CCTGCTATGCAATGTGAAGGGTTTTAGAGCTAGAAATAGCAAGTTAAA
U3b_LYM2_T2_R	CCTTCACATTGCATAGCAGGTGACCAATGTTGCTCCCTC
gRNA_LYM2-1_T3_F	TCTTCACAACTCTCGCCACAGTTTTAGAGCTAGAAATAGCAAGTTAAA
U6-1_LYM2-1_T3_R	TGTGGCGAGAGTTGTGAAGACAATCACTACTTCGTCTCTAACC
gRNA_LYM2-1_T4_F	CCTGCAATGCAATGTGAAGGGTTTTAGAGCTAGAAATAGCAAGTTAAA
U6-29_LYM2-1_T4_R	CCTTCACATTGCATTGCAGGCAATCTCTTAGTCGACTCTACCA

***in red is the target sites**

Supplemental Table 5.5. Primer pairs to assemble fragments coding for sgRNA into the pYLCRISPR/Cas9P$_{35S}$-N vector

Primer names	Sequences (5'->3')
Pgs_GA3	CCACGCATACGATTTAGGTGACACTATAGCGCATCCACTCCAAGCTCTTG
U_GA3	CGCTATAGTGTCACCTAAATCGTATGCGTGGTGGAATCGGCAGCAAAGG
Pgs_GA4	GTCGCTAGTTATTGCTCAGCGGCCAAGCTCATCCACTCCAAGCTCTTG
U_GA4	GAGCTTGGCCGCTGAGCAATAACTAGCGACTGGAATCGGCAGCAAAGG
Pgs_GG3	AGCGTGggtctcGtcttcacTCCATCCACTCCAAGCTC
Pps_GG3	TTCAGAggtctcTaagacttTGGAATCGGCAGCAAAGG
Pgs_GG4	AGCGTGggtctcGagtccttTCCATCCACTCCAAGCTC
Pps_GG4	TTCAGAggtctcTgactacaTGGAATCGGCAGCAAAGG
U-F	CTCCGTTTTACCTGTGGAATCG
gR-R	CGGAGGAAAATTCCATCCAC
Pps-GGL	TTCAGAggtctcTctcgACTAGTATGGAATCGGCAGCAAAGG
Pgs-GG2	AGCGTGggtctcGtcagggTCCATCCACTCCAAGCTC
Pps-GG2	TTCAGAggtctcTctgacacTGGAATCGGCAGCAAAGG
Pgs-GGR	AGCGTGggtctcGaccgACGCGTATCCATCCACTCCAAGCTC

Supplemental Table 5.6. Primer pairs for amplification of the sgRNA target site

Target genes	Sequences (5'->3')
PcLYM2-1 *P. alba* allele	Fw: GGGTTGAGCTACAGGCTAC Rv: CGAAGAATACTACATGCAGC
PcLYM2-1 *P. tremula* allele	Fw: GGGATGAGCTACAGGCTAT Rv: CGAAGAATACTACATGCAGC
PcLYM2-2 *P. alba* allele	Fw: GTAGCTGTCTTCAAATGTTGG Rv: GGCTAGAGTTGTGAAGATCC
PcLYM2-2 *P. tremula* allele	Fw: AGGCTCGTTGGCATTAAG Rv: GAGAAGCACCGTTTCTTACTAG

Supplemental Table 5.7. Primers for generating *PcLYM2*-constructs

Fragments	Primer pairs (5'->3')
35S:mVenus_PcLYM2-1	
p35S	Fw: GAATTGGGTACCGGCGCGGGTCCCCAGATTAGCCTTTTCAATTTC Rv: GGATCCCGGACCGCGGTC
SP_PcLYM2-1	Fw: GACCGCGGTCCGGGATCCATGGGTTTCCATTTCACTTCGC Rv: GGAAGAAGATCTTGAGTGGAGC
mVenus	Fw: GCTCCACTCAAGATCTTCTTCCATGGTGAGCAAGGGCGAG Rv: GTACAGCTCGTCCATGCC
LysM_PcLYM2-1	Fw: GGCATGGACGAGCTGTACAAGCACGCGGTGATGCAGACCTTCAAATGTAGC AC Rv: GAACTAGTGGATCCCCCGGGTCAAAGAAGATACACAAGAAGAAG
t35S	*
Destination Vector**	Fw: CCCGGGGGATCCACTAGTTC Rv: CGCGCCGGTACCCAATTC
35S:mVenus_PcLYM2-2.1	
P35S + SP_PcLYM2-like2.1+mVenus	Fw: GAATTGGGTACCGGCGCGGGTCCCCAGATTAGCCTTTTCAATTTC Rv: GTACAGCTCGTCCATGCC
PcLYM2-2.1 CDS	Fw: GGCATGGACGAGCTGTACAAGCACGCGGTGATGCAGCAAGCATTCAAGTGC AC Rv: GAACTAGTGGATCCCCCGGGTTAAAGAAGATATACAAGAAGCAGAATC
t35S	*
Destination vector**	Fw: CGCGCCGGTACCCAATTC Rv: CCCGGGGGATCCACTAGTTC
35S:mVenus_PcLYM2-2.2	
SP_PcLYM2-2.2	Fw: GACCGCGGTCCGGGATCCATGGGTTTCCATTTCATTC Rv: GGATGAAGATTTTGTGGGC
mVenus	Fw: GCCCACAAAATCTTCATCCATGGTGAGCAAGGGCGAG Rv: GTACAGCTCGTCCATGCC

LysM_PcLYM2-2.2	Fw: GGCATGGACGAGCTGTACAAGCACGCGGTGATGCAAACCTTCAAATGTAGC TCACC Rv: TTAAAGAAGATATACAAGAAGCAGAATC
t35S_PcLYM2-2.2	Fw: GATTCTGCTTCTTGTATATCTTCTTTAATCTAGAGTCCGCAAAAATCACC Rv: CTATAGGGCGAATTGGGTACCGGTCACTGGATTTTGGTTTTAGG
Destination vector**	Fw: CGCGCCGGTACCCAATTC Rv: CCCGGGGGATCCACTAGTTC

*On the vector backbone

**primer used for Inverse PCR

Blue =linkers

Red = overlapping sites to assemble the fragments trhough Gibson Assembly

Supplemental Table 5. 8. Recipes

Supplemental Table 5.8.1. CTAB RNA extraction buffer

Chemicals	Final concentration
CTAB (Hexadecyltrimethylammoniumbromid)	2%
Tris HCl	100 mM
EDTA	25 mM
NaCl	2 M
PVP K30	2%

Supplemental Table 5.8.2. SSTE

Chemicals	Final concentration
SDS	0.5 %
Tris HCl	10 mM
EDTA	1 mM
NaCl	1 M

Supplemental Table 5.8.3. Co-incubation medium (pH 5.8)

Materials	Final concentration
Murashige-Skoog (MS) including vitamin (Duchefa)	0.22 %
Sucrose	2 %
Plant agar (Duchefa)	0.7 %

Supplemental Table 5.8.4. Regeneration medium (pH 5.8)

Materials	Final concentration
Murashige-Skoog (MS) including vitamin (Duchefa)	0.22 %
Sucrose	2 %
Plant agar (Duchefa)	0.7 %
Pluronic-Thidiazuron	0.01% Pluronic and 0.01 µM Thidiazuron
Cefotaxime	150 mg/ l
Timentin	200 mg/ l

Supplemental Table 5.8.5. Selection medium (pH 5.8)

Materials	Final concentration
Murashige-Skoog (MS) including vitamin (Duchefa)	0.22 %
Sucrose	2 %
Plant agar (Duchefa)	0.7 %
Pluronic (Gibco, life technologies) and Thidiazuron (Duchefa)	0.01% Pluronic and 0.01 µM Thidiazuron
Cefotaxime (Duchefa)	150 mg/ l
Timentin (Duchefa)	200 mg/ l
Kanamycin (Roth)	50 mg/ l

8.6 Rooting medium (pH 5.8)

Materials	Final concentration
Murashige-Skoog (MS) including vitamin (Duchefa)	0.22 %
Sucrose	2 %
Plant agar (Duchefa)	0.7 %
Cefotaxime	150 mg/ l
Timentin	200 mg/ l
Kanamycin	50 mg/ l

Supplemental Table 5.8.6. Extraction buffer solution for total protein extract

Materials	Final concentration
Sucrose	250 mM
HEPES-KOH pH 7.5	100 mM
Glycerol	5%
Na2MoO4 + 2H2O	1 mM
NaF	25 mM
EDTA	10 mM
DTT	1 mM
Triton X-100	0.50%
Protease inhibitor cocktail (see table 12.8)	1:100

Supplemental Table 5.8.7. Protease inhibitor cocktail for total protein extraction buffer

Protease inhibitor cocktail (200 ml, 100x)	
4-(2-aminoethyl) benzenesulfonyl fluoride hydrochloride (AEBSF)	1 g
Bestatin hydrochloride	5 mg
Leupeptin hemisulfate	100 mg
Pepstatin A	10 mg
E-64 (trans-epoxysuccinyl-L-leucylamido-(4-guanidino)butane)	10 mg
Phenanthroline (1, 10-phenanthroline monohydrate)	10 g
All components were dissolved separately in a small amount of DMSO and further being combined and filled up with DMSO to a total volume of 200 ml. 2 ml Aliquot were made and stored at -20°C.	

Supplemental Table 5.8.8. Recipes for Western Blotting

SDS-PAGE gel buffer (250 ml)		
10% running gel buffer	1 M Tris-HCl, pH 8.8	143.6 ml
	10% SDS	3.79 ml
	ddH_2O	102.61 ml
Stacking gel buffer	1 M Tris-HCl, pH 6.8	38.58 ml
	SDS (10%)	3.06 ml
	ddH_2O	208.36 ml
SDS-PAGE gel (10 ml)		
10% running gel	10% running gel buffer	6.6 ml
	30% acrylamide	3.3 ml
	10% APS	0.1 ml
	TEMED	0.004 ml
Stacking gel	Stacking gel buffer	8.16 ml
	30% acrylamide	1.66 ml
	10% APS	0.05 ml
	TEMED	0.005 ml
SDS-PAGE and Immunoblot analysis		
10x SDS running buffer (1 l)	Glycine	144.2 g
	Tris-base	30.4 g
	10% SDS	100 ml
20x transfer buffer, pH 8.3 (1 l)	Tris-base	121.14 g

	Boric acid	61.83 g
20x TBS-T (1 l)	NaCl	175.32 g
	1M Tris-HCl, pH 8	200 ml
	Tween-20	10 ml
3% Milk solution	Milk powder (Roth)	3 g
	1x TBS-T	100 ml
AP buffer (1 l)	1 M Tris-HCl, pH 9.5	100 ml
	5 M NaCl	20 ml
	1 M $MgCl_2$	50 ml
4x SDS loading buffer (50 ml)	1 M Tris-HCl, pH 6.8	10 ml
	DTT	3.085 g
	SDS	4 g
	Gycerin	20 ml
	Bromphenolblue	50 mg
CBB staining solution (700 ml)	EtOH	300 ml
	ddH_2O	300 ml
	Acetic acid (10%)	100 ml
	Coomassie Brilliant Blue R-250	0.35 mg
Destaining solution for CBB	EtOH	300 ml
	ddH_2O	300 ml
	Acetic acid (10%)	100 ml

Supplemental Table 5.9. Transcript and protein sequences of genes encoding LysM-RLPs (PcLYM2) from *P. x canescens*

PcLYM2-1
***P. tremula* allele.** Used for generating construct.
ATGGGTTTCCATTTCACTTCGCTGCTTCTCACCCTACTCTTATTCTCCACGCTCCACTCAAGATCTTCTTCCCAGACCTT CAAATGTAGCACCCCCACCACGTGTCATTCCCTCATTGACTACATCTCTCCAAACGCGACAACTTTCTCCCACATCAAA ACCCTCTTCTCCGTCAAGAACATACACTCCATCTTAGCTGCCAACAACCTCCCTCTCTCCACGTTACCAAACTCTACCA TACCTGCAAACCAGCCCATCAAAATCTCATTTCCTTGCCTGTGCATCAACAACACTGGTCACTCAAACAAGCAACCAA TCTACACCGTTCAAAAGGATGATGGGCTTTCTCATATTGCAACAGAAGTTTTCTCAGGATTGGTAACATACCAAGAAA TTGCTGCTGTTAATAATATACCAGACGTTAATCTGATAAAGGTTGGGCAGAAGTTGTGGATTCCTTTACCTTGTAGTTG TGATGATGTTGATGGGGTCAAAGTTGTCCATTATGGACACGTGGTGGAAGCTGGCAGTTCTTTGGAGTTGATTGCTCA AGAATATGGGACCAGTACAGATACACTAGTGAAGCTTAATGGGGTTAATGACAGTTCTCTCTTAGCTGGTCAAGTTCT TGATGTCCCTCTGCAAGCTTGCAATTCATCGGTGAGAAGTGACTCAGTAGATTATCCACTACTTGTTCCTAACAACACC TATTTCTTCACTGCTAACAATTGTGTTAAATGCAAGTGTGATGCTGCAAACAACTGGACATTACAATGTGAAGCATCTG GGATTAAACCATCCAACTGGTCAACTTGCCCTGCTATGCAATGTGAAGGTGGCTTGTTATCCATCGACAACTCGACAA CTTCTGGTTGCAACATCACAACCTGTGCCTATGCCGGTTTTAGCAAGAACCAAAGCATCTTCACAACTCTCGCCACAA GGTCCACTTGTCCAGTTACTGCAGCTCCCGGCAGTTATGCTTCAAGGACTGGTTTGAGTTGGAACTACTTGTTCATGTC TCTTCACCTGATTCTTCTTCTTGTGTATCTTCTTTGA
MGFHFTSLLLTLLLFSTLHSRSSSQTFKCSTPTTCHSLIDYISPNATTFSHIKTLFSVKNIHSILAANNLPLSTLPNSTIPANQPIKI SFPCLCINNTGHSNKQPIYTVQKDDGLSHIATEVFSGLVTYQEIAAVNNIPDVNLIKVGQKLWIPLPCSCDDVDGVKVVHYG HVVEAGSSLELIAQEYGTSTDTLVKLNGVNDSSLLAGQVLDVPLQACNSSVRSDSVDYPLLVPNNTYFFTANNCVKCKCDA ANNWTLQCEASGIKPSNWSTCPAMQCEGGLLSIDNSTTSGCNITTCAYAGFSKNQSIFTTLATRSTCPVTAAPGSYASRTGLS WNYLFMSLHLILLLVYLL
***P. alba* allele**
ATGGGTTTCCATTTCACTCCGCTGCTTCTCACCCTACTGTTATTCTCCACGCTCCACTCAAGATCTTCTTCCCAAACCTT CAAATGTAGCACACCCACCACGTGTCATTCTCTCATTGACTACATCTCTCCAAACACAACAACTTTCTCCCACATCAAA ACCCTCTTCTCCGTCAAGAACATACACTCCATCTTAGCTGCCAACAACCTCCCTCTCTCCACGTTACCAAACTCTACCA TACCTGCAAACCAGCCCATCAAAATCTCATTTCCTTGCATGTGCATCAACAACACTGGTCACTCAAACAAGCAACCAA TCTACACCGTTCAAAAGGATGACGGGCTTTCTCATATTGCAACAGAAGTTTTCTCAGGATTGGTAACATACCAAGAAA TTGCTGCTGTTAATAATATACCAGACGTTAATCTGATTAAGGTTGGGCAGAAGTTGTGGATTCCTTTACCTTGTAATTG TGATGATGTTGATGGGGTCAAAGTTGTCCATTATGGACACGTGGTGGAAGCTGGCAGTTCTTTGGAGTTGATTGCTCA AGCATATGGGACCAGTACAGATACACTAGTGAAGCTTAATGGGGTTAATGACAGTTCTCTCTTAGCTGGTCAAGTTCT TGATGTCCCTCTGCAAGCTTGCAATTCATCGGTGAGAAGTGACTCGGTAGATTATCCACTACTTGTTCCTAACAACACC TATTTCTTCACTGCAAACAATTGTGTTAAATGCAAGTGTGATGCTGCAAACAACTGGACATTACAATGTGAAGCATCT GGGATTAAACCATCCAACTGGTCAACTTGCCCTGCTATGCAATGTGAAGGTGGCTTGTTATCCATCGACAACTCGACA ACTTCTGGTTGCAACGTCACAACCTGTGCCTATGCCGGTTTTATCAAGAACCAAAGCATCTTCACAACTCTCGCCACAC GGTCCGCTTGTCCAGTTACCGCAGCTCCCGGCAGTTATGCTTCAAGGACTGGTTTGAGTTGGAACTACTTGTTCATCTC TCTTCACCTGATTCTTCTTCTTGTGTATCTTCTTTGA

MGFHFTPLLLTLLLFSTLHSRSSSQTFKCSTPTTCHSLIDYISPNTTTFSHIKTLFSVKNIHSILAANNLPLSTLPNSTIPANQPIKI
SFPCMCINNTGHSNKQPIYTVQKDDGLSHIATEVFSGLVTYQEIAAVNNIPDVNLIKVGQKLWIPLPCNCDDVDGVKVVHY
GHVVEAGSSLELIAQAYGTSTDTLVKLNGVNDSSLLAGQVLDVPLQACNSSVRSDSVDYPLLVPNNTYFFTANNCVKCKC
DAANNWTLQCEASGIKPSNWSTCPAMQCEGGLLSIDNSTTSGCNVTTCAYAGFIKNQSIFTTLATRSACPVTAAPGSYASRT
GLSWNYLFISLHLILLLVYLL

PcLYM2-2.1

***P. tremula* allele**

ATGGGGTTTGCCATAATTCTAATGTGTCTGCTCTTCTACTCTTCTTTCACCACCATATCAGTAGCCCAGCAAGCATTCA
AGTGCACAGAAAGAACCACATGTCGTTCTTTGGTGGGTTATAAGTCCCCTAACACGACCTCCATCTCCTCCATCCAGA
AACTCTTTGGTGTCAAAAACCTACACTCTATTCTAGGAGCAAACAACCTTCCTTCCTCAACCTTACCAAACCACATGAT
CCAAGAGCAGCAAGTAATAAAAATCCCAATCCCATGCATATGTTTTAATGGGACAGGTGCCTCAAACAGGATGCCCAT
TTACACAGTCCAACCAGATGATGGGCTGTATTATATTGCAAACAATGTCTTCATGGGCTTGCTTGCATACCAAAGAAT
CCAACAAGTTAATAGGATAGAAAACGCTGATATGATCGAAGTGGGTCAGGAGCTCTGGATCCCACTTTCATGTAGCTG
TGAGGAAGTGGAAGGCGAGAGAGTTCTGCATTATGCACATTTGGTGGAAGAAGGGAGCACCGTGGAACAGATCGCAG
AAAAGTTCGGGACAACTAATGACACACTGTATAGGCTTAATGGGATTTCTAATAACAGTCAACTTATTGCAGCAACTG
CATTTGATGTTCCTCTTAAAGCTTGTAATTCATTGGTGAGAAATGACTCTCTGGATTTTCCGTTCCTTGTTCCTAATAAC
ACCTATTTCTTCACTGCTAACAATCGTGTGAAATGCAAGTGTGATGCCGCAAACAACTGGACATTACAATGCGAACCG
TCTGGAAATAAACCATCCAATTGGCCAACCTGTCCTGCTATGCAATGTGAAGATGGCTTGTCAACAATCGGCAACACT
ACAACTTCTGGTTGCAACACCACAACCTGTGCCTACGCCGGTTTTAGCAGGGACCAACGCATCTTCACAACTCTAGCC
ACACAGTCCACTTGTACAGCTCCCGGTGGAAGTCCTGGCAATTTCGCTTCAAGGATTGGTCTGAGTAGGAACTACTTG
TTCATCTGTATTCACATGATTCTGCTTCTTGTATATCTTCTTTAA

MGFAIILMCLLFYSSFTTISVAQQAFKCTERTTCRSLVGYKSPNTTSISSIQKLFGVKNLHSILGANNLPSSTLPNHMIQEQQVI
KIPIPCICFNGTGASNRMPIYTVQPDDGLYYIANNVFMGLLAYQRIQQVNRIENADMIEVGQELWIPLSCSCEEVEGERVLHY
AHLVEEGSTVEQIAEKFGTTNDTLYRLNGISNNSQLIAATAFDVPLKACNSLVRNDSLDFPFLVPNNTYFFTANNRVKCKCD
AANNWTLQCEPSGNKPSNWPTCPAMQCEDGLSTIGNTTTSGCNTTTCAYAGFSRDQRIFTTLATQSTCTAPGGSPGNFASRI
GLSRNYLFICIHMILLLVYLL

***P. alba* allele.** Used for generating construct.

ATGGGGTTTGCCATAATTCTAATGTGTCTGCTCTTCTACTCTTCTTTCACCACCATATCAGTAGCCCAGCAAGCATTCA
AGTGCACAGAAGGAACCGCATGTCGTTCTTTGGTGGGTTATAAGTCCCCTAACACGACCTCCATCTCCTCCATCCAGA
AACTCTTTGGTGTCAAAAACCTACACTCTCTTCTAGGAGCAAACAACCTTCCTTCCTCAACCTTACCAAACCACACGAT
CCAAGAGCAGCAAGTAATAAAAATCCCAATCCCATGCATATGTTTTAACGGGACAGGTGCCTCAAACAAGATGCCCA
TTTACACAGTCCAACCAGAAGATGGGCTGTATTATATTGCAAACAATGTCTTCATGGGCTTGCTTGCACACAAAAGAA
TCCAACAAGTTAATAGGATAGAAAACCCTGATATGATCGACGTGGGTCAGGAGCTCTGGATCCCGCTTCCATGTAGCT
GTGAAGAAGTGGACGGCGAGAGAGTTGTGCATTATGCACACTTGGTGGAAGAAGGGAGCACCGTGGAAGAGATCGC
AGAAAAGTTCGGGACAACTAATGATACACTGTATAGGCTTAATGGGATTTCTAATAACAGTCAACTTATTGCAGCAAC
TGCATTTGATGTTCCTCTTAAAGCTTGTAATTCATCGGTGAGAAGTGACTCTGTGGATTCTCCGTTCCTTGTTCCTAATA
ACACCTATTTCTTCACTGCTAACAATTGTGTGAAATGCAAGTGTGCTGCCGCAAACAACTGGACATTACAATGCGAAC
CGTCCGGAATTAAACCATCCAATCAGTCAACCTGTCCTGCTATGCAATGTGAAGGTGGCTTGTTAACAATCGGCAGCA
CTACAACTTCTGGTTGCAACACCACAACCTGTGCCTACGCCGGTTTTAGCGGGGACCAAAGGATCTTCACAACTCTAG
CCACACAGTCCACTTGTACAGCTCCCGGTGGAAGTCCTGGCAATTTCGCTTCAAGGATTGGTCCGAGTAGGAACTACT
TGTTCATCTGTATTCACATGATTCTGCTTCTTGTATATCTTCTTTAA

MGFAIILMCLLFYSSFTTISVAQQAFKCTEGTACRSLVGYKSPNTTSISSIQKLFGVKNLHSLLGANNLPSSTLPNHTIQEQQVI
KIPIPCICFNGTGASNKMPIYTVQPEDGLYYIANNVFMGLLAHKRIQQVNRIENPDMIDVGQELWIPLPCSCEEVDGERVVHY
AHLVEEGSTVEEIAEKFGTTNDTLYRLNGISNNSQLIAATAFDVPLKACNSSVRSDSVDSPFLVPNNTYFFTANNCVKCKCA
AANNWTLQCEPSGIKPSNQSTCPAMQCEGGLLTIGSTTTSGCNTTTCAYAGFSGDQRIFTTLATQSTCTAPGGSPGNFASRIG
PSRNYLFICIHMILLLVYLL

PcLYM2-2.2

***P. tremula* allele**

ATGGGTTTCCATTTCATTCCTCTACTTCTCACCCTACTCTTATTCTCTACACTGCCCACAAAATCTTCATCCCAAACCTT
CAAATGTAGCTCACCTTTAACATGTCGTTCCCTCATTGACTACATCTCTCCAAACACAACAACTCTTTCCCACATCAAA
ACCCTCTTTTCCATCAAAAACCTTCGTTCCATCTTAGGCGCGAACAACCTCGCTCTCTCCACGTTACCAAACTTTACAA
TACCTGCAAAACAGCCCATCAAGATCCCATTTACTTGCTTGTGCATCAACAACACTGGTCTCTCAAACAAGCAACCAA
TCTACACCGTCCAAAAAGATGATGGGCTTTATCATATAGCAGCAGAAGTTTTCTCAGGGCTGGTAACATACCAAGAAA
TTGCTGCTGTTAATAATGTAACAGACGTTAATTTGATCGAGGTTGGACAGAAGTTGTGGATTCCTTTGCCTTGTAGCTG
TGATGATGTTGATGGGGTTAAAGTGGCTCATTATGGACACGTGGTGGAAGCTGGGAGTTCTTTGGAGGTCATTGCTCA
GGAACACGGGACTAGTAGAAATACACTAATGAAGCTTAATGGGATTGCCAATGACAGCTCTCTTTTGGCTGGTCAAGT
TCTTGATGTCCCTCTCCAAGCTTGTAATTCATTGGTGAGAAATGACTCTCTGGATTTTCCGTTCCTTGTTCCTAATAACA
CCTATTTCTTCACTGCTAACAATCGTGTGAAATGCAAGTGTGATGCCGCAAACAACTGGACATTACAATGCGAACCGT
CTGGAAATAAACCATCCAATTGGCCAACCTGTCCTGCTATGCAATGTGAAGATGGCTTGTCAACAATCGGCAACACTA
CAACTTCTGGTTGCAACACCACAACCTGTGCCTACGCCGGTTTTAGCAGGGACCAACGCATCTTCACAACTCTAGCCA
CACAGTCCACTTGTACAGCTCCCGGTGGAAGTCCTGGCAATTTCGCTTCAAGGATTGGTCTGAGTAGGAACTACTTGTT
CATCTGTATTCACATGATTCTGCTTCTTGTATATCTTCTTTAA

MGFHFIPLLLTLLLFSTLPTKSSSQTFKCSSPLTCRSLIDYISPNTTTLSHIKTLFSIKNLRSILGANNLALSTLPNFTIPAKQPIKIP
FTCLCINNTGLSNKQPIYTVQKDDGLYHIAAEVFSGLVTYQEIAAVNNVTDVNLIEVGQKLWIPLPCSCDDVDGVKVAHYG
HVVEAGSSLEVIAQEHGTSRNTLMKLNGIANDSSLLAGQVLDVPLQACNSLVRNDSLDFPFLVPNNTYFFTANNRVKCKCD
AANNWTLQCEPSGNKPSNWPTCPAMQCEDGLSTIGNTTTSGCNTTTCAYAGFSRDQRIFTTLATQSTCTAPGGSPGNFASRI
GLSRNYLFICIHMILLLVYLL

***P. alba* allele.** Used for generating construct.
ATGGGTTTCCATTTCATTCCTCTACTTCTCACCCTACTCTTATTCTCTACACTGCCCACAAAATCTTCATCCCAAACCTT CAAATGTAGCTCACCTTTAACATGTCGTTCCCTCATTGACTACATCTCTCCAAACACAACAACTCTTTCCCACATCAAA ACCCTCTTTTCCATCAAAAACCTTCGTTCCATCTTAGGCGCGAACAACCTCGCTCTCTCCACGTTACCAAACTTTACAA TACCTGCAAAACAGCCCATCAAGATCCCATTTACTTGCTTGTGCATCAACAACACTGGTCTCTCAAACAAGCAACCAA TCTACACCGTCCAAAAAGATGATGGGCTTTATCATATAGCAGCAGAAGTTTTCTCAGGGCTGGTAACATACCAAGAAA TTGCTGCTGTTAATAATGTAACAGACGTTAATTTGATCGAGGTTGGACAGAAGTTGTGGATTCCTTTGCCTTGTAGCTG TGATGATGTTGATGGGGTTAAAGTGGTCCATTATGGACACGTGGTGGAAGCTGGGAGTTCTTTGGAGGTCATTGCTCA GGAATACGGGACTAGTAGAAATACACTAATGAAGCTTAATGGGATTGTCAATGACAGCTCTCTTTTGGCTGGTCAAGT TCTTGATGTCCCTCTCCAAGCTTGTAATTCATCGGTGAGAAGTGACTCTGTGGATTCTCCGTTCCTTGTTCCTAATAACA CCTATTTCTTCACTGCTAACAATTGTGTGAAATGCAAGTGTGCTGCCGCAAACAACTGGACATTACAATGCGAACCGT CCGGAATTAAACCATCCAATCAGTCAACCTGTCCTGCTATGCAATGTGAAGGTGGCTTGTTAACAATCGGCAGCACTA CAACTTCTGGTTGCAACACCACAACCTGTGCCTACGCCGGTTTTAGCGGGGACCAAAGGATCTTCACAACTCTAGCCA CACAGTCCACTTGTACAGCTCCCGGTGGAAGTCCTGGCAATTTCGCTTCAAGGATTGGTCCGAGTAGGAACTACTTGTT CATCTGTATTCACATGATTCTGCTTCTTGTATATCTTCTTTAA
MGFHFIPLLLTLLLFSTLPTKSSSQTFKCSSPLTCRSLIDYISPNTTTLSHIKTLFSIKNLRSILGANNLALSTLPNFTIPAKQPIKIP FTCLCINNTGLSNKQPIYTVQKDDGLYHIAAEVFSGLVTYQEIAAVNNVTDVNLIEVGQKLWIPLPCSCDDVDGVKVVHYG HVVEAGSSLEVIAQEYGTSRNTLMKLNGIVNDSSLLAGQVLDVPLQACNSSVRSDSVDSPFLVPNNTYFFTANNCVKCKCA AANNWTLQCEPSGIKPSNQSTCPAMQCEGGLLTIGSTTTSGCNTTTCAYAGFSGDQRIFTTLATQSTCTAPGGSPGNFASRIG PSRNYLFICIHMILLLVYLL

Supplemental Table 5.10. Domain prediction of PcLYM2 proteins. Signal peptide (SP), transmembrane domain (TM)

Gene	SP	LysM*	TM	Membrane attachment	Omega site
PcLYM2-1 (Potri.004G183500.1)	1-24	2 LysM predicted	-	GPI-anchored (both alleles)	at aa position 326, 100% specific
PcLYM2-2.1 (Potri.009G143300.1)	1-22	2 LysM predicted	-	GPI-anchored (both alleles)	at aa position 327, 100% specific
PcLYM2-2.2 (Potri.009G143300.2)	1-24	2 LysM predicted	-	GPI-anchored (both alleles)	at aa position 328, 100% specific

*InterPro Scan integrated in Geneious 8.1.8 (Quevillon et al., 2005) only predicted 2 extracellular LysM domain. However, protein alignment with OsCEBiP and AtLYM2 indicates that PcLYM2 proteins have 3 LysMs at the ectodomain.

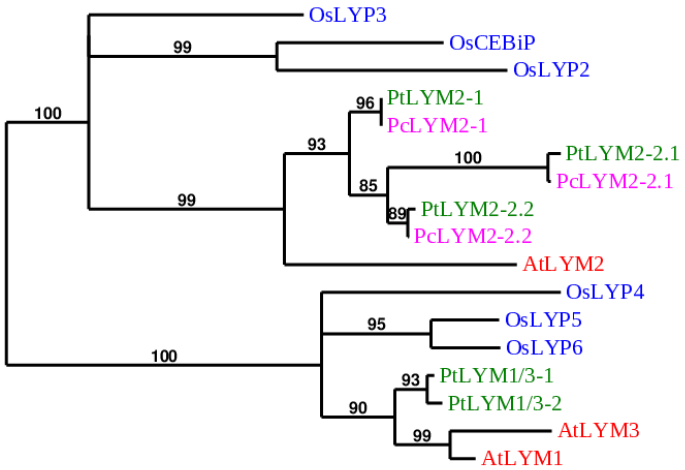

Supplemental Figure 5.1. The poplar genome codes for several LYM2 paralogs. A phylogenetic tree of LysM-RLPs was constructed based on sequence similarity of putative *P. trichocarpa* Nisqually proteins (green) and sequencing results of LysM-RLPs from *P. x canescens* (*P. tremula* allele in magenta) with well-characterized LysM-RLPs from *Arabidopsis thaliana* (red) and *Oryza sativa* (blue). Numbers on the clade are branch support values (%) from bootstrapping of 500 replicates (analyzed with PhyML for maximum likelihood).

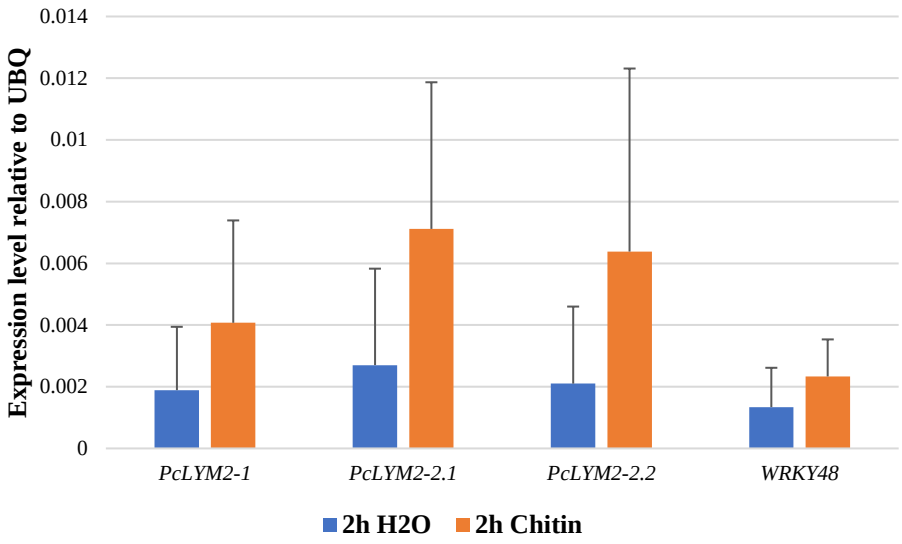

Supplemental Figure 5.2. Expression levels of *PcLYM2* genes in leaves of *P. x canescens* show a tendency to increase after chitin treatment. qPCR analysis was repeated twice with the same tendency. None of the repetition showed significant difference among the tested groups. Bars indicate standard deviation of three biological replicates (n = 3). For statistical analysis, two-way anova ($P \leq 0.05$) was performed.

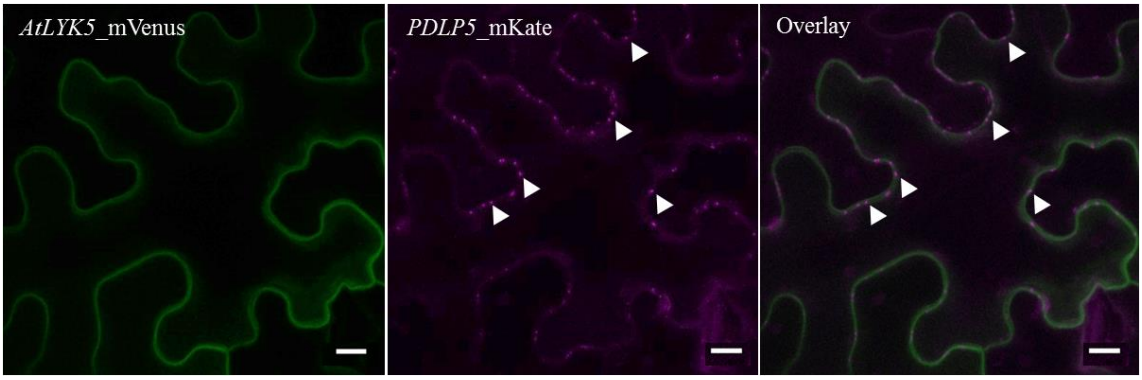

Supplemental Figure 5.3. AtLYK5 as a negative control for PD-PM localization shows localization only in PM. Constructs expressing *AtLYK5_mVenus* and *PDLP5_mKate* were co-infiltrated into the abaxial side of *N. benthamiana* leaves. In the left panel is the infiltration of *AtLYK5-mVenus* construct showing its localization only in PM. The central panel are images of PDLP5-mKate as a marker for PD-localization visible as magenta dots. In the right panel, overlay image of mVenus and mKate channels visualizes the PD-PM localization of only PDLP5-mKate (indicated by arrow heads). The protein localization was observed 72 hours post infiltration under CLSM SP5, and the displayed images are maximum projections of Z-stack series taken ~1 µm apart under 40x objective. Scale bar indicates 10 µm.

Supplemental Figure 5.4. Sequence analyses of edited sites in *PcLYM2* CRISPR/Cas9 lines.

Primers specific to *P. tremula* and *P. alba* alleles were used to amplify and sequence target sites. Edited taget sites showing loss of heterozygosity (no allele specific SNPs are detected) most likely have been repaired by homologous recombination (HR), involving the edited allele of one parental line. Sequences are displayed using Chromas (Technelysium Pty Ltd, Brisbane, Australia) software.

PcLYM2-1 P. alba allele editing in line T6#29. HR with *P. tremula* allele

Ref.

WT

T6#29

PcLYM2-1 P. tremula allele editing in line T6#29

Ref.

WT

T6#29

PcLYM2-1 P. alba allele editing in line T6#34b

Ref.

WT

T6#34b

PcLYM2-1 P. tremula allele editing in line T6#34b. HR with *P. alba* allele

Ref.

WT

T6#34b

PcLYM2-1 P. alba allele editing in line T6#10

Ref.

WT

T6#10

PcLYM2-1 P. tremula allele editing in line T6#10

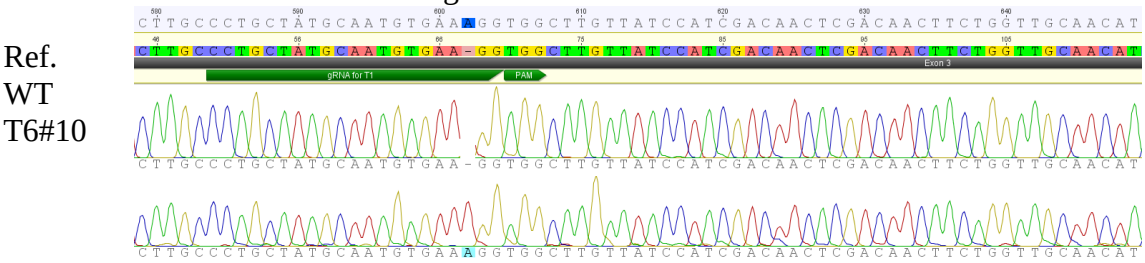

PcLYM2-1 P. alba allele editing in line T6#14. HR with *P. tremula* allele

PcLYM2-1 P. tremula allele editing in line T6#14

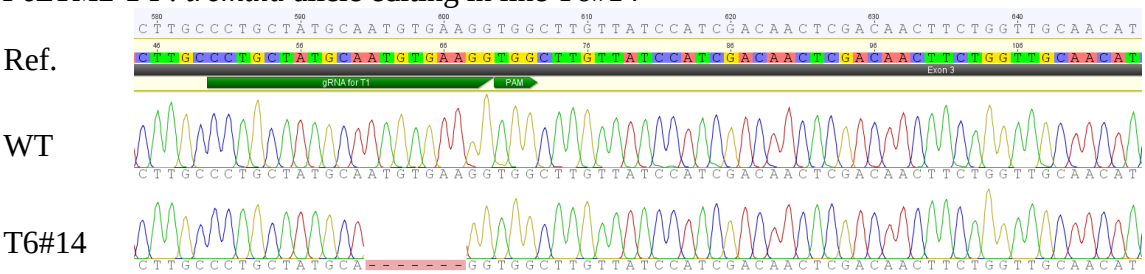

PcLYM2-1 P. alba allele editing in line T6#22c

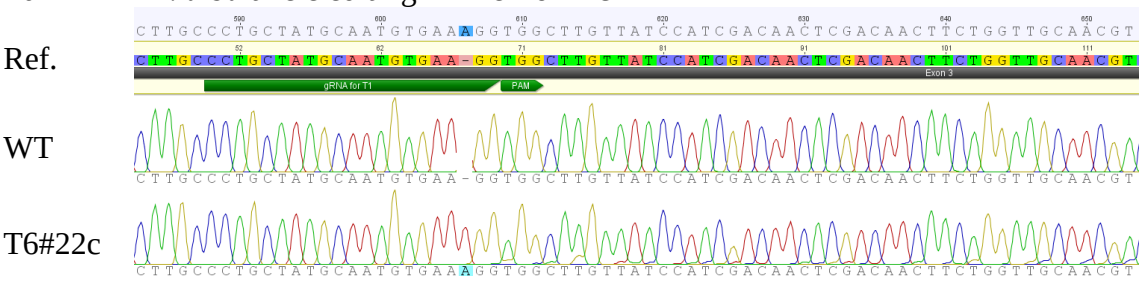

PcLYM2-1 P. tremula allele editing in line T6#22c

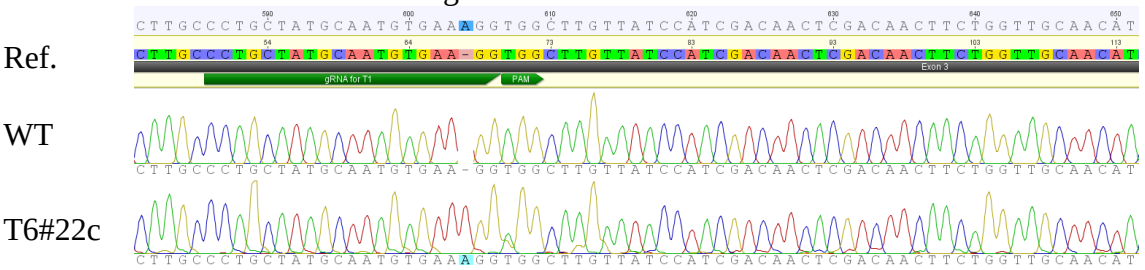

PcLYM2-1 P. alba allele editing in line T6#41a

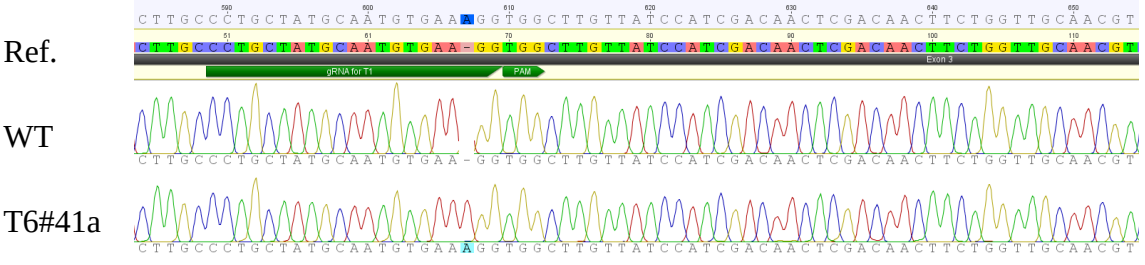

PcLYM2-1 P. tremula allele editing in line T6#41a

Ref.
WT
T6#41a

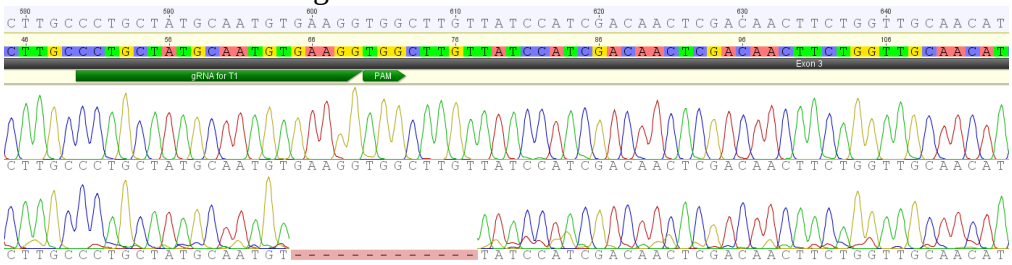

PcLYM2-2 *P. alba* allele editing in line T6#29

Ref.
WT
T6#29

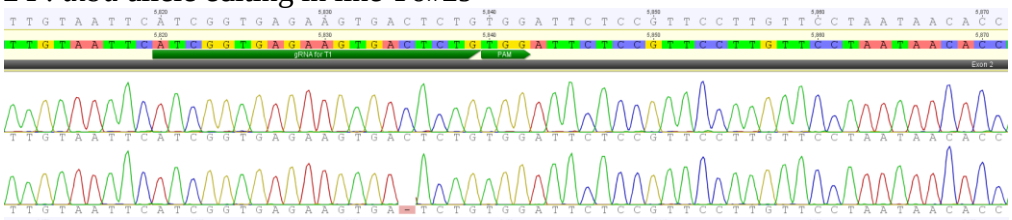

Ref.
WT
T6#29

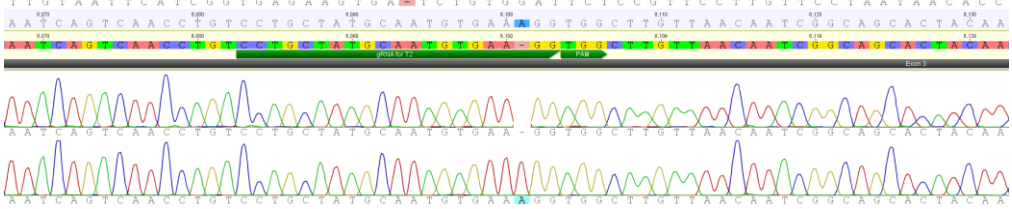

PcLYM2-2 *P. tremula* allele editing in line T6#29

Ref.
WT
T6#29

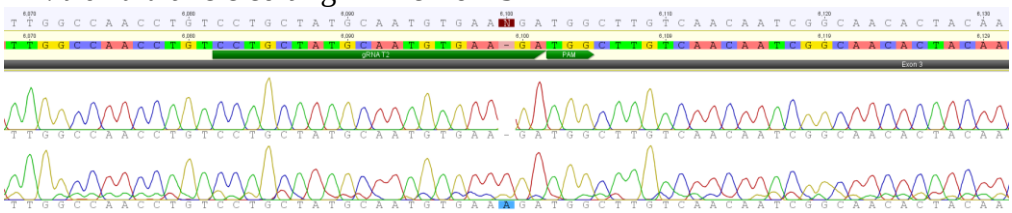

PcLYM2-2 *P. alba* allele in line T6#34b. HR with *P. tremula* allele

Ref.
WT
T6#34b

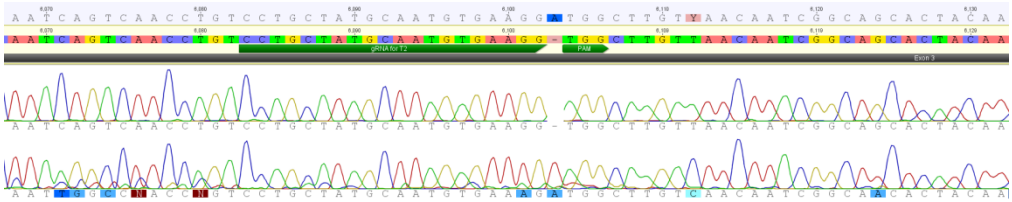

PcLYM2-2 *P. tremula* allele in line T6#34b

Ref.
WT
T6#34b

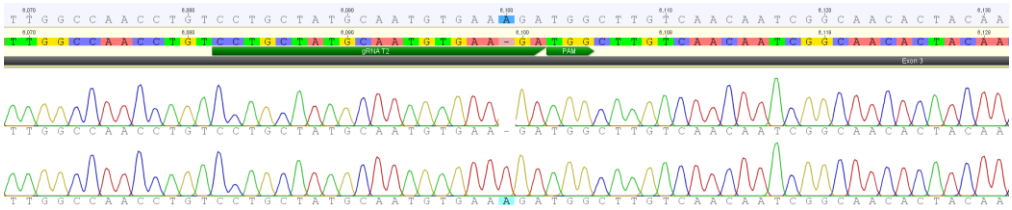

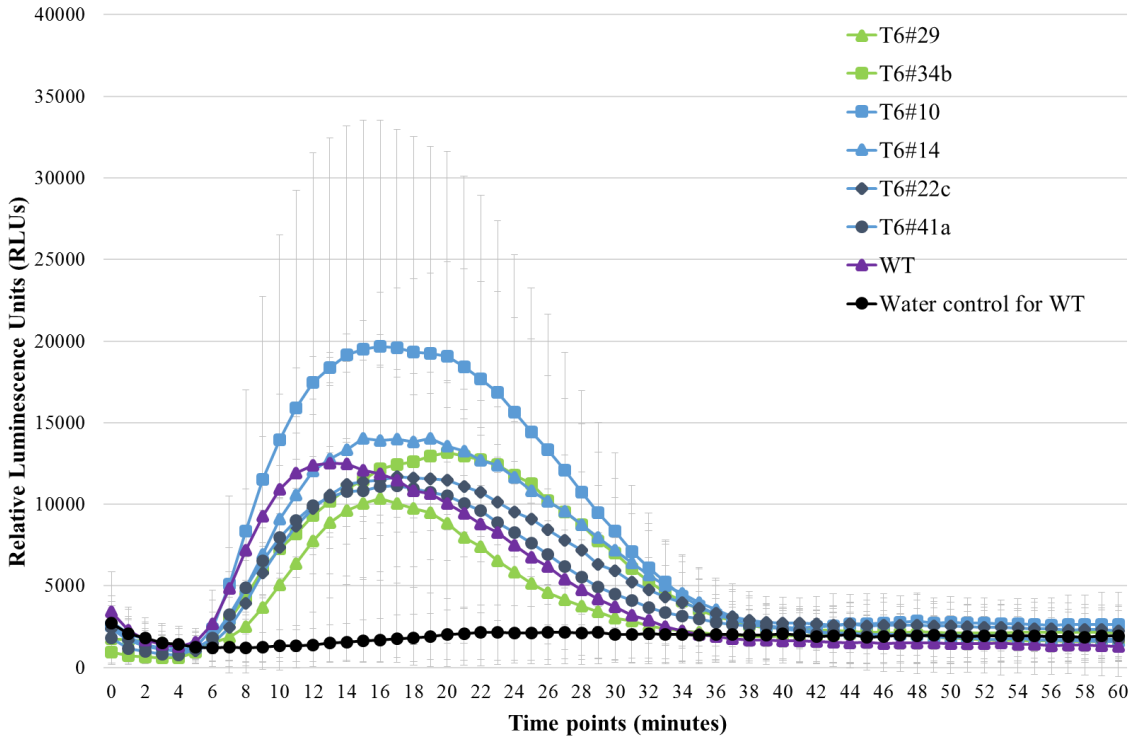

Supplemental Figure 5.5. *Pclym2-1* and *Pclym2-1 Pclym2-2* knock-out lines respond like wildtype to flg22. *LYM2* knock-out lines were generated through a CRISPR/Cas9 approach in *P. x canescens*. For ROS burst assays leaf discs were treated with 100 nM flg22 and the ROS production was measured for 1h. Two independent *Pclym2-1 Pclym2-2* double knock-out lines (green) and four independent *Pclym2-1* single knock-out lines (blue) were tested. Data are means ± SD (n = 8 biological replicates).

5.8 References

Aghaalikhani, A., Savuto, E., Di Carlo, A., & Borello, D. (2017). Poplar from phytoremediation as a renewable energy source: Gasification properties and pollution analysis. *Energy Procedia*, *142*, 924–931. https://doi.org/10.1016/j.egypro.2017.12.148

Antolín-Llovera, M., Petutsching, E. K., Ried, M. K., Lipka, V., Nürnberger, T., Robatzek, S., & Parniske, M. (2014). Knowing your friends and foes - plant receptor-like kinases as initiators of symbiosis or defence. *New Phytologist*, *204*(4), 791–802. https://doi.org/10.1111/nph.13117

Alberts, A. Johnson, J. Lewis, D. Morgan, M. Raff, K. Roberts, P. W. (2014). Molecular Biology of the Cell 6Th Edition. In *Garland Science, Taylor & Francis Group*. https://doi.org/10.1017/CBO9781107415324.004

Bates, D., Maechler, M., Bolker, B., Walker., S. 2015. Fitting Linear Mixed-Effects Models Using lme4. Journal of Statistical Software, 67(1), 1-48. doi:10.18637/jss.v067.i01.

Bradshaw, H. D., Ceulemans, R., Davis, J., & Stettler, R. (2000). Emerging model systems in plant biology: Poplar (Populus) as a model forest tree. *Journal of Plant Growth Regulation*, *19*(3), 306–313. https://doi.org/10.1007/s003440000030

Buendia, L., Girardin, A., Wang, T., Cottret, L., & Lefebvre, B. (2018). LysM receptor-like kinase and lysM receptor-like protein families: An update on phylogeny and functional characterization. *Frontiers in Plant Science*, *871*(October), 1–25. https://doi.org/10.3389/fpls.2018.01531

Buist, G., Steen, A., Kok, J., & Kuipers, O. P. (2008). LysM, a widely distributed protein motif for binding to (peptido)glycans. *Molecular Microbiology*, *68*(4), 838–847. https://doi.org/10.1111/j.1365-2958.2008.06211.x

Burch-Smith, T. M., & Zambryski, P. C. (2012). Plasmodesmata Paradigm Shift: Regulation from Without Versus Within. *Annual Review of Plant Biology*, *63*(1), 239–260. https://doi.org/10.1146/annurev-arplant-042811-105453

Cao, Y., Liang, Y., Tanaka, K., Nguyen, C. T., Jedrzejczak, R. P., Joachimiak, A., & Stacey, G. (2014). The kinase LYK5 is a major chitin receptor in Arabidopsis and forms a chitin-induced complex with related kinase CERK1. *ELife*, *3*(October). https://doi.org/10.7554/eLife.03766

Castro-Rodríguez, V., García-Gutiérrez, A., Canales, J., Cañas, R. A., Kirby, E. G., Avila, C., & Cánovas, F. M. (2016). Poplar trees for phytoremediation of high levels of nitrate and applications in bioenergy. *Plant Biotechnology Journal*, *14*(1), 299–312. https://doi.org/10.1111/pbi.12384

Chang, S., Puryear, J., & Cairney, J. (1993). A Simple and Efficient Method for Isolating RNA from Pine Trees. *Plant Molecular Biology Reporter*, *11*(2), 113–116.

Chaudhary, S., Khokhar, W., Jabre, I., Reddy, A. S. N., Byrne, L. J., Wilson, C. M., & Syed, N. H. (2019). Alternative splicing and protein diversity: Plants versus animals. *Frontiers in Plant Science*, *10*(June), 1–14. https://doi.org/10.3389/fpls.2019.00708

Chen, W. H., Lv, G., Lv, C., Zeng, C., & Hu, S. (2007). Systematic analysis of alternative first exons in plant genomes. *BMC Plant Biology*, *7*, 1–13. https://doi.org/10.1186/1471-2229-7-55

Chen, Z., Wang, J., Ye, M. X., Li, H., Ji, L. X., Li, Y., … An, X. M. (2013). A novel moderate constitutive promoter derived from poplar (Populus tomentosa carrière). *International Journal of Molecular Sciences*, *14*(3), 6187–6204. https://doi.org/10.3390/ijms14036187

Cheval, C., & Faulkner, C. (2018). Plasmodesmal regulation during plant–pathogen interactions. *New Phytologist*, *217*(1), 62–67. https://doi.org/10.1111/nph.14857

Cheval, C., Johnston, M., Samwald, S., Liu, X., Bellandi, A., Breakspear, A., … Faulkner, C. (2019). Chitin perception in plasmodesmata identifies subcellular, context-specific immune signalling in plants. *BioRxiv*, 611582. https://doi.org/10.1101/611582

Clark, S., Yu, F., Gu, L., & Min, X. J. (2019). Expanding alternative splicing identification by integrating multiple sources of transcription data in tomato. *Frontiers in Plant Science*, *10*(May), 1–12. https://doi.org/10.3389/fpls.2019.00689

Cui, W., & Lee, J. Y. (2016). Arabidopsis callose synthases CalS1/8 regulate plasmodesmal permeability during stress. *Nature Plants*, *2*(5). https://doi.org/10.1038/NPLANTS.2016.34

Dereeper, A., Guignon, V., Blanc, G., Audic, S., Buffet, S., Chevenet, F., … Gascuel, O. (2008). Phylogeny.fr: robust phylogenetic analysis for the non-specialist. *Nucleic Acids Research*, *36*(Web Server issue), 465–469. https://doi.org/10.1093/nar/gkn180

Dereeper, Alexis, Audic, S., Claverie, J. M., & Blanc, G. (2010). BLAST-EXPLORER helps you building datasets for phylogenetic analysis. *BMC Evolutionary Biology*, *10*(1), 8–13. https://doi.org/10.1186/1471-2148-10-8

Duplessis, S., Major, I., Martin, F., & Séguin, A. (2009). Poplar and pathogen interactions: Insights from populus genome-wide analyses of resistance and defense gene families and gene expression profiling. *Critical Reviews in Plant Sciences*, *28*(5), 309–334. https://doi.org/10.1080/07352680903241063

Ellinger, D., & Voigt, C. A. (2014). Callose biosynthesis in arabidopsis with a focus on pathogen response: What we have learned within the last decade. *Annals of Botany*, *114*(6), 1349–1358. https://doi.org/10.1093/aob/mcu120

Erwig, J., Ghareeb, H., Kopischke, M., Hacke, R., Matei, A., Petutschnig, E., & Lipka, V. (2017). Chitin-induced and CHITIN ELICITOR RECEPTOR KINASE1 (CERK1) phosphorylation-dependent endocytosis of Arabidopsis thaliana LYSIN MOTIF-CONTAINING RECEPTOR-LIKE KINASE5 (LYK5). *New Phytologist*, *215*(1), 382–396. https://doi.org/10.1111/nph.14592

Fankhauser, N., & Mäser, P. (2005). Identification of GPI anchor attachment signals by a Kohonen self-organizing map. *Bioinformatics*, *21*(9), 1846–1852. https://doi.org/10.1093/bioinformatics/bti299

Faulkner, C., Petutschnig, E., Benitez-Alfonso, Y., Beck, M., Robatzek, S., Lipka, V., & Maule, A. J. (2013). LYM2-dependent chitin perception limits molecular flux via plasmodesmata. *Proceedings of the National Academy of Sciences of the United States of America*, *110*(22), 9166–9170. https://doi.org/10.1073/pnas.1203458110

Fesel, P. H., & Zuccaro, A. (2016). β-glucan: Crucial component of the fungal cell wall and elusive MAMP in plants. *Fungal Genetics and Biology*, *90*, 53–60. https://doi.org/10.1016/j.fgb.2015.12.004

Fladung, M., Hoenicka, H., & Raj Ahuja, M. (2013). Genomic stability and long-term transgene expression in poplar. *Transgenic Research*, *22*(6), 1167–1178. https://doi.org/10.1007/s11248-013-9719-2

Fox, J. and Weisberg, S. 2019. An {R} Companion to Applied Regression, Third Edition. Thousand Oaks CA: Sage. URL: https://socialsciences.mcmaster.ca/jfox/Books/Companion/

Fuchs, M., van Bel, A. J. E., & Ehlers, K. (2010). Season-associated modifications in symplasmic organization of the cambium in Populus nigra. *Annals of Botany*, *105*(3), 375–387. https://doi.org/10.1093/aob/mcp300

Galian, C., Björkholm, P., Bulleid, N., & Von Heijne, G. (2012). Efficient glycosylphosphatidylinositol (GPI) modification of membrane proteins requires a C-terminal anchoring signal of marginal hydrophobicity. *Journal of Biological Chemistry*, *287*(20), 16399–16409. https://doi.org/10.1074/jbc.M112.350009

García-Angulo, P., Villar, I., Giner-Robles, L., & Centeno, M. L. (2018). In vitro regeneration of two Populus hybrid clones. The role of pectin domains in cell processes underlying shoot organogenesis induction. *Biologia Plantarum*, *62*(4), 763–774. https://doi.org/10.1007/s10535-018-0819-y

Gibson, D. G., Young, L., Chuang, R. Y., Venter, J. C., Hutchison, C. A., & Smith, H. O. (2009). Enzymatic assembly of DNA molecules up to several hundred kilobases. *Nature Methods*, *6*(5), 343–345. https://doi.org/10.1038/nmeth.1318

Gong, B. Q., Xue, J., Zhang, N., Xu, L., Yao, X., Yang, Q. J., … Li, J. F. (2017). Rice Chitin Receptor OsCEBiP Is Not a Transmembrane Protein but Targets the Plasma Membrane via a GPI Anchor. *Molecular Plant*, *10*(5), 767–770. https://doi.org/10.1016/j.molp.2016.12.005

Gow, N. A. R., Latge, J., Munro, C. A., De Groot, P. W. J., Hellingwerf, K. J., Klis, F. M., … Gil, C. (2003). Cell Wall Architecture in Yeast : New Structure and New Challenges MINIREVIEW Cell Wall Architecture in Yeast : New Structure and New Challenges †. *Yeast*, *9*(3), 3341–3354. https://doi.org/10.1128/microbiolspec.FUNK-0035-2016.Correspondence

Greco, M., Chiappetta, A., Bruno, L., & Bitonti, M. B. (2012). In Posidonia oceanica cadmium induces changes in DNA methylation and chromatin patterning. *Journal of Experimental Botany*, *63*(2), 695–709. https://doi.org/10.1093/jxb/err313

Grison, M. S., Brocard, L., Fouillen, L., Nicolas, W., Wewer, V., Dörmann, P., … Bayer, E. M. (2015). Specific membrane lipid composition is important for plasmodesmata function in arabidopsis. *Plant Cell*, *27*(4), 1228–1250. https://doi.org/10.1105/tpc.114.135731

Guerra, F., Gainza, F., Perez, R., & Zamudio, F. (2011). Phytoremidiation of heavy metals using poplars (Populus spp): a glimpse of the plant responses to copper, cadmium and zinc stress. *Nova Science Publishers, Inc.*, *ISBN: 978-*, 387–413.

Guo, M., Li, C., Facciotto, G., Bergante, S., Bhatia, R., Comolli, R., … Murphy, R. (2015). Bioethanol from poplar clone Imola: an environmentally viable alternative to fossil fuel? *Biotechnology for Biofuels*, *8*(1), 1–21. https://doi.org/10.1186/s13068-015-0318-8

Guseman, J. M., Lee, J. S., Bogenschutz, N. L., Peterson, K. M., Virata, R. E., Xie, B., … Torii, K. U. (2010). Dysregulation of cell-to-cell connectivity and stomatal patterning by loss-of-function mutation in Arabidopsis chorus (GLUCAN SYNTHASE-LIKE 8). *Development*, *137*(10), 1731–1741. https://doi.org/10.1242/dev.049197

Hacquard, S., Petre, B., Frey, P., Hecker, A., Rouhier, N., & Duplessis, S. (2011). The Poplar-Poplar Rust Interaction: Insights from Genomics and Transcriptomics. *Journal of Pathogens*, *2011*, 1–11. https://doi.org/10.4061/2011/716041

Han, Xiao, Hyun, T. K., Zhang, M., Kumar, R., Koh, E. ji, Kang, B. H., … Kim, J. Y. (2014). Auxin-Callose-Mediated Plasmodesmal Gating Is Essential for Tropic Auxin Gradient Formation and Signaling. *Developmental Cell*, *28*(2), 132–146. https://doi.org/10.1016/j.devcel.2013.12.008

Han, Xue, Ma, S., Kong, X., Takano, T., & Liu, S. (2013). Efficient Agrobacterium-mediated transformation of hybrid poplar Populus davidiana Dode × Populus bollena lauche. *International Journal of Molecular Sciences*, *14*(2), 2515–2528. https://doi.org/10.3390/ijms14022515

Harrison, X. A., Donaldson, L., Correa-Cano, M. E., Evans, J., Fisher, D. N., Goodwin, C. E. D., … Inger, R. (2018). A brief introduction to mixed effects modelling and multi-model inference in ecology. *PeerJ*, *2018*(5), 1–32. https://doi.org/10.7717/peerj.4794

Hayafune, M., Berisio, R., Marchetti, R., Silipo, A., Kayama, M., Desaki, Y., … Shibuya, N. (2014). Chitin-induced activation of immune signaling by the rice receptor CEBiP relies on a unique sandwich-type dimerization. *Proceedings of the National Academy of Sciences of the United States of America*, *111*(3). https://doi.org/10.1073/pnas.1312099111

Hellens, R. P., Edwards, E. A., Leyland, N. R., Bean, S., & Mullineaux, P. M. (2000). Biotechnology resources for arable crop transformation (bract)\npGreen: a versatile and flexible binary Ti vector for Agrobacterium-mediated plant transformation. *Plant Mol Biol*, *42*, 819–832. Retrieved from http://www.bract.org

Hothorn, T., Bretz, F., & Westfall, P. (2008). Simultaneous inference in general parametric models. *Biometrical Journal*, *50*(3), 346–363. https://doi.org/10.1002/bimj.200810425

Hou, J., Wei, S., Pan, H., Zhuge, Q., & Yin, T. (2019). Uneven selection pressure accelerating divergence of Populus and Salix. *Horticulture Research*, *6*(1). https://doi.org/10.1038/s41438-019-0121-y

Jansson, C., Wullschleger, S. D., Kalluri, U. C., & Tuskan, G. A. (2010). Phytosequestration: Carbon Biosequestration by Plants and the Prospects of Genetic Engineering. *BioScience*, *60*(9), 685–696. https://doi.org/10.1525/bio.2010.60.9.6

Kadota, Y., Sklenar, J., Derbyshire, P., Stransfeld, L., Asai, S., Ntoukakis, V., … Zipfel, C. (2014). Direct Regulation of the NADPH Oxidase RBOHD by the PRR-Associated Kinase BIK1 during Plant Immunity. *Molecular Cell*, *54*(1), 43–55. https://doi.org/10.1016/j.molcel.2014.02.021

Kaku, H., Nishizawa, Y., Ishii-Minami, N., Akimoto-Tomiyama, C., Dohmae, N., Takio, K., Minami, E., Shibuya, N. (2006). Plant cells recognize chitin fragments for defense signaling through a plasma membrane receptor. *Proceedings of the National Academy of Sciences of the United States of America*, *103*(29), 11086–11091. https://doi.org/10.1073/pnas.79.20.6304

Kouzai, Y., Mochizuki, S., Nakajima, K., Desaki, Y., Hayafune, M., Miyazaki, H., … Nishizawa, Y. (2014). Targeted gene disruption of OsCERK1 reveals its indispensable role in chitin perception and involvement in the peptidoglycan response and immunity in rice. *Molecular Plant-Microbe Interactions*, *27*(9), 975–982. https://doi.org/10.1094/MPMI-03-14-0068-R

Li, Q, Yeh, T., Yang, C., Song, J., Chen, Z., Sederoff, R., & Chiang, V. (2015). Populus trichocarpa. *Methods in Molecular Biology*, *1224*, 357–363. https://doi.org/10.1007/978-1-4939-1658-0

Li, Quanzi, Lin, Y. C., Sun, Y. H., Song, J., Chen, H., Zhang, X. H., … Chiang, V. L. (2012). Splice variant of the SND1 transcription factor is a dominant negative of SND1 members and their regulation in Populus trichocarpa. *Proceedings of the National Academy of Sciences of the United States of America*, *109*(36), 14699–14704. https://doi.org/10.1073/pnas.1212977109

Li, S., Zhen, C., Xu, W., Wang, C., & Cheng, Y. (2017). Simple, rapid and efficient transformation of genotype Nisqually-1: A basic tool for the first sequenced model tree. *Scientific Reports*, *7*(1), 1–10. https://doi.org/10.1038/s41598-017-02651-x

Littlewood, J., Guo, M., Boerjan, W., & Murphy, R. J. (2014). Bioethanol from poplar: A commercially viable alternative to fossil fuel in the European Union. *Biotechnology for Biofuels*, *7*(1), 1–12. https://doi.org/10.1186/1754-6834-7-113

Liu, S., Wang, J., Han, Z., Gong, X., Zhang, H., & Chai, J. (2016). Molecular Mechanism for Fungal Cell Wall Recognition by Rice Chitin Receptor OsCEBiP. *Structure*, *24*(7), 1192–1200. https://doi.org/10.1016/j.str.2016.04.014

Ma, X., Zhang, Q., Zhu, Q., Liu, W., Chen, Y., Qiu, R., … Liu, Y. G. (2015). A Robust CRISPR/Cas9 System for Convenient, High-Efficiency Multiplex Genome Editing in Monocot and Dicot Plants. *Molecular Plant*, *8*(8), 1274–1284. https://doi.org/10.1016/j.molp.2015.04.007

Ma, X., Zhu, Q., Chen, Y., & Liu, Y. G. (2016). CRISPR/Cas9 Platforms for Genome Editing in Plants: Developments and Applications. *Molecular Plant*, *9*(7), 961–974. https://doi.org/10.1016/j.molp.2016.04.009

Mach, J. (2014). When to hold them: Retention of duplicate genes in poplar. *Plant Cell*, *26*(6), 2283. https://doi.org/10.1105/tpc.114.128827

Mader, M., Le Paslier, M-C., Bounon, R., Bérard, A., Rampant, P.F., Fladung, M., Leplé, J.C., Kersten, B. 2018. P. tremula x P. alba, clone INRA 717-1B4 draft genome sequence. URGI database: https://urgi.versailles.inra.fr/Species/Forest-trees/Populus/Clone-INRA-717-1B4

Mélida, H., Sopeña-Torres, S., Bacete, L., Garrido-Arandia, M., Jordá, L., López, G., … Molina, A. (2018). Non-branched β-1,3-glucan oligosaccharides trigger immune responses in Arabidopsis. *Plant Journal*, *93*(1), 34–49. https://doi.org/10.1111/tpj.13755

Miya, A., Albert, P., Shinya, T., Desaki, Y., Ichimura, K., Shirasu, K., … Shibuya, N. (2007). CERK1, a LysM receptor kinase, is essential for chitin elicitor signaling in Arabidopsis. *Proceedings of the National Academy of Sciences of the United States of*

America, *104*(49), 19613–19618. https://doi.org/10.1073/pnas.0705147104

Movahedi, A., Zhang, J., Amirian, R., & Zhuge, Q. (2014). An efficient agrobacterium-mediated transformation system for poplar. *International Journal of Molecular Sciences*, *15*(6), 10780–10793. https://doi.org/10.3390/ijms150610780

Ner-Gaon, H., Leviatan, N., Rubin, E., & Fluhr, R. (2007). Comparative cross-species alternative splicing in plants. *Plant Physiology*, *144*(3), 1632–1641. https://doi.org/10.1104/pp.107.098640

New England Biolabs. (2014). NEBuilder HiFi DNA Assembly Master Mix. *Instruction Manual*, *1*(10), 1–23. Retrieved from https://www.neb.com/products/e5520-nebuilder-hifi-dna-assembly-cloning-kit?device=pdf

Nishiyama, R., Mizuno, H., Okada, S., Yamaguchi, T., Takenaka, M., Fukuzawa, H., & Ohyama, K. (1999). Two mRNA species encoding calcium-dependent protein kinases are differentially expressed in sexual organs of Marchantia polymorpha through alternative splicing. *Plant and Cell Physiology*, *40*(2), 205–212. https://doi.org/10.1093/oxfordjournals.pcp.a029529

Pereira, S., Costa, M., Carvalho, M., & Rodrigues, A. (2016). Potential of poplar short rotation coppice cultivation for bioenergy in Southern Portugal. *Energy Conversion and Management*, *125*. https://doi.org/10.1016/j.enconman.2016.03.068

Petersen, T. N., Brunak, S., Von Heijne, G., & Nielsen, H. (2011). SignalP 4.0: Discriminating signal peptides from transmembrane regions. *Nature Methods*, *8*(10), 785–786. https://doi.org/10.1038/nmeth.1701

Petutschnig, E. K., Jones, A. M. E., Serazetdinova, L., Lipka, U., & Lipka, V. (2010). The Lysin Motif Receptor-like Kinase (LysM-RLK) CERK1 is a major chitin-binding protein in Arabidopsis thaliana and subject to chitin-induced phosphorylation. *Journal of Biological Chemistry*, *285*(37), 28902–28911. https://doi.org/10.1074/jbc.M110.116657

Pierleoni, A., Martelli, P., & Casadio, R. (2008). PredGPI: A GPI-anchor predictor. *BMC Bioinformatics*, *9*, 1–11. https://doi.org/10.1186/1471-2105-9-392

Porth, I., Klápště, J., McKown, A. D., La Mantia, J., Hamelin, R. C., Skyba, O., … Douglas, C. J. (2014). Extensive functional pleiotropy of REVOLUTA substantiated through forward genetics. *Plant Physiology*, *164*(2), 548–554. https://doi.org/10.1104/pp.113.228783

Quevillon, E., Silventoinen, V., Pillai, S., Harte, N., Mulder, N., Apweiler, R., & Lopez, R. (2005). InterProScan: Protein domains identifier. *Nucleic Acids Research*, *33*(SUPPL. 2), 116–120. https://doi.org/10.1093/nar/gki442

R Core Team. 2019. R: A language and environment for statistical computing. R Foundation for Statistical Computing, Vienna, Austria. URL https://www.R-project.org/.

Radutoiu, S., Madsen, L. H., Madsen, E. B., Felle, H. H., Umehara, Y., Grønlund, M., … Stougaard, J. (2003). Plant recognition of symbiotic bacteria requires two LysM receptor-like kinases. *Nature*, *425*(6958), 585–592. https://doi.org/10.1038/nature02039

Ren, L. L., Liu, Y. J., Liu, H. J., Qian, T. T., Qi, L. W., Wang, X. R., & Zeng, Q. Y. (2014). Subcellular relocalization and positive selection play key roles in the retention of

duplicate genes of Populus class III peroxidase family. *Plant Cell*, *26*(6), 2404–2419. https://doi.org/10.1105/tpc.114.124750

Roberts, A. G., & Oparka, K. J. (2003). Plasmodesmata and the control of symplastic transport. *Plant, Cell and Environment*, *26*(1), 103–124. https://doi.org/10.1046/j.1365-3040.2003.00950.x

Ruel, K., Joseleau, J-P. 1991. Involvement of an extracellular glucan sheath during degradation of Populus wood by Phanerochaete chrysosporium. Applied and Environmental Microbiology 57(2): 374-384

Sablok, G., Powell, B., Braessler, J., Yu, F., & Min, X. J. (2017). Comparative landscape of alternative splicing in fruit plants. *Current Plant Biology*, *9–10*, 29–36. https://doi.org/10.1016/j.cpb.2017.06.001

Sager, R. E., & Lee, J. Y. (2018). Plasmodesmata at a glance. *Journal of Cell Science*, *131*(11), 1–7. https://doi.org/10.1242/jcs209346

Sager, R., & Lee, J. Y. (2014). Plasmodesmata in integrated cell signalling: Insights from development and environmental signals and stresses. *Journal of Experimental Botany*, *65*(22), 6337–6358. https://doi.org/10.1093/jxb/eru365

Sannigrahi, P., Ragauskas, A., & Tuskan, G. (2009). Poplar as a feedstock for biofuels: a review of compositional characteristics. *Biofuels, Bioproducts and Biorefining*, *4*, 209–226. https://doi.org/10.1002/bbb

Shimizu, T., Nakano, T., Takamizawa, D., Desaki, Y., Ishii-Minami, N., Nishizawa, Y., … Shibuya, N. (2010). Two LysM receptor molecules, CEBiP and OsCERK1, cooperatively regulate chitin elicitor signaling in rice. *Plant Journal*, *64*(2), 204–214. https://doi.org/10.1111/j.1365-313X.2010.04324.x

Shinya, T., Motoyama, N., Ikeda, A., Wada, M., Kamiya, K., Hayafune, M., … Shibuya, N. (2012). Functional characterization of CEBiP and CERK1 homologs in arabidopsis and rice reveals the presence of different chitin receptor systems in plants. *Plant and Cell Physiology*, *53*(10), 1696–1706. https://doi.org/10.1093/pcp/pcs113

Singh, D., & Chen, S. (2008). The white-rot fungus Phanerochaete chrysosporium: Conditions for the production of lignin-degrading enzymes. *Applied Microbiology and Biotechnology*, *81*(3), 399–417. https://doi.org/10.1007/s00253-008-1706-9

Song, J., Lu, S., Chen, Z. Z., Lourenco, R., & Chiang, V. L. (2006). Genetic transformation of Populus trichocarpa genotype Nisqually-1: A functional genomic tool for woody plants. *Plant and Cell Physiology*, *47*(11), 1582–1589. https://doi.org/10.1093/pcp/pcl018

Song, W.-Y., Choi, Y.-I., Shim, D., Kim, D.-Y., Noh, E.-W., Martinoia, E., & Lee, Y. (2007). Transgenic Poplar for Phytoremediation. *Biotechnology and Sustainable Agriculture 2006 and Beyond*, 265–271. https://doi.org/10.1007/978-1-4020-6635-1_40

Tallis, M. J., Casella, E., Henshall, P. A., Aylott, M. J., Randle, T. J., Morison, J. I. L., & Taylor, G. (2013). Development and evaluation of ForestGrowth-SRC a process-based model for short rotation coppice yield and spatial supply reveals poplar uses water more efficiently than willow. *GCB Bioenergy*, *5*(1), 53–66. https://doi.org/10.1111/j.1757-1707.2012.01191.x

Tuskan, G., DiFazio, S., Jansson, S., & Al., E. (2006). The Genome of Black Cottonwood Populus trichocarpa (Torr. & Gray). *Science*, *313*(September), 1596–1604.

Vanneste, K., Maere, S., & Van de Peer, Y. (2014). Tangled up in two: A burst of genome duplications at the end of the Cretaceous and the consequences for plant evolution. *Philosophical Transactions of the Royal Society B: Biological Sciences*, *369*(1648). https://doi.org/10.1098/rstb.2013.0353

Vatén, A., Dettmer, J., Wu, S., Stierhof, Y. D., Miyashima, S., Yadav, S. R., … Helariutta, Y. (2011). Callose Biosynthesis Regulates Symplastic Trafficking during Root Development. *Developmental Cell*, *21*(6), 1144–1155. https://doi.org/10.1016/j.devcel.2011.10.006

Verma, Deshpal S & Hong, Z. (2001). Plant Callose Synthase Complexes. *Plant Molecular Biology*, *47*, 693–701. https://doi.org/10.1023/A

Wan, J., Tanaka, K., Zhang, X. C., Son, G. H., Brechenmacher, L., Nguyen, T. H. N., & Stacey, G. (2012). LYK4, a lysin motif receptor-like kinase, is important for chitin signaling and plant innate immunity in Arabidopsis. *Plant Physiology*, *160*(1), 396–406. https://doi.org/10.1104/pp.112.201699

Wang, S., Hastings, A., Wang, S., Sunnenberg, G., Tallis, M. J., Casella, E., … Smith, P. (2014). The potential for bioenergy crops to contribute to meeting GB heat and electricity demands. *GCB Bioenergy*, *6*(2), 136–141. https://doi.org/10.1111/gcbb.12123

Willmann, R., Lajunen, H. M., Erbs, G., Newman, M. A., Kolb, D., Tsuda, K., … Nürnberger, T. (2011). Arabidopsis lysin-motif proteins LYM1 LYM3 CERK1 mediate bacterial peptidoglycan sensing and immunity to bacterial infection. *Proceedings of the National Academy of Sciences of the United States of America*, *108*(49), 19824–19829. https://doi.org/10.1073/pnas.1112862108

Wu, S. W., Kumar, R., Iswanto, A. B. B., & Kim, J. Y. (2018). Callose balancing at plasmodesmata. *Journal of Experimental Botany*, *69*(22), 5325–5339. https://doi.org/10.1093/jxb/ery317

Xie, B., Wang, X., Zhu, M., Zhang, Z., & Hong, Z. (2011). CalS7 encodes a callose synthase responsible for callose deposition in the phloem. *Plant Journal*, *65*(1), 1–14. https://doi.org/10.1111/j.1365-313X.2010.04399.x

Zavaliev, R., Dong, X., & Epel, B. L. (2016). Glycosylphosphatidylinositol (GPI) modification serves as a primary plasmodesmal sorting signal. *Plant Physiology*, *172*(2), 1061–1073. https://doi.org/10.1104/pp.16.01026

Zavaliev, R., Ueki, S., Epel, B. L., & Citovsky, V. (2011). Biology of callose (β-1,3-glucan) turnover at plasmodesmata. *Protoplasma*, *248*(1), 117–130. https://doi.org/10.1007/s00709-010-0247-0

Zhang, C., Yang, H., & Yang, H. (2015). Evolutionary Character of Alternative Splicing in Plants. *Bioinformatics and Biology Insights*, *9s1*, 47–52. https://doi.org/10.4137/BBI.S33716

6. General Discussion

6.1 Chitin perception and signaling in poplar

Components of the chitin receptor complex in poplar are similar to Arabidopsis. In Arabidopsis, the known components of the chitin receptor are three LysM-RLKs with AtCERK1 as the kinase active receptor that associates with AtLYK4 and AtLYK5 for a competent signaling complex (Miya et al., 2007; Wan et al., 2008; Petutschnig et al., 2010; Shinya et al., 2012; Liu et al., 2012). In poplar (*P. x canescens*), genes encoding CERK1, LYK4 and LYK5 are present in more than one copy that include two homologs of *CERK1* (Muhr, unpublished), four homologs of *LYK4*, and two homologs of *LYK5* (**Figure 4.1**). The two homologs of *CERK1*, *PcCERK1-1* and *PcCERK1-2*, have an ORF. For *LYK4/5* genes, only two homologs of *LYK4* and one homolog of *LYK5* have been retained as functional copies during evolution while the rest are pseudogenes. All corresponding homologs have a protein domain organization similar to the corresponding proteins in *Arabidopsis*: PcCERK1 proteins were predicted to employ an active kinase, whereas PcLYK4/PcLYK5 proteins likely harbor inactive kinases based on the absence of amino acid residues important for the enzymatic activity (**Figure 4.3A** and Supplemental Figure 4.3). Functional characterization of these components in this study revealed that these proteins exhibit the same function as the corresponding homologs in *Arabidopsis*. The responses of the double knock-out lines of *PcCERK1* (*PcCerk1-1 PcCerk1-2*) to chitin are abolished as shown by the absence of ROS production and MAPK activation upon chitin treatment, while they respond normally to flg22 (personal communication Mascha Muhr). Moreover, the plants still show response to chitin when only one *PcCERK1* gene is knocked out (*PcCerk1-1* has normal ROS burst but strongly impaired MAPK activation, *PcCerk1-2* shows both normal ROS production and MAPK activation), indicating redundancy. Both PcCERK1 proteins seem to be equally involved in ROS burst, but for MAPK PcCERK1-1 is likely more important. For functional characterization of PcLYK4/PcLYK5, complementation studies were carried out by expressing the genes in the *Atlyk4-1 Atlyk5-2* double knock-out mutant, which does not respond to chitin treatment with a ROS burst and MAPK activation (Cao et al., 2014). Constructs expressing *PcLYK4-1*, *PcLYK4-2* and *PcLYK5-2* under the *AtLYK5* promoter in fusion with mCitrine, were generated and transformed into the double knock-out mutant. The generated lines were further tested for their response to chitin via ROS burst and MAPK assays. The results of these complementation studies showed that expression of *PcLYK4*/*PcLYK5* partially restored the responses of the *Atlyk4-1 Atlyk5-2* mutant to chitin,

with respect to ROS burst and MAPK activation (**Figure 4.5**, **Figure 4.6** and Supplemental Figure 4.14), while the lines had a wildtype-like response to flg22 in both assays (Supplemental Figure 4.10, Supplemental Figure 4.11, Supplemental Figure 4.13 and Supplemental Figure 4.15).

PcLYK4/PcLYK5 proteins are internalized into endosomes upon chitin perception (**Figure 4.9**), and this endocytosis was shown to be CERK1-dependent (at least for PcLYK5-2 that was analysed during this research, **Figure 4.10**) similar to endocytosis of AtLYK5 that was used as a positive control during the experiments. AtLYK5 is endocytosed while AtCERK1 stays at the plasma membrane following chitin perception (Erwig et al., 2017). Endocytosis upon elicitor treatment is common for pathogen recognition receptors (PRRs) and essential for receptor-mediated signaling (Robatzek et al., 2006), even though it may be also one mechanism for receptor degradation through ubiquitination. Ligand-induced internalization of a receptor is often followed by degradation, such as the endocytosis of FLS2 upon flg22 perception. Bacterial flagellin receptor, FLS2, was shown to signal from endosomes, prior to intracellular degradation (Robatzek et al., 2006). Signaling from endosomes can occur only if the internalized receptors are fully functional to induce signaling, while in the case of AtLYK5 endocytosis, endosomes contain a protein that is kinase inactive, making downstream signal transduction unlikely, unless AtLYK5 interacts with a kinase active component in the endosome. According to *in silico* analyses, PcLYK4/PcLYK5 are also kinase inactive and signaling from endosomes containing only these proteins should not occur.

Besides LysM-RLKs, the LysM-RLP LYM2 was identified as an additional chitin receptor in *Arabidopsis* that plays a role in a chitin-induced signaling pathway, different from that initiated by chitin-activated AtCERK1 (Faulkner et al., 2013; Cheval et al., 2019). AtLYM2 mediates chitin-induced plasmodesmal closure that also contributes to the regulation of plant immunity. Two homologs of *LYM2* are present in poplar, in which the second homolog shows differential splicing resulting in two splicing variants (**Figure 5.1** and **Figure 5.2**). All identified poplar PcLYM2 proteins have a domain organization similar to AtLYM2 with three extracellular LysM domains and a predicted GPI anchor at the C-terminus (**Figure 5.3**). Knocking out both *PcLYM2* paralogs in poplar abolishes chitin-induced plasmodesmal closure (**Figure 5.9** and **Figure 5.10**), indicating that *PcLYM2* exhibits a function similar to *AtLYM2*. However, the single knock-out lines of *PcLYM2-1* also showed no chitin-induced PD closure after chitin treatment. The transcript of *PcLYM2-1* is more abundant in all analysed tissues of *P. x canescens* and the protein showed the

highest capacity to bind chitin among all identified PcLYM2 proteins, suggesting PcLYM2-1 as the primary poplar LYM2 protein involved in chitin-triggered PD closure. It is speculation, but conceivable that the other paralog, *PcLYM2-2* (including the splicing variants), acquired a new function. PcLYM2-2 could modulate receptor characteristics as a heterodimeric partner of PcLYM2-1 in the receptor complex or PcLYM2-2 may be involved in a not yet identified process that is different from chitin-induced PD closure. PcLYM2-2 may even perceive other ligands than chitin to regulate plasmodesmal flux or act in a different pathway, which has not been identified yet. A receptor can bind different ligands and work in multiple signaling pathways, depending on the interacting partner (Macho and Zipfel, 2014). AtCERK1, for instance, shows preferential binding to longer-chain chitin oligosaccharides and requires N-acetyl glucosamine residues for binding (Iizasa et al., 2010; Petutschnig et al., 2010; Liu et al., 2012). Bacterial peptidoglycan (PGN) also contains N-acetyl glucosamine residues, but it does not bind to AtCERK1, which could be due to the inhibition by the bulky peptide group cross-linked to N-acetylmuramic acid residues in PGN (Iizasa et al., 2010). However, in association with AtLYM1 and AtLYM3, AtCERK1 can perceive PGN (Willmann et al., 2011). Moreover, *in silico* docking analyses showed that AtCERK1 also binds to ligands beside chitin, such as to the linear 1,3-β-D glucans (Mélida et al., 2018).The preference of PcLYM2 ligand-binding, especially of the PcLYM2-2 splicing variants, needs to be examined, since these proteins also bind to chitin but the chitin-binding capacity is lower compared to PcLYM2-1.

6.2 Gene duplication in the poplar genome resulted in functional diversity of LysM-RLK and LysM-RLP paralogs

Single-gene or whole genome duplication (WGD) occurs during evolution in which one gene is doubled into two genes that cannot be functionally distinguished from each other, mostly leading to genetic redundancy (Flagel and Wendel, 2009; Magadum et al., 2013). Several rounds of duplication may even multiply gene copies. Gene duplication occurs through several mechanisms including unequal crossing over, retroposition, duplicative transposition and polyploidization (Magadum et al., 2013). Unequal crossing often results in a tandem duplication and, depending on the segmental position of the crossing over, the duplicated region can contain part of the gene, the entire gene or several genes. Retroposition is the integration of reverse transcribed mRNA into the genome that rarely results in an expressed, full-length coding sequence, but the coding sequence is separated from its regulatory element, lacks introns and has a poly-A tail.

Subsequently, the duplicated genes undergo modification through accumulation of mutations, which results in differentiation of the duplicates. During this process, natural selection occurs by elimination of the non-functional duplicates (which become pseudogenes) and retention of the functional ones (Mach, 2014; Vanneste et al., 2014). Thus, WGD followed by massive gene loss and gene specialization contributes to innovation in evolution. The retained functional genes might undergo further mutations resulting in pseudogenization, conservation of gene function, subfunctionalization and neofunctionalization, which generates novel functions that can lead to speciation (Vanneste et al., 2014). The existence of gene families in which some members arose from a common ancestor is an evidence that gene duplication has occurred. Gene duplicates that share a common ancestor and stay in the same genome are defined as paralogs, which differ from orthologs present in different genomes. These originated from the same ancestor as a result of speciation (Hurles, 2004). The presence of more than one gene copy can help the genome to escape from extinction (Crow and Wagner, 2006) due to gene loss during the evolution. Gene duplication is common with the Salicaceae family such as *Populus* and *Salix* that were reported to have a paralogous segment in almost every chromosomal region of their genomes and share lineage-specific whole genome duplications (salicoid duplication) (Hou et al., 2019).

Identification and functional characterization of genes encoding the LysM-RLKs LYK4/LYK5 and the LysM-RLPs LYM2 in poplar provides evidence for an evolutionary process in poplar that involves gene duplication followed by both gene loss and probable gene neofunctionalization. Four homologs of *LYK4* and two homologs of *LYK5* are present in *P. x canescens* as a result of gene duplication (**Table 4.1**). Only *PcLYK4-1* and *PcLYK4-2* were maintained by positive selection and retained during evolution, while the other two homologs of PcLYK4 were inactivated through pseudogenization. For PcLYK5, only one homolog was retained. The remaining duplicates (*PcLYK4-1*, *PcLYK4-2* and *PcLYK5-2*) have a similar domain organization. Complementation studies with the *Atlyk4-1 lyk5-2* mutant as well as the fact that the genes are expressed in the same tissues indicate functional redundancy.

In contrast, both retained *LYM2* duplicates in poplar are translated into full length proteins. The two homologs of *LYM2, PcLYM2-1* and *PcLYM2-2*, were identified on different chromosomes of *P. x canescens. PcLYM2-1* is located on chromosome 4 and *PcLYM2-2* on chromosome 9. The poplar LYM2 paralogs have the same domain organization like AtLYM2 (**Figure 5.3**). The *PcLYM2* genes might have originated from the same ancestor as the orthologs in *Arabidopsis* (*AtLYM2*) and rice (*OsCEBiP*). However,

unlike OsCEBiP that acts as a main component of the chitin receptor complex in rice, PcLYM2 as well as AtLYM2 have a different function. AtLYM2 perceives chitin but mediates chitin-triggered plasmodesmal closure rather than chitin-induced ROS production and MAPK activation as described for OsCEBiP. Similar to AtLYM2, PcLYM2 proteins in poplar are also chitin-binding proteins that facilitate the closure of plasmodesmata upon chitin perception (**Figure 5.9** and **Figure 5.10**). However, possible functional differentiation within the two paralogs of PcLYM2 remains to be characterized.

The second homolog of *PcLYM2*, *PcLYM2-2*, generates two alternative transcripts as a result of alternative splicing (**Figure 5.2**). During the splicing event, alternative splicing might occur that results in two or more mRNAs derived from the same precursor (Chaudhary et al., 2019). Alternative splicing can occur through intron retention, exon skipping, or alternative 5' or 3' end donor sites. Alternative splicing in plants mostly occurs through intron retention (Chaudhary et al., 2019; Clark et.al., 2019), but the splicing event in *PcLYM2-2* occurs through mutually exclusive splicing of the first exon, which is not common in plants (Zhang et al., 2015). In this splicing mode, the pre-mRNA has two mutually exclusive exons, but only one of them is present in each mRNA variant, which usually results in alternative trancripts with identical ORF lengths (Zhang et al., 2015; Chen et.al., 2007). The *PcLYM2-2* gDNA has two alternative first exons that are mutually exclusive. The translated products of the transcripts show that these two alternative first exons encode the same protein domains (the LysM domains), whereas the rest of the sequence is identical. Mutually exclusive splicing was investigated in detail for a gene encoding a CALCIUM-DEPENDENT CALMODULIN-INDEPENDENT PROTEIN KINASE (CDPK) in *Marchantia polymorpha* (Nishiyama et al., 1999). This CDPK has 9 exons, and the 6^{th} exon is almost identical with the 7^{th} exon (further renamed as exon 6A and 6B). Mutually exclusive alternative splicing of these two exons resulted in two splicing variants of CDPK, each containing only one of the two nearly identical exons. mRNA that contains both alternative exons was not detected. Chen et.al. (2007) identified data sets of mutually exclusive splicing events of the first exon in Arabidopsis and rice, and found 79 and 84 evidences, respectively. They also observed that alternative splicing through this mechanism results in an unchanged protein domain organization, and thus hypothesized that the splicing variants resulting from mutually exclusive splicing may have tissue or stage-specificity (Chen et.al., 2007). This is also the case for *PcLYM2* splicing variants, which differ at the first exon but still encode two full-size proteins with similar domain organization.

6.3 Formation of alternative pathogen recognition receptor (PRR) complexes related to different signaling pathways

PAMP-triggered immunity (PTI) is the first layer of plant defenses which is mediated by surface-localized pathogen recognition receptors (PRRs) perceiving PAMPs or DAMPs (Antolín-Llovera et al., 2014). PRRs usually work in a collaborative manner through homo- or heterodimerization and can be involved in different pathways depending on the interacting partners (Macho and Zipfel, 2014). Chitin perception in the plant model *Arabidopsis* is mediated by two receptor complexes, which use different signaling pathways. One pathway is the CERK1-mediated pathway that involves the association of LysM-RLKs CERK1, LYK4 and LYK5 for chitin perception and proper chitin-induced signal transduction (Miya et al., 2007; Wan et al., 2008; Petutschnig et al., 2010; Shinya et al., 2012; Liu et al., 2012; Wan et al., 2012; Cao et al., 2014; Erwig et al., 2017). Elicitation of this pathway is manifested by several chitin-triggered plant responses such as cytosolic calcium elevation, ROS production, MAPK activation, as well as chitin-related gene expression. The other chitin-triggered pathway described in Arabidopsis is facilitated by the LysM-RLP LYM2 to control chitin-triggered plasmodesmal closure. AtLYM2 was postulated to associate with the LysM-RLK LYK4 to form a signaling competent complex (Faulkner et al., 2013; Cheval and Faulkner, 2018; Cheval et al., 2019). However, LYK4 has an inactive kinase (Wan et al., 2012; Cao et al., 2014; Petutschnig et al., 2010). Hence, association of only LYM2 and LYK4 is not sufficient to inititate signal transduction and requires an interacting partner that is able to mediate intracellular signaling. In rice, the homolog of *AtLYM2*, *OsCEBiP*, heterodimerizes with OsCERK1 upon chitin perception and acts in a pathway comparable to the signaling that is mediated by CERK1 in a complex with LYK4/5 in *Arabidopsis* (Kaku et al., 2006; Miya et al., 2007; Shimizu et al., 2010; Hayafune et al., 2014; Kouzai et al., 2014).

Results of this study and, in addition, research on poplar CERK1 homologs (Mascha Muhr, personal communication), indicate that the formation of chitin receptor complexes in poplar is comparable to Arabidopsis. Since there are two putatively functional homologs of *LYK4* in poplar, *PcLYK4-1* and *PcLYK4-2*, alternative receptor complex formations are conceivable, including one or the other of these two *LYK4* homologs.

The poplar homolog of LYM2 mediates chitin-induced PD closure comparable to AtLYM2 (Faulkner et al., 2013; Cheval et al., 2019). However, one difference between chitin control of plasmodesmal flux in Arabidopsis and poplar is the presence of more than one *LYM2* copy in poplar, which might also affect the complex formation as discussed for the P*cLYK4*

paralogs. The molecular binding mechanism of LysM-RLP to chitin was described in rice CEBiP, showing that OsCEBiP homodimerizes upon binding to chitin (Liu et al., 2016; Hayafune et al., 2014) and the dimer forms a complex with OsCERK1 for downstream signaling (Shimizu et al., 2010; Kouzai et al., 2014). There are two homologs of LYM2 (and three LYM2 proteins due to the alternative splicing of the second homolog) in *P. x canescens*, and the transcripts show tissue-specific abundance making alternative complex formation with different LYM partners conceivable. As a consequence of tissue-specific expression and tissue-specific splicing of poplar *LYM2* genes, tissue-specific LYM2 complexes may form. Homo- or heterodimerization among PcLYM2 proteins might occur upon chitin treatment (**Figure 5.12**). However, this complex still needs to associate with another protein that harbors an intracellular active signaling domain to mediate downstream signaling pathways.

6.4 Regulation of plasmodesmal flux contributes to plant immunity

Plasmodesmata (PD) are not only used as a conduit for plant defense signaling molecules, but also utilized by pathogens for spreading. Several viruses such as *tobacco mosaic virus* (TMV) (Guenoune-Gelbart et al., 2008) and potato virus Y^{NTN} (PVY^{NTN}) (Dobnik et al., 2013) were reported to spread via PD, facilitated by movement proteins (MPs). Similar to the facilitation of viral spreading by MPs, the cell to cell transport of pathogen-induced compounds is required for plant defense. Effectors released by fungal or bacterial pathogens were also proposed to counteract PD-located, innate immune responses to regulate PD permeability and exploit PD as a channel for spreading from cell to cell (Cheval and Faulkner, 2018). Therefore, PD permeability is under the tight control of signaling components that recognize attackers and facilitate ligand-induced signal transduction to prevent infection. LYM2 is a receptor that mediates ligand-induced PD-closure upon the perception of fungal chitin in *Arabidopsis* (Faulkner et al., 2013; Cheval et al., 2019) and in poplar, as shown in this study. This response is independent of CERK1-mediated chitin-induced signaling, in which the perception of chitin triggers the early responses of plants that include ROS burst and MAPK activation. The *Atcerk1-2* mutant does not exhibit chitin-induced ROS burst and MAPK activation (Miya et al., 2007), but it has a PD closure like WT upon chitin treatment (Faulkner et al., 2013). *PcLYM2* loss-of-function mutations also do not affect chitin induced ROS burst and MAPK activation but abolish the PD-response (**Figure 5.8** and **Figure 5.10**). However, chitin-induced PD closure assays by particle

bombardment have to be performed in *PcCerk1* knockout mutants to confirm that these pathways are also independent of CERK1 in poplar.

ROS production has been associated with the regulation of PD connectivity since the application of exogenous ROS decreases PD permeability (Cui and Lee, 2016). However, chitin-induced ROS production in *Atlym2-1* does not affect PD permeability, suggesting that LYM2-mediated chitin-triggered PD closure is independent of other chitin-induced responses. Beside chitin, bacterial flg22 was also reported to induce PD closure (Faulkner et al., 2013; Xu et al., 2017). flg22-induced PD closure through callose deposition is mediated by CALMODULIN LIKE41 (CML41), a plasmodesmal-localized Ca^{2+}-binding protein, which acts downstream of flg22 recognition by FLS2. However, it is not clear whether CML41 directly stimulates the synthesis of callose or inhibits the constitutive process of callose degradation. Callose deposition requires flg22-triggered Ca^{2+} signaling via CML41. Whether PcLYM2 functions in callose deposition remains to be examined by performing callose staining on the knock-out lines with and without chitin treatment, and analyse whether the callose deposition is reduced in comparison to chitin-treated wildtype plant as a control.

7. General conclusions and outlook

Components important for chitin perception that have been described in Arabidopsis are also present in poplar. These include the three LysM-RLKs: *CERK1*, *LYK4*, *LYK5* and the LysM-RLP *LYM2*. Regarding LysM-RLKs, there are four homologs of *LYK4* and two homologs of *LYK5* in poplar, but two *LYK4* paralogs and one *LYK5* paralog are pseudogenes with premature stop codons. Domain prediction on PcLYK4-1, PcLYK4-2 and PcLYK5-2, encoded by homologs with an open reading frame, revealed domain organization similar to AtLYK4 and AtLYK5 with three extracellular LysM domains, a transmembrane domain, and an intracellular kinase domain that lacks subdomains necessary for its enzymatic activity. Expressing *PcLYK4*/*PcLYK5* in the *Atlyk4*-1 *Atlyk5*-2 mutant partially restores the responses of this double knock-out mutant to chitin as shown via chitin-induced ROS production and MAPK activation. Subcellular localization studies indicate that the characterized PcLYK4/PcLYK5 proteins are plasma membrane-localized LysM-RLKs that undergo endocytosis following chitin treatment. The endocytosis of PcLYK5-2 was shown to be CERK1-dependent. The data provide evidences that PcLYK4/PcLYK5 proteins are involved in chitin perception and signaling. However, to determine whether these components are indispensable for chitin-induced signal transduction, single or triple knock-out lines of PcLYK4/PcLYK5 need to be generated and analysed for reduced or abolished chitin responses. Knocking-out *PcLYK4*/*PcLYK5* individually or simultaneously will also show if these genes are functionally redundant. The presence of more than one homolog for *LYK4*, *PcLYK4-1* and *PcLYK4-2*, suggests that alternative receptor complexes with CERK1 may form with each including only one of these paralogs. Investigation of the interaction of these proteins can be done by conducting co-immunoprecipitation assays, or via FLIM-FRET analyses.

Identification of LYM2 homologs in poplar revealed that there are two *LYM2* paralogs, *PcLYM2-1* and *PcLYM2-2*, as a result of gene duplication. Domain analysis of the protein sequences predicts that PcLYM2 proteins are GPI-anchored proteins that employ three extracellular LysM domains similar to AtLYM2. One of the paralogs exhibits tissue-specific alternative splicing resulting in the two splicing variants, *PcLYM2-2.1* and *PcLYM2-2.2*, which differ only at the first exon encoding the LysM domains. All identified PcLYM2 proteins are chitin-binding proteins that localize at both plasma membrane (PM) and plasmodesmata (PD), with PcLYM2-1 showing the highest chitin-binding capacity. Knocking-out both *PcLYM2* genes simultaneously does not impair chitin-induced ROS

production and MAPK activation, but abolishes chitin-induced PD closure. This suggests that *PcLYM2* acts like *AtLYM2* in Arabidopsis, which mediates chitin-induced PD closure. Moreover, knocking out *PcLYM2-1* is sufficient to abolish the chitin-induced PD closure, suggesting that PcLYM2-1 is the primary LysM-RLP in poplar involved in this process. This result also indicates that there is no functional redundancy between the two paralogs. Expression analysis of *PcLYM2* genes in different tissues showed that the *PcLYM2-1* transcript is more abundant in all analysed tissues (roots, woods, developing xylems, barks and leaves) than the mRNA of both *PcLYM2-2* splicing variants. The highest transcript abundance of *PcLYM2-1* was found in bark. Moreover, comparing the *PcLYM2-2* splicing variants, *PcLYM2-2.1* is significantly more abundant in wood than in the other tissues while *PcLYM2-2.2* is significantly more abundant in bark with the same tendency in leaves. These results together with the chitin binding capacity data support the hypothesis that PcLYM2-1 is more important than the other PcLYM2 proteins in mediating chitin perception and chitin-induced PD closure.

PcLYM2 proteins might homo- or heterodimerize to form tissue-specific complexes upon binding to chitin. PcLYM2 proteins are GPI-anchored proteins that do not have an intracellular signaling domain and, therefore, they require association with other components in order to mediate downstream signaling. Complex formation among PcLYM2 proteins as well as their interaction with other components needs to be further investigated. The homo- or heterodimerization of PcLYM2 paralogs can be examined by co-expressing the genes in fusion with a distinct fluorescent tag and further conduct chitin pull-down assays or Fluorescence Lifetime Imaging Microscopy-Förster Resonance Energy Transfer (FLIM-FRET analyses).

8. References

Aghaalikhani, A., Savuto, E., Di Carlo, A., & Borello, D. (2017). Poplar from phytoremediation as a renewable energy source: Gasification properties and pollution analysis. *Energy Procedia*, *142*, 924–931. https://doi.org/10.1016/j.egypro.2017.12.148

Antolín-Llovera, M., Petutsching, E. K., Ried, M. K., Lipka, V., Nürnberger, T., Robatzek, S., & Parniske, M. (2014). Knowing your friends and foes - plant receptor-like kinases as initiators of symbiosis or defence. *New Phytologist*, *204*(4), 791–802. https://doi.org/10.1111/nph.13117

Ao, Y., Li, Z., Feng, D., Xiong, F., Liu, J., Li, J. F., … Wang, H. Bin. (2014). OsCERK1 and OsRLCK176 play important roles in peptidoglycan and chitin signaling in rice innate immunity. *Plant Journal*, *80*(6), 1072–1084. https://doi.org/10.1111/tpj.12710

Arrighi, J. F., Barre, A., Ben Amor, B., Bersoult, A., Soriano, L. C., Mirabella, R., … Gough, C. (2006). The Medicago truncatula lysine motif-receptor-like kinase gene family includes NFP and new nodule-expressed genes. *Plant Physiology*, *142*(1), 265–279. https://doi.org/10.1104/pp.106.084657

B. Alberts, A. Johnson, J. Lewis, D. Morgan, M. Raff, K. Roberts, P. W. (2014). Molecular Biology of the Cell 6Th Edition. In *Garland Science, Taylor & Francis Group*. https://doi.org/10.1017/CBO9781107415324.004

Bateman, A., & Bycroft, M. (2000). The structure of a LysM domain from E. coli membrane-bound lytic murein transglycosylase D (MltD). *Journal of Molecular Biology*, *299*(4), 1113–1119. https://doi.org/10.1006/jmbi.2000.3778

Bayer, E. M., Mongrand, S., & Tilsner, J. (2014). Specialized membrane domains of plasmodesmata, plant intercellular nanopores. *Frontiers in Plant Science*, *5*(SEP), 1–3. https://doi.org/10.3389/fpls.2014.00507

Beck, M., Zhou, J., Faulkner, C., Mac, D. L., & Robatzek, S. (2012). Spatio-temporal cellular dynamics of the Arabidopsis flagellin receptor reveal activation status-dependent endosomal sorting. *Plant Cell*, *24*(10), 4205–4219. https://doi.org/10.1105/tpc.112.100263

Benitez-Alfonso, Y., Faulkner, C., Pendle, A., Miyashima, S., Helariutta, Y., & Maule, A. (2013). Symplastic Intercellular Connectivity Regulates Lateral Root Patterning. *Developmental Cell*, *26*(2), 136–147. https://doi.org/10.1016/j.devcel.2013.06.010

Bielnicki, J., Devedjiev, Y., Derewenda, U., Dauter, Z., Joachimiak, A., & Derewenda, Z. S. (2006). B. subtilis ykuD protein at 2.0 Å resolution: Insights into the structure and function of a novel, ubiquitous family of bacterial enzymes. *Proteins: Structure, Function and Genetics*, *62*(1), 144–151. https://doi.org/10.1002/prot.20702

Blackman, L., & Overall, R. (1998). Immunolocalization of the cytoskeleton to plasmodesmata of Chara corallina. *The Plant Journal*, *14*(6), 733–741.

Böhlenius, H., Huang, T., Charbonnel-Campaa, L., Brunner, A. M., Jansson, S., Strauss, S. H., & Nilsson, O. (2006). CO/FT regulatory module controls timing of flowering and seasonal growth cessation in trees. *Science*, *312*(5776), 1040–1043. https://doi.org/10.1126/science.1126038

Boller, T., & Felix, G. (2009). A Renaissance of Elicitors: Perception of Microbe-Associated

Molecular Patterns and Danger Signals by Pattern-Recognition Receptors. *Annual Review of Plant Biology*, *60*(1), 379–406. https://doi.org/10.1146/annurev.arplant.57.032905.105346

Bozsoki, Z., Cheng, J., Feng, F., Gysel, K., Vinther, M., Andersen, K. R., … Stougaard, J. (2017). Receptor-mediated chitin perception in legume roots is functionally separable from Nod factor perception. *Proceedings of the National Academy of Sciences of the United States of America*, *114*(38), E8118–E8127. https://doi.org/10.1073/pnas.1706795114

Bradshaw, H. D., Ceulemans, R., Davis, J., & Stettler, R. (2000). Emerging model systems in plant biology: Poplar (Populus) as a model forest tree. *Journal of Plant Growth Regulation*, *19*(3), 306–313. https://doi.org/10.1007/s003440000030

Broghammer, A., Krusell, L., Blaise, M., Sauer, J., Sullivan, J. T., Maolanon, N., … Stougaard, J. (2012). Legume receptors perceive the rhizobial lipochitin oligosaccharide signal molecules by direct binding. *Proceedings of the National Academy of Sciences of the United States of America*, *109*(34), 13859–13864. https://doi.org/10.1073/pnas.1205171109

Buendia, L., Girardin, A., Wang, T., Cottret, L., & Lefebvre, B. (2018). LysM receptor-like kinase and lysM receptor-like protein families: An update on phylogeny and functional characterization. *Frontiers in Plant Science*, *871*(October), 1–25. https://doi.org/10.3389/fpls.2018.01531

Buendia, L., Wang, T., Girardin, A., & Lefebvre, B. (2016). The LysM receptor-like kinase SlLYK10 regulates the arbuscular mycorrhizal symbiosis in tomato. *New Phytologist*, *210*(1), 184–195. https://doi.org/10.1111/nph.13753

Buist, G., Steen, A., Kok, J., & Kuipers, O. P. (2008). LysM, a widely distributed protein motif for binding to (peptido)glycans. *Molecular Microbiology*, *68*(4), 838–847. https://doi.org/10.1111/j.1365-2958.2008.06211.x

Burch-Smith, T. M., Stonebloom, S., Xu, M., & Zambryski, P. C. (2011). Plasmodesmata during development: Re-examination of the importance of primary, secondary, and branched plasmodesmata structure versus function. *Protoplasma*, *248*(1), 61–74. https://doi.org/10.1007/s00709-010-0252-3

Burch-Smith, T. M., & Zambryski, P. C. (2012). Plasmodesmata Paradigm Shift: Regulation from Without Versus Within. *Annual Review of Plant Biology*, *63*(1), 239–260. https://doi.org/10.1146/annurev-arplant-042811-105453

Cantrill, L. C., Overall, R. L., & Goodwin, P. B. (1999). Cell-to-cell communication via plant endomembranes. *Cell Biology International*, *23*(10), 653–661. https://doi.org/10.1006/cbir.1999.0431

Cao, Y., Liang, Y., Tanaka, K., Nguyen, C. T., Jedrzejczak, R. P., Joachimiak, A., & Stacey, G. (2014). The kinase LYK5 is a major chitin receptor in Arabidopsis and forms a chitin-induced complex with related kinase CERK1. *ELife*, *3*(October). https://doi.org/10.7554/eLife.03766

Castro-Rodríguez, V., García-Gutiérrez, A., Canales, J., Cañas, R. A., Kirby, E. G., Avila, C., & Cánovas, F. M. (2016). Poplar trees for phytoremediation of high levels of nitrate and applications in bioenergy. *Plant Biotechnology Journal*, *14*(1), 299–312. https://doi.org/10.1111/pbi.12384

Chang, S., Puryear, J., & Cairney, J. (1993). A Simple and Efficient Method for Isolating RNA from Pine Trees. *Plant Molecular Biology Reporter*, *11*(2), 113–116.

Chaudhary, S., Khokhar, W., Jabre, I., Reddy, A. S. N., Byrne, L. J., Wilson, C. M., & Syed, N. H. (2019). Alternative splicing and protein diversity: Plants versus animals. *Frontiers in Plant Science*, *10*(June), 1–14. https://doi.org/10.3389/fpls.2019.00708

Chen, W. H., Lv, G., Lv, C., Zeng, C., & Hu, S. (2007). Systematic analysis of alternative first exons in plant genomes. *BMC Plant Biology*, *7*, 1–13. https://doi.org/10.1186/1471-2229-7-55

Chen, X. Y., & Kim, J. Y. (2009). Callose synthesis in higher plants. *Plant Signaling and Behavior*, *4*(6), 489–492. https://doi.org/10.4161/psb.4.6.8359

Chen, Z., Wang, J., Ye, M. X., Li, H., Ji, L. X., Li, Y., … An, X. M. (2013). A novel moderate constitutive promoter derived from poplar (Populus tomentosa carrière). *International Journal of Molecular Sciences*, *14*(3), 6187–6204. https://doi.org/10.3390/ijms14036187

Cheval, C., & Faulkner, C. (2018). Plasmodesmal regulation during plant–pathogen interactions. *New Phytologist*, *217*(1), 62–67. https://doi.org/10.1111/nph.14857

Cheval, C., Johnston, M., Samwald, S., Liu, X., Bellandi, A., Breakspear, A., … Faulkner, C. (2019). Chitin perception in plasmodesmata identifies subcellular, context-specific immune signalling in plants. *BioRxiv*, 611582. https://doi.org/10.1101/611582

Chinchilla, D., Zipfel, C., Robatzek, S., Kemmerling, B., Nürnberger, T., Jones, J. D. G., … Boller, T. (2007). A flagellin-induced complex of the receptor FLS2 and BAK1 initiates plant defence. *Nature*, *448*(7152), 497–500. https://doi.org/10.1038/nature05999

Choi, H. W., & Klessig, D. F. (2016). DAMPs, MAMPs, and NAMPs in plant innate immunity. *BMC Plant Biology*, *16*(1), 1–10. https://doi.org/10.1186/s12870-016-0921-2

Clark, S., Yu, F., Gu, L., & Min, X. J. (2019). Expanding alternative splicing identification by integrating multiple sources of transcription data in tomato. *Frontiers in Plant Science*, *10*(May), 1–12. https://doi.org/10.3389/fpls.2019.00689

Clough, S. J., & Bent, A. F. (1998). Floral dip: A simplified method for Agrobacterium-mediated transformation of Arabidopsis thaliana. *Plant Journal*, *16*(6), 735–743. https://doi.org/10.1046/j.1365-313X.1998.00343.x

Crow, K. D., & Wagner, G. P. (2006). What is the role of genome duplication in the evolution of complexity and diversity? *Molecular Biology and Evolution*, *23*(5), 887–892. https://doi.org/10.1093/molbev/msj083

Cui, W., & Lee, J. Y. (2016). Arabidopsis callose synthases CalS1/8 regulate plasmodesmal permeability during stress. *Nature Plants*, *2*(5). https://doi.org/10.1038/NPLANTS.2016.34

Dangl, J. L., & Jones, J. D. G. (2001). Defence Responses To Infection. *Nature*, *411*(June).

Den Camp, R. O., Streng, A., De Mita, S., Cao, Q., Polone, E., Liu, W., … Geurts, R. (2011). LysM-type mycorrhizal receptor recruited for rhizobium symbiosis in nonlegume Parasponia. *Science*, *331*(6019), 909–912. https://doi.org/10.1126/science.1198181

Dereeper, A., Guignon, V., Blanc, G., Audic, S., Buffet, S., Chevenet, F., … Gascuel, O.

(2008). Phylogeny.fr: robust phylogenetic analysis for the non-specialist. *Nucleic Acids Research*, *36*(Web Server issue), 465–469. https://doi.org/10.1093/nar/gkn180

Dereeper, Alexis, Audic, S., Claverie, J. M., & Blanc, G. (2010). BLAST-EXPLORER helps you building datasets for phylogenetic analysis. *BMC Evolutionary Biology*, *10*(1), 8–13. https://doi.org/10.1186/1471-2148-10-8

Desaki, Y., Miyata, K., Suzuki, M., Shibuya, N., & Kaku, H. (2018). Plant immunity and symbiosis signaling mediated by LysM receptors. *Innate Immunity*, *24*(2), 92–100. https://doi.org/10.1177/1753425917738885

Dobnik, D., Baebler, Š., Kogovšek, P., Pompe-Novak, M., Štebih, D., Panter, G., … Gruden, K. (2013). β-1,3-glucanase class III promotes spread of PVYNTN and improves in planta protein production. *Plant Biotechnology Reports*, *7*(4), 547–555. https://doi.org/10.1007/s11816-013-0300-5

Dodds, P. N., & Rathjen, J. P. (2010). Plant immunity: Towards an integrated view of plantĝ€" pathogen interactions. *Nature Reviews Genetics*, *11*(8), 539–548. https://doi.org/10.1038/nrg2812

Doxey, A. C., Yaish, M. W. F., Moffatt, B. A., Griffith, M., & McConkey, B. J. (2007). Functional divergence in the Arabidopsis β-1,3-glucanase gene family inferred by phylogenetic reconstruction of expression states. *Molecular Biology and Evolution*, *24*(4), 1045–1055. https://doi.org/10.1093/molbev/msm024

Duplessis, S., Major, I., Martin, F., & Séguin, A. (2009). Poplar and pathogen interactions: Insights from populus genome-wide analyses of resistance and defense gene families and gene expression profiling. *Critical Reviews in Plant Sciences*, *28*(5), 309–334. https://doi.org/10.1080/07352680903241063

Ehlers, K., & Kollmann, R. (2001). Primary and secondary plasmodesmata: Structure, origin, and functioning: Review article. *Protoplasma*, *216*(1–2), 1–30. https://doi.org/10.1007/BF02680127

Ellinger, D., & Voigt, C. A. (2014). Callose biosynthesis in arabidopsis with a focus on pathogen response: What we have learned within the last decade. *Annals of Botany*, *114*(6), 1349–1358. https://doi.org/10.1093/aob/mcu120

Epel, B. L. (2009). Plant viruses spread by diffusion on ER-associated movement-protein-rafts through plasmodesmata gated by viral induced host β-1,3-glucanases. *Seminars in Cell and Developmental Biology*, *20*(9), 1074–1081. https://doi.org/10.1016/j.semcdb.2009.05.010

Erwig, J., Ghareeb, H., Kopischke, M., Hacke, R., Matei, A., Petutschnig, E., & Lipka, V. (2017). Chitin-induced and CHITIN ELICITOR RECEPTOR KINASE1 (CERK1) phosphorylation-dependent endocytosis of Arabidopsis thaliana LYSIN MOTIF-CONTAINING RECEPTOR-LIKE KINASE5 (LYK5). *New Phytologist*, *215*(1), 382–396. https://doi.org/10.1111/nph.14592

Fankhauser, N., & Mäser, P. (2005). Identification of GPI anchor attachment signals by a Kohonen self-organizing map. *Bioinformatics*, *21*(9), 1846–1852. https://doi.org/10.1093/bioinformatics/bti299

Faulkner, C. (2013). Receptor-mediated signaling at plasmodesmata. *Frontiers in Plant Science*, *4*(DEC), 1–6. https://doi.org/10.3389/fpls.2013.00521

Faulkner, C., Akman, O. E., Bell, K., Jeffree, C., & Oparka, K. (2008). Peeking into pit fields: A multiple twinning model of secondary plasmodesmata formation in tobacco. *Plant Cell*, *20*(6), 1504–1518. https://doi.org/10.1105/tpc.107.056903

Faulkner, C., Petutschnig, E., Benitez-Alfonso, Y., Beck, M., Robatzek, S., Lipka, V., & Maule, A. J. (2013). LYM2-dependent chitin perception limits molecular flux via plasmodesmata. *Proceedings of the National Academy of Sciences of the United States of America*, *110*(22), 9166–9170. https://doi.org/10.1073/pnas.1203458110

Fesel, P. H., & Zuccaro, A. (2016). β-glucan: Crucial component of the fungal cell wall and elusive MAMP in plants. *Fungal Genetics and Biology*, *90*, 53–60. https://doi.org/10.1016/j.fgb.2015.12.004

Fladung, M., Hoenicka, H., & Raj Ahuja, M. (2013). Genomic stability and long-term transgene expression in poplar. *Transgenic Research*, *22*(6), 1167–1178. https://doi.org/10.1007/s11248-013-9719-2

Friedrich, L., Vernooij, B., Gaffney, T., Morse, A., & Ryals, J. (1995). Characterization of tobacco plants expressing a bacterial salicylate hydroxylase gene. *Plant Molecular Biology*, *29*(5), 959–968. https://doi.org/10.1007/BF00014969

Fuchs, M., van Bel, A. J. E., & Ehlers, K. (2010). Season-associated modifications in symplasmic organization of the cambium in Populus nigra. *Annals of Botany*, *105*(3), 375–387. https://doi.org/10.1093/aob/mcp300

Galian, C., Björkholm, P., Bulleid, N., & Von Heijne, G. (2012). Efficient glycosylphosphatidylinositol (GPI) modification of membrane proteins requires a C-terminal anchoring signal of marginal hydrophobicity. *Journal of Biological Chemistry*, *287*(20), 16399–16409. https://doi.org/10.1074/jbc.M112.350009

García-Angulo, P., Villar, I., Giner-Robles, L., & Centeno, M. L. (2018). In vitro regeneration of two Populus hybrid clones. The role of pectin domains in cell processes underlying shoot organogenesis induction. *Biologia Plantarum*, *62*(4), 763–774. https://doi.org/10.1007/s10535-018-0819-y

Garvey, K. J., Saedi, M. S., & Ito, J. (1986). Nucleotide sequence of Bacillus phage ø29 genes 14 and 15: Homology of gene 15 with other phage lysozymes. *Nucleic Acids Research*, *14*(24), 10001–10008. https://doi.org/10.1093/nar/14.24.10001

Geldner, N., Hyman, D. L., Wang, X., Schumacher, K., & Chory, J. (2007). Endosomal signaling of plant steroid receptor kinase BRI1. *Genes and Development*, *21*(13), 1598–1602. https://doi.org/10.1101/gad.1561307

Geurts, R., & Bisseling, T. (2002). Rhizobium nod factor perception and signalling. *Plant Cell*, *14*(SUPPL.), 239–249. https://doi.org/10.1105/tpc.002451.These

Gibson, D. G., Young, L., Chuang, R. Y., Venter, J. C., Hutchison, C. A., & Smith, H. O. (2009). Enzymatic assembly of DNA molecules up to several hundred kilobases. *Nature Methods*, *6*(5), 343–345. https://doi.org/10.1038/nmeth.1318

Gimenez-Ibanez, S., Hann, D. R., Ntoukakis, V., Petutschnig, E., Lipka, V., & Rathjen, J. P. (2009). AvrPtoB Targets the LysM Receptor Kinase CERK1 to Promote Bacterial Virulence on Plants. *Current Biology*, *19*(5), 423–429. https://doi.org/10.1016/j.cub.2009.01.054

Gong, B. Q., Xue, J., Zhang, N., Xu, L., Yao, X., Yang, Q. J., … Li, J. F. (2017). Rice Chitin

Receptor OsCEBiP Is Not a Transmembrane Protein but Targets the Plasma Membrane via a GPI Anchor. *Molecular Plant*, *10*(5), 767–770. https://doi.org/10.1016/j.molp.2016.12.005

Gow, N. A. R., Latge, J., Munro, C. A., De Groot, P. W. J., Hellingwerf, K. J., Klis, F. M., … Gil, C. (2003). Cell Wall Architecture in Yeast : New Structure and New Challenges MINIREVIEW Cell Wall Architecture in Yeast : New Structure and New Challenges †. *Yeast*, *9*(3), 3341–3354. https://doi.org/10.1128/microbiolspec.FUNK-0035-2016.Correspondence

Greco, M., Chiappetta, A., Bruno, L., & Bitonti, M. B. (2012). In Posidonia oceanica cadmium induces changes in DNA methylation and chromatin patterning. *Journal of Experimental Botany*, *63*(2), 695–709. https://doi.org/10.1093/jxb/err313

Grison, M. S., Brocard, L., Fouillen, L., Nicolas, W., Wewer, V., Dörmann, P., … Bayer, E. M. (2015). Specific membrane lipid composition is important for plasmodesmata function in arabidopsis. *Plant Cell*, *27*(4), 1228–1250. https://doi.org/10.1105/tpc.114.135731

Gronnier, J., Crowet, J. M., Habenstein, B., Nasir, M. N., Bayle, V., Hosy, E., … Mongrand, S. (2017). Structural basis for plant plasma membrane protein dynamics and organization into functional nanodomains. *ELife*, *6*, 1–24. https://doi.org/10.7554/eLife.26404

Gubaeva, E., Gubaev, A., Melcher, R. L. J., Cord-Landwehr, S., Singh, R., Gueddari, N. E. El, & Moerschbacher, B. M. (2018). Slipped sandwich' model for chitin and chitosan perception in arabidopsis. *Molecular Plant-Microbe Interactions*, *31*(11), 1145–1153. https://doi.org/10.1094/MPMI-04-18-0098-R

Guenoune-Gelbart, D., Elbaum, M., Sagi, G., Levy, A., & Epel, B. L. (2008). Tobacco mosaic virus (TMV) replicase and movement protein function synergistically in facilitating TMV spread by lateral diffusion in the plasmodesmal desmotubule of Nicotiana benthamiana. *Molecular Plant-Microbe Interactions*, *21*(3), 335–345. https://doi.org/10.1094/MPMI-21-3-0335

Guerra, F., Gainza, F., Perez, R., & Zamudio, F. (2011). Phytoremidiation of heavy metals using poplars (Populus spp): a glimpse of the plant responses to copper, cadmium and zinc stress. *Nova Science Publishers, Inc.*, *ISBN: 978-*, 387–413.

Guo, M., Li, C., Facciotto, G., Bergante, S., Bhatia, R., Comolli, R., … Murphy, R. (2015). Bioethanol from poplar clone Imola: an environmentally viable alternative to fossil fuel? *Biotechnology for Biofuels*, *8*(1), 1–21. https://doi.org/10.1186/s13068-015-0318-8

Guseman, J. M., Lee, J. S., Bogenschutz, N. L., Peterson, K. M., Virata, R. E., Xie, B., … Torii, K. U. (2010). Dysregulation of cell-to-cell connectivity and stomatal patterning by loss-of-function mutation in Arabidopsis chorus (GLUCAN SYNTHASE-LIKE 8). *Development*, *137*(10), 1731–1741. https://doi.org/10.1242/dev.049197

Hacquard, S., Petre, B., Frey, P., Hecker, A., Rouhier, N., & Duplessis, S. (2011). The Poplar-Poplar Rust Interaction: Insights from Genomics and Transcriptomics. *Journal of Pathogens*, *2011*, 1–11. https://doi.org/10.4061/2011/716041

Hamel, L. P., Miles, G. P., Samuel, M. A., Ellis, B. E., Séguin, A., & Beaudoin, N. (2005). Activation of stress-responsive mitogen-activated protein kinase pathways in hybrid

poplar (Populus trichocarpa x Populus deltoides). *Tree Physiology*, *25*(3), 277–288. https://doi.org/10.1093/treephys/25.3.277

Han, Xiao, Huang, L. J., Feng, D., Jiang, W., Miu, W., & Li, N. (2019). Plasmodesmata-Related Structural and Functional Proteins: The Long Sought-After Secrets of a Cytoplasmic Channel in Plant Cell Walls. *International Journal of Molecular Sciences*, *20*(12). https://doi.org/10.3390/ijms20122946

Han, Xiao, Hyun, T. K., Zhang, M., Kumar, R., Koh, E. ji, Kang, B. H., … Kim, J. Y. (2014). Auxin-Callose-Mediated Plasmodesmal Gating Is Essential for Tropic Auxin Gradient Formation and Signaling. *Developmental Cell*, *28*(2), 132–146. https://doi.org/10.1016/j.devcel.2013.12.008

Han, Xue, Ma, S., Kong, X., Takano, T., & Liu, S. (2013). Efficient Agrobacterium-mediated transformation of hybrid poplar Populus davidiana Dode × Populus bollena lauche. *International Journal of Molecular Sciences*, *14*(2), 2515–2528. https://doi.org/10.3390/ijms14022515

Hanks, S. K., & Hunter, T. (1995). The eukaryotic protein kinase superfamily: Kinase (catalytic) domain structure and classification. *FASEB Journal*, *9*(8), 576–596.

Harrison, X. A., Donaldson, L., Correa-Cano, M. E., Evans, J., Fisher, D. N., Goodwin, C. E. D., … Inger, R. (2018). A brief introduction to mixed effects modelling and multi-model inference in ecology. *PeerJ*, *2018*(5), 1–32. https://doi.org/10.7717/peerj.4794

Hayafune, M., Berisio, R., Marchetti, R., Silipo, A., Kayama, M., Desaki, Y., … Shibuya, N. (2014). Chitin-induced activation of immune signaling by the rice receptor CEBiP relies on a unique sandwich-type dimerization. *Proceedings of the National Academy of Sciences of the United States of America*, *111*(3). https://doi.org/10.1073/pnas.1312099111

Hellens, R. P., Edwards, E. A., Leyland, N. R., Bean, S., & Mullineaux, P. M. (2000). Biotechnology resources for arable crop transformation (bract)\npGreen: a versatile and flexible binary Ti vector for Agrobacterium-mediated plant transformation. *Plant Mol Biol*, *42*, 819–832. Retrieved from http://www.bract.org

Hothorn, T., Bretz, F., & Westfall, P. (2008). Simultaneous inference in general parametric models. *Biometrical Journal*, *50*(3), 346–363. https://doi.org/10.1002/bimj.200810425

Hou, J., Wei, S., Pan, H., Zhuge, Q., & Yin, T. (2019). Uneven selection pressure accelerating divergence of Populus and Salix. *Horticulture Research*, *6*(1). https://doi.org/10.1038/s41438-019-0121-y

Hurles, M. (2004). Gene duplication: The genomic trade in spare parts. *PLoS Biology*, *2*(7). https://doi.org/10.1371/journal.pbio.0020206

Iizasa, E., Mitsutomi, M., & Nagano, Y. (2010). Direct binding of a plant LysM receptor-like kinase, LysM RLK1/CERK1, to chitin in vitro. *Journal of Biological Chemistry*, *285*(5), 2996–3004. https://doi.org/10.1074/jbc.M109.027540

Iswanto, A. B. B., & Kim, J. Y. (2017). Lipid raft, regulator of plasmodesmal callose homeostasis. *Plants*, *6*(2), 257s-278s. https://doi.org/10.3390/plants6020015

Jansson, C., Wullschleger, S. D., Kalluri, U. C., & Tuskan, G. A. (2010). Phytosequestration: Carbon Biosequestration by Plants and the Prospects of Genetic Engineering. *BioScience*, *60*(9), 685–696. https://doi.org/10.1525/bio.2010.60.9.6

Jansson, S., & Douglas, C. J. (2007). Populus : A Model System for Plant Biology . *Annual Review of Plant Biology*, *58*(1), 435–458. https://doi.org/10.1146/annurev.arplant.58.032806.103956

Kadota, Y., Sklenar, J., Derbyshire, P., Stransfeld, L., Asai, S., Ntoukakis, V., … Zipfel, C. (2014). Direct Regulation of the NADPH Oxidase RBOHD by the PRR-Associated Kinase BIK1 during Plant Immunity. *Molecular Cell*, *54*(1), 43–55. https://doi.org/10.1016/j.molcel.2014.02.021

Kaku, H., Nishizawa, Y., Ishii-Minami, N., Akimoto-Tomiyama, C., Dohmae, N., Takio, K., Minami, E., Shibuya, N. (2006). Plant cells recognize chitin fragments for defense signaling through a plasma membrane receptor. *Proceedings of the National Academy of Sciences of the United States of America*, *103*(29), 11086–11091. https://doi.org/10.1073/pnas.79.20.6304

Kohler, A., Rinaldi, C., Duplessis, S., Baucher, M., Geelen, D., Duchaussoy, F., … Martin, F. (2008). Genome-wide identification of NBS resistance genes in Populus trichocarpa. *Plant Molecular Biology*, *66*(6), 619–636. https://doi.org/10.1007/s11103-008-9293-9

Koornneef, M., Alonso-Blanco, C., Peeters, A., & Soppe, W. (1998). Genetic control of flowering time in Arabidopsis. *Annu. Rev. Plant Physiol. Plant Mol. Biol.*, *49*, 345–370. https://doi.org/10.3389/fpls.2015.00207

Kouzai, Y., Mochizuki, S., Nakajima, K., Desaki, Y., Hayafune, M., Miyazaki, H., … Nishizawa, Y. (2014). Targeted gene disruption of OsCERK1 reveals its indispensable role in chitin perception and involvement in the peptidoglycan response and immunity in rice. *Molecular Plant-Microbe Interactions*, *27*(9), 975–982. https://doi.org/10.1094/MPMI-03-14-0068-R

Krogh, A., Larsson, B., Von Heijne, G., & Sonnhammer, E. L. L. (2001). Predicting transmembrane protein topology with a hidden Markov model: Application to complete genomes. *Journal of Molecular Biology*, *305*(3), 567–580. https://doi.org/10.1006/jmbi.2000.4315

Lee, J. Y., Wang, X., Cui, W., Sager, R., Modla, S., Czymmek, K., … Lakshmanana, V. (2011). A plasmodesmata-localized protein mediates crosstalk between cell-to-cell communication and innate immunity in arabidopsis. *Plant Cell*, *23*(9), 3353–3373. https://doi.org/10.1105/tpc.111.087742

Levy, A., Erlanger, M., Rosenthal, M., & Epel, B. L. (2007). A plasmodesmata-associated β-1,3-glucanase in Arabidopsis. *Plant Journal*, *49*(4), 669–682. https://doi.org/10.1111/j.1365-313X.2006.02986.x

Li, Q, Yeh, T., Yang, C., Song, J., Chen, Z., Sederoff, R., & Chiang, V. (2015). Populus trichocarpa. *Methods in Molecular Biology*, *1224*, 357–363. https://doi.org/10.1007/978-1-4939-1658-0

Li, Quanzi, Lin, Y. C., Sun, Y. H., Song, J., Chen, H., Zhang, X. H., … Chiang, V. L. (2012). Splice variant of the SND1 transcription factor is a dominant negative of SND1 members and their regulation in Populus trichocarpa. *Proceedings of the National Academy of Sciences of the United States of America*, *109*(36), 14699–14704. https://doi.org/10.1073/pnas.1212977109

Li, S., Zhen, C., Xu, W., Wang, C., & Cheng, Y. (2017). Simple, rapid and efficient transformation of genotype Nisqually-1: A basic tool for the first sequenced model tree.

Scientific Reports, *7*(1), 1–10. https://doi.org/10.1038/s41598-017-02651-x

Liang, Y., Cao, Y., Tanaka, K., Thibivilliers, S., Wan, J., Choi, J., … Stacey, G. (2013). Nonlegumes respond to rhizobial nod factors by suppressing the innate immune response. *Science*, *341*(6152), 1384–1387. https://doi.org/10.1126/science.1242736

Liesche, J., Gao, C., Binczycki, P., Andersen, S. R., Rademaker, H., Schulz, A., & Martens, H. J. (2019). Direct comparison of leaf plasmodesma structure and function in relation to phloem-loading type. *Plant Physiology*, *179*(4), 1768–1778. https://doi.org/10.1104/pp.18.01353

Lim, G. H., Shine, M. B., De Lorenzo, L., Yu, K., Cui, W., Navarre, D., … Kachroo, P. (2016). Plasmodesmata Localizing Proteins Regulate Transport and Signaling during Systemic Acquired Immunity in Plants. *Cell Host and Microbe*, *19*(4), 541–549. https://doi.org/10.1016/j.chom.2016.03.006

Limpens, E., Franken, C., Smit, P., Willemse, J., Bisseling, T., & Geurts, R. (2003). LysM Domain Receptor Kinases Regulating Rhizobial Nod Factor-Induced Infection. *Science*, *302*(5645), 630–633. https://doi.org/10.1126/science.1090074

Littlewood, J., Guo, M., Boerjan, W., & Murphy, R. J. (2014). Bioethanol from poplar: A commercially viable alternative to fossil fuel in the European Union. *Biotechnology for Biofuels*, *7*(1), 1–12. https://doi.org/10.1186/1754-6834-7-113

Liu, B., Li, J. F., Ao, Y., Qu, J., Li, Z., Su, J., … Wang, H. Bin. (2012). Lysin motif-containing proteins LYP4 and LYP6 play dual roles in peptidoglycan and chitin perception in rice innate immunity. *Plant Cell*, *24*(8), 3406–3419. https://doi.org/10.1105/tpc.112.102475

Liu, S., Wang, J., Han, Z., Gong, X., Zhang, H., & Chai, J. (2016). Molecular Mechanism for Fungal Cell Wall Recognition by Rice Chitin Receptor OsCEBiP. *Structure*, *24*(7), 1192–1200. https://doi.org/10.1016/j.str.2016.04.014

Liu, T., Liu, Z., Song, C., Hu, Y., Han, Z., She, J., … Chai, J. (2012). Chitin-induced dimerization activates a plant immune receptor. *Science*, *336*(6085), 1160–1164. https://doi.org/10.1126/science.1218867

Lu, D., Lin, W., Gao, X., Wu, S., Cheng, C., Avila, J., … Shan, L. (2011). Direct ubiquitination of pattern recognition receptor FLS2 attenuates plant innate immunity. *Science*, *332*(June), 1439–1442. https://doi.org/10.1126/science.1204903

Ma, X., Zhang, Q., Zhu, Q., Liu, W., Chen, Y., Qiu, R., … Liu, Y. G. (2015). A Robust CRISPR/Cas9 System for Convenient, High-Efficiency Multiplex Genome Editing in Monocot and Dicot Plants. *Molecular Plant*, *8*(8), 1274–1284. https://doi.org/10.1016/j.molp.2015.04.007

Ma, X., Zhu, Q., Chen, Y., & Liu, Y. G. (2016). CRISPR/Cas9 Platforms for Genome Editing in Plants: Developments and Applications. *Molecular Plant*, *9*(7), 961–974. https://doi.org/10.1016/j.molp.2016.04.009

Mach, J. (2014). When to hold them: Retention of duplicate genes in poplar. *Plant Cell*, *26*(6), 2283. https://doi.org/10.1105/tpc.114.128827

Macho, A. P., & Zipfel, C. (2014). Plant PRRs and the activation of innate immune signaling. *Molecular Cell*, *54*(2), 263–272. https://doi.org/10.1016/j.molcel.2014.03.028

Madsen, E. B., Madsen, L. H., Radutoiu, S., Olbryt, M., Rakwalska, M., Szczyglowski, K., … Stougaard, J. (2003). A receptor kinase gene of the LysM type is involved in legume perception of rhizobial signals. *Nature*, *425*, 637–640.

Magadum, S., Banerjee, U., Murugan, P., Gangapur, D., & Ravikesavan, R. (2013). Gene duplication as a major force in evolution. *Journal of Genetics*, *92*(1), 155–161. https://doi.org/10.1007/s12041-013-0212-8

Maillet, F., Poinsot, V., André, O., Puech-Pagés, V., Haouy, A., Gueunier, M., … Dénarié, J. (2011). Fungal lipochitooligosaccharide symbiotic signals in arbuscular mycorrhiza. *Nature*, *469*(7328), 58–64. https://doi.org/10.1038/nature09622

Malinsky, J., Opekarová, M., Grossmann, G., & Tanner, W. (2013). Membrane Microdomains, Rafts, and Detergent-Resistant Membranes in Plants and Fungi. *Annual Review of Plant Biology*, *64*(1), 501–529. https://doi.org/10.1146/annurev-arplant-050312-120103

Manevski, K., Jakobsen, M., Kongsted, A. G., Georgiadis, P., Labouriau, R., Hermansen, J. E., & Jørgensen, U. (2019). Effect of poplar trees on nitrogen and water balance in outdoor pig production – A case study in Denmark. *Science of the Total Environment*, *646*, 1448–1458. https://doi.org/10.1016/j.scitotenv.2018.07.376

Martins, S., Dohmann, E. M. N., Cayrel, A., Johnson, A., Fischer, W., Pojer, F., … Vert, G. (2015). Internalization and vacuolar targeting of the brassinosteroid hormone receptor BRI1 are regulated by ubiquitination. *Nature Communications*, *6*. https://doi.org/10.1038/ncomms7151

Mbengue, M., Bourdais, G., Gervasi, F., Beck, M., Zhou, J., Spallek, T., … Robatzek, S. (2016). Clathrin-dependent endocytosis is required for immunity mediated by pattern recognition receptor kinases. *Proceedings of the National Academy of Sciences of the United States of America*, *113*(39), 11034–11039. https://doi.org/10.1073/pnas.1606004113

Mélida, H., Sopeña-Torres, S., Bacete, L., Garrido-Arandia, M., Jordá, L., López, G., … Molina, A. (2018). Non-branched β-1,3-glucan oligosaccharides trigger immune responses in Arabidopsis. *Plant Journal*, *93*(1), 34–49. https://doi.org/10.1111/tpj.13755

Miya, A., Albert, P., Shinya, T., Desaki, Y., Ichimura, K., Shirasu, K., … Shibuya, N. (2007). CERK1, a LysM receptor kinase, is essential for chitin elicitor signaling in Arabidopsis. *Proceedings of the National Academy of Sciences of the United States of America*, *104*(49), 19613–19618. https://doi.org/10.1073/pnas.0705147104

Miyata, K., Hayafune, M., Kobae, Y., Kaku, H., Nishizawa, Y., Masuda, Y., … Nakagawa, T. (2016). Evaluation of the role of the LysM receptor-like kinase, OsNFR5/OsRLK2 for AM symbiosis in rice. *Plant and Cell Physiology*, *57*(11), 2283–2290. https://doi.org/10.1093/pcp/pcw144

Miyata, K., Kozaki, T., Kouzai, Y., Ozawa, K., Ishii, K., Asamizu, E., … Nakagawa, T. (2014). The bifunctional plant receptor, OsCERK1, regulates both chitin-triggered immunity and arbuscular mycorrhizal symbiosis in rice. *Plant and Cell Physiology*, *55*(11), 1864–1872. https://doi.org/10.1093/pcp/pcu129

Mongrand, S., Stanislas, T., Bayer, E. M. F., Lherminier, J., & Simon-Plas, F. (2010). Membrane rafts in plant cells. *Trends in Plant Science*, *15*(12), 656–663.

https://doi.org/10.1016/j.tplants.2010.09.003

Movahedi, A., Zhang, J., Amirian, R., & Zhuge, Q. (2014). An efficient agrobacterium-mediated transformation system for poplar. *International Journal of Molecular Sciences*, *15*(6), 10780–10793. https://doi.org/10.3390/ijms150610780

Mulder, L., Lefebvre, B., Cullimore, J., & Imberty, A. (2006). LysM domains of Medicago truncatula NFP protein involved in Nod factor perception. Glycosylation state, molecular modeling and docking of chitooligosaccharides and Nod factors. *Glycobiology*, *16*(9), 801–809. https://doi.org/10.1093/glycob/cwl006

Ner-Gaon, H., Leviatan, N., Rubin, E., & Fluhr, R. (2007). Comparative cross-species alternative splicing in plants. *Plant Physiology*, *144*(3), 1632–1641. https://doi.org/10.1104/pp.107.098640

New England Biolabs. (2014). NEBuilder HiFi DNA Assembly Master Mix. *Instruction Manual*, *1*(10), 1–23. Retrieved from https://www.neb.com/products/e5520-nebuilder-hifi-dna-assembly-cloning-kit?device=pdf

Nishiyama, R., Mizuno, H., Okada, S., Yamaguchi, T., Takenaka, M., Fukuzawa, H., & Ohyama, K. (1999). Two mRNA species encoding calcium-dependent protein kinases are differentially expressed in sexual organs of Marchantia polymorpha through alternative splicing. *Plant and Cell Physiology*, *40*(2), 205–212. https://doi.org/10.1093/oxfordjournals.pcp.a029529

Onaga, S., & Taira, T. (2008). A new type of plant chitinase containing LysM domains from a fern (Pteris ryukyuensis): Roles of LysM domains in chitin binding and antifungal activity. *Glycobiology*, *18*(5), 414–423. https://doi.org/10.1093/glycob/cwn018

Oparka, K. J., Roberts, A. G., Boevink, P., Cruz, S. S., Roberts, I., Pradel, K. S., … Epel, B. (1999). Simple, but not branched, plasmodesmata allow the nonspecific trafficking of proteins in developing tobacco leaves. *Cell*, *97*(6), 743–754. https://doi.org/10.1016/S0092-8674(00)80786-2

Otegui, M. S., & Spitzer, C. (2008). Endosomal functions in plants. *Traffic*, *9*(10), 1589–1598. https://doi.org/10.1111/j.1600-0854.2008.00787.x

Overall, R. L., & Blackman, L. M. (1996). A model of the macromolecular structure of plasmodesmata. *Trends in Plant Science*, *1*(9), 307–311. https://doi.org/10.1016/1360-1385(96)88177-5

Paez Valencia, J., Goodman, K., & Otegui, M. S. (2016). Endocytosis and Endosomal Trafficking in Plants. *Annual Review of Plant Biology*, *67*(1), 309–335. https://doi.org/10.1146/annurev-arplant-043015-112242

Pereira, S., Costa, M., Carvalho, M., & Rodrigues, A. (2016). Potential of poplar short rotation coppice cultivation for bioenergy in Southern Portugal. *Energy Conversion and Management*, *125*. https://doi.org/10.1016/j.enconman.2016.03.068

Petersen, T. N., Brunak, S., Von Heijne, G., & Nielsen, H. (2011). SignalP 4.0: Discriminating signal peptides from transmembrane regions. *Nature Methods*, *8*(10), 785–786. https://doi.org/10.1038/nmeth.1701

Petre, B., Lorrain, C., Saunders, D. G. O., Win, J., Sklenar, J., Duplessis, S., & Kamoun, S. (2016). Rust fungal effectors mimic host transit peptides to translocate into chloroplasts. *Cellular Microbiology*, *18*(4), 453–465.

https://doi.org/10.1111/cmi.12530

Petre, B., Saunders, D. G. O., Sklenar, J., Lorrain, C., Win, J., Duplessis, S., & Kamoun, S. (2015). Candidate effector proteins of the rust pathogen Melampsora larici-populina target diverse plant cell compartments. *Molecular Plant-Microbe Interactions*, *28*(6), 689–700. https://doi.org/10.1094/MPMI-01-15-0003-R

Petutschnig, E. K., Jones, A. M. E., Serazetdinova, L., Lipka, U., & Lipka, V. (2010). The Lysin Motif Receptor-like Kinase (LysM-RLK) CERK1 is a major chitin-binding protein in Arabidopsis thaliana and subject to chitin-induced phosphorylation. *Journal of Biological Chemistry*, *285*(37), 28902–28911. https://doi.org/10.1074/jbc.M110.116657

Petutschnig, E. K., Stolze, M., Lipka, U., Kopischke, M., Horlacher, J., Valerius, O., … Lipka, V. (2014). A novel Arabidopsis CHITIN ELICITOR RECEPTOR KINASE 1 (CERK1) mutant with enhanced pathogen-induced cell death and altered receptor processing. *New Phytologist*, *204*(4), 955–967. https://doi.org/10.1111/nph.12920

Pierleoni, A., Martelli, P., & Casadio, R. (2008). PredGPI: A GPI-anchor predictor. *BMC Bioinformatics*, *9*, 1–11. https://doi.org/10.1186/1471-2105-9-392

Porth, I., Klápště, J., McKown, A. D., La Mantia, J., Hamelin, R. C., Skyba, O., … Douglas, C. J. (2014). Extensive functional pleiotropy of REVOLUTA substantiated through forward genetics. *Plant Physiology*, *164*(2), 548–554. https://doi.org/10.1104/pp.113.228783

Quevillon, E., Silventoinen, V., Pillai, S., Harte, N., Mulder, N., Apweiler, R., & Lopez, R. (2005). InterProScan: Protein domains identifier. *Nucleic Acids Research*, *33*(SUPPL. 2), 116–120. https://doi.org/10.1093/nar/gki442

Radutoiu, S., Madsen, L. H., Madsen, E. B., Felle, H. H., Umehara, Y., Grønlund, M., … Stougaard, J. (2003). Plant recognition of symbiotic bacteria requires two LysM receptor-like kinases. *Nature*, *425*(6958), 585–592. https://doi.org/10.1038/nature02039

Radutoiu, S., Madsen, L. H., Madsen, E. B., Jurkiewicz, A., Fukai, E., Quistgaard, E. M. H., … Stougaard, J. (2007). LysM domains mediate lipochitin-oligosaccharide recognition and Nfr genes extend the symbiotic host range. *EMBO Journal*, *26*(17), 3923–3935. https://doi.org/10.1038/sj.emboj.7601826

Raffaele, S., Bayer, E., Lafarge, D., Cluzet, S., Retana, S. G., Boubekeur, T., … Mongrand, S. (2009). Remorin, a solanaceae protein resident in membrane rafts and plasmodesmata, impairs potato virus X movement. *Plant Cell*, *21*(5), 1541–1555. https://doi.org/10.1105/tpc.108.064279

Ren, L. L., Liu, Y. J., Liu, H. J., Qian, T. T., Qi, L. W., Wang, X. R., & Zeng, Q. Y. (2014). Subcellular relocalization and positive selection play key roles in the retention of duplicate genes of Populus class III peroxidase family. *Plant Cell*, *26*(6), 2404–2419. https://doi.org/10.1105/tpc.114.124750

Rey, T., Nars, A., Bonhomme, M., Bottin, A., Huguet, S., Balzergue, S., … Jacquet, C. (2013). NFP, a LysM protein controlling Nod factor perception, also intervenes in Medicago truncatula resistance to pathogens. *New Phytologist*, *198*(3), 875–886. https://doi.org/10.1111/nph.12198

Rinne, P. L. H., Kaikuranta, P. M., & Van Schoot, C. Der. (2001). The shoot apical meristem restores its symplasmic organization during chilling-induced release from dormancy. *Plant Journal*, *26*(3), 249–264. https://doi.org/10.1046/j.1365-313X.2001.01022.x

Robatzek, S., Chinchilla, D., & Boller, T. (2006). Ligan-induced endocytosis of the pattern recognition receptor FLS2 in Arabidopsis. *Reserach Communication: Genes & Development*, *20*, 537–542. https://doi.org/10.1101/gad.366506.nized

Roberts, A. G., & Oparka, K. J. (2003). Plasmodesmata and the control of symplastic transport. *Plant, Cell and Environment*, *26*(1), 103–124. https://doi.org/10.1046/j.1365-3040.2003.00950.x

Sablok, G., Powell, B., Braessler, J., Yu, F., & Min, X. J. (2017). Comparative landscape of alternative splicing in fruit plants. *Current Plant Biology*, *9–10*, 29–36. https://doi.org/10.1016/j.cpb.2017.06.001

Sager, R. E., & Lee, J. Y. (2018). Plasmodesmata at a glance. *Journal of Cell Science*, *131*(11), 1–7. https://doi.org/10.1242/jcs209346

Sager, R., & Lee, J. Y. (2014). Plasmodesmata in integrated cell signalling: Insights from development and environmental signals and stresses. *Journal of Experimental Botany*, *65*(22), 6337–6358. https://doi.org/10.1093/jxb/eru365

Sannigrahi, P., Ragauskas, A., & Tuskan, G. (2009). Poplar as a feedstock for biofuels: a review of compositional characteristics. *Biofuels, Bioproducts and Biorefining*, *4*, 209–226. https://doi.org/10.1002/bbb

Schleifer, K. H., & Kandler, O. (1972). Peptidoglycan types of bacterial cell walls and their taxonomic implications. *Bacteriological Reviews*, *36*(4), 407–477.

Sevilem, I., Miyashima, S., & Helariutta, Y. (2013). Cell-to-cell communication via plasmodesmata in vascular plants. *Cell Adhesion and Migration*, *7*(1), 27–32. https://doi.org/10.4161/cam.22126

Shi, X., Sun, X., Zhang, Z., Feng, D., Zhang, Q., Han, L., … Lu, T. (2014). GLUCAN SYNTHASE-LIKE 5 (GSL5) plays an essential role in male fertility by regulating callose metabolism during microsporogenesis in rice. *Plant and Cell Physiology*, *56*(3), 497–509. https://doi.org/10.1093/pcp/pcu193

Shibuya, N., & Minami, E. (2001). Oligosaccharide signalling for defence responses in plant. *Physiological and Molecular Plant Pathology*, *59*(5), 223–233. https://doi.org/10.1006/pmpp.2001.0364

Shimizu, T., Nakano, T., Takamizawa, D., Desaki, Y., Ishii-Minami, N., Nishizawa, Y., … Shibuya, N. (2010). Two LysM receptor molecules, CEBiP and OsCERK1, cooperatively regulate chitin elicitor signaling in rice. *Plant Journal*, *64*(2), 204–214. https://doi.org/10.1111/j.1365-313X.2010.04324.x

Shinya, T., Motoyama, N., Ikeda, A., Wada, M., Kamiya, K., Hayafune, M., … Shibuya, N. (2012). Functional characterization of CEBiP and CERK1 homologs in arabidopsis and rice reveals the presence of different chitin receptor systems in plants. *Plant and Cell Physiology*, *53*(10), 1696–1706. https://doi.org/10.1093/pcp/pcs113

Simpson, C., Thomas, C., Findlay, K., Bayer, E., & Maule, A. J. (2009). An arabidopsis GPI-anchor plasmodesmal neck protein with callose binding activity and potential to regulate cell-to-cell trafficking. *Plant Cell*, *21*(2), 581–594.

https://doi.org/10.1105/tpc.108.060145

Singh, D., & Chen, S. (2008). The white-rot fungus Phanerochaete chrysosporium: Conditions for the production of lignin-degrading enzymes. *Applied Microbiology and Biotechnology*, *81*(3), 399–417. https://doi.org/10.1007/s00253-008-1706-9

Sivaguru, M., Fujiwara, T., Samaj, J., Baluska, F., Yang, Z., Osawa, H., … Matsumoto, H. (2000). Aluminum-induced 1→3-β-D-glucan inhibits cell-to-cell trafficking of molecules through plasmodesmata. A new mechanism of aluminum toxicity in plants. *Plant Physiology*, *124*(3), 991–1005.

Smit, P., Limpens, E., Geurts, R., Fedorova, E., Dolgikh, E., Gough, C., & Bisseling, T. (2007). Medicago LYK3, an entry receptor in rhizobial nodulation factor signaling. *Plant Physiology*, *145*(1), 183–191. https://doi.org/10.1104/pp.107.100495

Song, J., Lu, S., Chen, Z. Z., Lourenco, R., & Chiang, V. L. (2006). Genetic transformation of Populus trichocarpa genotype Nisqually-1: A functional genomic tool for woody plants. *Plant and Cell Physiology*, *47*(11), 1582–1589. https://doi.org/10.1093/pcp/pcl018

Song, W.-Y., Choi, Y.-I., Shim, D., Kim, D.-Y., Noh, E.-W., Martinoia, E., & Lee, Y. (2007). Transgenic Poplar for Phytoremediation. *Biotechnology and Sustainable Agriculture 2006 and Beyond*, 265–271. https://doi.org/10.1007/978-1-4020-6635-1_40

Sun, Y., Huang, D., & Chen, X. (2019). Dynamic regulation of plasmodesmatal permeability and its application to horticultural research. *Horticulture Research*, *6*(1). https://doi.org/10.1038/s41438-019-0129-3

Takata, N., & Eriksson, M. E. (2014). *A simple and efficient transient transformation for hybrid aspen (Populus tremula × P . A simple and efficient transient transformation for hybrid aspen (Populus tremula × P . tremuloides).* (August 2012), 1–10. https://doi.org/10.1186/1746-4811-8-30

Tallis, M. J., Casella, E., Henshall, P. A., Aylott, M. J., Randle, T. J., Morison, J. I. L., & Taylor, G. (2013). Development and evaluation of ForestGrowth-SRC a process-based model for short rotation coppice yield and spatial supply reveals poplar uses water more efficiently than willow. *GCB Bioenergy*, *5*(1), 53–66. https://doi.org/10.1111/j.1757-1707.2012.01191.x

Thomas, C. L., Bayer, E. M., Ritzenthaler, C., Fernandez-Calvino, L., & Maule, A. J. (2008). Specific targeting of a plasmodesmal protein affecting cell-to-cell communication. *PLoS Biology*, *6*(1), 0180–0190. https://doi.org/10.1371/journal.pbio.0060007

Tilsner, J., Nicolas, W., Rosado, A., & Bayer, E. M. (2016). Staying Tight: Plasmodesmal Membrane Contact Sites and the Control of Cell-to-Cell Connectivity in Plants. *Annual Review of Plant Biology*, *67*(1), 337–364. https://doi.org/10.1146/annurev-arplant-043015-111840

Tuskan, G., DiFazio, S., Jansson, S., & Al., E. (2006). The Genome of Black Cottonwood Populus trichocarpa (Torr. & Gray). *Science*, *313*(September), 1596–1604.

Vanneste, K., Maere, S., & Van de Peer, Y. (2014). Tangled up in two: A burst of genome duplications at the end of the Cretaceous and the consequences for plant evolution. *Philosophical Transactions of the Royal Society B: Biological Sciences*, *369*(1648).

https://doi.org/10.1098/rstb.2013.0353

Vatén, A., Dettmer, J., Wu, S., Stierhof, Y. D., Miyashima, S., Yadav, S. R., … Helariutta, Y. (2011). Callose Biosynthesis Regulates Symplastic Trafficking during Root Development. *Developmental Cell*, *21*(6), 1144–1155. https://doi.org/10.1016/j.devcel.2011.10.006

Verma, Deshpal S & Hong, Z. (2001). Plant Callose Synthase Complexes. *Plant Molecular Biology*, *47*, 693–701. https://doi.org/10.1023/A

Vogler, H., Kwon, M. O., Dang, V., Sambade, A., Fasler, M., Ashby, J., & Heinlein, M. (2008). Tobacco mosaic virus movement protein enhances the spread of RNA silencing. *PLoS Pathogens*, *4*(4). https://doi.org/10.1371/journal.ppat.1000038

Wan, J., Tanaka, K., Zhang, X. C., Son, G. H., Brechenmacher, L., Nguyen, T. H. N., & Stacey, G. (2012). LYK4, a lysin motif receptor-like kinase, is important for chitin signaling and plant innate immunity in Arabidopsis. *Plant Physiology*, *160*(1), 396–406. https://doi.org/10.1104/pp.112.201699

Wan, J., Zhang, X. C., Neece, D., Ramonell, K. M., Clough, S., Kim, S. Y., … Stacey, G. (2008). A LysM receptor-like kinase plays a critical role in chitin signaling and fungal resistance in Arabidopsis. *Plant Cell*, *20*(2), 471–481. https://doi.org/10.1105/tpc.107.056754

Wang, S., Hastings, A., Wang, S., Sunnenberg, G., Tallis, M. J., Casella, E., … Smith, P. (2014). The potential for bioenergy crops to contribute to meeting GB heat and electricity demands. *GCB Bioenergy*, *6*(2), 136–141. https://doi.org/10.1111/gcbb.12123

White, R. G., Badelt, K., Overall, R. L., & Vesk, M. (1994). Actin associated with plasmodesmata. *Protoplasma*, *180*(3–4), 169–184. https://doi.org/10.1007/BF01507853

Willmann, R., Lajunen, H. M., Erbs, G., Newman, M. A., Kolb, D., Tsuda, K., … Nürnberger, T. (2011). Arabidopsis lysin-motif proteins LYM1 LYM3 CERK1 mediate bacterial peptidoglycan sensing and immunity to bacterial infection. *Proceedings of the National Academy of Sciences of the United States of America*, *108*(49), 19824–19829. https://doi.org/10.1073/pnas.1112862108

Wu, S. W., Kumar, R., Iswanto, A. B. B., & Kim, J. Y. (2018). Callose balancing at plasmodesmata. *Journal of Experimental Botany*, *69*(22), 5325–5339. https://doi.org/10.1093/jxb/ery317

Xie, B., Wang, X., Zhu, M., Zhang, Z., & Hong, Z. (2011). CalS7 encodes a callose synthase responsible for callose deposition in the phloem. *Plant Journal*, *65*(1), 1–14. https://doi.org/10.1111/j.1365-313X.2010.04399.x

Xu, B., Cheval, C., Laohavisit, A., Hocking, B., Chiasson, D., Olsson, T. S. G., … Gilliham, M. (2017). A calmodulin-like protein regulates plasmodesmal closure during bacterial immune responses. *New Phytologist*, *215*(1), 77–84. https://doi.org/10.1111/nph.14599

Yan, L., Ma, Y., Liu, D., Wei, X., Sun, Y., Chen, X., … Lou, Z. (2012). Structural basis for the impact of phosphorylation on the activation of plant receptor-like kinase BAK1. *Cell Research*, *22*(8), 1304–1308. https://doi.org/10.1038/cr.2012.74

Yuan, C, Lazarowitz, S., & Citovsky, V. (2018). crossm The Plasmodesmal Localization

Signal of TMV MP Is. *MBIO*, *9*(4), 1–8. https://doi.org/10.1128/mBio.01314-18

Yuan, Cheng, & Lazarowitz, S. G. (2016). Identification of a Functional Plasmodesmal Localization Signal in a. *Mbio*, *7*(1), 1–10. https://doi.org/10.1128/mBio.02052-15.Editor

Zambryski, P., & Crawford, K. (2000). Plasmodesmata: Gatekeepers for Cell-to-Cell Transport of Developmental Signals in Plants. *Annual Review of Cell and Developmental Biology*, *16*(1), 393–421. https://doi.org/10.1146/annurev.cellbio.16.1.393

Zavaliev, R., Dong, X., & Epel, B. L. (2016). Glycosylphosphatidylinositol (GPI) modification serves as a primary plasmodesmal sorting signal. *Plant Physiology*, *172*(2), 1061–1073. https://doi.org/10.1104/pp.16.01026

Zavaliev, R., Ueki, S., Epel, B. L., & Citovsky, V. (2011). Biology of callose (β-1,3-glucan) turnover at plasmodesmata. *Protoplasma*, *248*(1), 117–130. https://doi.org/10.1007/s00709-010-0247-0

Zhang, C., Yang, H., & Yang, H. (2015). Evolutionary Character of Alternative Splicing in Plants. *Bioinformatics and Biology Insights*, *9s1*, 47–52. https://doi.org/10.4137/BBI.S33716

Zhang, X. C., Wu, X., Findley, S., Wan, J., Libault, M., Nguyen, H. T., … Stacey, G. (2007). Molecular evolution of lysin motif-type receptor-like kinases in plants. *Plant Physiology*, *144*(2), 623–636. https://doi.org/10.1104/pp.107.097097

Zhang, X., Dong, W., Sun, J., Feng, F., Deng, Y., He, Z., … Wang, E. (2015). The receptor kinase CERK1 has dual functions in symbiosis and immunity signalling. *Plant Journal*, *81*(2), 258–267. https://doi.org/10.1111/tpj.12723

Zhou, J., Liu, D., Wang, P., Ma, X., Lin, W., Chen, S., … Shan, L. (2018). Regulation of Arabidopsis brassinosteroid receptor BRI1 endocytosis and degradation by plant U-box PUB12/PUB13-mediated ubiquitination. *Proceedings of the National Academy of Sciences of the United States of America*, *115*(8), E1906–E1915. https://doi.org/10.1073/pnas.1712251115

Acknowledgement

I do not like the idea to put acknowledgment at the last page, because I want the readers to know that this doctoral dissertation does not only belong to me, but also belongs to these kind-hearted people, “I dedicate this doctorate to you”.

I won’t be able to accomplish this doctoral studies without receiving so much support from others. I know that my words will never be enough to deliver my gratitude, and I can’t really do anything to pay them back on everything they have ever done for me, but I promise that I will pay it forward...to people whom I’ll meet in my future life, “They will also feel your kindness”.

PD. Dr. Thomas Teichmann. Thank you so much for giving me a chance to be involved in this project. To finally come to this point, I still can’t believe it. I might have made your days harder during the last three years, so thank you to always have your door open for me. You didn’t only provide me ideas and solutions to any problems and difficulties during the research, but also mentally support me to reach the finish line. I will remember you as a great supervisor! And Poplar has been and will still be my favourite plant!

Dr. Elena Petutschnig, thank you so much for the critical questions and insightful discussion throughout the project. I’m so glad that I can always come to you anytime I meet problems during the experiments. And despite your busy work, you always have time to answer my questions and help me out from the problems. I think I’m not exaggerating to say that I admire you as a dedicated researcher.

Prof. Dr. Volker Lipka, thank you very much for the opportunity to work in your department, a very nice working environment. It’s an honor for me that I can just call you ‘Volker’, if I wouldn’t know you, I might have to call you with the ‘Prof.’ The questions were too hard, the suggestions were so true, and the ideas were so brilliant. The three phrases: use your brain, do the control and talk to people! I will keep them in mind.

My two personal mentors: Viktor Korzun (Global Lead Scientific Affairs, KWS SAAT SE Co. KgaA) and Rizal Fajar Hariadi (Assistant Professor, Arizona State University). During my PhD life, BMBF (Bundesministeriums für Bildung und Forschung) through the Plant 2030 Academy provided a mentoring program, and I have two mentors for my personal development. Thanks to both of you who are willing to be my forever mentors, to provide me some insightful advices for my future personal and professional life.

All further members of the examination board: PD Dr. Marcel Wiermer, Prof. Dr. Andrea Polle, PD Dr. Till Ischebeck and Prof. Dr. Stefan Jakobs for your willingness to be my examiners. Many thanks in advance.

Dr. Hassan Ghareeb, thank you for giving me advice and providing me the bifluorescent plasmid for the particle bombardment assays. It really helps to analyse the PD flux, which was not easy in the beginning.

Robert Hänsch, Professor at the Department of Plant Biology, Technische Universität Braunschweig. Thanks for sharing the method and giving me short training to perform particle bombardment on poplar leaves.

Dennis Janz, a statistical expert and a friend of Thomas who helps analyzing the statistics of particle bombardment data.

Birgit Kersten from Thünen Institute, for sharing the transcript sequence of *PcLYM2-1 P. alba* allele.

Thanks to Prof. Dr. Andrea Polle and the gardener for providing greenhouse space at the forestry institute and taking care of the plants.

I want to thank Dr. Corina Thurow for showing me how to use the Biolistic® PDS-1000/He particle delivery system and thanks to the department of Prof. Gatz for giving me space to use this equipment.

Heinrich Ralf, Professor of Molecular Neuropharmacology of Behavior, who had ever given me a space to work with SP2 confocal in his Lab. for the DANS assay, which unfortunately did not work out well and couldn't make it into this dissertation because I switch into particle bombardment instead.

All members of Plant Cell Biology Department, thanks for listening to my progress report, giving me nice input and sharing research info. It helps improving the process and the outcomes of my experiments.

Thanks to all collaborators of ChitoPop project: Matthias Fladung and Khira Lettkemann from Johann Heinrich von Thünen Institute, as well as Stephanie Wemer and Christine Hallmann from Julius Kühn-Institute (JKI) for the discussion during the meetings and also providing information related to the project. Also thanks to BMBF for the funding.

Mascha Muhr (formerly Mascha Brinkkötter), I am so thankful that I have a mate in this project, and that it was you. To remember the days we've been through along the project, I am a bit sad that we can't do the defense at the same day (for a beautiful reason). Well, the day that we've talked a lot has finally come, I am happy...but also sad to realize that it means we are not working together anymore. I wish you a best of luck for your future!

Merlin Muhr and Maria Paulat, a former post doc and a former technician in Poplar Lab., respectively, who helped me getting to know the Lab. in the beginning of my stay here, and introduced me to poplar work.

Greta Niemann and Merle Münier, master and bachelor students respectively, who had spent long days in the Lab. with me. We were a great team! Some of the results are in chapter 2, yeayyyyy!!! ☺

Patricia (a former master student of Mascha), you're such a nice companion in the Lab. who often carry out nice conversation and funny jokes. I will always miss our conversations while we are having lunch in the Mensa.

All technicians: Feli, Susanne, Gaby, Sabine, Melanie, Ludmilla. I want to thank them for making my Lab. life easier, for being so helpful and friendly. Especially Feli who helped me the most. So sad that I cannot speak German, otherwise we can chat more.

Anja Auspurg, the secretary of Plant Cell Biology Department, thank you for helping me with the administrative stuff, especially when most of documents are in German.

All PhD students: Denise, Daniel, Sina, Julia, Chrissie, Lena, Leonie, Mohammed and Dimitri. Thanks for sharing the space with me in the Lab. and being supportive to each other. For Sina, thank you for taking care of me during my writing time, I will not forget to eat my pudding ^^. For the new PhD students: Qiqy, Andrea, Konrad…fighting! You are at the right place with good companions and under best supervision.

Hiking mates: Merlin and Mascha Muhr for giving me a ride to go for hiking, Maria Paulat, Anja Auspurg and Sabine Laukamm, you all gave me an alternative to escape from the Lab. *_^. I have some nice memories to bring to home ☺.

Finally, my family members: Bapak (Busra'i), Ibu (Hafilah) dan adik-adik (Mofidatul Jannah, Muswiatul Jannah, Mamluul Jannah). Terima kasih sudah mendukung semua keputusan dan langkah saya sejauh ini, terutama dalam hal pendidikan. I do not stay close to you physically but my heart and mind are always with you. This doctorate is partially dedicated to my parents, the most beloved people in my life. My brother in law (Syahril Aliif), thank you for being the only brother and the second man in our family and taking care of them when I am not there. The last is my new-born nephew (Akmal Ahsanul Aliif), I will meet you soon ☺.

Most importantly, Thanks God, thank You! There are many times that I was away from you and being sucked into my experiments during this reasearch, please forgive me!